

# **Development of a Point-of-Care Immunoassay System for Rapid Diagnosis of Severe Dengue**

**Thesis submitted for the degree of  
Doctor of Philosophy (Science)  
of**

**Jadavpur University**

**Department of Life Science & Biotechnology**



**By**

**Moumita Paul**

**School of Tropical Medicine**

**Department of Laboratory Medicine**

**Kolkata-700073**

**India**

**October, 2024**



# **CALCUTTA SCHOOL OF TROPICAL MEDICINE**

GOVERNMENT OF WEST BENGAL

108 Chittaranjan Avenue, Kolkata - 700073

Phone : 033 2212 3695/96/97 Fax : 033 2212 3698

Website : [stmkolkata.org](http://stmkolkata.org)

---

## **Certificate**

This is to certify that work described in this thesis entitled “**Development of a point-of-care immunoassay system for rapid diagnosis of severe dengue.**” is the result of investigations carried out by Moumita Paul, who got her name registered for the award of Ph.D. (Science) degree of Jadavpur University (**Index No. 39/22/LifeSc./27**), under our guidance and that the results presented here have previously not formed the basis for the award of any other diploma, degree, or fellowship.

*Sumi Mukhopadhyay*

**Dr. Sumi Mukhopadhyay, Ph.D.**

**(Research Supervisor)**

**Research Associate (W.B.G.S)**

**Department of Laboratory Medicine**

**Calcutta School of Tropical Medicine**

**Dept of Health and Family Welfare,**

**Govt of West Bengal, India**

**Date:**

## **Author's Declaration**

I declare that the work described in this thesis was carried out in accordance with the regulations of Jadavpur University. The work is original, except where indicated by references in the text. No part of this work has been submitted for any other academic award.

*Moumita Paul*

**Moumita Paul**

**Ph.D. Scholar**

**Department of Laboratory Medicine**

**Calcutta School of Tropical Medicine**

**Kolkata, India**

**Date: - 1/10/2024**

## Acknowledgement

This work would not have been possible without the support and advice provided by my Ph.D. supervisor **Dr. Sumi Mukhopadhyay, Ph.D., Research Associate (W.B.G.S) and Biological Scientist, Department of Laboratory Medicine, Calcutta School of Tropical Medicine, Kolkata, West Bengal, India.** In addition to her scientific prowess, creativity, and curiosity, I have been inspired by how she managed the whole group and project.

I am thankful to my Ph.D. clinical expert **Dr. Sudeshna Mallik, Associate Professor and Prof. (Dr.) Bibhuti Saha, Head of the Department of Tropical Medicine, Calcutta School of Tropical Medicine, Kolkata, West Bengal** for guiding me with the intuitive knowledge regarding clinical observation, patient handling, and case studies.

It gives me immense pleasure to express my deep sense of gratitude to the **Director, Calcutta School of Tropical Medicine, Kolkata, West Bengal, India** for providing me with the infrastructure and facility to carry out my research work.

I thank **Jadavpur University.** I also acknowledge **LSRB-DRDO** govt. of India and **WBHESTBT** (India). I am thankful to **IIT-Bombay** for the LC-MS/MS study, **ICAR, Kolkata** for DLS, **CRNN** for TEM, and the research team of **Viharilal College, Kolkata** for their guidance and suggestions with sample preparation of TEM and **NBRI, Lucknow** for plagiarism check.

I express my sincere thanks to all my **patients** and their family members for cooperating with me during my study period at Calcutta School of Tropical Medicine, Kolkata, West Bengal, India.

I would like to thank all my present and past lab members for creating a vibrant environment in the lab. I thank **Priyank Jaiswal, Dr. Goutam Patra, Dr. Nilotpal Banerjee, Susraba Chatterjee, and Akrite Mishra,** Department of Laboratory Medicine, Calcutta School of Tropical Medicine Kolkata, West Bengal, India.

I am deeply grateful to **Dr. Indranil Dhar, Assistant Professor & Head** and **all the members of the Department of Laboratory Medicine** for their support and guidance. I would like to extend a special thanks to **Rima Das**, who has been a wonderful friend since the day I joined the institute. Additionally, I am particularly indebted to **Sk Samimuddin Ahmed**, who has always been there to assist me with everything from providing distilled water to drinking water. He helped me to obtain patient details. His unwavering kindness and helpfulness have been invaluable to me, and I am truly thankful for his support.



I am eternally grateful to **Sourav Datta** for his support and guidance throughout my Ph.D. journey and for helping me to find a suitable lab where I can start my PhD journey. His insightful suggestions were invaluable in navigating challenges and preparing for coursework. I am thankful to him for helping me with the experiments. Without his mentorship, I may not have had the courage to pursue my PhD or find such a supportive lab environment. His patience and kindness are beyond words, and I am truly fortunate to have such a helpful friend.

Throughout my Ph.D. journey, I was fortunate enough to have two friends **Sukla Das** and **Sumona Basu** who were always there to lend a listening ear, offer comfort, and provide invaluable companionship, especially during the most challenging times.

I thank all CSTM colleagues and friends with whom I have interacted during my PhD.

My sincere apologies to my friends and people if I have missed any of your names in my acknowledgment.

I would also like to express my sincere gratitude to **Dr. Arup Kumar Mitra, Ph.D., Associate Professor, Department of Microbiology, St. Xavier's College, Kolkata**, who provided me with my first research opportunity after completing my Master's degree. This invaluable experience played a pivotal role in igniting my passion for research and ultimately led me to pursue my Ph.D. journey.

Beyond my Lab members, I want to acknowledge the invaluable friendship of my two friends **Puja Singh** and **Pallabi Adak** who have always been there for me. Their constant presence, even from afar, has been a source of encouragement and inspiration. I am grateful to **Puja Singh** for her timely assistance, which was invaluable in the final stages of my Ph.D.

I would like to express my sincere gratitude to my husband **Dr. Abhik Paul, Ph.D.** His consistent guidance and positive problem-solving approach have been invaluable to my career. His ability to extract valuable lessons from every situation has helped me grow professionally. I am truly grateful for the opportunity to learn from him.

I am thankful to my brother **Mr. Amarnath Paul** and my Sister-in-law **Mrs. Pallabi Paul** for their unwavering support and their creation of a peaceful home environment, which has been instrumental in allowing me to focus on my PhD work. I would also like to extend a special thanks to my daughter-in-law **Debadrita Paul**, whose active energy has always inspired me to maintain a positive outlook.

Last but not least, I would like to express my deepest gratitude to my parents, **Mr. Rabindranath Paul** and **Mrs. Manisha Paul** whose immense support and belief in me have been instrumental in my PhD journey. They always encouraged me to pursue my passions without fear, and their unconditional love and sacrifices have made this achievement possible.

## List of Figures

Figure 1.1.	Pathogenesis of dengue infection.....	6
Figure 1.2.:	Global scenario of dengue infection.....	7
Figure 1.3.	(A) States with highest dengue cases in 2023 in India. (B) Scenario of dengue cases in West Bengal from the year 2020 to 2024. Abbreviation: - WB: West Bengal.....	9
Figure 1.4:	Schematic view of a lateral flow test strip.....	22
Figure 1.5.:	General Structure of antibody.....	24
Figure 1.6.:	Lateral flow immunostrip with sandwich format (185).....	27
Figure 2.1.:	Dengue outbreak work at affected region in West Bengal.....	36
Figure 2.2.	Diagram of participates evaluated and enrolled in this study.....	37
Figure 2.3.	Protein can bind with NP through several types of interactions : A- Electrostatic, B - Hydrophobic, C - Dative bonds.....	46
Figure 3.1.:	Dengue outbreak work at affected regions in West Bengal (A)Phlebotomy for sample collection (B)Medical team visiting the affected area (C) Clinicians providing treatment guidelines to patients (D) Dengue patient with rash (E) USG showing Gall bladder thickening of affected patient (F) X ray showing fluid accumulation in dengue patient.....	53
Figure 3.2.:	Level of CICs in sera of Dengue WithOut Warning Sign (DwoWS), Dengue With Warning Sign (DwWS), and Severe Dengue (SD) patients. The horizontal line indicates the mean value. **** P<0.0001, significantly different from each category. ....	55
Figure 3.3.:	(A) Purification fold of different categories of enrolled subjects (i) Severe dengue (ii) Nonsevere (iii) Healthy. (B) Elution profile of different categories of enrolled subjects (i) Severe dengue. (ii) Nonsevere dengue (iii) Healthy. ....	55
Figure 3.4.:	(A) Mass spectrometric analysis of (i) Severe, (ii) Nonsevere and (iii) Healthy; data revealed list of up and down regulated proteins in severe dengue as compared to non severe dengue.Data submitted in PRIDE Database Project accession: PXD051713; B(i) 7.5 % SDS-PAGE profile of purified CIC antigens in lane 1 Severe; lane 2 Nonsevere; lane 3 Healthy, stained with Silver. D(ii) 7.5 % SDS-PAGE profile of purified CIC antigens in lane 4 Severe; lane 5 Healthy; lane 6 Nonsevere stained with coomassie. ....	56
Figure 3.5.	A. Levels of <i>Thrombospondin 1</i> (TSP1) of dengue without warning sign (DwoWS), dengue with warning signs (DWWS), and severe dengue (SD). Study subjects are significantly different from each category. The Kruskal-Wallis test was used in a one-way ANOVA to compare several study categories, and Dunn's multiple test was used to compare repeated measures. Symbols (*) represent statistically significant differences ( $P<0.05$ ) between different groups. B. Receiver operating characteristics curve analysis obtained the cutoff value (4818 ng/ml), AUC=0.9234, Sensitivity-90%, and Specificity-82.98 %. C. MS-MS Spectra of Thrombospondin-1 (TSP-1). ....	59

Figure 3.6.	a–b Multiple receiver operating characteristic (ROC) curve as a function of sensitivity vs 1-specificity to compare the performance of markers and combos for TSP-1 PLATELET and HCT. ....	60
Figure 3.7.:	A) Levels of VTN of Nonsevere and Severe, Healthy and OFI, B) Level of MASP-1 of nonsevere, severe, healthy and OFI. C) Receiver operating characteristics curve analysis of VTN level in Severe and Non-severe Dengue infected patients obtained the AUC=0.8730. D) Receiver operating characteristics curve analysis of MASP-1 level in Severe and Non-severe Dengue infected patients obtained the AUC=0.8817.E) Validation of VTN using western blotting image. (F) Validation of MASP-1 using western blotting image. G) MS-MS Spectra of Vitronectin (VTN). H) MS-MS Spectra of Mannan associated serine protease-1 (MASP-1). ....	62
Figure 3.8.:	STRING analysis uncovering protein-protein interactions of upregulated proteins in severe dengue as compared to nonsevere dengue. A.& D: Proteins identified in different cells.B.& E Biological functions of proteins. C,F,G & H: Basic settings of string analysis. A protein is represented by each node, and an interaction, including a functional or physical relationship, is represented by each edge. The only interactions displayed are those with a high confidence score of 0.7.....	63
Figure 3.9.:	STRING analysis uncovering protein-protein interactions of downregulated proteins in severe dengue as compared to nonsevere dengue.A.& D: Proteins identified in different cells.B.& E Biological functions of proteins. C,F,G & H: Basic settings of string analysis. A protein is represented by each node, and an interaction, including a functional or physical relationship, is represented by each edge. The only interactions displayed are those with a high confidence score of 0.7.....	64
Figure 3.10.	Correlation of MASP-1 and VTN with viral load. (A) MASP-1 versus viral load and (B) VTN versus viral load.....	66
Figure 3.11.:	Schematic view of a lectin-based lateral flow test strip using VTN-MAb conjugated AuNPs. ....	67
Figure 3.11.	A. Sample pad standardization, B. Conjugate pad standardization, C. NC membrane standardization, D. Absorbent pad standardization, E. table shows flow time of different categories of components.....	69
Figure 3.12.	Test and control line optimisation using point-of-care assay analysis. ANOVA is used first, then the Kruskal-Wallis test (K). A) Variations in MAA ( <i>Maackia amurensis</i> agglutinin) concentration. B) Graph represents color intensity of different concentration of one lectin, i.e., of MAA ( <i>Maackia amurensis</i> agglutinin). C) Graph represents color intensity of different concentration of another lectin, i.e., of DSA ( <i>Datura stramonium</i> agglutinin). D) Different concentration of DSA ( <i>Datura stramonium</i> agglutinin). E) Graph represents color intensity of different concentration of control line, i.e. <i>Goat anti-mouse IgG antibody</i> . F) Different concentration of control line ( <i>Goat anti-mouse IgG antibody</i> ).....	71

Figure 3.13.:	A) Chemical reaction behind the synthesis of Silver Nanoparticle Synthesis, B) Figure shows colour of solution of Silver nanoparticles gradually changed, C) Characteristic UV-Vis spectrum, with maximum absorbance at 401 nm, D) Bar graph represents size distribution of AgNPs. E) Transmission electron microscope (TEM) image of the synthesised AgNPs. ....	72
Figure 3.14.:	Dynamic light scattering (DLS) size distribution curves for AgNPs (A.[i] - A.[v] ) and AgNPs + Ab (B [i] - B [ii]):- (A1) intensity vs size of AgNPs, (B1) Correlation coefficient vs time of AgNPs , (C1) Number vs size of AgNPs, (A2) intensity vs size of AgNPs + Ab, (B2) Correlation coefficient vs time of AgNPs +Ab, (C2) Number vs size of AgNPs + Ab, (D1) Zeta potential graph of AgNPs, (D2) Zeta potential of AgNPs +Ab .....	73
Figure 3.15	A) TEM micrograph of the Silver dispersion kit, B.i) Intensity vs size of AgNPs, ii) Correlation coefficient vs time of AgNPs, iii) Number vs Size distribution of AgNPs, iv & v) zeta potential graph of AgNPs of silver dispersion kit, vi) Statistical table of AgNPs of Silver dispersion kit.....	74
Figure 3.16.:	Dynamic light scattering (DLS) size distribution curves for AgNPs of Silver dispersion kit which conjugated with antibody. A.i) Intensity vs Size of Ab conjugated AgNPs after 30 minutes, ii) Correlation coefficient vs time of Ab conjugated AgNPs, iii) Number vs Size, iv) Zeta potential graph of AgNPs, v) Statistical table of Ab conjugated AgNPs, B. i) Intensity vs Size of Ab conjugated AgNPs after 1 hr, ii) Correlation coefficient vs time of Ab conjugated AgNPs, iii) Number vs Size, iv) Zeta potential graph of Ab conjugated AgNPs, v) Statistical table of Ab conjugated AgNP. ....	74
Figure 3.17.:	A i)-iii) Density gradient centrifugation method, B.i)-vi) TEM micrograph of AgNPs, C. AGE assay.i-ia) Ab conjugated AgNPs, ii-ia) AgNPs, iii-ia) Ab conjugated AgNPs binds with analytes present in patient sample. ii) MASP-1 conjugated AgNPs, iii) Ab conjugated AgNPs further bind with analytes present in patient sample, D i) Graph shows DLS of AgNPs- Intensity vs Size and ii) Correlation coefficient vs time of AgNPs. ....	75
Figure 3.18.	A) Graph represents Zeta potential of only AgNPs and value of zeta potential represents in statistical tabulate form, B) Graph represents zeta potential of Ab conjugated AgNPs and statistical table shows value of zata potential.....	76
Figure 3.12.:	Schematic view of a lectin-based lateral flow test strip using MASP-1-MAb conjugated AgNPs. ....	77
Figure 3.19.	Point of care immunoassay analysis of test and control line optimization. ANOVA followed by Kruskal-wallis test (K). (A) Obtained colour intensity by using ImageJ software, (B) Different concentration of Goat anti-mouse IgG antibody in lateral flow assay, (C) Graph represents colour intensity of different concentration of control line i.e. Goat anti-mouse IgG antibody. (D) Different concentration of Masp-1 polyclonal (test line) antibody in lateral flow assay, (E) Graph represents colour intensity of different concentration of test line.....	78

Figure 3.20. Validation of the newly developed assay using clinical samples. A) A graph showed the logarithmic color intensity of the LFIA strip when using DSA lectin, B) A receiver operating characteristic (ROC) curve analysis was performed to evaluate the diagnostic accuracy of the newly developed point-of-care assay using DSA lectin, C) A graph showed the logarithmic color intensity of the LFIA strip when using MAA lectin, D) A receiver operating characteristic (ROC) curve analysis was performed to evaluate the diagnostic accuracy of the newly developed point-of-care assay using MAA lectin, E) A graph showed the logarithmic color intensity of the LFIA strip when using MASP-1 protein, F) A receiver operating characteristic (ROC) curve analysis was performed to evaluate the diagnostic accuracy of the newly developed point-of-care assay using MASP-1 protein, G) A graph showed the severity scores of dengue patients as calculated by a nomogram, H) A receiver operating characteristic (ROC) curve analysis was performed to evaluate the diagnostic accuracy of the severity score of dengue patients as calculated by a nomogram. .... 80

## List of Tables

Table 1.1:	Dengue Severity Classification, PAHO (Pan American Health Organization) /WHO (World Health Organization) .....	10
Table 3.1.:	Demographic study and clinical parameters of enrolled subjects. ....	52
Table 3.2:	Basic laboratory parameter study of enrolled subjects .....	54
Table 3.3.:	Represented gene ontology terms associated with differential proteins in SD patients compared to non-severe dengue patients. ....	57
Table 3.4.:	The performance of combination of biomarkers via receiver operating characteristic (ROC) curve analysis .....	60
Table 3.5.:	Association of MASP-1 and VTN with biochemical parameters of severe dengue patients .....	65
Table 3.6.:	Inter- and intra-assay variation. ....	81

# Table of Contents

Certificate .....	i
Author's Declaration .....	ii
Acknowledgement.....	iii
List of Figures .....	v
List of Tables.....	ix
Table of Contents .....	x
List of Abbreviations .....	xiv
Units .....	xvi
Statistical Notations.....	xvii
Abstract.....	xviii
List of Publications.....	xx
CHAPTER - 1	
Introduction.....	1
1.1. Dengue .....	1
1.2. History of Dengue disease.....	2
1.3. Vector of Dengue infection.....	3
1.4. Host of Dengue infection .....	3
1.5. Environmental factors of Dengue infection: .....	3
1.6. Dengue Virus Transmission.....	4
1.7. Immune Response to Dengue Infection .....	5
1.8 Epidemiology of Dengue infection.....	6
1.8.1 Global Scenario.....	6
1.8.2 Indian Scenario .....	8
1.9 Clinical Aspects of Dengue Infection .....	10
1.10 Vector Control and Dengue Vaccine .....	11
1.11 Complement system in dengue infection .....	13
1.11.1. Mannose Associated Serine Protease -1 (MASP-1) .....	14
1.11.2 Vitronectin .....	15
1.12 Thrombospondin-1.....	17
1.13 Point of Care Diagnostics.....	19
1.13.1 Lateral flow immunoassay (LFIA).....	20
1.13.2 General Principles and the Components of LFIAs.....	21

1.13.3 Sample Pad .....	22
1.13.4 Conjugate Pad .....	22
1.13.5 Nitrocellulose Membrane (NCM) .....	23
1.13.6 Absorbent Pad .....	24
1.14 Bio-recognition elements used in lateral flow assay .....	24
1.14.1. Antibody .....	24
1.15 Working mechanism of lateral flow Immunoassay .....	25
1.15.1 Sandwich-format .....	25
1.15.2 Competitive format .....	27
1.15.3 Immunothreshold format .....	28
1.16 Labels used in lateral flow assay .....	29
1.16.1 Colloid gold/Gold nanoparticles (AuNPs) .....	30
1.16.2 Silver nanoparticles (AgNP) .....	30
1.16.3 Carbon nanoparticles (CNPs) .....	31
1.16.4 Magnetite nanoparticles (MNPs) .....	32
1.16.5 Up-converting phosphor nanoparticles (UCPs) .....	32
1.16.6 Latex bead and liposomes .....	32
1.16.7 Other LFA labels .....	33
Aims and Objectives .....	34
CHAPTER - 2	
Materials and Methods .....	35
2.1. Ethical Statement .....	35
2.2. Study population .....	35
2.3. Quantification of Biochemical parameters .....	37
2.4. Dengue viral load determination .....	38
2.5. Quantification of Circulating Immune Complexes .....	38
2.6. Gradient gel electrophoresis and SDS-PAGE analysis used for Characterization of CICs .....	39
2.7. Sample preparation for affinity purification .....	39
2.8. Zip Tipping & LC-MS/MS .....	40
2.9. SDS-PAGE and Western blotting .....	40
2.10. Determination of Circulating Proteins Titers .....	41
2.11. Protein Network Analysis .....	41
2.12. Nitrocellulose membrane selection .....	42
2.13. Sample-pad, conjugate-pad, and absorbent-pad selection .....	42



2.14. Assembly of the immunostrip for the detection of Dengue severity .....	42
2.15. Preparation of Gold nanoparticle conjugated antibody .....	43
2.16. Control line and test line optimization for AuNPs .....	43
2.17. LFIA strips with Gold nanoparticles testing with clinical samples .....	44
2.18. Synthesis of Silver nanoparticles. ....	44
2.19. UV-Visible Spectroscopy .....	45
2.20. Transmission electron microscopy (TEM) .....	45
2.21. Preparation of Silver nanoparticle conjugated antibody .....	46
2.22. Dynamic Light Scattering (DLS).....	47
2.23. Density gradient centrifugation Method.....	48
2.24. Agarose Gel Electrophoresis assay .....	49
2.25. Control line and test line optimization for AgNP .....	50
2.26. LFIA strips with Silver nanoparticles testing with clinical samples .....	50
2.27. Quantification of color intensity .....	50
2.28. Statistics .....	51
<b>CHAPTER - 3</b>	
Results .....	52
3.1. Demography & Clinical parameters .....	52
3.2. Laboratory parameters .....	54
3.3. CICs estimation by PEG index .....	54
3.4. Affinity Purification of CIC antigens .....	55
3.5. Plasma Proteomic Changes .....	56
3.6. Quantifying TSP-1 Protein Levels and CombiROC analysis .....	58
3.7. Individual Sample Analysis: Quantifying Protein Levels .....	61
3.8. Evaluating Protein Biomarkers for Dengue Diagnosis: A Western Blot Approach .....	61
3.9. Functional Data Analysis of differentially Expressed Proteins .....	62
3.10. Correlation in between MASP-1, VTN with Blood Parameters .....	65
3.11. Correlation in between MASP-1, VTN with Viral load .....	65
3.12 Preparation of immunostrip for Lectin-based LFIA using AuNPs.....	66
3.13 Morphological analysis of the NCM (Nitrocellulose membrane).....	67
3.14 Morphology analysis of Sample pad, Conjugate pad and Absorbent pad .....	67
3.15 Characterization of Gold nanoparticles by using UV-Vis Spectrophotometry .....	69
3.16 Control line optimization for AuNPs-Lectin-based LFIA.....	69

3.17 Test line MAA ( <i>Maackia amurensis agglutinin</i> ) and DSA ( <i>Datura stramonium agglutinin</i> ) optimization for AuNPs- Lectin-based LFIA.....	70
3.18 Synthesis of Silver Nanoparticles (AgNPs).....	71
3.19 Characterization of Silver nanoparticles through TEM and UV-Vis Spectrophotometry .....	71
3.20 Characterization of Ab-conjugated AgNPs .....	72
3.21 Characterization of AgNPs, Ab conjugated AgNPs and Conjugated AgNPs with targated analytes present in plasma.....	75
3.22 Preparation of immunostrip for MASP-1-based LFIA using AgNPs.....	76
3.23 Control and Test line optimization for LFIA by using AgNPs .....	77
3.24 Validation of the newly developed Lectin-based assay using clinical samples .....	78
3.25 Validation of the newly developed MASP-1-based assay using clinical samples .....	79
3.26 Comparison between assays with nomogram.....	79
CHAPTER - 4	
Discussion.....	82
CHAPTER - 5	
Summary & Future directions.....	91
References.....	96
Permission for Figure .....	121

## List of Abbreviations

Ab:	Antibody
AgNPs:	Silver nanoparticles
ALB:	Albumin
AUC:	Area Under Curve
AuNPs:	Gold nanoparticles
CICs:	Circulating immune complexes
CRP:	C-reactive protein
CV:	Coefficient variation
DAB:	Diaminobenzidine
DENV:	Dengue Virus
DLS:	Dynamic Light Scattering
DSA:	Datura stramonium Agglutinin
DWOWS:	Dengue without warning sign
DWWS:	Dengue with warning sign
ELISA:	Enzyme-linked immunosorbent assay
GLB:	Globulin
HCT:	Hematocrit
HD:	Healthy Donor
HRP:	Horseradish peroxidase
IgM:	Immunoglobulin
IQR:	Interquartile ranges
LCMS:	Liquid Chromatography mass spectrometry
LFIA:	Lateral flow immunoassay
MAA:	Maackia amurensis Agglutinin
MASP-1:	Mannose associated serine protease-1
MBL:	Mannan binding lectin
NC:	Nitrocellulose
NS:	Nonstructural
OD:	Optical density
OFI:	Other febrile illness

PBS:	Phosphate buffered saline
PLT:	Platelet
PoC:	Point of Care
ROC:	Receiver operating characteristic
SAS:	Saturated Ammonium Sulphate
SD:	Severe Dengue
SDS-PAGE:	Sodium dodecyl sulfate polyacrylamide gel electrophoresis
SGOT:	Serum Glutamic Oxaloacetic Transaminase
SGPT:	Serum Glutamic Pyruvic Transaminase
TEM:	Transmission Electron Microscopy
TMB:	Tetramethylbenzidine
VTN:	Vitronectin
WHO:	World Health Organization

## Units

mM:	millimole
μM:	micromole
IU:	International unit
g:	gram
mg:	milligram
μg:	microgram
pg:	picogram
ml:	milliliter
dl:	deciliter
μl:	microliter
mm:	millimeter
nm:	nanometer
kDa:	kilodalton
ng:	nanogram

## Statistical Notations

P:	Probability
SEM:	Standard error mean
SD:	Standard deviation
<:	Less than
>:	Greater than
±:	Plus minus
r:	Spearman rank coefficient
%:	Percentage
AUC:	Area under curve

# Development of Point-of-Care Immunoassay System for rapid Diagnosis of Severe Dengue

## Abstract

**Background:** Dengue an arboviral infection, has recorded a dramatic increase in prevalence in the past few decades. The majority of these cases are asymptomatic, with a minor fraction of them resulting in mortality. Current assays cannot predict the severity of the infection due to a lack of identifiable associated protein biomarkers. The absence of specific protein biomarkers significantly hampers the early identification of individuals at high risk of developing severe dengue. This can therefore result in inadequate or delayed interventions, which could worsen the disease's progression and raise the chance of death. By focusing early intervention efforts on high-risk people, healthcare providers may be able to lower the prevalence of severe dengue fever and enhance patient outcomes.

Additionally, the availability and promptness of dengue diagnosis and severity evaluation would be greatly improved by the founding of point-of-care diagnostic tools that incorporate these novel biomarkers. These tests could be used in distant or resource-constrained environments, where prompt and precise diagnosis is essential for efficient disease management.

**Aim:** This research focuses on the identification, validation, and utilization of protein biomarkers associated with dengue severity. This endeavor involves applying advanced proteomic techniques to comprehensively analyze the protein profiles of dengue patients with severe and nonsevere illnesses. By comparing the proteomic mode of severe and non-severe cases, we aim to uncover differentially expressed proteins that could serve as potential biomarkers for predicting disease progression. The ultimate goal of this research is to apply these identified and validated biomarkers to develop a lateral flow immunoassay (LFIA) for the rapid and accurate assessment of dengue severity. LFIA technology offers several advantages, including its ease of use and cost-effectiveness, making it suitable for point-of-care (PoC) applications. By incorporating the identified biomarkers into LFIA strips, we aim to create a diagnostic tool that can provide clinicians with a rapid and reliable assessment of dengue severity, causing timely and appropriate management decisions.

**Methodology:** To identify potential biomarkers associated with dengue severity, we employed LC-MS/MS-based proteomic analysis on the protein profiles of patients with severe and non-

severe dengue infections. The identified biomarkers were subsequently validated using Western blotting and ELISA. Building upon these findings, we developed a lateral-flow-immunoassay (LFIA) incorporating the validated biomarkers. The newly developed assay was then evaluated using confirmed dengue samples to determine its sensitivity, specificity, positive predictive value, and negative predictive value. The newly developed assay could conclusively identify severe cases of infection.

**Result:** Proteomics analysis revealed 144 up-regulated and 89 down-regulated proteins between severe and nonsevere dengue cases. MASP-1, VTN, and TSP-1 were selected for this study due to their roles in the complement system and coagulation cascade, respectively. These pathways are known to be dysregulated in severe dengue, suggesting their potential involvement in disease pathogenesis. This research found that the levels of MASP-1 (Mannan Associated Serine Protease-1), TSP-1(Thrombospondin-1), and VTN (Vitronectin) were significantly altered in patients with severe dengue compared to those with non-severe infections. The combination of TSP-1 and platelet counts was evaluated for their predictive performance which showed almost 100% sensitivity and specificity and 1.000 for AUC (Area Under Curve). Using lateral flow immunoassay (LFIA), these biomarkers (MASP-1 and VTN) could effectively differentiate between severe and mild cases of dengue. This suggests that a combination of TSP-1 with platelet and LFIA-based testing of MASP-1 and Lectin-based LFIA with VTN could be a valuable tool for early identification of patients at risk of severe dengue and inform timely clinical management.

**Conclusion:** This study leveraged proteomics to conduct a comprehensive analysis of proteins on a large scale. A significant breakthrough was achieved by combining TSP-1 with platelet counts using CombiROC and developing a point-of-care immunoassay utilizing the identified biomarkers MASP-1 and VTN. The newly developed assay, successfully employed gold and silver nanoparticles as probes, which can differentiate between severe and non-severe dengue cases. This combination of TSP-1 with platelet counts and the point-of-care test using MASP-1 and VTN offers promising potential for rapid and convenient dengue severity detection in clinical settings.

**Keywords:** Dengue fever, LC-MS/MS, Lateral flow immunoassay (LFIA), Mannan-binding lectin-associated serine protease-1(MASP-1), Thrombospondin-1 (TSP-1), Vitronectin (VTN), Complement pathway.



## List of Publications

- **Paul, M.**, Saha, B., & Mukhopadhyay, S. (2023). Development of a novel lectin-based gold nanoparticle point-of-care immunoassay for rapid diagnosis of patients with severe Dengue infection. *Journal of Immunoassay and Immunochemistry*, 1-18. <https://pubmed.ncbi.nlm.nih.gov/37789768/>.
- **Paul, M.**, Basu, D., Mallik, S. *et al.* Decreased Thrombospondin-1 Titers Are Hallmarks of Patients with Severe Dengue Infection. *Proc. Natl. Acad. Sci., India, Sect. B Biol. Sci.* (2024). <https://doi.org/10.1007/s40011-024-01586-4>.
- **Paul, M.**, Misra, S., Patra, G., Datta, S., Saha, B., & Mukhopadhyay, S. (2021). In Silico Molecular Docking and in Vitro Analysis of Eugenol as Free Radical Scavenger in Patients with Dengue Infection. In *Advances in Medical Physics and Healthcare Engineering* (pp. 583- 594). Springer, Singapore. <https://ouci.dntb.gov.ua/en/works/4k6eJMG7/>.
- Datta, S., Ghosh, M., **Paul, M.**, Haldar, P., Mallik, S., Mukhopadhyay, S., ... & Kundu, P. K. Comprehensive Investigation of Fever cases enrolled during 2019 Dengue outbreaks from three hyperendemic regions of North 24 Parganas district of West Bengal, India. *Journal of Medical Virology* 2021 (November). <https://pubmed.ncbi.nlm.nih.gov/34730296/>.

# CHAPTER - 1

## Introduction

### 1.1. Dengue

In the tropics and subtropics area, dengue viral infections are more frequent. Due to its worldwide distribution in more than 100 countries and the potential for large-scale outbreaks of potentially fatal disease, at present, dengue virus stands as the most prominent virus carried by arthropods. Dengue fever is currently the most significant arthropod-borne viral disease. The vectors are primarily *Aedes aegypti*, and *Aedes albopictus* [1], responsible for the transmission of dengue infection. A member of the genus *Flavivirus* and family *Flaviviridae* is the dengue virus (DENV). The dengue virus (DENV), a member of the *Flaviviridae* family and genus *Flavivirus*, is the reason behind dengue infection [2]. It contains a single-stranded positive-sense ribonucleic acid. Any one of the four viruses known as DENV- (1,2,3 &4), which have a serological connection, can cause dengue infections. Another serotype, DENV-5, was identified in October 2013 in the Malaysian state of Sarawak. It largely has a sylvatic non-human transmission cycle, which results in a milder version of the disease. The electron-dense core of mature DENV particles, which have a diameter of 500 nm, is encased in a lipid bi-layer, into which two transmembrane viral proteins are inserted to create a glycoprotein shell [3]. The envelope (E) and membrane protein (prM/M) are present in 180 copies within the clearly defined glycoprotein shell. At least 10 mature proteins are produced by the co- and post-translational cleavage of the viral polyprotein. Three structural proteins (capsid, prM, and E) are encoded at the polyprotein's N-terminus, and the remaining seven NS proteins (NS1-NS2A-NS2B-NS3-NS4A-NS4B-NS5) are encoded at the ORF. Host and viral proteases perform the polyprotein maturation process. PrM, E, NS1, and NS4B's N-termini are cleaved by the host signal peptidase at the ER lumen, whereas the majority of the other NS proteins and the capsid protein's C-terminus are processed by the viral protease NS2B3 in the cytoplasm of infected cells [4]. It has been discovered that NS1 (48–50 kDa) interacts with virus-induced vesicles that are produced inside cells, secreted to the cell surface, or discharged into the circulation of infected people [5]. A barrel-shaped structure with a diameter of about 10 nm and a height of about 9 nm, it is composed of charged lipids such as phosphatidylcholine and phosphatidylethanolamine as well as triglycerides, cholesterol, and trimers of sNS1 dimers [6]. Virus RNA synthesis and viral particle assembly have both been linked to the tiny hydrophobic

integral membrane protein NS2A (22 kDa) [7]. The NS2B-NS3 protease cleaves the NS2B protein after translation, adding 130 residues to the final product. Three hydrophobic regions that span the membrane are thought to make up NS2B. The 69 kDa NS3 protein performs a variety of enzymatic functions that are crucial for the replication of viral genomic RNA, including Nucleoside triphosphatase (NTPase), RNA helicase, and RNA nucleoside 5' triphosphatase (RTPase) all facilitated by its C-terminal domain and processing of viral polyproteins by protease N-terminal domain serine protease. Additionally, NS5 has terminal transferase activity, which can obstruct in vitro tests that measure the NS5 protein's capacity to copy RNA from a template [8].

## **1.2. History of Dengue disease**

The origin of the name "dengue fever" is obscured in history. "Ka-dinga pepo" (a seizure similar to cramps brought on by a malevolent spirit) is the Kiswahili phrase from which the English name "dengue" is derived [9]. The word "dengue" was eventually borrowed into West Indian Spanish and eventually found its way into English. There is another explanation for the name. The term "dengue" is derived from the Spanish word "fastidiousness" or "affectation," which describes the mannerisms and stances of individuals afflicted with the illness, which were supposed to mimic those of a dandy [10].

The West Indies is where the term "dengue" was originally used. There, it was referred to as "dandy fever" because of the patients' rigid posture and unwillingness to move. The extreme pain in the joints and bones was sometimes referred to as "breakbone fever" [10].

The first historical record of a probable dengue fever case dates back to the Jin Dynasty (226-420 CE) in China, which referred to a "Water poison" associated with flying insects. Through trade and human mobility, it spread over the world, with notable outbreaks in the 18th century in places like Cairo, Jakarta, and Philadelphia.

After 1828, the term "dengue" became commonly used, however, it's still not clear where the name came from. It is thought that African slaves brought it to the West Indies, where it subsequently dispersed to other areas. The disease, which still poses a serious threat to global health, is commonly referred to as "dengue" despite its ambiguous history.

### **1.3. Vector of Dengue infection**

Female *Aedes* mosquitoes transmit the dengue virus to non-immune people by feeding on the blood of an infected person, usually up to 5–12 days after the onset of symptoms, or the period of viremia. The primary vector of dengue transmission, *Aedes aegypti*, is widely distributed in tropical and subtropical regions worldwide [11,12]. Within seven days, the adult mosquito emerges from its eggs, which are laid on damp surfaces somewhat above the waterline. If the temperature drops, this could take several weeks. The mosquito's most significant survival trait is its ability to survive for over a year in arid conditions and to reemerge in seven days when it comes into touch with water. The virus can stay dormant in the egg for the same amount of time before becoming active when it transforms into larvae.

*Aedes albopictus* is a mosquito that excels in temperate climates and is increasingly linked to epidemics in numerous states and locations [13]. The usual life spans of *Aedes aegypti* and *Aedes albopictus* are 30 days and 8 weeks, respectively, yet they may grow longer during the rainy season. *Aedes albopictus* favors natural settings like tree holes, rubber containers, etc., while *Aedes aegypti* typically inhabits household waters and the home environment. All *Aedes* mosquitoes bite between five and seven people at a time during the day (peak biting occurs early in the morning and in the evening just before dusk). They can also fly up to a restricted 400 meters [14].

### **1.4. Host of Dengue infection**

After evolving from mosquitoes, dengue viruses then adapted to non-human primates and then to humans. They can all serve as dengue virus carriers and reservoirs. Human viremia accumulates high viral titers two days before the development of fever (non-febrile) and persists for 5-7 days following the start of fever (febrile). Only in these two-time frames does the vector species become infected. Humans then serve as a dead-end host for the transmission. Human susceptibility is influenced by both genetic predisposition and immunological conditions [15-17]. Humans and monkeys are both amplifying hosts for the virus, which is spread by mosquito eggs.

### **1.5. Environmental factors of Dengue infection:**

The environment greatly affects the vectors' activity and transmissibility. The ideal conditions for vector growth are 16–30°C and 60–80% relative humidity. Additionally, this causes the extrinsic incubation period to shorten. The information above explains in detail why infections

in Indian cities are becoming more prevalent after rains, which typically occur in late July and early August. Vector transmission is only allowed to occur between sea level and 1000 feet above sea level. By the year 2100, average global temperatures are expected to rise by 2.0 to 4.5 degrees Celsius due to global warming [18], which may have a noticeable influence on vector-borne diseases [19]. On the other hand, a 2 °C rise in temperature will shorten the extrinsic incubation period of DENV and extend the amount of infected mosquitoes that are accessible. Apart from that, dehydration causes mosquitoes to bite more frequently, increasing the amount of time that people spend in the company of mosquitoes [20].

## **1.6. Dengue Virus Transmission**

A cycle of transmission from human to mosquito to human allows the dengue virus to spread. A person often develops viremia, a condition in which there is a high level of the dengue virus in the blood, four days after being bitten by an infected *Aedes aegypti* mosquito [21]. An essential mechanism, the ubiquitin-proteasome, plays a crucial role in controlling the transmission of infectious DENV via vectors [22]. While the DENV is being transmitted to the host, the salivary glands get infected and virions are released into the host's saliva [23]. For the propagation of four DENV serotypes into the host, blood cells and plasma are crucial media. After the dengue virus attaches to the target cell through contact between multiple cell surface receptors and the viral envelope (E) protein, the person becomes infected with DENV. All categorized serotypes interact with the mannose, heparan sulfate, nLc4Cer, and DCSIGN/L-SIGN receptors in mammalian cells. After receptor-mediated endocytosis, DENV virion fuses with acidic lysosomes, and its genomic RNA (11000 bases positive-sense, a single-stranded RNA) is released into the cytoplasm. After that, it is translated into polyproteins of 3400 amino acids which are further cleaved into 3 structural (Capsid: C, Envelop: E and Membrane: M) and 7 non-structural proteins (NS1, NS2A, NS2B, NS3, NS4A, NS4B and NS5) [24].

During DENV replication, host components, viral proteins, and genomic RNA are all incorporated by a membrane-bound replication complex assembly. In this instance, positive-strand (+) DENV genomic RNA serves as a template to create complementary negative-strand (-) RNA, which is sequentially employed to produce numerous (+) RNA genomes available for translation and replication cycle regulation or packaging into virions [25]. Although DENV itself encodes RNA-dependent RNA polymerases, other cellular factors catalyze this virus' infection cycle. The presence of DENV genomic RNA in the salivary glands of *Aedes aegypti*,

as demonstrated by Raquin and Lambrechts, suggests that DENV is actively replicating in its vector before transmission [26].

### **1.7. Immune Response to Dengue Infection**

The immune system possesses more defenses to combat the dengue virus. Human Langerhans cells and dermal/interstitial dendritic cells are first infected by DENV. These cells then move to lymph nodes where they present viral antigens to T cells, triggering humoral and cellular immune responses [27]. Small proteins known as interferons, which belong to a broad class of proteins known as cytokines, are produced and released by infected cells. Interferons activate both the innate and adaptive immune systems and can obstruct the reproduction of viruses. They assist in identifying dengue-infected cells by the immune system and aid in preventing infection of uninfected cells. Tumor necrosis factor, platelet-activating factor, interleukin-1 $\alpha$ , interleukin-1 $\beta$ , and interleukin-6 are all produced by the infected monocytes and macrophages. All these factors along with complement proteins like C3a, C3b, and histamine protein correlate with the severity of dengue infection, playing a role in plasma leakage, and increased vascular permeability which are hallmarks of severe dengue infection [28]. In response to the dengue infection, B cells generate IgM and IgG antibodies, which are then released into the bloodstream and lymphatic fluid. These antibodies are specifically designed to identify and neutralize dengue viral particles, predominantly directed against the E and M glycoproteins of DENV are produced to develop acquired immunity to the infecting serotype. The initial encounter with DENV infection, referred to as primary infection, is distinguished by a gradual and low-titer antibody reaction. Antibodies of immunoglobulin M (IgM) are the first to emerge. After the fever starts, IgM antibodies start to show up within 5 days, peak two weeks later, and then gradually drop to undetectable levels over the following few months. Within a week of the fever starting, immunoglobulin G (IgG) antibodies can be found at low titers, and they gradually rise over time [29]. A secondary antibody response arises from a second exposure to DENV. IgM antibody levels are significantly lower during a secondary DENV infection. IgG antibodies are produced during the acute phase of the infection and titers rise dramatically to high levels in the following two weeks. Due to antibody-dependent enhancement (ADE), a person with a heterologous serotype secondary DENV infection is highly susceptible to developing a severe illness. The new DENV serotype after secondary infection is recognized by the preexisting heterologous dengue antibody specific for the virus serotype from the main infection in ADE, resulting in the formation of a non-neutralizing antigen-antibody complex. The antigen-antibody complex's Fc portion binds to Fc receptors on the cell surface, allowing

the virus to attach. The virus then becomes internalized by the cell, which makes it possible for it to multiply [30].

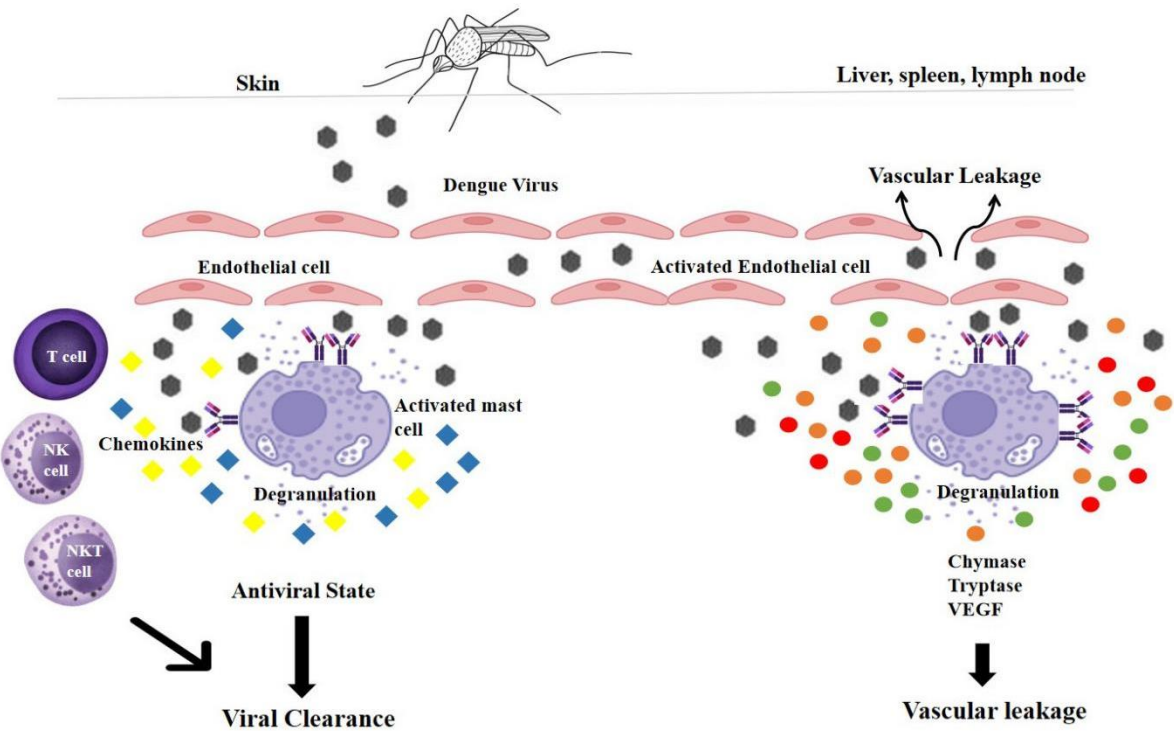


**Figure 1.1. Pathogenesis of dengue infection**

## 1.8 Epidemiology of Dengue infection

### 1.8.1 Global Scenario

Due to globalization, dengue has grown dramatically over the past 60 years, with an almost 30-fold rise in incidence [31]. According to recent data, the annual prevalence of infection is estimated to be around 390 million (95% confidence interval: 284-528 million). However, only one-fourth (24.61%) of cases (96 million, 95% CI: 67-136 million) present clinically and are diagnosed [32]. According to an additional assessment, 128 countries and 3.9 billion individuals are in danger of contracting the dengue virus [33]. Jakarta, Indonesia, and Cairo, Egypt all reported the first dengue outbreaks in 1779 [34]. The Philadelphia outbreak in 1780 was a DENV outbreak that was confirmed in North America [35]. In Thailand in 1958 and the Philippines in 1953–1954, the first dengue epidemics were officially reported [36]. More than 2.38 million cases of dengue were reported during the greatest dengue outbreak ever recorded in the US in 2016. With 1.5 million patients, Brazil had the largest contribution to this outbreak. With more than 3 million incidences, dengue incidents have dramatically exploded in 2019 in the US [37]. From the start of the 19th century, dengue epidemics were documented in the

West, East, and South Africa [38]. After World War II, dengue outbreaks became a problem in Southeast Asian nations, primarily because of urbanization [39]. The Philippines reported the first two dengue hemorrhagic fever outbreaks in 1953 and 1956, respectively [36]. In Southeast-Asian nations like the Philippines, Myanmar, Bangkok, Singapore, Thailand, Vietnam, Bhutan, Brunei, Cambodia, East Timor, Indonesia, Laos, and Malaysia dengue epidemics have been cyclically occurring every year since 1950 [41]. In Indonesia between 2009 and 2010, serotype-4 caused the majority of dengue cases [42]. Dengue virus was first isolated by Hotta and Kimura in 1943. They inoculated a diseased patient’s serum in suckling mice [43]. In 1944, Sabin et al. identified comparable viruses from US troops stationed in India, New Guinea, and Hawaii. Three dengue strains were discovered between 1942 and 1945 by the use of mouse-brain passage experiments, which involved injecting blood from a dengue patient into the minds of subsequent generations of white mice [44].

More than 10 million dengue cases and more than 5,000 dengue-related fatalities have been reported from 80 nations and territories since the start of 2024. The WHO PAHO region has recorded the majority of cases worldwide. Two times as many cases were reported in 2023 as there were in 2024, with almost nine million cases recorded by PAHO. Brazil recorded more than eight million cases in the region in 2024, followed by Argentina, Paraguay, Peru, and Colombia [45].

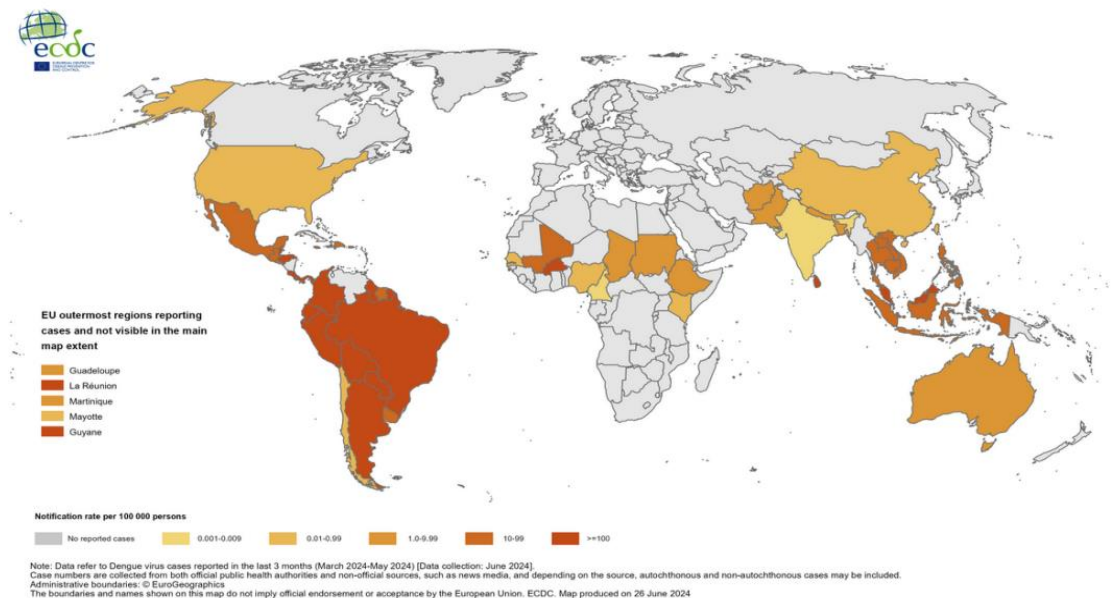


**Figure 1.2.: Global scenario of dengue infection**  
 Ref:- <https://www.ecdc.europa.eu/en/dengue-monthly>



In total, up until June 16, 2024, 1,180 cases of dengue were documented in La Reunion, as per the Epidemiological Bulletin released on the same day. Dengue circulation is wider now than it was in 2023, and during the past four weeks, there has been a decline in cases. According to reports from the regional offices (SEARO, South-East Asia Regional Offices) and (WPRO, Western - Pacific Regional Offices, respectively), dengue circulation has also been documented in Africa and South-East Asia the WHO Regions. As of June 2024 The SEARO report, released on June 12, 2024, states that although dengue cases in Bangladesh, Sri Lanka, and Thailand have decreased from prior years, there have been rises in dengue cases reported in the Maldives (totaling 1, 234 cases reported until May 2024). The WPRO (Western - Pacific Regional Offices) update Dengue Situation from June 13, 2024 states that although there have been increases in cases in Vietnam, as of May 26, there had been fewer cases reported overall than there had been during the same period in 2023. Meanwhile, Malaysia, which had previously reported an increase in cases, has seen a decrease in cases, with a total of 62,107 cases reported as of week 21 (up 34% from the same period in 2023). In Africa, 44 956 cases of dengue have been reported this year from Burkina Faso, Cameroon, Cabo Verde, Chad, Ethiopia, Kenya, Mali, Mauritius, Sao Tome & Principe, Senegal, and Sudan, according to the Africa CDC Epidemic Intelligence Report of June 22, 2024.

### **1.8.2 Indian Scenario**

Due to its favorable environment, the Indian subcontinent has seen several cases of dengue outbreaks including all serotypes except DENV-5 [45]. Although dengue was once only found in cities, it has since expanded to rural areas. In addition to union territories like the Andaman and Nicobar Islands, Dadra, and Nagar Haveli, the disease is endemic in other states, including Assam, Bihar, Jharkhand, Orissa, and Uttarakhand. Over the past few decades, there have been major changes to the dengue infection scenario in India. Dengue has become more common in many states since 2010, with an annual incidence of roughly 15 per million people. In India, there are more than 100,000 infections and 200–400 fatalities per year [46]. In terms of history, the dengue virus was originally identified in 1945, many years before the Philippines saw its first notable outbreak (1954). The first clinical case was documented in Vellore in 1956. The first dengue epidemic was noted in Kolkata seven years later. In different areas of WB, particularly in the Jalpaiguri, Darjeeling, Siliguri, and Kolkata domains, infection rates with all DENV serotypes were found in 2019–2020.

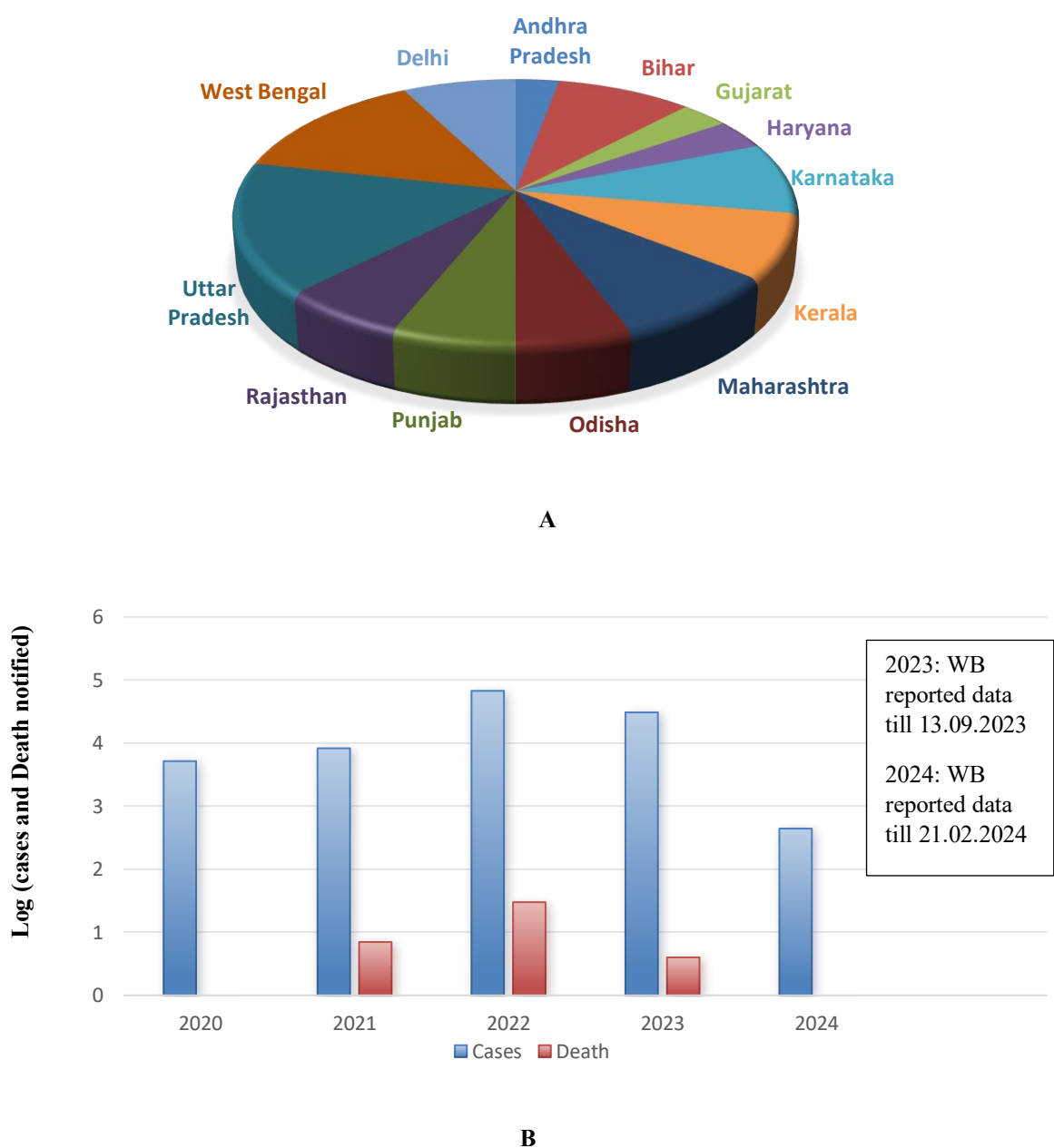


**Figure 1.3. (A) States with highest dengue cases in 2023 in India. (B) Scenario of dengue cases in West Bengal from the year 2020 to 2024. Abbreviation: - WB: West Bengal**

West Bengal, one of the hardest-hit states in India, reported 67,271 cases and 30 fatalities in 2022. Dengue cases in the state increased dramatically in 2022 compared to 2021, with 8,264 cases and 5,166 cases in 2020. In 2024, the dengue condition in West Bengal remained a cause for worry. 441 cases of dengue were reported in the state as of February 21, 2024. Even though there have been fewer cases in 2024 than in 2023, the state is still susceptible to dengue epidemics.

### 1.9 Clinical Aspects of Dengue Infection

In the majority of instances, asymptomatic or mildly symptomatic courses of DENV infection represent a promising approach for disease progression [47]. In November 2009, the World Health Organization (WHO) issued a new guideline that classified dengue severity based on the symptoms i.e., Dengue Without Warning Sign (DWOWS), Dengue With Warning Sign (DWWS), and Severe Dengue (SD). DWOWS and DWWS are considered as Non-Severe Dengue infection. A febrile person who has travelled to or lives in a Dengue-endemic area is considered to have dengue if they have  $\geq 2$  clinical symptoms [184].

**Table 1.1: Dengue Severity Classification, PAHO (Pan American Health Organization) /WHO (World Health Organization)**

Dengue Without Warning Signs (DWOWS)	Dengue With Warning Signs (DWWS)	Severe Dengue (SD)
Live in/ travel to dengue endemic area Fever and 2 of the following criteria: Nausea Rash Aches and pains Tourniquet test (+ve) Any warning sign laboratory confirmed dengue	Abdominal pain or tenderness Persistent vomiting Clinical fluid accumulation Mucosal bleed Lethargy, restlessness Laboratory : increase in HCT concurrent with rapid decrease in platelet count	Severe plasma leakage leading to: Shock (DSS) Fluid accumulation with respiratory distress Severe bleeding as evaluated by clinician Severe organ involvement Liver: high AST or ALT Heart and other organs

Clinical findings include vomiting, rash, nausea, positive tourniquet test are considered the symptoms of Dengue without warning sign. Abdominal pain or tenderness, clinical fluid accumulation, persistent vomiting, mucosal bleeding, fatigue, restlessness, and liver enlargement are all included in the warning sign of dengue infection. Severe dengue is characterized as having any of the following symptoms: severe bleeding; severe transaminase elevations 1,000 IU/L; impaired consciousness; severe organ dysfunction; or severe plasma leakage leading to shock or fluid accumulation with respiratory distress [48].

Based on the number of days following the start of the dengue infection, the WHO (2009) divided the dengue season into three parts. They are the crucial period (4-6 days), the recuperation phase ( $\geq 7$  days), and the febrile phase (1-3 days). Symptoms of the febrile phase include fever, nausea, headache, arthralgia, myalgia, and/or vomiting. Mild hemorrhagic

manifestations like petechiae and mucosal bleeding can also happen, and dehydration can also become apparent [49,50]. In the crucial phase of dengue, enhanced capillary permeability and fluid extravasation are the disease's pathophysiological hallmarks [51].

During this critical time, it is common to find leukocytopenia, thrombocytopenia, and plasma leak as clinically indicated by hemoconcentration, pleural effusion, and/or ascites; shock and severe bleeding are also conceivable [52]. The majority of dengue patients will then go into the recovery phase, which lasts for 24 to 48 hours and is when the extravasated fluid is reabsorbed into the intravascular compartment. If intravenous fluids were given in excess, pulmonary edema could develop. Dengue patients often recover during convalescence, while some may experience an itchy or non-itchy erythematous rash [53]. Pediatric patients often experience the clinical phases and symptoms of dengue that have been proposed by the WHO [54,55]. Adults with severe dengue may potentially develop a variety of additional clinical manifestations throughout the dengue clinical course, especially during the patient's critical phase. This is especially true for those with comorbidities and/or elderly patients. Examples of these manifestations include bacterial sepsis and multi-organ failure [56,57].

### **1.10 Vector Control and Dengue Vaccine**

There isn't yet a vaccine that can be used to prevent DENV infection, and there aren't many resources available to do so, including controlling mosquito populations. Insecticides and bed nets are two vector management strategies that can aid in lowering mosquito-mediated transmission. There is an urgent need for vaccine development or preventive measures because the number of people at risk for infection is rising and there are no cures for active diseases.

Although various companies are developing dengue vaccines, there are currently no licensed vaccinations available in India as of 2024. Currently, two commercially available dengue vaccines: Dengvaxia (CYD-TDV) developed by Sanofi Pasteur, and Qdenga (TAK-003) developed by Takeda [58,59]. Dengvaxia is a live-attenuated vaccine, administered in three doses spaced six months apart. It is only advised for those between the ages of 9 and 45 who have already caught dengue, as it raises the risk of severe dengue in people who have never had the illness [60].

Another vaccine is Qdenga. The four dengue virus serotypes have been weakened in this live-attenuated vaccine. In environments with high dengue transmission intensity, children aged 6-16 years are administered it in a 2- doses series with a 3- months gap between doses [61]. On

May 10, 2024, WHO prequalified Qdenga, allowing UN agencies to purchase it. Clinical development for a second dengue vaccine created by the National Institute of Allergy and Infectious Diseases in the United States is close to completion [62]. For its Qdenga vaccine, Takeda has recently started conducting local clinical studies in India.

All four of the dengue virus serotypes that have been licensed by the US NIH are being used to create live attenuated vaccines by Serum Institute of India (SII) and Panacea Biotec. A Phase 1/2 trial conducted by Panacea Biotec in 100 healthy people demonstrated the production of antibodies against all four serotypes, while a Phase 1 trial conducted by SII in Australia demonstrated the safety and well-tolerated nature of the vaccine [63]. The International Centre for Genetic Engineering and Biotechnology (ICGEB) has developed a vaccine called Virus-Like Particle that uses specific dengue envelope protein regions to inhibit antibody-dependent enhancement (ADE). This vaccine has shown 100% protection in animal trials, however, human testing has not yet taken place. Although DNA vaccines can be produced more affordably and kept at room temperature, they might not elicit as potent an immune response. Following successful animal testing, nano-plasmids are currently being used to optimize this candidate. In conclusion, while the VLP and DNA vaccines from ICGEB and TIFR are still in preclinical development, the live attenuated vaccines from SII, Panacea, and IIL are the most advanced, having either entered or finished early human trials [64].

A dengue vaccine's first-ever Phase 3 clinical trial has begun in India, according to a statement released by Panacea Biotec and the Indian Council of Medical Research (ICMR) on 14th August 2024 by PIB Delhi. DengiAll, an indigenous tetravalent dengue vaccine created in India by Panacea Biotec, will be tested for effectiveness in this historic experiment. [65].

While dengue remains a significant global health concern, the lack of a vaccine suitable for all age groups underscores the need for effective prevention and treatment strategies. Accurately predicting the severity of dengue infections remains a significant challenge in clinical management. While existing biomarkers, provide valuable insights, their limitations in sensitivity and specificity hinder early diagnosis and intervention. The identification of novel, reliable biomarkers is crucial to improve patient outcomes and optimize resource allocation. MASP-1, VTN, and TSP-1 were selected for this study due to their roles in the complement system and coagulation cascade, respectively. These pathways are known to be dysregulated in severe dengue, suggesting their potential involvement in disease pathogenesis. By

investigating these biomarkers, we aim to impart the development of a more comprehensive and predictive diagnostic tool for dengue severity.

### **1.11 Complement system in dengue infection**

An essential part of the innate immune response, the complement system is a series of about thirty serum proteins that work together to destroy infections. This complex system is essential to the host's defense against viruses and other infectious invaders. A major worldwide health burden is caused by the flavivirus known as dengue virus, which is endemic to tropical and subtropical countries. The complement system's role in the pathophysiology of dengue infection has become a focus of research [66]. Three different pathways—the lectin, alternative, and classical pathways—all lead to the same effector phase when the complement system is active. Traditionally, the classical route is started when antibodies attach to pathogen surface antigens to form immune complexes. The initial complement component, C1q, interacts with this complex, which sets off a series of enzymatic events that result in the production of C3 convertase, an essential enzyme in complement activation [67]. When interaction with foreign surfaces, like microbial pathogens, amplifies the alternative pathway, which is constitutively active at a low level in the circulation. In this route, factor B binds to C3(H<sub>2</sub>O), which is produced by the spontaneous hydrolysis of C3. The other form of C3 convertase is produced by further activation stages [68]. The lectin pathway, on the other hand, is not dependent on antibodies and recognizes the carbohydrate structures on the pathogen surface through the use of pattern recognition molecules like mannose-binding lectin (MBL). Similar to the conventional pathway, MBL and MASP proteases work together to activate the complement system. Because it doesn't involve the development of antibodies, the lectin pathway is thought to respond more quickly than the other two pathways [69,70]. The three routes have different roles in dengue infection, even though they eventually converge to produce the C5 convertase, which cleaves C5 into C5b and C5a starting the creation of the membrane attack complex (MAC). Cell lysis is caused by the MAC, a cytolytic complex that penetrates the pathogen's membrane. However, compared to other effector activities, complement-mediated lysis is less significant in the setting of viral infections [71]. The function of the complement system in dengue infection is complex. On the one hand, it uses direct lysis, neutralization, and opsonization to help remove the virus. Complement elements have the ability to attach to the dengue virus, making it easier for phagocytic cells to recognize and absorb it. Complement activation products also work to neutralize the virus by preventing it from adhering to host cells. Moreover, the MAC may lyse contaminated cells, which would

prevent the virus from replicating. Conversely, the pathophysiology of severe dengue sickness has been linked to dysregulated complement activation. The hallmark symptoms of severe dengue include increased vascular permeability and organ destruction, which might result from excessive complement activation. Severe disease symptoms are partly due to endothelial cell damage and complement-mediated inflammation [72]. Developing efficacious therapeutic strategies requires a precise understanding of the mechanisms underpinning complement activation and control in dengue infection. A promising treatment strategy is to modulate complement activity, either by increasing its antiviral effects or by preventing excessive activation. Furthermore, finding complement activation indicators may help with early identification and risk assessment of dengue patients.

#### **1.11.1. Mannose Associated Serine Protease -1 (MASP-1)**

The complement system serves as a crucial link between the innate immune system and the adaptive immune system. It is one of the main innate immune system effectors [73]. The complement system contains about 50 plasma and membrane-associated proteins. A proteolytic cascade that is triggered by complement activation results in the recruitment of inflammatory cells, phagocytosis, and cell lysis [74]. The lectin, alternative, and classical routes can all be used to activate complement. The C1 complex's attachment to immunological complexes, mostly to IgM or IgG but also to apoptotic cells, pentraxins, and pathogens, triggers the activation of the classical pathway. On the other hand, spontaneous plasma C3 hydrolysis triggers the activation of the alternate pathway. When pattern recognition molecules (PRMs) attach to acetylated residues or carbohydrates found on the surface of microbes (sometimes referred to as PAMPs or pathogen-associated molecular patterns), the lectin pathway is activated [75]. In 1992, Matsushita and Fujita published a seminal paper on the mechanism of the lectin pathway's activation by MBL and MASPs [76]. Numerous PRMs activate the lectin pathway: oligomers of mannose-binding lectin (MBL), heteromers of collectins 10 and 11 (COLEC10, also called collectin liver 1 or CL-L1, and COLEC11, also called collectin kidney 1 or CL-K1), and oligomers of Ficolin-1, 2 or 3 [77]

The "MBL-associated" serine proteases, commonly referred to as MASPs, begin life as proenzymes (zymogens) and then combine to form complexes with the trimeric structural subunits of these PRMs' dimers, trimers, and/or higher oligomers [78]. Recent data from many authors show that MASP-1, which also autoactivates, is crucial for activating MASP-2 [79]. The finding that about 70% of MBL circulate in the blood as tetramers of trimeric subunits

(MBLIV-III) associated with MASP-2 or MASP-3, or as trimers of trimeric subunits (MBL-III-III) associated with MASP-1 or MASP-19, suggests a major role for inter-complex cross-activation in the start of the complement cascade [80].

MASP-1, a C1s-like protein linked to MBL, was found in 1992 [76]. The MASP-1 protein has 699 amino acid residues and 19 amino acids leader peptide [81]. Its expression is mostly found in the liver and is induced by IL-6 during the acute phase response [82]. Normal serum/plasma MASP-1 concentration is 20 times more than MASP-2 concentration [83].

Among people with different cardio- and cerebrovascular diseases, MASP-1 levels were lowest in acute ischaemic stroke patients and greatest in subacute myocardial infarction patients [84]. Additionally, primary uterine leiomyosarcoma and HCV-infected hepatocyte cell lines also showed increased MASP-1 expression [85]. MASP-1 creates 60% of the C2a necessary for the production of C3 convertase by activating MASP-2 in heterocomplexes of large oligomeric MBL [86]. MASP-1 autoactivation appears to regulate the start of the lectin pathway [87]. Despite having a lower catalytic efficiency than thrombin, MASP-1 was found to play a function in the coagulation, cleaving factor XIII and fibrinogen, and mediating the synthesis of cross-linked fibrin [88]. Through the protease-activated receptor 4 (PAR4), the proteolytic activity of MASP-1 activates the NF-kappaB, Ca<sup>2+</sup> signaling, and p38 MAPK pathways in endothelial cells [89]. This activity triggers the release of IL-6 and IL-8, which activate neutrophil granulocytes' chemotaxis [89].

### **1.11.2 Vitronectin**

A multifunctional glycosylated protein, vitronectin (VTN) is found in the extracellular matrix of tissues, blood, amniotic fluid, and urine [91]. Hepatocytes and endothelial cells in the liver are primarily responsible for producing VTN, which circulates as a plentiful plasma protein [94]. VTN's physiological actions as an extracellular matrix component include cell adhesion, cell necrosis, which is mediated by complement action, and fibrinolysis, which prevents damage to tissues [92]. Similar to fibronectin, VTN is an adhesion protein found in plasma that contains the RGD (arginine, glycine, and aspartic acid) domain [93]. Human glycoproteins are generally glycosylated in two ways: N-linked and O-linked, where glycan is coupled with asparagines or serine and threonine residues, respectively. According to Plough et al. (2000), the RGD domain of VTN interacts with receptors such as  $\alpha\text{v}\beta 3$  and  $\alpha\text{v}\beta 5$  integrin. It interacts with several other proteins as well. In addition to its ability to stick to cells, VTN activates the intracellular



signaling molecules of integrins, such as FAK (also referred to as PTK2), one of the main integrin transducers. FAK activation requires Y397 phosphorylation. FAK phosphorylation at Y397 is crucial for TNF $\alpha$ -stimulated IL-6 production, suggesting that FAK may be a signaling node for cytokine regulation [94]. Both integrin and the uPA receptor, which are expressed on VSMCs (Vascular Smooth Muscle Cells), are bound by VTN. These receptors' interactions with vitronectin control the migration of VSMCs in vitro [95].

VTN also plays a crucial function in blocking the lytic action of the complement membrane attack complex, which is made up of the proteins C5b, C6, C7, C8, and C9 [96]. A brief heparin-binding domain is located near the carboxy terminus and is believed to be the location of molecular interactions with the thrombin-antithrombin complex, the terminal complement complex, and the plasminogen activator inhibitor type 1 (PAI-1) [97]. Comparable to protamine sulfate, a known inhibitor of the TCC, in terms of amino acid composition, this extremely basic sequence of 42 amino acids consists of 12 arginines and 3 lysines[98,99]. In order for the formation of lytic pores, the positively charged domain of vitronectin may attach to a complementary negatively charged domain on the C9 molecule. Since C6, C7, and C8 also contain the same cysteine-rich sections [100], it has been postulated that the heparin-binding domain is responsible for vitronectin's binding to C5b-7. Most of VTN's biological activities are dependent upon and/or synchronized with its conformational state(s) because of its structural labile nature [101]. It improves platelet adherence and integrates with blood clots like fibrin. According to in vivo research, thrombi develop in response to vascular injury and become unstable in the absence of VTN, delaying blood vessel closure and causing recurrent reopening. By binding to plasminogen activator inhibitor-1, VTN functions as a thrombus stabilizer and may prevent fibrin from lysing [102]. Important steps necessary to stop bleeding include platelet adhesion, aggregation, and the creation of the polymerized fibrin matrix at the site of vascular damage. Using a monoclonal anti-VTN antibody, fresh evidence indicated that VTN enhances platelet adhesion and aggregation, supporting the findings of an earlier antibody investigation, despite the fact that it has the potential to both stabilize the fibrin matrix and fasten  $\beta$ 3-integrin. Thus, it has been documented that VTN plays a supporting role in thrombosis [103,104].

The glycosylated portion of human VTN is about 30%. Variations in the glycosylation of plasma VTN could be linked to various physiological states or cellular functions [105]. Mass spectrometry and chromatography reveal that VTN contains an N-glycan with outer

fucosylation [107]. Proteins undergo post-translational alteration known as glycosylation, which attaches carbohydrates, or glycans, to particular locations on the backbone of the protein. N-linked oligosaccharides are found in all six species of animal plasma VTNs, as determined by a lectin binding assay, and 10–20% of their mass is composed of carbohydrates [107]. In cirrhosis and liver regeneration, VTN's glycosylation varies [108,109]. Furthermore, it has been shown that in humans, swine, and mice, de N-glycosylation and desialylation of VTN enhance collagen-binding ability [110]. When compared to control VTN, desensitized VTN (deNeu-VN) significantly reduces the spread of hepatic stellate cells and dermal fibroblasts, but not deN-glycosylated VTN (deN-gly-VN) [111]. A promising approach for the direct and precise identification of functional glycans on intact glycoproteins while accounting for accessibility is the lectin binding-based method. Natural proteins known as lectins are extensively distributed and attach to particular glycans. Because of their diversity and selectivity, lectins can be helpful tools in molecular biology.

### **1.12 Thrombospondin-1**

Thrombospondin is a large, multimeric glycoprotein secreted by various cell types, including platelets, endothelial cells, and fibroblasts. It is composed of three distinct domains: the N-terminal domain, the central region, and the C-terminal domain. Each domain contributes to the diverse functions of TSP [112]. The N-terminal domain contains a calcium-binding motif and is involved in interactions with other proteins, including matrix metalloproteinases and integrins. The central region that contains a thrombospondin type I repeat domain, which is important for binding to other proteins and extracellular matrix components and the C-terminal domain which is involved in interactions with fibrinogen and other coagulation factors.

Thrombospondin is heavily glycosylated, with approximately 30% of its mass consisting of carbohydrates. The carbohydrate modifications on TSP are diverse and include O-linked glycosylation, N-linked glycosylation, and C-mannosylation. O-linked glycosylation is the result of attaching a monosaccharide, usually galactose or N-acetylgalactosamine, to a serine or threonine residue in the backbone of a protein. The C-terminal region of TSP has a high concentration of O-linked glycosylation. N-linked glycosylation is a kind of glycosylation that happens when an asparagine residue in the protein backbone is connected to a complex oligosaccharide. TSP has N-linked glycosylation in both its central domain and N-terminal domains. When a mannose residue in the protein backbone is joined to a tryptophan residue forms a kind of glycosylation known as C-mannosylation. Although it is somewhat uncommon,

TSP's N-terminal domain has been found to contain C-mannosylation. The carbohydrate modifications on TSP play a crucial role in its structure, stability, and interactions with other molecules. Carbohydrates have a number of important roles in TSP, including Protein folding and stability. Through the formation of hydrogen bonds with amino acid residues, carbohydrates can aid in the stabilisation of protein structure. By interacting with lectins on the surface of other cells, carbohydrates on TSP can encourage cell adhesion and aggregation. TSP can interact with other proteins, including integrins and growth factors, through the mediation of carbohydrates. TSP's biological activity can be controlled by the proteolytic processing that carbohydrates affect. Strong platelet agonist thrombospondin can cause platelets to aggregate and become activated [113]. One important factor in controlling vascular permeability is thrombospondin. Increased vascular permeability in dengue can result in hypotension and plasma leakage, two symptoms that are specific to severe dengue. Thrombospondin plays a role in controlling inflammatory reactions. By stimulating inflammatory pathways and drawing immune cells to the infection site, it can exacerbate inflammation. In certain situations, though, thrombospondin may also have anti-inflammatory properties. Thrombospondin (TSP-1) suppresses NO synthesis and VEGF enhances endothelial permeability by inducing NO, the two have an antagonistic interaction that contributes to the pathophysiology of illness [114]. The goal of the current investigation was to determine whether TSP-1, when used in conjunction with other laboratory measures, may enhance the sensitivity and specificity limits for the diagnosis of severe dengue cases. TSP-1 may be in charge of capillary architecture, according to recent studies [115]. According to reports, downregulating TSP-1 in diabetic wounds caused capillaries to become more permeable and caused a delay in the healing process [116-118].

Numerous variables, including VEGF, activation of NF- $\kappa$ B, and cytokines like TNF- $\alpha$  and dengue NS1 antigen, are thought to be contributory contributors to this increase in vascular permeability [119-124]. TSP-1 is closely linked to TNF- $\alpha$  production and is a powerful activator of the NF- $\kappa$ B pathway [125].

Therefore, it is necessary to assess TSP-1's function in vascular leakage and how it relates to the severity of dengue. Numerous studies have demonstrated that older patients have a higher mortality rate due to their increased susceptibility to this infection. Further research is necessary to determine the underlying source of this infection and manage its severity, to ameliorate the situation.

### 1.13 Point of Care Diagnostics

An accurate result is typically obtained through lengthy and intricate procedures using traditional laboratory-based analytical techniques like gas chromatography (GC), real-time polymerase chain reaction (qPCR), enzyme-linked immunosorbent assay (ELISA), mass spectrometry (MS), and high-performance liquid chromatography (HPLC) however, a number of circumstances frequently call for an immediate on-site analyte identification. Point-of-care testing (POCT) is the term used to describe medical diagnostic testing conducted at the time and site of patient care (Kost, 2002). This indicates that the test can be carried out by individuals with minimal training in a hospital, an emergency room, a doctor's office, or at home. Additionally, the results are available right now rather than having to wait for them to be returned from a central facility, which could take hours or days [126]. One of the main factors influencing the future of the in-vitro diagnostics industry will be point-of-care testing, which is rapidly expanding with a growth rate of about 10% in clinical diagnostics [127]. Thus, infectious illnesses and coagulation monitoring are the two high-growth sectors that are primarily driving the market. The market for infectious diseases is expanding as a result of rising infection rates, the discovery of novel illnesses, and genetic abnormalities. The expansion of testing in patient homes and the rise of patient services are both contributing to the activity monitoring market's explosive growth [128]. To perform sophisticated biological tests at the location where they are most needed, diagnostic testing equipment must be lightweight, portable, and simple to use. Rapid tests are sold by a number of businesses worldwide. They have created several devices and technologies that cut down the testing period to hours or even minutes. These technologies can be divided into three groups: Purely disposable and permanently integrated with disposable components are the three types of medical devices [129]. Permanent integrated instruments are made for high-throughput work that requires quick and reliable findings, but even if those tools were sufficiently affordable, they couldn't be regarded as point-of-care tools because they require trained workers. Even when using microfluidic components, carryover must be avoided by rinsing the component with cleaning solutions between testing. Additionally, periodic calibration is required to maintain the settings by the standards [129]. The term "disposables" refers to analytical tests that use a disposable substrate (such as paper), are typically based on a microfluidic device (such as a lateral flow test), and rely on relatively cheap components and reagents that can be produced as commercial off-the-shelf (COTS) products using large-scale production techniques. One of the most common point-of-care formats, It is common practice to employ

lateral flow immunoassay (LFIA), also called immunochromatographic test strip (ICTS), for clinical diagnostics, environmental monitoring, and food analysis (Ji et al., 2015). The commercial usage of lateral flow assays for the detection of many analytes extends approximately over thirty years. They can be made to detect antigens or antibodies and can be applied to a variety of specimens. Most of them are designed to last longer than a year at room temperature without refrigeration, and some of them perform analytically on par with reference-level laboratory techniques [130]. Several operating mechanisms for lateral flow devices were created based on various target characteristics; the most popular ones are the sandwich format and competitive format. The next sections will cover the specifics of the lateral flow assay, including the biorecognition components, operational mechanisms, and labels. Disposable tests offer Point-of-Care (POC) diagnostics in locations without access to clinical laboratories with adequate equipment and people. Such disposable-based tests can be easily performed by users without the need for frequent training. Because of this, POC tests are crucial in circumstances where timing is crucial (such as emergency triage), when laboratory facilities are lacking (such as military or alien functions), and where resources are scarce (such as in underdeveloped nations). They support the fast and appropriate administration of care while enhancing clinical results [98-100]. Currently, available disposable tests have a variety of drawbacks. They still fall short of laboratory results in terms of sensitivity, specificity, and accuracy. Additionally, they frequently only offer a yes/no response. When compared to integrated equipment, the disposable has the advantages of being able to save calibrates and not requiring the reader to be cleaned in between samples. Due to this compromise, good performance and affordable test costs are possible. This strategy is the ideal POC option for hospitals where numerous tests must be performed each day at the patient's bedside. As a result, more sophisticated diagnostic procedures based on low-cost disposables are required to meet the needs of POC applications for use in poor countries and at the patient's home.

### **1.13.1 Lateral flow immunoassay (LFIA)**

One of the most used technologies for POC testing is Lateral flow immunoassay (LFIA) [134]. One of the most successful immunoassay-based analytical platforms for organised or point-of-care testing strategies that need little to no supporting infrastructure is the lateral flow immunoassay strategy (LFIA), also known as the immunochromatographic strip test (ICST) or the rapid diagnostic test (RDT). One (bio)analytical technique that can be used on-site to identify target molecules is the LFIA, which is paper-based. It requires adding the sample to a

standalone device, and results can be acquired in a matter of minutes. LFIAs met every requirement for the perfect POCT, including being "ASSURED" (affordable, sensitive, specific, user-friendly, robust, rapid, and equipment-free and delivered) [135]. The ASSURED standards were first used to describe diagnostic tests for STDs (Sexually Transmitted Diseases), but they are now the standard for all point-of-care testing (POCT) and, more broadly, all point-of-need (PON) tests.

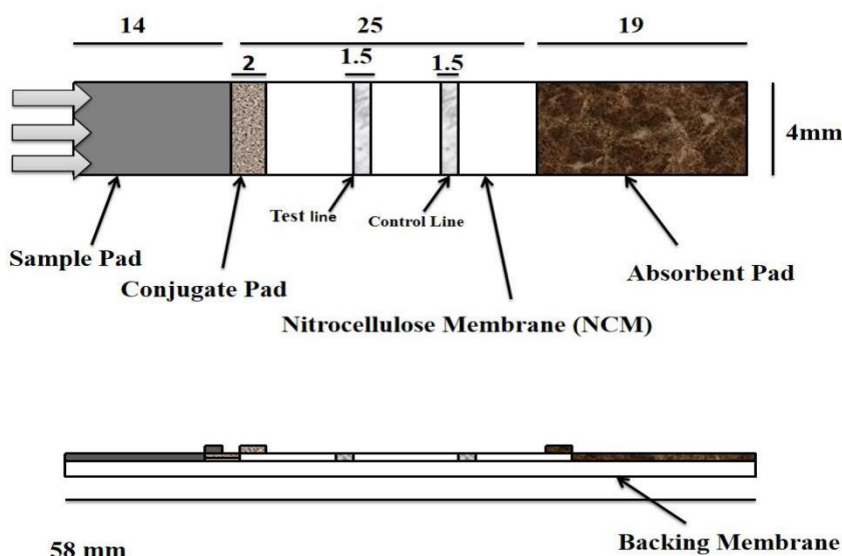
The LFIA's success is evident when one considers their place in the business world. The global market for lateral flow testing was valued at over US \$5.98 billion in 2019 and is expected to increase to US \$10.36 billion by 2027, with a compound annual growth rate (CAGR) of 7.7% between 2020 and 2027 [136].

Additionally, the LFIA has embodied a paradigm change from sample-to-lab to lab-to-sample to enhance decision-making and turnaround time. Kind of like a lab-in-a-hand [137].

LFIA's very appealing features are what make it so generally recognized and appealing. Consequently, the use of LFIA has expanded swiftly across numerous industries, including forensic analysis, veterinary medicine, environmental control, food and feed safety, and many more, starting with the identification of hormones, parasites, bacteria, viruses, cells, and biological markers for medicinal purposes [138,139].

### **1.13.2 General Principles and the Components of LFIAs**

Figure 1.4. reports the general structure of the LFIA, which is made up of a collection of parts that provide mechanical, chemical, and physical properties [140-142]. It basically looks like a multi-layered strip. A thin layer of porous nitrocellulose membrane sticks to a backing plastic substrate. The backing support gives the device physical stiffness and serves as a platform for the assembly of the various test components. The main components of the lateral flow immunoassay (LFIA), also known as lateral flow testing (LFT), as they relate to the materials employed and how they are integrated with the assay conditions, are covered in this section. The figure shows the main part of the lateral flow immunoassay system i.e. Sample pad, Conjugate pad, Nitrocellulose membrane (NC Membrane), and Absorbent pad.



Schematics of the LFIA assembly (measurements in mm)

Figure 1.4: Schematic view of a lateral flow test strip

### 1.13.3 Sample Pad

The sample pad is the first part of the lateral flow immunoassay strip. The sample pad's primary responsibility is to guarantee uniform distribution and regulate the sample's flow rate to the conjugate pad. The material of the sample pad is glass fiber. High absorption capacity and no protein binding are displayed by glass fiber sample pad type GFB. It serves as the platform on which the sample or analyte is placed during testing. Glass fiber material has neither reactive nor binding qualities, allowing the analyte to flow steadily and uniformly while preventing sample components from non-specifically adhering to the pad. GFB pads are offered in sheet and strip form in the usual thicknesses of 0.35 mm and 0.60 mm (GFBR4, GFBR7L) [143].

### 1.13.4 Conjugate Pad

Another pad, known as the conjugate pad, is positioned betwixt the sample pad and the commencement of the nitrocellulose membrane. This pad is often composed of polyester or glass fiber, which was first fixed at the appropriate position with a 2-3 mm overlap on the nitrocellulose membrane. After being impregnated with an appropriate labeled immunoreagent solution (often gold/ silver nanoparticle-tagged antibodies), the conjugation pad is dried [144,145]. The conjugate pad's principal job is to keep the dried detection reagents in storage until a liquid test sample is placed to the sample pad, at which point it makes sure that both the detection reagent and the test sample are uniformly transferred to the membrane. Studies have

suggested that the ideal conjugate pad material has to comprise the following attributes. A polyester matrix makes up a conjugate pad. The assay detection conjugate, such as a gold conjugate, is placed on this platform when it is dried. By re-hydrating the test sample, the conjugate pad's synthetic material composition ensures its speedy and effective release. The 'detection conjugate-analyte' complex travels into and up the nitrocellulose membrane.

### **1.13.5 Nitrocellulose Membrane (NCM)**

In 1832, nitrocellulose (NC) was first developed. It is a highly combustible substance that is created when cellulose is nitrated with potent nitrating agents like nitric acid (Henri, 1832) [146]. The membrane is the component of a lateral flow test strip that matters the most. These could consist of one Control line and one or more Test lines, which are designated regions. The purpose of the test lines is to provide proof of the interaction with the target molecule or molecules and, as a result, the necessary data. By binding with the probe independently of the target's presence, the control line guarantees that the test will run correctly [140]. The membrane for lateral flow test strips needs to firmly bind capture reagents at the test or control lines.

Studies have suggested that the NC membrane and other components must be fastened to a plastic backing to create a lateral flow test. Such pre-assembled membrane, adhesive, and plastic sub-assemblies are known as laminates or cards. These are easy to use for applying reagents and for later cutting into strips to finish the test.

According to the membrane manufacturer, membrane laminates show some following advantages i.e. Permit immediate development and increase scale for production, can be specially made to accommodate cassette or dipstick designs that already exist, Each element has been tested to ensure that it won't impede the immunoassays.

Applying the liquid sample to the sample pad is the first step in the LFIA. The tagged immunoreagents are resuspended in the solution from the conjugate pad, and the analytes and labeled probe are forced through the lines and along the membrane by capillary forces, where immunoreactions occur. The liquid sample is usually all that is needed to complete the experiment; no additional reagents are usually needed. Findings can usually be quickly and easily interpreted without the need for equipment for qualitative testing [137].



### 1.13.6 Absorbent Pad

The absorbent, also known as a wick or waste pad, is utilized to maintain a capillary flow that is consistently directed and flowing at the correct rate through the membrane. The sample will flow back into the membrane if there isn't or isn't enough of an absorption pad, which could increase the background or lead to false positives. A variety of materials, including cotton, cellulose, glass fibers, and porous polymers, are used to make lateral flow absorbent pads. To meet the needs of the test, non-woven cellulose fiber sheets in a range of thicknesses and densities are often used to make absorption pads.

### 1.14 Bio-recognition elements used in lateral flow assay

Bio-recognition components are substances that can recognize particular target molecules while avoiding cross-activity with other compounds. In lateral flow tests, aptamers/nucleic acids and antibodies are crucial bio-recognition components. Lateral flow assays (LFA) can be classified into three groups based on how antibodies and nucleic acid are used. Lateral flow immunoassays (LFIA) exclusively use antibodies. The term "nucleic acid lateral flow assay" (NALF) refers to tests that use nucleic acid [147]. A nucleic acid lateral flow immunoassay, or NALFIA, is created when both an antibody and a nucleic acid are employed in the LFA.

#### 1.14.1. Antibody

Immunoglobulins, another name for antibodies, are big, Y-shaped proteins that are created by plasma cells. They are utilized by the immune system to neutralize invaders including viruses and bacteria.

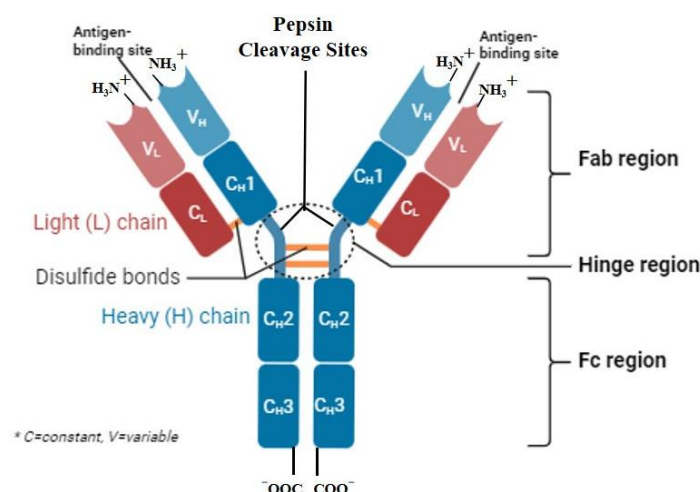


Figure 1.5.: General Structure of antibody

Antibodies have two 'Fab' domains for binding to antigens and a 'Fc' region for effector activities such as attaching to cell receptors. Ion-dipole bonds, hydrogen, van der Waals, and hydrophobic are only a few examples of the "weak interactions" that contribute to the link between antigen and antibody. The range of typical bond energy is 54–150 kJ/mol [148].

A small part of the molecules, consisting of only a couple of amino acids, are involved in this interaction (Vanoss, 1995) [149]. In lateral flow tests, antibodies are a great choice for determining the analyte because they primarily interact with specific antigens through immunoreactions. Lateral flow immunoassays (LFIA) are the common name for lateral flow assays that depend on an antibody. Primary antibody and secondary antibody are the two types of antibodies utilized in lateral flow experiments. Primary antibodies are those that can bind to a particular analyte (target analyte). Despite not having a direct affinity for the target analyte, the secondary antibody can still interact with the primary antibody and the immunocomplex that was created by the primary antibody and the target analyte. Primary antibodies are employed as detection elements in common LFIA, while secondary antibodies serve the purpose of the control line. An immunochromatographic device's total performance is significantly influenced by the antibody's affinity, particularly the primary antibody. Throughout the entire process of developing lateral flow sensors, the creation of antibodies plays a key role. If other factors are correctly managed, an antibody with strong affinity can typically provide exceptional sensitivity. However, compared to antibodies with mediate performance, these are typically significantly more expensive. Some of them aren't even sold commercially. On the one hand, additional elements like the target detection limit, price, and

The required quantity of strips should also be considered, particularly while a commercial LFA product is still in the research and development stage. Nevertheless, maximizing additional strip features like immunoreagent concentrations and nitrocellulose membrane type can also aid in enhancing the performance of the sensing system.

## **1.15 Working mechanism of lateral flow Immunoassay**

### **1.15.1 Sandwich-format**

Analytes having more than two distinct epitopes can typically bind to two different types of antibodies at once. Based on this concept, the sandwich format was created. The pregnancy test, which Unipath invented in 1984 and uses to measure human chorionic gonadotropin (HCG), is one of the earliest applications of the sandwich assay (Wild, 2013) [150]. Two

unique primary antibodies are employed in the sandwich configuration. A pre-coated version of one of them is present on the nitrocellulose membrane. Capturing the target antigen is its purpose. This antibody is known as a "detection antibody." 'Test line' refers to the area covered with the detecting antibody. The second kind of antibody is called "reaction antibody," and applying it on the conjugate pad [151]. Typically, reaction-specific antibodies are coupled to additional labels like magnetic nanoparticles (MNPs), silver nanoparticles (AgNPs), or gold nanoparticles (AuNPs). These labels can display the ultimate location of response antibodies on the test strip following the measurement, which can aid in understanding the outcomes. Secondary antibodies are immobilized in a different location following the test line known as the "control line" in addition to the test line. Every antibody and immunocomplex in existence (the result of an immunoreaction), which are not caught by the test sequence, is captured using secondary antibodies. The validity of the assay is also demonstrated by the control line. In the event that the control line is signal-free, the measurement may be deemed invalid. After the sample is placed on the sample pad, capillary force will cause the solution to move down the membrane. When the targeted antigen reaches the conjugate pad, it will interact with the corresponding antibody in the solution to form an immunocomplex. The detection antibody will then bind to the immunocomplex on the test line. Depending on the label employed in the assay, the buildup of immunocomplex on the testing line may be seen by unaided eyes or by various lateral-flow-strip readers when the concentration of the target analyte reaches a specified level. A positive result, for instance, would show two red stripes on the strip if the response antibody was labeled with AuNPs. This indicates that the target analyte's concentration in the sample solution exceeds the detection limit. On the contrary hand, if the analyte level is less than the detection limit, a neg result with just one red zone (control line) can be observed on the membrane.

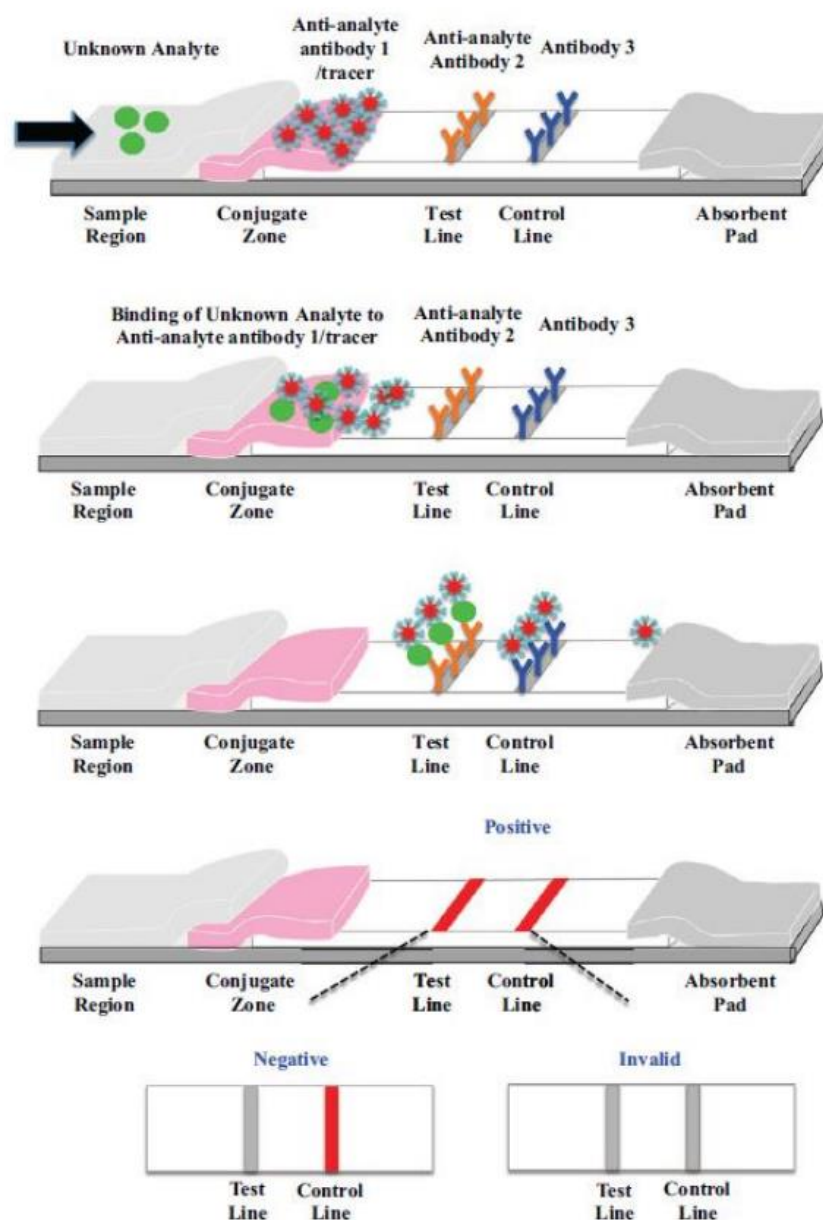


Figure 1.6.: Lateral flow immunostrip with sandwich format (185)

The sandwich configuration has several key advantages, including the ability to apply multiple signal-enhancing techniques to the strip, which significantly boosts sensitivity. In recent years, lateral flow assays have become increasingly popular, and the sandwich format has benefited from this.

### 1.15.2 Competitive format

Small compounds that are inappropriate for the sandwich format were the focus of the development of the competing format. One sort of antibody is utilized in the competitive format. The competitive format has two possible layouts. The initial one uses the antibody as

a "detection antibody," This is on the testing line's pre-coated, similar to the sandwich format. Nanomaterials were used to mark a known quantity of analyte, which was subsequently entrapped on the conjugate pad. Those tagged analytes will disintegrate into the sample solution and proceed with the flow once it reaches the conjugation pad. The labeled analyte and any unbound analytes in the sample will compete with one another for the antibody's constricting sites when the liquid reaches the testing line. As a result, the sign on the testing line will have a negative correlation with the concentration of the target analyte. This implies that the lower the analyte concentration in the sample solution, the higher the color intensity on the test line. The "reaction antibody" in the second scenario is a primary antibody that has been tagged and printed on the conjugate pad. Antigen-protein conjugate was coated on the testing line at the same time. The protein known as bovine serum albumin (BSA) is frequently utilized to conjugate with antigens. There are two phases to the whole reaction process:

First, the free analyte will interact with the antibody and create an immunocomplex before the sample even reaches the test line. Second, the immunocomplex will pass through the test line and be caught aside the control line while the free response antibodies will be caught by the test line when the sample passes through the test line.

There are two main factors in competitive format that describe the strip's sensitivity. One is the term "limit of detection" (LOD), which describes the lowest analyte concentration at which the sign on the testing line can become noticeably weaker than the signal in the negative control [152]. The other is known as 'cut-off' value. It indicates that the signal on the test line disappears at the lowest analyte concentration (Chen et al., 2016) [153].

### **1.15.3 Immunothreshold format**

The immunothreshold format is less common in lateral flow assays than the other two techniques, and there aren't many papers on it either. Sandwich format is comparable to how its results are interpreted. The 'test line' and 'control line' in this procedure, however, are not predetermined. According to Posthuma-Trumpie et al. (2009), the two sections are simply referred to as "line one/1st line" (the line close to the conjugate pad) and "line two/2nd line" (the line close to the absorbent pad) [154]. Only the signal on the first line is visible when the concentration of the target analyte is below the detection threshold. On the other hand, if the antigen concentration is more than the detection limit, a signal can be seen in the second line. Additionally, in this case, the color intensity in the first line will vary based on the analyte

concentrations. A signal won't appear in the first area if the concentration exceeds a particular threshold, which is analogous to a competitive mechanism. When the analyte is present, two bands are discernible at concentrations between moderate and high. Consequently, this approach also has the capacity for semi-quantification.

The immune threshold approach was initially inspired by the risk of result interpretation in a competitive mechanism. When this method is employed by untrained individuals, issues could arise since the signal strength in competing mechanisms is negatively connected to analyte concentration [154].

The immune threshold method has several shortcomings even if it can prevent some unclear result interpretations in competitive format. First off, test lines typically use more than a purely competitive process to consume immunoreagents. Because when evaluating blank samples, a nearly 100% of 45 antibody absorbency is required for the first line. When the amount of analyte is relatively low, the second line won't be capable of obtaining the immunocomplex if the concentration of immunoreagents is not high enough. The cost as well as the optimization processes will go up as a result. Additionally, it will be challenging to determine the concentration of the analyte because it depends not only on the signal strength on the second line but also on the first line. The creation of a trustworthy quantification methodology will face extra challenges if these two intensities are taken into consideration simultaneously.

Finally, there is no further evidence that the immunothreshold technique outperforms competitive mechanisms in terms of total sensing performance. Very little information has been written about this strategy in the literature in recent years following the deployment of combined labels in competitive mechanisms.

### **1.16 Labels used in lateral flow assay**

Labels/tracers are primarily proteins and nanomaterials that can produce detectable signals when aggregated in the testing line and control line of an NCM. They are employed in lateral flow assays. Labels are first coupled with biorecognition components during the production of a lateral flow strip, and then they are deposited onto the conjugate pad or combined with sample solution prior to testing. In lateral flow assays, tracers are crucial because they have a significant impact on sensor performance. In this section, a number of frequently used LFA labels will be discussed.

### **1.16.1 Colloid gold/Gold nanoparticles (AuNPs)**

Colloidal gold, commonly referred to as gold nanoparticles (AuNPs), has a long history of use in human society. The initial documented usage of AuNP for medical purposes dates back to roughly 2500 years [155]. One of the earliest uses of AuNP in a lateral flow device was reported in 2002. Shyu et al. created a device based on a sandwich structure for ricin detection. Later, it can be increased to 100pg/ml by employing a silver enhancement approach [156]. Numerous articles relating to AuNP-based LFIA have now been published. In addition to antibodies, AuNPs are employed to label aptamers and other DNA probes, as well as other biorecognition components. To determine thrombin, developed an LFA using aptamers as the detecting unit and AuNP as the labeling substance. A DNA-based lateral flow test for the identification of the 35S promoter, a regulatory component frequently present in genetically modified (GM) crops, was created by Kolm et al. The detection limit is 0.5% GM content, which complies with the European regulation requiring the labeling of any product or feed containing more than 0.9% GM content [157]. The many benefits of AuNPs include their simple production, great chemical stability, outstanding biocompatibility, customizable size, relative affordability, and high molar extinction coefficient. Additionally, due to its wide surface area, it is possible to combine it with other biomolecules, such as enzymes, which opens up the possibility of further enhancing the signal [158,159]. These characteristics have made AuNPs one of the most widely used labels in lateral-flow-assay in recent years.

### **1.16.2 Silver nanoparticles (AgNP)**

Silver nanoparticles (AgNPs) are growing in popularity in a range of fields, including those involving industries, medicine, food, and consumer goods because of their unique physical and chemical properties [160-162]. Among them include high electrical conductivity as well as optical, electrical, thermal energy, and medical qualities. Due to their unusual qualities, they have been used for a wide range of applications. These include the pharmaceutical and food industries, diagnostics, orthopedics, drug delivery, antibacterial agents, consumer goods, medical equipment coatings, sensors for optics, and healthcare products. In the end, they have also been used to enhance the tumor-killing actions of anticancer medications [163]. AgNPs have recently been widely used in a variety of fabrics, keyboards, dressings for injuries, and biomedical equipment [164,165]. It's significant to note that biologically produced AgNPs exhibit great yield, solubility, and stability. Among the several synthetic techniques for AgNPs, biological techniques appear to be straightforward, quick, non-toxic, trustworthy, and

environmentally friendly ways that may generate well-defined size and morphology under ideal circumstances for translational research. The production of AgNPs using green chemistry has great potential, in the end. Because of their simplicity of production, chemical stability, high conductivity, and antibacterial capabilities, silver nanoparticles (AgNPs) have gained a lot of interest. Silver ions are reduced in aqueous solution in the presence of a capping agent, such as citrate molecules, which imparts negative surface charges that inhibit nanoparticle aggregation through repulsion forces. This process is a common way to create AgNP [166]. AgNPs have a significant increase in surface energy due to the abundance of surface atoms. It has been noticed that they have a propensity to interact with nearby components that have donating or accepting sites in order to lower their high surface energy. According to data published in the literature, when nanoparticles are put into a biological environs, proteins tend to act and form a protein corona shell [167, 168].

### **1.16.3 Carbon nanoparticles (CNPs)**

Another significant type of coloured biomarker is carbon nanoparticles (CNPs), commonly referred to as colloidal carbon or carbon black. Strong black coloration gives CNPs a high signal-to-noise ratio that enables visual detection down to the picomolar range [169]. In addition to their excellent sensitivity, CNPs also exhibit outstanding stability, non-toxicity, ease of preparation, and lack of activation [170]. The use of CNPs in lateral flow tests was first described in 2003. Aldus et al.'s lateral flow immunostrip enabled the simultaneous identification of verotoxin and E. Coli O157:H7 in milk that had been experimentally inoculated [171].

Since then, numerous articles pertaining to CNPs in lateral flow tests have been published. For example, Blaková et al. created an immunostrip to quickly identify the genus *Cronobacter* using carbon-neutravidin conjugate as the marker. The detection limit for the test was 8ng/ml, and it may be completed in 10 minutes. According to Blaková et al. (2011), the LFIA results showed excellent agreement with those from traditional microbiological techniques [172]. The performance of conventional CNP-based LFA has recently been improved by research. For the purpose of detecting DNA, created a lateral-flow-biosensor with fluorescent carbon nanoparticles (FCN). The benefits of carbon nanoparticles and fluorescent labeling are combined in FCN [173].



#### **1.16.4 Magnetite nanoparticles (MNPs)**

Scientists have recently discovered magnetite nanoparticles (MNPs), which offer some distinct advantages as a label for lateral flow assays. MNPs have a brilliant brown hue that is good for optical identification in qualitative tests. However, their magnetic characteristics make them ideally suited for quantitative assay [174]. Quantitative analysis is typically done through conventional optical lateral flow tests using readers that gauge the brightness of reflected light or fluorescence. The ability to preserve the strip after experiments for further verification is made possible by the long-term stability of the magnetic signals produced by MNPs [175]. Beads of Magnetic are considerably less likely to experience background noise in biological samples, which typically contain turbidity, natural fluorescence, and hue [176].

#### **1.16.5 Up-converting phosphor nanoparticles (UCPs)**

Another kind of luminescent and fluorescent probes are up-converting phosphor nanoparticles (UCPs), which may "emit high-energy visible or UV light when irradiated with low energy infrared light" [177]. Owing to their narrow bandwidth, variable emission colors, low cytotoxicity, and excellent chemical and photo rigidity, UCPs have been receiving a lot of attention recently [178]. Long fluorescence lifetimes are another benefit of UCPs; These lifetimes can improve the signal-to-noise ratio and decrease background autofluorescence, which can raise vulnerability by a few orders of magnitude [179].

#### **1.16.6 Latex bead and liposomes**

According to Quesada-Gonzalez and Merkoci (2015), latex beads (LBs) are homogeneous-size particles that can be employed as labels after being colored. It is a fairly traditional marker used in lateral flow experiments, much like AuNP [159]. The research by Greenwald et al. indicates that LBs have greater sensitivity than AuNP in the lateral flow assay for the identification of *Mycobacterium bovis* [180]. Even though LBs are less common than AuNPs in lateral flow devices, certain lateral flow experiments using LBs have been described recently. Deoxyribonucleic acid in plasma was measured using a quantitative lateral flow nucleic acid biosensor (LFNB) created by Mao et al. An LBs-based lateral flow device designed by Reiko et al. can detect 10<sup>3</sup>-10<sup>4</sup> focus-forming units/mL of ebolaviruses. It is regarded as a useful technique for tracking the virus in underdeveloped African nations [181].

### **1.16.7 Other LFA labels**

Traditional labels may not always be able to match the sensitivity or quantification requirements during the determination of particular analytes due to the rapid development of immunochromatography technology. Scientists worked hard to create new labels for lateral flow devices as a result. New tracers can be broadly divided into two categories. The first is the combining and integrating of conventional labels [173,182]. The other sort of label is constructed from unusual substances. For example, Liang et al. developed the label for Europium (III) chelate microparticles, which are used in LFIA to measure antibodies to the hepatitis B virus (anti-HBV). The instrument has a wide linear range of 0.63-640IU/mL and can quantitatively measure anti-HBV levels with a limit of detection of 0.31IU/mL [183]. Another chromatographic device used fluorescein isothiocyanate as the label to determine the presence of *E. coli* O157:H7. The LOD was approximately 1CFU/mL. According to articles that have been published, these labels have demonstrated exceptionally excellent sensing performance in the lab and are quite promising moving forward. There is still much work to be done before these innovative tracers can be used commercially, thus it is still unclear if they will continue to perform similarly in field applications.

## **Aims and Objectives**

- Identification of dengue severity biomarkers through using several established methodology like LC-MS/MS, ELISA, Western Blot.
- Development of a point of care immunoassay for diagnosis of Severe Dengue by performing extensive optimization experiments for the different parameters.
- Validation of the newly developed assay by estimating analytical and diagnostic sensitivity, specificity limits along with NPV(Negative-Predictive-Value), PPV(Positive-Predictive-Value) and establishing a ROC(Receiver Operating Characteristic) curve of the new assay.

## **CHAPTER - 2**

### **Materials and Methods**

#### **2.1. Ethical Statement**

Blood samples were collected from patients of the School of Tropical Medicine, Kolkata after explaining the benefit and objective of the study to the patient and his/her family members. All enrolled patients and the healthy control group gave written informed consent, with the assurance that their identities would be kept private (from parents or legal guardians in the case of pediatric patients). They also had the option to remove their names from the study if they wanted to. After appropriate explanation, Study subjects were chosen for the research. As agreed upon, the members of the medical team gathered demographic information such as age, sex, type and length of treatment, and clinical complaints. Following the initial screening, 5 milliliters of venous blood were drawn into vials containing EDTA and those without anticoagulants. Routine blood test of all the enrolled subjects was also performed was also run. The School of Tropical Medicine, Kolkata's Clinical Research Ethics Committee examined and accepted the study sites' ethical considerations as well as those of the department's outdoor and indoor departments of dermatology and tropical medicine [CREC-STM/ IEC Ref No:2018-AG2 dated 18/06/2018 & CREC-STM/ IEC Ref No: 2022-AS07, dated 06/07/2022].

#### **2.2. Study population**

Five milliliters (5.0 ml) of venous blood were obtained by venepuncture from patients who had symptoms similar to dengue and preserved in EDTA anticoagulant tube and no- anticoagulant tube. NS1 ELISA, IgM/IgG ELISA, and RT-PCR were performed on plasma that had been separated by centrifugation at 3000 rpm. The study was conducted in India at the Calcutta School of Tropical Medicine during the period of July 2019 to December 2023. Apart from the Calcutta School of Tropical Medicine, we also collected blood from three other Govt. Hospital i.e. Barasat, Habra of North 24 Parganas and Bongaon, in the state of West Bengal at the time of the dengue outbreak.



**Figure 2.1.: Dengue outbreak work at affected region in West Bengal**

We got 782 dengue suspected patients. From suspected patients, 302 dengue confirmed samples were collected and categorized into three groups based on clinical symptoms. Among 302 confirmed dengue suspected patients, 176 were considered as DWOWS, 106 patients were considered as DWWS and 20 patients were considered as SD. DWOWS and DWWS are considered as Nonsevere dengue infection. Additionally, 30 other febrile illness (OFI) and 30 healthy donors (HD) were included in this investigation as control individuals. The plasma was collected for the entire study and stored at  $-20^{\circ}\text{C}$  until future study.

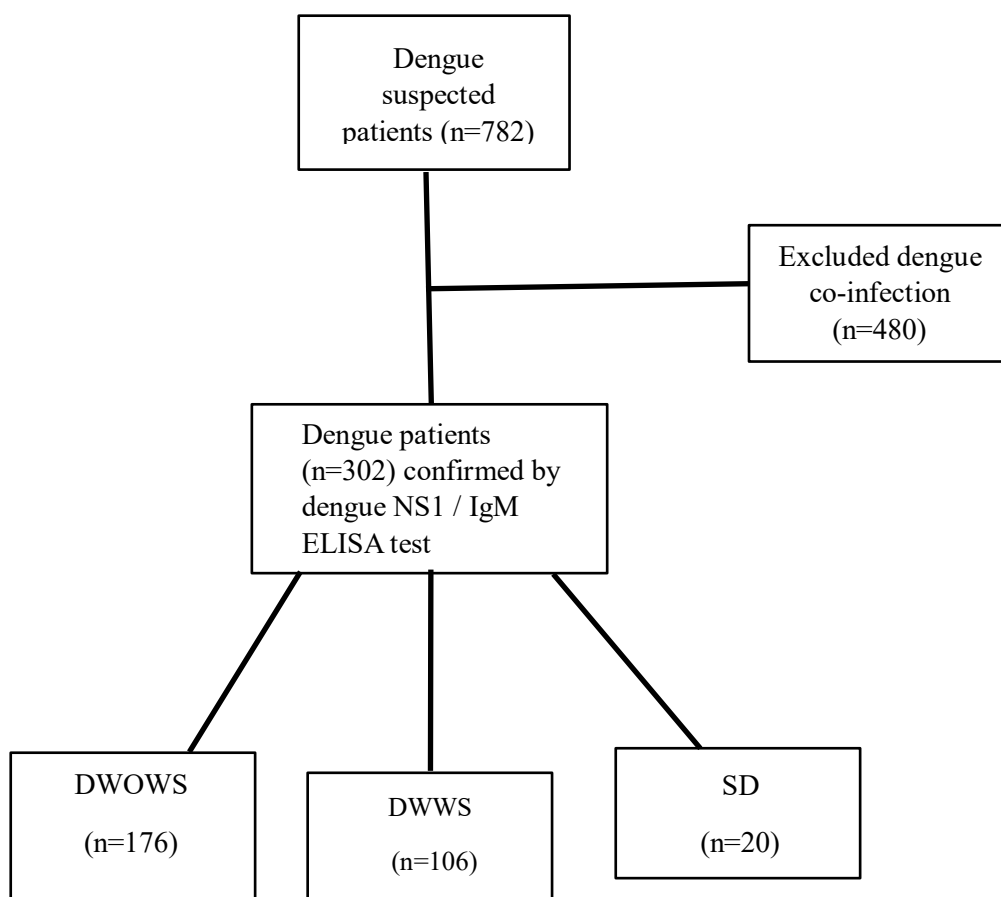


**Figure 2.2. Diagram of participates evaluated and enrolled in this study**

### **2.3. Quantification of Biochemical parameters**

To characterize the pathophysiological condition of the study subjects a detailed biochemical analysis of the blood samples was measured using a standard autoanalyzer (ERBA Model No- EM360). These included Serum glutamic oxaloacetic transaminase (SGOT)/ Aspartate transaminase (AST), Serum glutamic pyruvic transaminase (SGPT)/Alanine transaminase (ALT), globulin (GLB), albumin (ALB). Additionally, WBC (White Blood Cell) count, RBC (Red Blood Cell) count, hematocrit (HCT), and platelet (PLT) count, were measured by using Automated Cell counter (SYSMEX Model No- KX100). Following the manufacturer's instruction manual, The tests were accomplished. All the samples were tested in triplicates and the mean value was taken for analysis. These data typically involved plotting patient data on a chart i.e. Dengue nomogram to determine the risk of severe and nonsevere dengue-infected patients. The nomogram incorporated vomiting, NS1 levels, platelet count, and AST levels as key parameters to calculate a severity score for dengue-infected patients [216].

**2.4. Dengue viral load determination**

DENV-infected individuals in the febrile phase were chosen for real-time PCR-based viral RNA quantification in order to measure the viral burden. In summary, 140 µl of samples of serum were subjected to viral RNA extraction using a Qiagen Viral RNA kit. Taqman-based Real-Time PCR was used to measure the dengue virus load in the patient's sera (Genome Diagnostic Pvt. Ltd.) [186]. Reagents and enzymes for both the specific amplicon's direct detection in the fluorescence domain FAM (fluorescent 6-carboxyfluorescein) and the specific amplification of the Dengue genome are included in the kit's Specific Master Mix. The gene load may be measured according to the external positive standards provided in the kit. PCR was conducted in real time by using the ABI-Prism (7500) instrument.

The immunological pathophysiology of several diseases, such as dengue, measles, chronic hepatitis, persistent viral infections, and malaria has been linked to circulating immune complexes (CICs). These complexes, formed by the binding of antigens to antibodies, can trigger a cascade of inflammatory responses that contribute to tissue damage and disease progression. To elucidate the specific role of CICs in dengue infection, researchers have conducted studies exploring the formation, composition, and biological effects of these complexes in the context of dengue pathogenesis. By understanding the mechanisms underlying CIC-mediated immune responses, scientists aim to identify potential therapeutic targets for mitigating the severity of dengue illness.

**2.5. Quantification of Circulating Immune Complexes**

The polyethylene glycol precipitation method of Creighton was used to extract the immune complex from the plasma of dengue patients as well as healthy control [187]. In summary, the plasma was diluted 1:3 ratio with 0.1 M borate buffer at pH 8.4. It was then combined with 2 ml of 4.16% PEG 6000 in borate buffer [4.16 gm PEG MW-6000 dissolved in 100 ml borate buffer saline (BBS)] and incubated for one hour at 4°C temperature. The turbidity caused by the precipitation of CIC in the PEG-containing tube was determined at 450 nm using a spectrophotometer, which was compared to the absorbance of the control sample that contained borate buffer.

The outcome was given as the PEG-index, which was obtained using the formula below.

PEG index = 
$$\frac{\text{Absorbance with PEG}}{\text{Absorbance with BBS}} \times 1000$$

## **2.6. Gradient gel electrophoresis and SDS-PAGE analysis used for Characterization of CICs**

Serum was incubated with 8% PEG 6000 for a whole night at 4°C in order to extract circulating immune complexes from it. After removing the supernatants, the precipitates were rinsed and resuspended in 3% PEG in PBS (pH 7.2), and they were centrifuged once more at 13,000 rpm for 20 minutes at 4°C. After that, the precipitates were dissolved in equal parts of PBS, the supernatants were removed, and the mixture was kept incubated for an hour at the temp of 37°C [188]. After the incubation period, 7.5% SDS-PAGE was used to analyze the complexes. For 3.5 hours, the isolated patient CIC was exposed to a continuous voltage of 70 V. After 20 minutes of incubation in coomassie staining, the gel was destained and photographed. Using a protein ladder, the molecular weight of the unidentified patient proteins CIC was determined based on the relative mobility of the proteins.

Moreover, By using denaturing gradient gel electrophoresis, bands of protein were separated. In conclusion, 50µg of the CICs solution was used for the electrophoresis, and 5%–15% of an SDS PAGE gradient gel was created, which was run for 1.5 hours at a fixed voltage of 110V. Coomassie brilliant blue stain was used to visualize the protein bands in the gel [189].

## **2.7. Sample preparation for affinity purification**

Different categories of DENV patients' plasma samples i.e., Severe and Nonsevere were pooled down separately and CICs were precipitated by a 50% saturated solution of ammonium sulfate as described by [190]. After that, the samples were dialyzed for 48 hours at 4°C using Dialysis tubing (Sigma-Aldrich) and repeated 1000-ml PBS changes. In order to make it easier to detect low abundant proteins, high abundant plasma proteins were eliminated using depletion column resins. This method followed the manufacturer's directions and involved utilizing the Albumin Depletion kit (Pierce-85170) to remove highly abundant proteins like albumin. Albumin-depleted samples were treated with Glycine—HCL buffer to dissociate the antigen-antibody complex [191, 192]. After that, the acid-dissociated CICs were affinity-purified for 45 minutes at room temperature (RT) using an equilibrated Protein A Sepharose 4B column (Invitrogen, USA). The glycosylated CICs antigenic fraction was purified by subjecting the antibody-free CICs antigen fraction to an m-phenyl boronic acid column (Sigma) for an overnight period at room temperature [192, 193]. After being eluted with a solution of Taurine-NaOH (50 mM, pH 8.7), the Glycosylated Fractions were dialyzed using Dialysis Tubes (Sigma-



Aldrich) and continuous 1,000 ml PBS exchanges for 24 hours at 4°C [9]. The Lowry technique was used to measure the protein content.

The Glycated Fractions were dialyzed using Dialysis Tubing (Sigma-Aldrich) and repeated 1,000 ml PBS changes for 24 hours at 4°C after being eluted with 50 mM Taurin-NaOH solution, pH 8.7 [194]. Protein concentration was measured by the Lowry method [195].

## **2.8. Zip Tipping & LC-MS/MS**

After being dried using centrifugation of speed-vacuum, protein samples were dried after being resuspended in 40 µL of 0.1% formic acid and eluted with acetonitrile again. The specimens were replenished with 0.1% formic acid (15 µl). The various peptides in the polypeptide solution were isolated using nano-LC prior to MS. Using the LC 1200 system [ Easy-nano, Thermo Scientific] connected to a mass spectrometer [Q Exactive Plus Orbitrap, Thermo Scientific], peptides were examined by electrospray ionization mass spectrometry. Six microliters of tryptic digested peptide were briefly placed onto a PepMap 100µm × 2 cm, nanoviper C18, 5µm, 100A nano-precolumn (Thermo Fisher Scientific Acclaim). The peptides were separated using a linear gradient of water, 0.1% formic acid (v/v) 80% acetonitrile in a nano column of HPLC (100A, 75µm × 50 cm, ES 803 PepMap RSLC C18 2µm). The samples were then sprayed with ion into MS with a spray-voltage (1.90KV) and 300°C of capillary temperature. Additionally, Proteome Discoverer Software 2.2 (Thermo Scientific) was used to analyze raw data and identify proteins of interest. The following criteria were applied: Mass values: Max Missed Cleavages: 2, Monoisotopic, SequestHT Uniprot Human database; database; Precursor mass tolerance: 10 ppm, Protein mass: Unrestricted, Fragment mass tolerance: 0.05Da. Variable modifications: Oxidation (M). The label-free quantification option was chosen when conducting searches [196]. Via the PRIDE member repository, the proteomics data acquired by liquid chromatography-mass spectrometry (LC-MS/MS) were submitted to the Proteome-Xchange-Consortium. Proteome Xchange offers data under the identifier number PXD051713.

## **2.9. SDS-PAGE and Western blotting**

To validate the identification of upregulated dengue severity biomarkers, the expression of VTN and MASP-1 were validated with western blot analysis. Thirty micrograms of affinity-purified CIC antigens from Dengue patient plasma were electrophoresed in SDS PAGE. The samples were run on a 7.5% resolving gel that was prepared with 1.5M Tris-HCl (pH-8.8),

30% acrylamide and bisacrylamide solution, 10% SDS, 10% APS, and 5 $\mu$ lTEMED. Mini protean tetra cells (Bio-Rad, USA) were used for the electrophoresis, and the electrophoresis buffer (Tris 0.025M, glycine 0.19M, and SDS 0.1%) was used. Using monoclonal biotin-tagged VTN anti-human antibody (BIOSS, USA) and biotin-tagged MASP-1 (Mybiosource, San Diego, USA), a Western blot was conducted. Subsequently, HRP-avidin anti-human IgG secondary antibody monoclonal IgG (1:1000) (Sigma-Aldrich, Cat#: A0170) was applied, and it was visualized by using DAB substrate kit (Pierce, USA) [197].

## **2.10. Determination of Circulating Proteins Titers**

In 1971 and 1972, the ELISA technology was initially introduced. It is based on the useful theories and research of Engvall and Perlmann, who provided a methodology for determining the level of immunoglobulin G in human serum [198]. The procedure entails adding sera/plasma for analysis after the suggested antigen /antibody has been bound in a solid phase [199]. Circulating proteins like TSP-1, VTN, and MASP-1 were involved in DENV pathogenesis [200, 201]. To evaluate their levels of TSP-1, VTN, and the key components of the MBL pathway i.e. MASP-1 in DENV illness, stored plasma of DENV patients were thawed at room temperature, and levels of TSP-1, VTN, and MASP-1 were evaluated using standard ELISA kits (Ray Biotech and Fine test). The tests were carried out as per the manufacturer's instructions. The sample used for this assay included HD and the patient with Severe dengue, Nonsevere dengue, and OFI.

## **2.11. Protein Network Analysis**

A comprehensive analysis of protein networks was carried out in order to clarify the functional connections between the identified proteins. First, the human gene symbols that matched the proteins found by LC-MS/MS analysis were carefully chosen. After that, these gene symbols were added to the STRING database (version 11.0), which is a well-known resource for creating useful protein association networks. Interactions and linkages between the proteins of interest were deduced by utilizing STRING's large knowledgebase and computational techniques, which offered important insights into their possible functional interplay [202]. A gene ontology (GO) enrichment study was carried out to examine these protein networks' biological importance in more detail [203]. In order to provide light on the possible cellular roles and pathways involved, this research sought to discover biological process phrases that were over-represented among the proteins under study.

### **2.12. Nitrocellulose membrane selection**

Nitrocellulose is commonly used as a membrane for strip development (i.e. NCM). Easypack membrane kit device was made available by Advanced Microdevices Pvt. Ltd., based in Ambala, Haryana, India. The package includes 8 $\mu$ m (CNPF-SN12-L2-H50), 10 $\mu$ m (CNPF-SN12-L2-H50), 12 $\mu$ m (CNPF-SS12-L2-H500, and 15 $\mu$ m (CNPC-SS12-L2-H50) NCM pore sizes, which were utilized during the standardization procedure. Because the NCM pore size influences how fluid flows through the strip, the porosity of the strip is important. Flow time is a crucial morphology for choosing NCM with the right size of pores since it allows us to examine the flow time of various porosities of the NCM lump combined on the strips.

### **2.13. Sample-pad, conjugate-pad, and absorbent-pad selection**

For developing a lateral flow assay, we used different components like a Conjugate pad (glass fiber; GFB-R7L, GFB-R4), Sample pad (Cellulose fiber; PT-R7 and PT-R5), and Absorbent Pad (Cellulose; AP080 and AP045), procured from Advanced Microdevices Pvt. Ltd. Ambala, Haryana, India.

### **2.14. Assembly of the immunostrip for the detection of Dengue severity**

The Lateral Flow Immunoassay (LFIA) strip is a composite element that has a plastic backing that has been laminated. Plastic backing laminate (4 × 25 mm) requires three elements on the surface, every component has distinct characteristics and attributes and is essential to the test process's performance. The first component is the sample pad, different materials like cellulose, glass fibers, etc. are used to produce sample pads. The sample pad sheet (4 × 14 mm) adhered to the backing laminate so that it overlapped the conjugate pad. The sample pad receives the sample, retains it while forwarding it to the conjugate pad, and then releases it to the NCM. The conjugate pad maintains the stability of the protein bioconjugates throughout LFIA's shelf life. The conjugate pad should release the bioconjugate consistently and efficiently during the LFIA analysis. Because of its advantages in terms of stability, capillary flow, ease of fabrication, and high fluid holding capacity, glass fiber is the material of choice for the conjugate pad. The conjugate pad is normally dipped in the bioconjugate mixture and then dried in preparation for installation on the LFIA strip. Using a paper cutter, a sheet of the conjugate pad (4 × 2 mm) was cut, the adhesive label on the sample pad side was removed, and the conjugate pad sheet was assembled on the backing laminate with a 2 mm overlap on NCM (nitrocellulose membrane). The membrane used for LFIA strip development, or NCM is

usually nitrocellulose. It has several advantages, such as inexpensive cost, strong mechanical properties, high capacity for binding proteins, simplicity in handling, effective capillary flow, etc. This section of the LFIA assembly is where the actual analysis is done. Different proteins have been immobilized on the surface of the control and test parts of NCM as detection markers. On the other side of the strip, the absorbent pad sheet ( $4 \times 19$  mm) adhered in a similar pattern. Attached to the opposite end of the strip, the absorbent pad was placed with a 2 mm overlap at the NCM. Because the absorbent pad acts as an engine to move fluid from the strip to the end, this overlap is an important consideration. The strip must be dried as soon as the replacement kit packet is received since any moisture that has been absorbed or adsorbed onto the kit's component surfaces could interfere with the LFIA process. If moisture is present, the fluid may seep throughout the pad, altering the flow pattern. Following the placement of the required parts on the plastic backing laminate, the sheet was cut into strips that were 4 mm wide.

### **2.15. Preparation of Gold nanoparticle conjugated antibody**

We used a Gold Conjugated Kit (40nm, 200D, ab154873) for the preparation of Gold conjugated Antibody. Stock antibody (Vitronectin Monoclonal Antibody) was diluted with the Gold antibody diluent provided in the kit to 0.1 mg/ml. For each reaction in a clean 1.5 ml microfuge tube 42  $\mu$ l of Gold reaction buffer was added followed by 12  $\mu$ l of diluted antibody. 45  $\mu$ l of the mixture was added to a vial of Gold. This was allowed to stand at room temperature for 15 minutes. Finally, 5  $\mu$ l of EL Gold Quencher was added to yield 50  $\mu$ l of 20 OD conjugate. To confirm the successful conjugation of the antibody to the gold nanoparticles, UV spectra of both the unconjugated gold nanoparticles and the antibody-conjugated gold nanoparticles were analyzed individually.

### **2.16. Control line and test line optimization for AuNPs**

The components, such as an absorbent pad at the plastic backing laminate that has been preassembled with NCM, are assembled according to the standard operating protocol for LFIA development. Initially, standardization was done using a laminated NC membrane. Initially, the NC membrane was dried out for 20 minutes at 55°C in a hot air oven. One microlitre of various concentrations of the capture antibody (Goat Anti-Mouse IgG Antibody, #31160 Invitrogen) was used for the control line optimization, and two lectins (MAA, vector lab-L-1310) and DSA, vector lab-L-1180) in varying concentrations were used for the test line optimization. The NCM was then dried at room temperature for the entire night in front of the

dehumidifier. After that microcentrifuge tubes were obtained. A microcentrifuge tube was prepared with different concentrations of the capture antibody (i.e., 0.25, 0.5, 1, and 2  $\mu\text{g}/\mu\text{l}$ ) and lined on the NCM. A microcentrifuge tube was prepared with different concentrations of lectins (i.e., 10, 5, 2.5, and 1.25  $\mu\text{g}/\mu\text{l}$ ) on the test line and lined on the NC membrane. A conjugated detection antibody (Anti-VTN mAb) in the form of a microcentrifuge tube was applied on the conjugated pad and left overnight at room temperature. An optimized lectin concentration was used for the detection of severe and nonsevere dengue-infected patients.

### **2.17. LFIA strips with Gold nanoparticles testing with clinical samples**

By loading human plasma from Dengue-infected patients, the viability of the generated immunostrips as instruments for determining the severity of Dengue infection was examined in triplicate trials. A sample pad containing 50  $\mu\text{l}$  of positive or negative human plasma was added to the case of strips where the conjugates were made up of AuNP-anti-VTN mAb. During the first five minutes of the test, capillary pressures led samples to move from the conjugate pad to the membrane, where they contacted the lectin test lines and control lines before entering the absorbent pad. The results were visually evaluated after thirty minutes. The color intensity of each strip's test and control lines was further measured using the Image J application. Sensitivity, specificity, and the intra- and inter-assay coefficient of variation (CV) were used to calculate the assay performance. To calculate the reproducibility of this assay, samples in triplicate from each set were assayed by two independent experiments. Further assay performance is validated through standard ELISA determining VTN titers of severe and nonsevere Dengue patients.

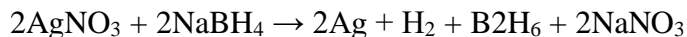
### **2.18. Synthesis of Silver nanoparticles.**

The unique properties of silver nanoparticles make them promising candidates for a wide range of applications, from medical devices to water purification. Silver nanoparticles have acquired significant scientific interest due to their exceptional optical, electrical, and catalytic properties. This study seeks to investigate synthesis methods for tailoring their characteristics to specific applications.

Sodium borohydride ( $\text{NaBH}_4$ ) was used as the reducing agent in a straightforward chemical reduction process to create AgNPs [204]. An Erlenmeyer flask was filled with 30.0 mL of 0.002 M aqueous  $\text{NaBH}_4$  solution, and 10.0 mL of 0.001 M  $\text{AgNO}_3$  solution was added while

vigorously swirling at a rate of around 1 drop per second. The solution was left to react until it changed from a pale yellow to a brighter yellow color.

One way to express the AgNO<sub>3</sub> reduction process is as



To stabilize the colloidal AgNPs, 1.0 mL of 0.02 M TSC solution was added at the end. Because of the repulsive interaction between the particles and the net negative charge on their surface, TSC stabilized the colloidal AgNP in a colloidal form. 0.1 M K<sub>2</sub>CO<sub>3</sub> was used to bring the pH of AgNP down to 9.0.

## **2.19. UV-Visible Spectroscopy**

For the initial characterization of synthesized nanoparticles, UV-vis spectroscopy is a highly helpful and trustworthy method. It is also used to track the synthesis and stability of AgNPs [205]. AgNPs have distinctive optical characteristics that cause them to interact strongly with particular light wavelengths. Additionally, UV-vis spectroscopy is quick, simple, sensitive, selective for various types of NPs, only requires a small amount of time for measurement, and lastly, calibration is not necessary for particle characterization of colloidal suspensions [206].

## **2.20. Transmission electron microscopy (TEM)**

To gain a deeper understanding of the structural properties of silver nanoparticles (AgNPs), transmission electron microscopy (TEM) is an indispensable tool. TEM allows for direct visualization of particle size, shape, and crystal structure, providing valuable insights into their physical and chemical properties. TEM was carried out using a JEOL (JEM-2100 HR WITH EELS) apparatus at an accelerating voltage of 80 kV after a drop of aqueous AgNPs on copper that had been coated with carbon-dried. Prior to loading on a specimen holder, TEM grid samples were dried and vacuum-stored in desiccators. AgNPs' particle size distribution was assessed utilizing the Model 963 GIF Quantum Imaging Filter System. Quantitative measurements of particle and/or grain size, size distribution, and morphology are obtained using the useful, popular, and significant TEM technique for the characterization of nanomaterials [207]. The distance between the objective lens and the specimen and the distance between the objective lens and its image plane mostly define the magnification of TEM. Compared to SEM, TEM has two advantages: higher spatial resolution and the ability to

conduct extra analytical measurements [208]. Therefore, sample preparation is extremely important in order to obtain the highest-quality images possible.

## 2.21. Preparation of Silver nanoparticle conjugated antibody

The preparation of antibodies coupled with silver nanoparticles has the potential to revolutionize diagnostics. These conjugates provide early illness diagnosis and surveillance by enabling the detection and quantification of biomarkers in a range of biological samples. To 10.0 mL of AgNP solution, an additional 60.0  $\mu$ L of 1.0 mg/mL Anti-MASP-1 Ab was added dropwise. Following a one-hour period of gentle agitation at 37  $^{\circ}$ C, monodentate or bidentate bonding allowed Ab to bind to the colloidal AgNP surface. After adding 2.5 milliliters of 5.0 wt% BSA solution to the combination, which blocked the non-coated colloidal AgNP surfaces for 15 minutes, the mixture was centrifuged for 20 minutes at 6000 rpm. After two rounds of washing, the supernatant unconjugated antibody was removed by centrifugation at 6000 rpm for 20 minutes, yielding colloidal AgNP conjugated Ab in soft pellet form. Once more, the pellet was cleaned using PBST solution. At last, Ag- conjugated Ab was reconstituted in 50.0  $\mu$ L of PBS (pH 7.4) solution and kept cold for storage [209].

### Different types of protein interaction with nanoparticles:-

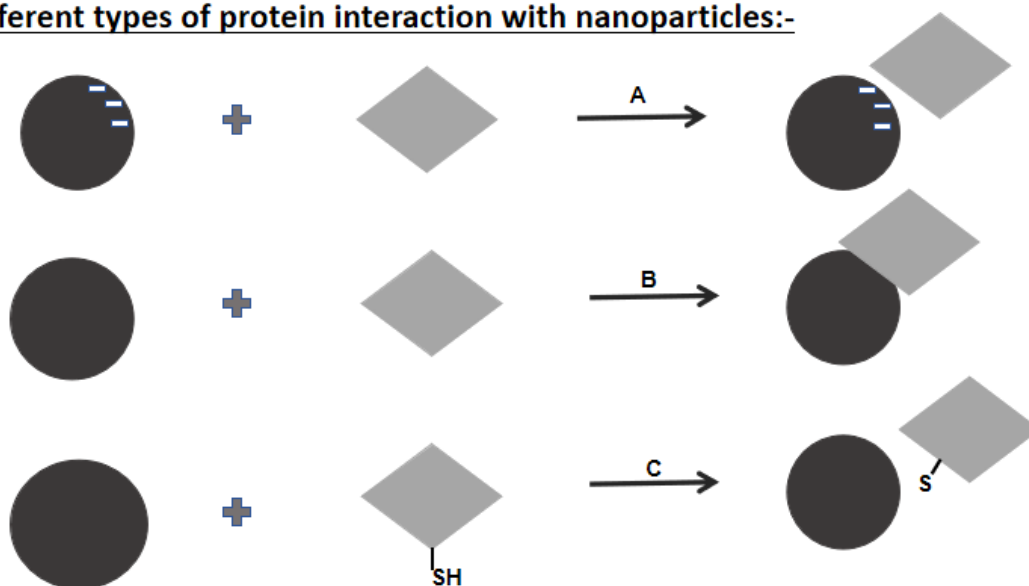


**Figure 2.3. Protein can bind with NP through several types of interactions : A- Electrostatic, B - Hydrophobic, C - Dative bonds.**

## 2.22. Dynamic Light Scattering (DLS)

A useful method for precisely determining the size distribution of silver nanoparticles is Dynamic Light Scattering (DLS). By measuring a particle's Brownian motion in solution, DLS enables us to determine its hydrodynamic size and comprehend the homogeneity of the nanoparticle population. The stability, biocompatibility, and molecular interactions of silver nanoparticles are significantly influenced by their surface charge. Through the measurement of the particles' electrophoretic mobility, DLS can be utilized to infer information regarding the colloidal stability of the surface charge. For the dynamic light scattering (DLS) experiments, a Malvern Nano ZS light scattering equipment (Malvern Instruments Ltd., Malvern, UK) was employed. Every 10s, 15 acquisitions were made in order to measure the time-dependent autocorrelation function of the photocurrent. A 633 nm laser was used to illuminate the materials, and an avalanche photodiode was used to gauge the light's intensity as it was reflected at a 173 degree angle. The manufacturer's software was used to determine the hydrodynamic mean diameters (dz), polydispersity (PDI), and distribution profiles of the samples. The samples listed here were measured: 1) AgNPs that have been citrate-stabilized 2) Coated AgNP with an antibody and incubated for 1 hour at 37°C with gentle, constant stirring 3) An antibody-coated AgNP was incubated for two hours at 37°C while being gently and continuously stirred. For the investigation of biological activities utilizing radiation scattering techniques, the physicochemical characterization of produced nanomaterials is crucial [210]. DLS is capable of measuring the size distribution of tiny particles in suspension or solution on a scale ranging from submicron to one nanometer. A technique that relies on light and particle interaction is dynamic light scattering. This technique can be used to measure tiny particle size distributions, particularly in the 2- to 500-nm range [211]. The most often utilized method for the characterization of nanoparticles is DLS. DLS primarily depends on Rayleigh scattering from the suspended nanoparticles to quantify the light scattered from a laser that passes through a colloid. Next, the time-dependent modification of scattered light intensity is examined, and the hydrodynamic size of the particles can be calculated [212]. Particle size and size distributions are the main uses of DLS in aqueous or physiological fluids. It's possible that Brownian motion has an impact on why the size acquired from DLS is frequently larger than that from TEM. The average diameter of nanoparticles scattered in liquids can be determined using the nondestructive technique known as DLS. It offers the unique benefit of simultaneously probing a high number of particles, but it has a number of sample-specific restrictions [213].



### **2.23. Density gradient centrifugation Method**

To produce pure and precisely defined populations of nanoparticles by sorting particles according to their density, is the density gradient centrifugation method, a useful method for separating silver nanoparticles from impurities like a complicated heterogenic mixture of particles.

One of the most significant separation methods utilized extensively in cellular and molecular biology as well as colloid science is centrifugation. Gravity causes items thicker than liquids to settle on their own. This procedure may take a very long time; for minuscule particles (such as in nanoparticles). The particles won't settle at all when exposed to thermal energy. Still, Particles can travel radially away from the axis with the assistance of centrifugal forces.

Density gradient centrifugation is one of the methods, where particles are spun in a liquid column that supports a density gradient (such that the buoyant force changes inside the tube). Carefully layering liquids with varying concentrations on top of one another can produce a density gradient, which causes the density of the tube to grow from top to bottom. This method has two variations: (i) isopycnic centrifugation and (ii) rate zonal centrifugation.

Successful applications of isopycnic centrifugation for diameter-dependent separation have been made. In the isopycnic method, the item densities that need to be separated must lie between the gradient's lowest and maximum values for the column. On top of the gradient, the sample is typically applied as a thin layer. Only when the density of each particle matches the gradient will it settle at that location in the centrifuge tube; only then will it stay there. Consequently, the isopycnic method divides particles into zones based only on the variations in their buoyant densities. Though longer centrifugation periods do not further affect the positions of the particles, the run time must be adequate for the particles to separate to their isopycnic points. The sample density in the rate zonal centrifugation (RZC) process is higher than that of the gradient's greatest density part. A tiny layer of the sample is put to the tube's top, and when it is centrifuged, the particles start to settle into distinct zones based on their size, shape, and density as they go along the gradient. However, the separation must end before the divided particles reach the tube's bottom, in contrast to the isopycnic approach.

Particles from distinct zones can be easily removed using a pipette syringe or needle in both the RZC and isopycnic procedures.

Pure sucrose was dissolved in deionized water and stirred to create the sucrose gradients. Thus, from bottom to top of a test tube, four sucrose solutions with volumes of 2 ml and fractions of 10, 20, 30, and 40% were placed on top of one another in 15 ml vials. Next, using a syringe, load 4 ml of the colloidal silver nanoparticle solution onto the prepared sucrose gradient. Centrifuge for 2 hours at 5°C at 6000 rpm. Subsequently, the distinct layers were gathered using a syringe, cleaned three times in deionized water, centrifuged to eliminate any leftover material, and then distributed in deionized water for subsequent research [214].

## **2.24. Agarose Gel Electrophoresis assay**

By comparing the migration patterns of silver nanoparticles, antibody-conjugated silver nanoparticles, and binding with targeted analytes present in the sample on agarose gel, we can estimate the efficiency of the conjugation process. This information is valuable for optimizing the preparation of antibody-conjugated nanoparticles and conjugated with targeted analytes as well.

The technique known as agarose gel electrophoresis (AGE) assay is frequently used in the study and separation of macromolecules such as DNA and RNA. Nevertheless, its usefulness goes beyond biomolecules because it works well for describing other types of nanoparticles, such as silver nanoparticles (AgNPs) [215]. The AGE concept is simple to understand. To adjust pore size, a porous matrix made from seaweed called agarose gel is created in different quantities. Charged particles migrate through the pores in the gel according to their size, shape, and charge when an electric field is applied across it. Smaller particles go through the gel more quickly and easily through the pores. Bigger particles move more slowly and face greater resistance. The agarose gel electrophoresis, or AGE, test has been widely used to characterize mixtures of synthetic or pure NPs. Firstly, an agarose gel of 0.3% was prepared. 0.3% agarose gel contains 0.3 gm agarose powder in 100ml 0.5x TBE containing 0.2% SDS. 0.5x TBE (Tris-Borate-EDTA) was used as the electrophoresis buffer (EB) and 1% SDS was used as a stabilizing agent. The various AgNPs were combined with a loading buffer (LB) (ratio 1:1) which contains glycerol (30% m/m). AgNPs and LB were combined before being injected into the wells (15  $\mu$ L of sample volume per well). The power supply was attached to the electrophoresis cell, which was operated for 30 minutes at a constant voltage of 150 V, or a potential gradient of 10 V/cm.

### **2.25. Control line and test line optimization for AgNP**

The components, such as an absorbent pad at the plastic backing laminate that has been preassembled with NCM, are assembled according to the standard operating protocol for LFIA development. Initially, standardization was done using a laminated NC membrane. Initially, the NC membrane was dried out for 20 minutes at 55°C in a hot air oven. One microlitre of the capture antibody, Goat Anti-Mouse IgG Antibody (#31160 Invitrogen), and various test antibody concentrations, such as Anti-MASP-1 Ab (PA5-119268, Invitrogen), were lined up on the NCM and allowed to dry overnight at room temperature in front of the dehumidifier. Following that, tubes for microcentrifuges were taken. In a microcentrifuge tube, test antibodies at different concentrations (i.e., 5, 4, 3, 2, and 1 µg/µl) were made and lined on the NC membrane. Two microgrammes of gold-conjugated detection antibody (Anti-MASP-1 Mab) were then applied to the conjugated pad and left overnight at room temperature. With an optimal test antibody concentration, the LFIA strip is also utilized for the identification of patients with dengue infection, both severe and nonsevere.

### **2.26. LFIA strips with Silver nanoparticles testing with clinical samples**

The usefulness of the produced immunostrips as tools for assessing the severity of Dengue infection was investigated in triplicate experiments by loading human plasma from individual infected patients. A sample pad containing 50 µl of positive or negative human plasma was added to the case of strips where the conjugates were made up of AgNP-anti-MASP-1Mab. Capillary pressures caused samples to travel from the conjugate pad to the membrane, where they met the test lines and control lines and finally into the absorbent pad during the first 5 min of the test, and the findings were visually assessed within 30 min. The color intensity of each strip's test and control lines was further measured using the Image J application. Sensitivity, specificity, and the intra- and inter-assay coefficient of variation (CV) were used to calculate the assay performance. To calculate the reproducibility of this assay, samples in triplicate from each set were assayed by two independent experiments. Further assay performance is validated through standard ELISA determining MASP-1 titers of both severe and nonsevere Dengue patients.

### **2.27. Quantification of color intensity**

The program ImageJ 1.49 v was used to quantify the intensity of the lines. After converting the photos to RGB format, the proper color was chosen. Software enabled selection of an area

whose intensity was measured along with the area, minimum, and maximum values. A plot profile throughout the illuminated region was created using a rectangle that was drawn. Column averages of the data to the left and right of the location were used to create a baseline. Depending on the exposure times used, the signals were scaled appropriately.

## **2.28. Statistics**

All graphs were plotted in Graph Pad Prism statistical program (Graph-Pad Software Inc., San Diego, CA), and Microsoft Excel 2016. Initially, each data set underwent to a normality test using the D'Agostino and Pearson normality tests. Analyses using a single nonparametric ANOVA (i.e. Kruskal–Wallis test) and t-test (Mann-Whitney-Test) were performed. Data representation was done by Box plots to show Tukey whiskers values and *P* values below 0.05 were considered statistically significant. Values for each set of experiments were analyzed by calculating their respective mean, medians, and Standard error of the mean. A cut-off value of circulating proteins (MASP-1 and VTN, TSP-1) was determined by using the Youden index. Efficiency was analyzed using receiver operating characteristic (ROC) curves. Values for specificity and sensitivity were computed for the same at various thresholds. Also computed were statistically significant areas under the curve (AUC) values. The Spearman's correlation was applied. Using CombiROC (area under the curve), the most efficient parameter combinations with the corresponding sensitivity, specificity, and accuracy were selected.

# CHAPTER - 3

## Results

### 3.1. Demography & Clinical parameters

In this study, 302 confirmed dengue patients were enrolled out of 782 suspected patients. They were confirmed by the NS1/IgM test. On the basis of the clinical symptoms, 176 patients were included in DWOWS, 106 patients were included in DWWS and 20 patients were included in the SD category. According to WHO guidelines, classification was based on the clinical history and characteristics of a subset of patients. As shown in table 3.1. the Mean  $\pm$  SEM age of dengue patients with DWOWS was (31.07  $\pm$  1.09) years with male preponderance; 101 out of 176 (57.38%) were male and 75 (42.61%) were female. For DWWS, the Mean  $\pm$  SEM of age was (34.29  $\pm$  1.25) years. Among the patients infected with DWWS, approximately 66.98% (n=71) were male and 33.01% (n=35) were female. Among the SD patients, approximately 65% (n=13) were male and 35% (n=7) were female and the age of Mean  $\pm$  SEM was (38.25  $\pm$  2.69) years. Among the patients with OFI, 66.66% (n=20) patients were male 33.33% (n=10) patients were female and the Mean  $\pm$  SEM of the age of OFI was (34.77  $\pm$  2.81). For healthy donors, the males and females were 50% (n=15) and the Mean  $\pm$  SEM of age was (36.37 $\pm$  2.09). All patients observed (respectively DWOWS, DWWS, SD, OFI) had fever, myalgia (61.36%, 41.5%, 40%, 56.66%), vomiting (32.38%, 23.58%, 50%, 6.66%), Rash (34.09%, 16.47%, 15%, 0%), abdominal pain (29.54%, 23.58%, 50%, 0%) hemorrhage (0%, 4.71%, 15%, 0%).

**Table 3.1.: Demographic study and clinical parameters of enrolled subjects.**

	DWOWS	DWWS	SD	HD	OFI
<b>Total number of population</b>	(n=176 )	(n=106 )	(n=20)	(n=30)	(n=30)
<b>Male (%)</b>	57.38 %	66.98 %	65 %	50 %	66.66 %
<b>Female (%)</b>	42.61 %	33.01 %	35 %	50 %	33.33 %
<b>Age (Mean <math>\pm</math>SEM)</b>	31.07 $\pm$ 1.09	34.29 $\pm$ 1.25	38.25 $\pm$ 2.69	36.37 $\pm$ 2.09	34.77 $\pm$ 2.81
<b>Clinical Parameters</b>					
<b>Day of Fever (Mean <math>\pm</math> SEM)</b>	4.54 $\pm$ 0.18	4.81 $\pm$ 0.2	5.2 $\pm$ 0.32	-	4.13 $\pm$ 0.56

	DWOWS	DWWS	SD	HD	OFI
<b>Rash (%)</b>	34.09 %	16.47 %	15 %	-	0 %
<b>Abdominal Pain (%)</b>	29.54 %	23.58 %	50 %	-	16.66 %
<b>Nausea (%)</b>	37.5 %	25.47 %	45 %	-	43.33 %
<b>Vomiting (%)</b>	32.38 %	23.58 %	50 %	-	6.66 %
<b>Fluid accumulation (%)</b>	3.4 %	0.94 %	20 %	-	0 %
<b>Myalgia (%)</b>	61.36 %	41.5 %	40 %	-	56.66 %
<b>Headache (%)</b>	65.34 %	46.22 %	40 %	-	83.33 %
<b>Haemorrhage (%)</b>	0 %	4.71 %	15 %	-	0 %



**Figure 3.1.: Dengue outbreak work at affected regions in West Bengal (A)Phlebotomy for sample collection (B)Medical team visiting the affected area (C) Clinicians providing treatment guidelines to patients (D) Dengue patient with rash (E) USG showing Gall bladder thickening of affected patient (F) X ray showing fluid accumulation in dengue patient**

3.2. Laboratory parameters

The results of biochemical parameters of dengue-infected patients showed lower levels (median) of platelet (33000 X 103/ µl) in SD patients than DWOWS and DWWS. Further, a 5-fold increased C-reactive protein (CRP) was observed in SD as compared to patients with DWOWS, whereas almost 4.1-fold lower CRP was observed in DWWS compared to SD. Increased hematocrit (HCT) was observed in patients with SD compared to nonsevere dengue-infected patients (DWOWS and DWWS) whereas decreased levels of Albumin and globulin were observed in SD patients compared to nonsevere dengue-infected patients. Mann-Whitney analysis between Nonsevere and SD with respect to, platelet (p<0.0001), albumin (p<0.0001), globulin (p=0.0052), and hematocrit (p=0.2442) showed significant differences as shown in table 3.2.

Table 3.2: Basic laboratory parameter study of enrolled subjects

BiochemicalParameters	DWOWS	DWWS	SD	ANOVA analysis (p* value)	Mann-WhitneyTest (Nonsevere vs Severe) (p* value)
	Mean ± SEM	Mean ± SEM	Mean ±SEM		
Platelet (/µl)	152977 ± 4398	75236 ± 4441	40000 ± 4479	<0.0001	<0.0001
CRP (mg/l)	10.74 ± 2.10	13.15 ± 1.273	54.65 ± 6.29	0.0111	<0.0001
Albumin (gm/dl)	3.939 ± 0.04	3.582 ± 0.05	3.2 ± 0.09	<0.0001	<0.0001
Globulin (gm/dl)	3.203 ± 0.04	3.05 ± 0.05	2.77 ± 0.09	0.0007	0.0052
Haematocrit (%)	37.45 ± 0.52	37.67 ± 0.55	40.59 ± 1.47	0.1705	0.2442

Table shows biochemical parameter of dengue infected patients @ANOVA followed by Kruskal-Wallis test (K). Biochemical results showed the value of Mean ± SEM

3.3. CICs estimation by PEG index

For nonsevere, severe, and HD, the corresponding Mean ±SEM of the PEG index were 115.5 ± 6.891, 205.0 ± 10.13, and 62.77 ± 1.605 respectively. As a result, CICs in nonsevere were 1.84 times higher than in HD, and SD patients had 3.26-fold higher CICs than HD patients. An ANOVA comparison between the groups showed a statistically significant P value of less than 0.0001.

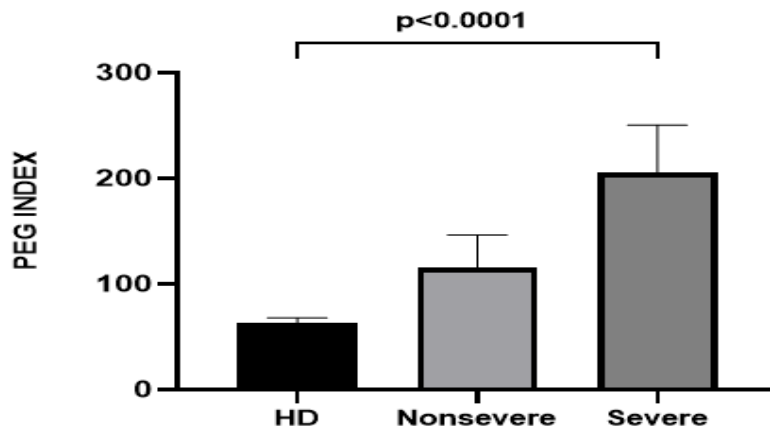


**Figure 3.2.:** Level of CICs in sera of Dengue WithOut Warning Sign (DwoWS), Dengue With Warning Sign (DwWS), and Severe Dengue (SD) patients. The horizontal line indicates the mean value. \*\*\*\* P<0.0001, significantly different from each category.

### 3.4. Affinity Purification of CIC antigens

Affinity purification is a powerful technique for the isolation of highly specific CIC antigens. A pooled Plasma sample that contained a combination of proteins was progressively purified and the concentration of proteins dropped as it was run through the columns.

Figure 3.3. (A) demonstrated the degree of purification of affinity-purified CIC in each category of dengue patients. Figure 3.3. (B) also showed the elution profile of affinity purification. The Elution profile describes how the target proteins separate from the other proteins during elution [217].

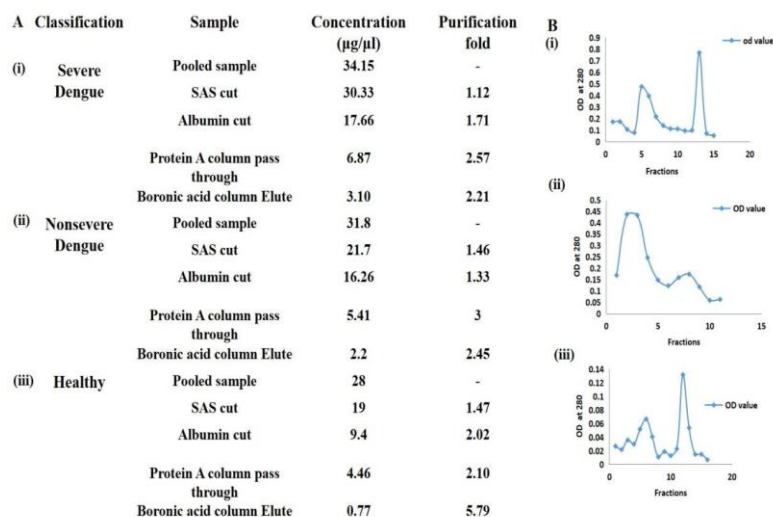


**Figure 3.3.:** (A) Purification fold of different categories of enrolled subjects (i) Severe dengue (ii) Nonsevere (iii) Healthy. (B) Elution profile of different categories of enrolled subjects (i) Severe dengue. (ii) Nonsevere dengue (iii) Healthy.



3.5. Plasma Proteomic Changes

To compare protein profiles across severe and nonsevere dengue infection, we isolated and processed plasma samples from dengue patients with varying clinical presentations. These samples underwent proteomic analysis, involving in-solution digestion followed by high-performance liquid chromatography-tandem mass spectrometry (nano LC-MS/MS) using a mass spectrometer (Q-Exactive Plus orbitrap). Samples were run in triplicate sets for each comparison: (i) severe vs nonsevere, allowing us to identify proteins with differential abundance between these groups.

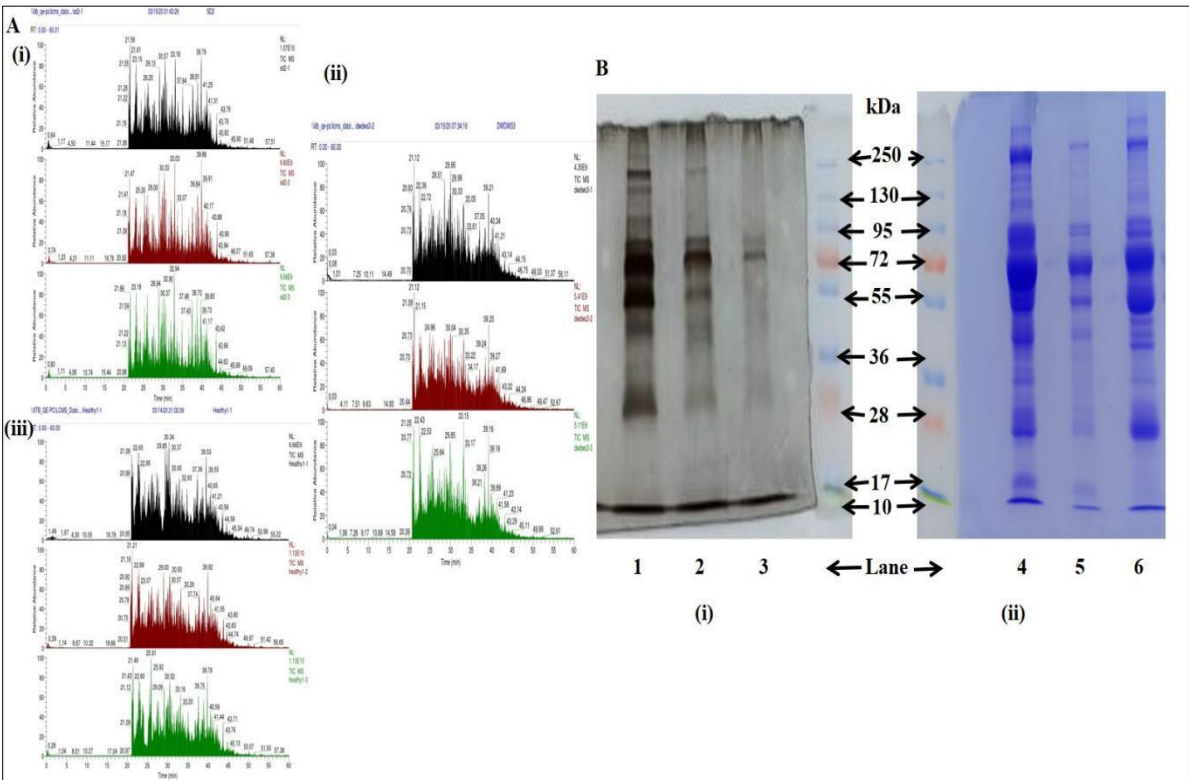


**Figure 3.4.:** (A) Mass spectrometric analysis of (i) Severe, (ii) Nonsevere and (iii) Healthy; data revealed list of up and down regulated proteins in severe dengue as compared to non severe dengue. Data submitted in PRIDE Database Project accession: PXD051713; B(i) 7.5 % SDS-PAGE profile of purified CIC antigens in lane 1 Severe; lane 2 Nonsevere; lane 3 Healthy, stained with Silver. D(ii) 7.5 % SDS-PAGE profile of purified CIC antigens in lane 4 Severe; lane 5 Healthy; lane 6 Nonsevere stained with coomassie.

Characteristics of different categories of dengue subjects are presented in **Table 3.3**. Of these 144 proteins were upregulated in severe cases compared to nonsevere cases, and 89 proteins were downregulated in severe cases as compared to nonsevere cases. This analysis examined the fold change, which represented the relative increase or decrease in abundance, of each identified protein across patient groups. This study aimed to pinpoint protein signatures

common to all groups in the experiment ( severe vs. nonsevere ). These potential biomarkers could serve as valuable tools for predicting dengue severity and, more importantly, differentiating its severity stages, leading to improved disease management strategies. Interestingly, several proteins, such as C-reactive protein, Apolipoprotein B, Alpha-2 macroglobulin, Complement C3, Complement C4A, Complement C4B, Plasminogen, ITIH4, Apolipoprotein A, were up-regulated (fold change >1) in severe dengue group. Some proteins like Haptoglobin, Alpha-1 acid glycoprotein, and Apolipoprotein E showed 2 times upregulation and lectin galactoside binding soluble 3 binding protein, Myosin reactive immunoglobulin, Complement component C8 (beta chain), Fibulin-1 showed almost 3 times upregulation in severe dengue as compared to nonsevere dengue. Ficolin-3 is also upregulated (fold change >1) in severe dengue infection compared with nonsevere which activates the complement system, which acts against dengue virus. Complement proteins such as C5, C4BPB, C3, C8, MASP-2, showed upregulation in SD patients. Some proteins showed downregulation (fold change <1) in Severe dengue cases. These were Apolipoprotein A, Antithrombin III, Fibrinogen alpha chain, Fibronectin -1, etc. Proteins such as Mannan binding lectin serine protease -1 (MASP-1), Vitronectin (VTN), and Thrombosondin-1 (TSP-1) were significantly up-regulated in severe patients with dengue infection as compared to nonsevere patients with dengue infection. In this study, we investigated the status of MASP-1, TSP-1, and VTN in dengue infection.

**Table 3.3.: Represented gene ontology terms associated with differential proteins in SD patients compared to non-severe dengue patients.**

Protein	Proteins regulation in dengue patient	Biological process	Associated molecules
Upregulated	144	Innate Immune response	C5, C4BPB, C3, MASP1, C4BPA, C1RL, CRP, GSN, APCS, CLU, FCN3, CFH, C7, C1QB, C8A, JCHAIN, C8B, C8G, CFH, C1QC
		Transport	APOM, APOA1, APOE, APOC1, LCAT, APOA2, CLU
		Coagulation	F10, PLG, F2, KLKB1, F5, VWF, FBLN1, ACTB, C4BPB, FBLN1, SERPINA1, HBB, TSP-1
		Inflammatory responses	ITIH4, CRP, APCS, VCAM1, F2, ORM2, HPR, APOA2, A2M, KLKB1, SERPINA2, SERPINA1
		Defense responses	GSN, PRDX2, HPR, CD5L, C1QB, C1QC, CRP, VCAM1, C3, MASP-1, FCN3, CFH, ITIH4, C5, F2, A2M, JCHAIN, KLKB1

Protein	Proteins regulation in dengue patient	Biological process	Associated molecules
Downregulated	89	Endocytosis	ACTB, VTN, FCN3, CD5L
		Opsonization	C3, MASP-1, FCN3
		Innate Immune response	C1R, ACTR3, GAPDH, PGLYRP2, APOA4, HPX, KRT16, FGB, FGA
		Cell adhesion	TGFB1, AZGP1, AMBP, LRG1, FGA, FGB, FGC, VCL, LRG1
		Defense responses	HPX, SERPING1, C1R, ACTR3, GAPDH, HP, APOA4, FGA, FGB, KRT16, PGLYRP2
		Coagulation	F13B, FGA, FGB, FGC, VCL, PROS, SERPIND1, SERPING, TSP-1

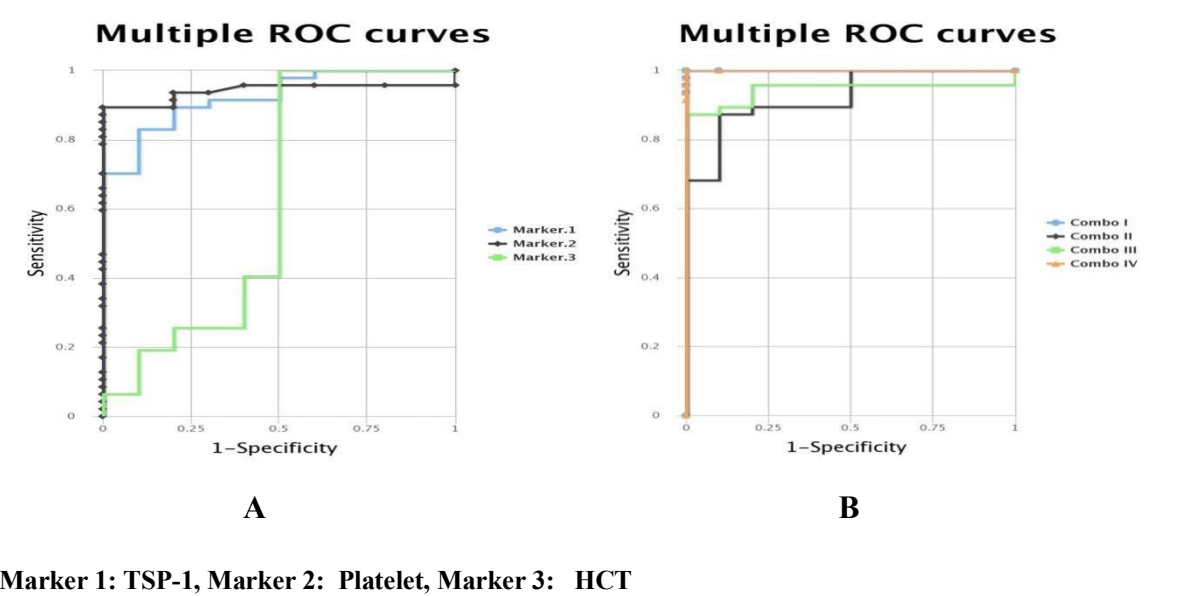
After that, We carried out a comparative study of the detected proteins' expression levels in several groups of dengue-infected individuals in order to confirm their diagnostic usefulness. Our aim was to determine whether these proteins could effectively differentiate severe cases from non-severe dengue infections.

### 3.6. Quantifying TSP-1 Protein Levels and CombiROC analysis

Decreased Thrombospondin-1 titers ( $P<0.0001$ ) were obtained in severe dengue infection. In vitro suppression of TSP-1 transcription in endothelial cells was observed during viral infections, leading to a reduction in TSP-1 protein accumulation in the extracellular matrix of endothelial cells [219]. TSP-1 levels may have decreased as a result of a comparable molecular reaction during dengue infection. Among patients with severe dengue infection, TSP-1 level is 2.14-fold lower in DWOWS, 2.14-fold lower in DWWS, and 3.92-fold lower in SD than in healthy donors (HD). TSP-1 level is upregulated in HD with “Mean  $\pm$  SEM” value of  $16109 \pm 1121$  ng/ ml as compared DWOWS ( $7519 \pm 557.9$  ng/ml), DWWS ( $7496 \pm 421.8$  ng/ml) and SD ( $4102 \pm 251.9$  ng/ml) (Fig. 3.5.). In addition, TSP-1 cutoff of 4818 ng/ mL with a promising AUC-0.9234 showed its potential to be a novel indicator of dengue severity. It was reported that increased consumption or insufficient production of TSP-1 may lead to impairment of the integrity of capillary and small vessels.



evaluated, is accessible at <http://CombiROC.eu> and was used to investigate the best marker combination. Based on the maximum area under the curve (AUC), sensitivity (SE), and specificity (SP), the ideal marker or marker combination is selected.



Marker 1: TSP-1, Marker 2: Platelet, Marker 3: HCT

Combo I : TSP-1 & Platelet, Combo II: TSP-1 & HCT, Combo III: Platelet & HCT, Combo IV: TSP-1 & Platelet & HCT

Figure 3.6. a–b Multiple receiver operating characteristic (ROC) curve as a function of sensitivity vs 1-specificity to compare the performance of markers and combos for TSP-1 PLATELET and HCT.

Table 3.4.: The performance of combination of biomarkers via receiver operating characteristic (ROC) curve analysis

TSP-1	0.923	0.830	0.9	0.786
Platelet	0.941	0.894	1.0	0.810
HCT	0.617	1.000	0.5	0.657
TSP-1 & Platelet	1.000	1.000	1.0	0.500
TSP-1 & HCT	0.923	0.872	0.9	0.715
Platelet & HCT	0.943	0.872	1.0	0.824
TSP-1 & Platelet & HCT	1.000	1.000	1.0	0.500

### **3.7. Individual Sample Analysis: Quantifying Protein Levels**

Apart from the LC-MS studies, we employed enzyme-linked immunosorbent assay (ELISA) to quantify the other upregulated proteins like MASP-1 and VTN in individual samples from various dengue groups: non-severe and severe. Notably, MASP-1 levels were significantly higher in the severe group (Mean  $\pm$  SEM:  $20.12 \pm 0.7427$   $\mu\text{g/ml}$ ) compared to the non-severe ( $9.713 \pm 0.4126$   $\mu\text{g/ml}$ ) whereas VTN levels were significantly lower in the severe group ( $920.2 \pm 69.39$   $\mu\text{g/ml}$ ) as compared to nonsevere ( $1679 \pm 50.89$   $\mu\text{g/ml}$ ) as shown in figure. Among patients with severe dengue infection, the MASP-1 level is almost 2.07-fold higher and the VTN level is 1.82-fold lower in SD than in nonsevere dengue infected patients. In addition, MASP-1 and VTN cut-offs of  $15.54\mu\text{g/ml}$  and  $941\mu\text{g/ml}$  with an encouraging AUC value of 0.8813 and 0.8730 indicated its potential to serve as novel dengue severity markers.

### **3.8. Evaluating Protein Biomarkers for Dengue Diagnosis: A Western Blot Approach**

Western blot analysis was employed to corroborate the proteomic identification of differentially expressed proteins. Pooled samples from severe and non-severe dengue patients were utilized for this experiment. Equal protein loading across lanes was verified using Ponceau staining. As anticipated from the proteomics data, Western blots demonstrated a clear overexpression of MASP-1 protein in the severe patient group compared to the non-severe group, whereas VTN showed three isoforms with different molecular weights as reported in (Poole-Smith BK,.. et al. 2014) [218] were downregulated in severe dengue infection as compared to nonsevere suggesting its potential as a biomarker for dengue severity. Using ImageJ software, we were able to determine the western blot's color intensity, which shows that individuals with severe dengue had about nine times higher color intensity than those with less severe dengue.

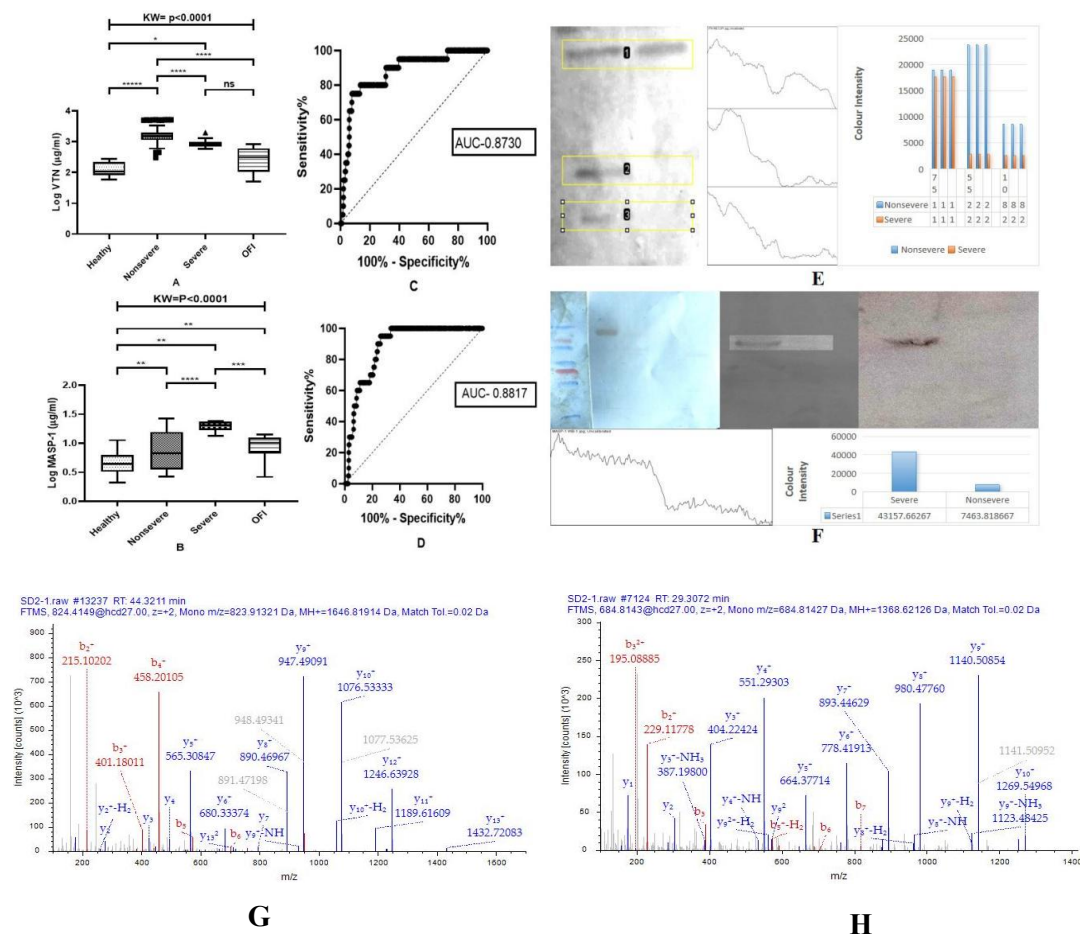


**Figure 3.7.:** A) Levels of VTN of Nonsevere and Severe, Healthy and OFI, B) Level of MASP-1 of nonsevere, severe, healthy and OFI. C) Receiver operating characteristics curve analysis of VTN level in Severe and Non-severe Dengue infected patients obtained the AUC=0.8730. D) Receiver operating characteristics curve analysis of MASP-1 level in Severe and Non-severe Dengue infected patients obtained the AUC=0.8817. E) Validation of VTN using western blotting image. (F) Validation of MASP-1 using western blotting image. G) MS-MS Spectra of Vitronectin (VTN). H) MS-MS Spectra of Mannan associated serine protease-1 (MASP-1).

### 3.9. Functional Data Analysis of differentially Expressed Proteins

To understand the biological processes impacted by the protein with altered abundance in severe dengue patients compared to non-severe patients we employed STRING analysis. Protein interaction networks were generated for a group comparison (severe vs. nonsevere) using the STRING database (**Figures 3.8 & 3.9**). Utilizing the identified proteins, we then conducted gene ontology analysis, which revealed changes in biological functions primarily associated with defense, inflammatory, and innate immune responses. Details of the up- and down-regulated proteins in a comparison group (severe vs. nonsevere) are provided in **Table 3.3**.



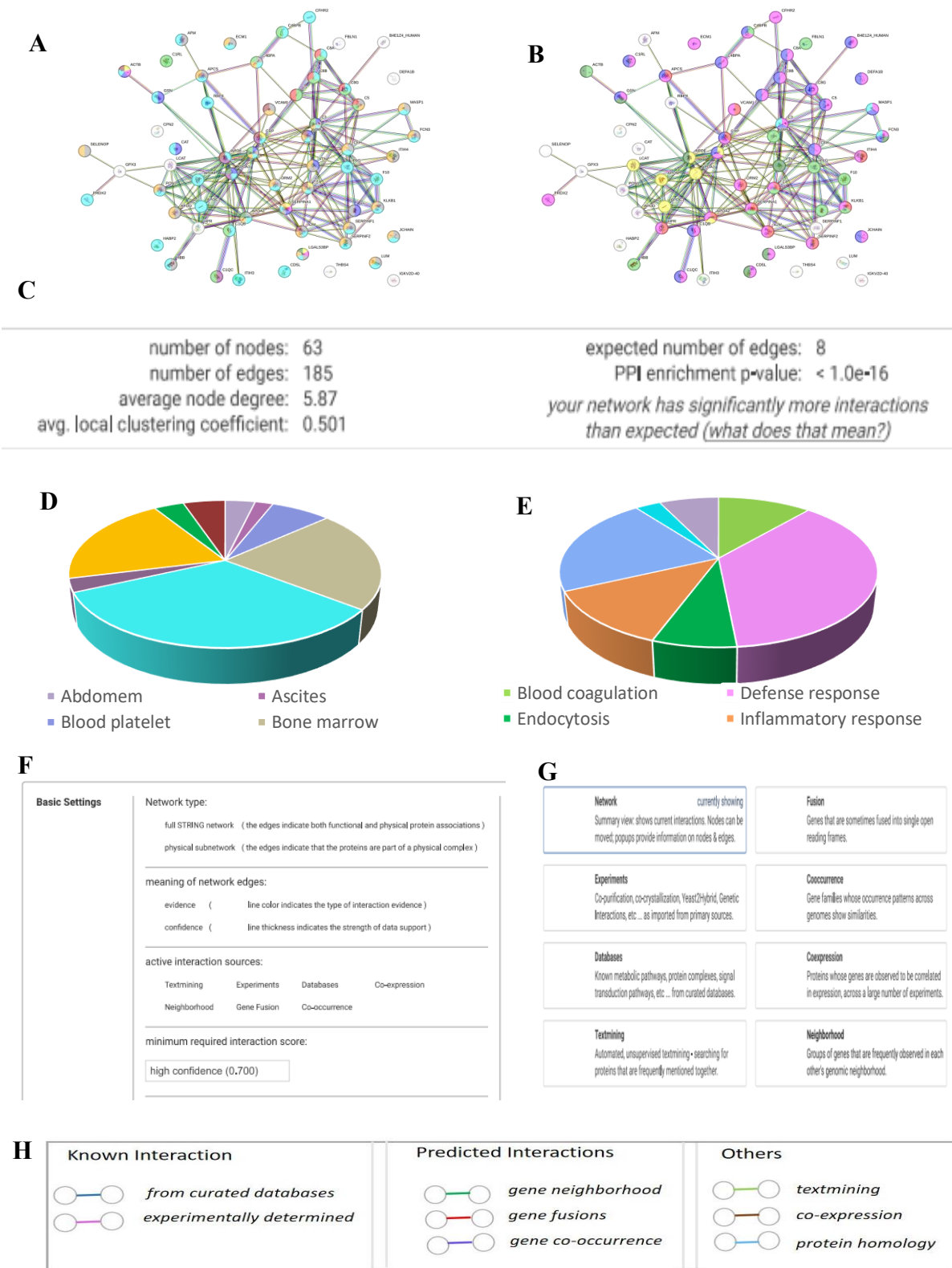


**Figure 3.8.: STRING analysis uncovering protein-protein interactions of upregulated proteins in severe dengue as compared to nonsevere dengue. A.& D: Proteins identified in different cells.B.& E Biological functions of proteins. C,F,G & H: Basic settings of string analysis. A protein is represented by each node, and an interaction, including a functional or physical relationship, is represented by each edge. The only interactions displayed are those with a high confidence score of 0.7.**



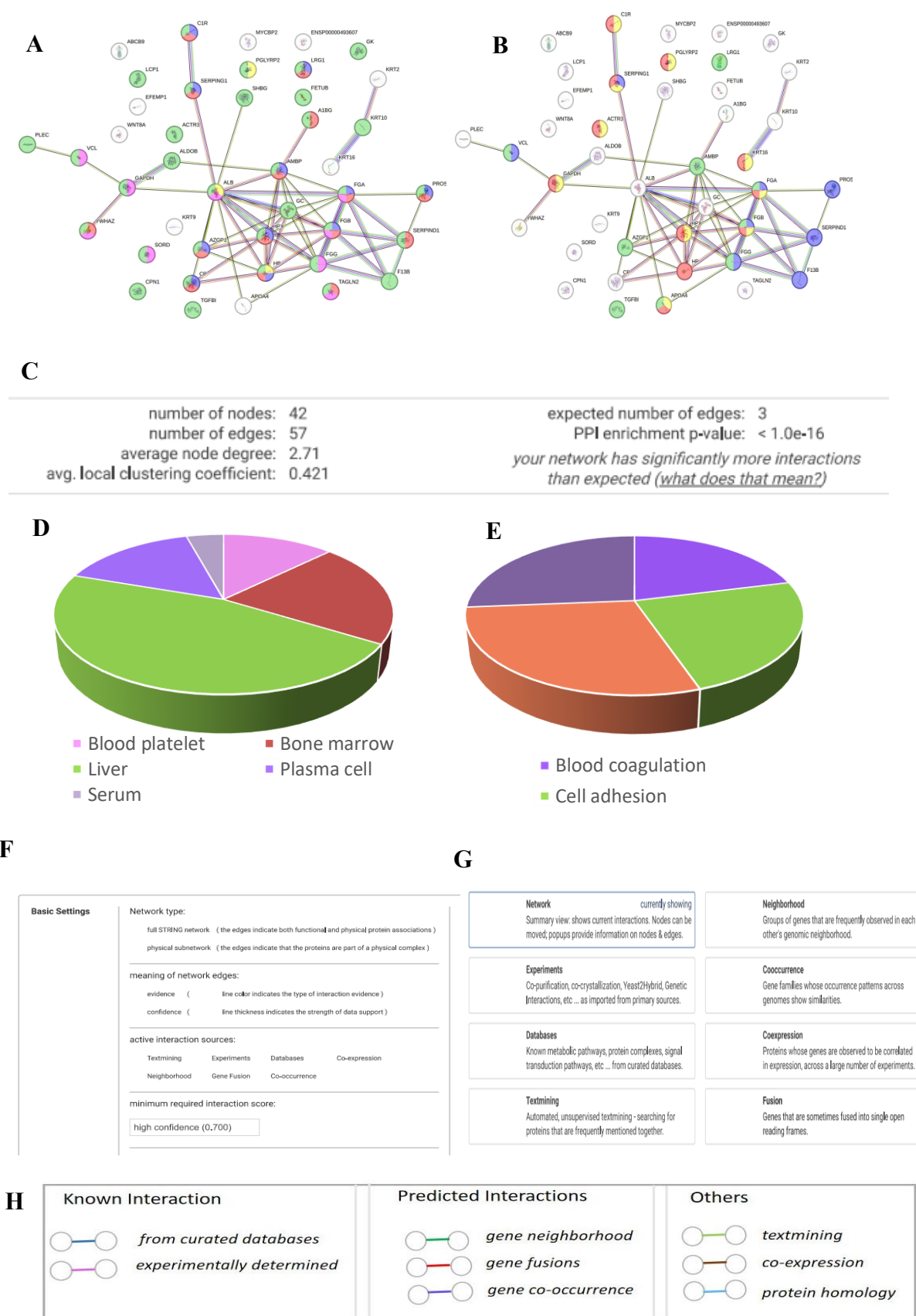


**Figure 3.9.: STRING analysis uncovering protein-protein interactions of downregulated proteins in severe dengue as compared to nonsevere dengue. A.& D: Proteins identified in different cells. B.& E Biological functions of proteins. C,F,G & H: Basic settings of string analysis. A protein**

is represented by each node, and an interaction, including a functional or physical relationship, is represented by each edge. The only interactions displayed are those with a high confidence score of 0.7.

Gene ontology mining of the identified proteins revealed alteration in the biological functions, mostly involved in inflammatory and immune response and transporter activity (Table 3.3).

3.10. Correlation in between MASP-1, VTN with Blood Parameters

According to Nguyen et al. (2004), dengue fever is frequently associated with changes in hepatic functioning. Increased SGOT levels were positively correlated with MASP-1 (r=0.614 with p<0.0001) and negatively correlated with VTN (r=-0.1898 with p=0.0009) whereas platelet was negatively correlated with MASP-1 (r=-0.5781 with p<0.0001) and positively correlated with VTN (r=0.5081 with p<0.0001). Further, HCT was found to be negatively correlated with the levels of VTN and positively correlated with MASP-1 respectively.

Table 3.5.: Association of MASP-1 and VTN with biochemical parameters of severe dengue patients

		SGOT (IU/L)	SGPT (IU/L)	Platelet (µl)	CRP (mg/L)	HCT (%)	ALB (gm/dl)	GLB (gm/dl)	MASP-1 (µg/ml)	VTN (µg/ml)
SGOT (IU/L)	r value	0.0000	0.8657	-0.4788	0.1973	0.0616	-0.3230	-0.1751	0.6140	-0.1898
	P value	0.0000	<0.0001	<0.0001	0.0006	0.2852	<0.0001	0.0023	<0.0001	0.0009
SGPT (IU/L)	r value	0.8657	0.0000	-0.3400	0.1472	0.1373	-0.1723	-0.1253	0.5298	-0.1292
	P value	<0.0001	0.0000	<0.0001	0.0104	0.0169	0.0027	0.0295	<0.0001	0.0247
Platelet (µl)	r value	-0.4788	-0.3400	0.0000	-0.2565	-0.1077	0.3397	0.3225	-0.5781	0.5081
	P value	<0.0001	<0.0001	0.0000	<0.0001	0.0617	<0.0001	<0.0001	<0.0001	<0.0001
CRP (mg/L)	r value	0.1973	0.1472	-0.2565	0.0000	0.1200	-0.0746	-0.1145	0.2309	-0.2330
	P value	0.0006	0.0104	<0.0001	0.0000	0.0371	0.1961	0.0468	<0.0001	<0.0001
HCT (%)	r value	0.0616	0.1373	-0.1077	0.1200	0.0000	0.2373	0.0198	0.0746	-0.0373
	P value	0.2852	0.0169	0.0617	0.0371	0.0000	<0.0001	0.7314	0.1957	0.5185
ALB (gm/dl)	r value	-0.3230	-0.1723	0.3397	-0.0746	0.2373	0.0000	0.2294	-0.2890	0.1277
	P value	<0.0001	0.0027	<0.0001	0.1961	<0.0001	0.0000	<0.0001	<0.0001	0.0265
GLB (gm/dl)	r value	-0.1751	-0.1253	0.3225	-0.1145	0.0198	0.2294	0.0000	-0.2292	0.1662
	P value	0.0023	0.0295	<0.0001	0.0468	0.7314	<0.0001	0.0000	<0.0001	0.0038
MASP-1 (µg/ml)	r value	0.6140	0.5298	-0.5781	0.2309	0.0746	-0.2890	-0.2292	0.0000	-0.2526
	P value	<0.0001	<0.0001	<0.0001	<0.0001	0.1957	<0.0001	<0.0001	0.0000	<0.0001
VTN (µg/ml)	r value	-0.1898	-0.1292	0.5081	-0.2330	-0.0373	0.1277	0.1662	-0.2526	0.0000
	P value	0.0009	0.0247	<0.0001	<0.0001	0.5185	0.0265	0.0038	<0.0001	0.0000

3.11. Correlation in between MASP-1, VTN with Viral load

RT-PCR-based nucleic acid detection is one of the innovative molecular techniques for accurately diagnosing dengue infection. Here, we employed real-time polymerase chain reaction (RT-PCR) to detect the acute phase infection of the DENV population. A total of seventy-six DENV patients were recruited to investigate the relationship between the dengue viral load and the biomarkers found. During the fever phase of the disease, a higher viral load ( $2 \times 10^7$  copies/ml) was found compared to the defervescence period ( $3 \times 10^5$  copies/ml).

Patients in the acute phase with higher viral loads may have experienced a cellular immune response that eliminated the plasma viremia during the defervescence phase. According to our data, during the febrile phase of infection, viral load was negatively connected with VTN ( $r = -0.246$ ,  $p = 0.03$ ) and positively correlated with MASP-1 ( $r = 0.266$ ,  $p = 0.01$ ), suggesting that these biomarkers may be directly correlated with viral load.

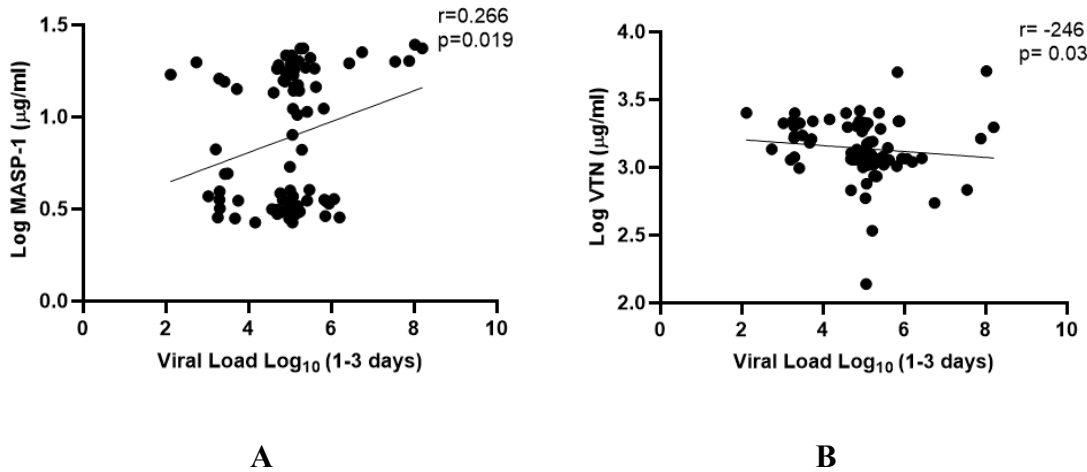


**Figure 3.10. Correlation of MASP-1 and VTN with viral load. (A) MASP-1 versus viral load and (B) VTN versus viral load.**

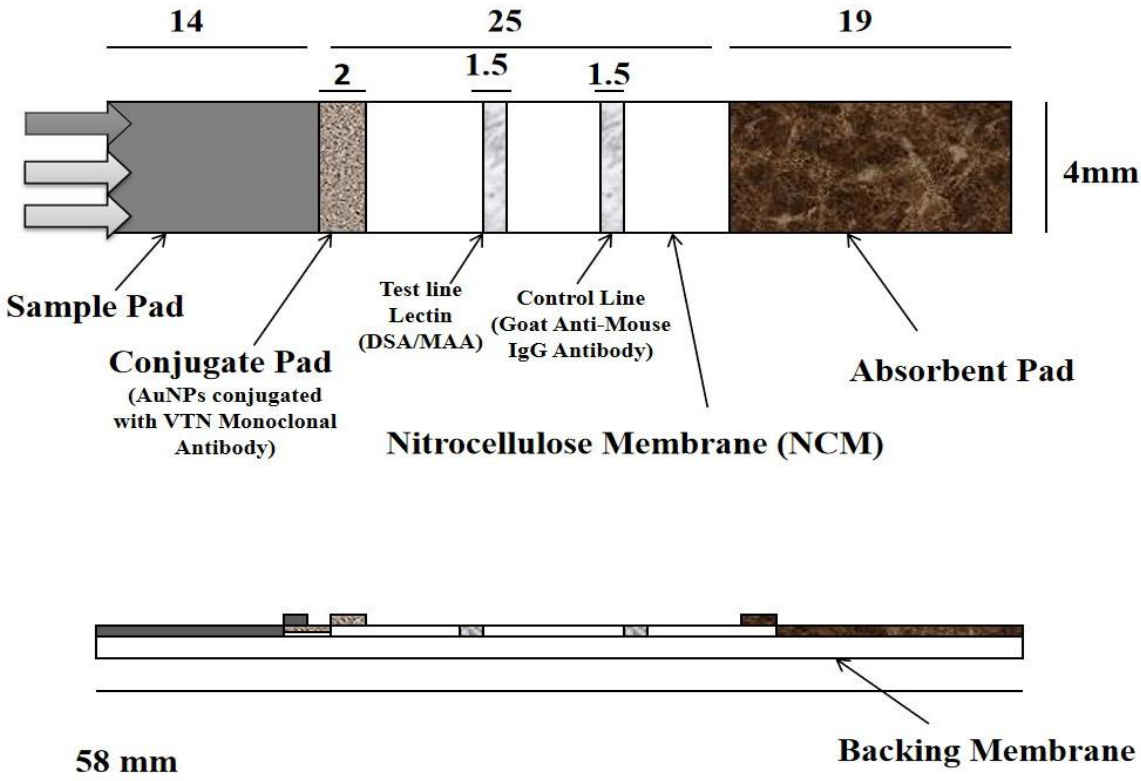
MASP-1: Mannose Associated Serine Protease-1, VTN: Vitronectin.

From the LC-MS, ELISA, and Western blot technique MASP-1 and VTN proteins could be validated as dengue severity biomarkers. Subsequently, these proteins were utilized for the development of lateral flow strips or point-of-care assays. Development of these assays required standardization of various components, which are described in detail in the following sections. The following sections describe the development of two LFIA systems. With VTN a lectin-based gold nanoparticle LFIA system was developed. Whereas utilizing MASP-1 a silver nanoparticle-based LFIA system was developed.

### 3.12 Preparation of immunostrip for Lectin-based LFIA using AuNPs

To conduct these experiments, we used a backing laminate with a pre-assembled Nitrocellulose Membrane (NCM). A conjugate pad, containing VTN monoclonal Antibody conjugated AuNPs, was placed on the NCM with 2 mm overlap. A sample pad was then placed on the conjugate pad with a 1 mm overlap. Finally, an absorbent pad was placed on the opposite end of the NCM with a 2 mm overlap. The overlap between each component is crucial for fluid wicking and efficient flow. For the test line, we used two types of lectins (DSA and MAA),

while a goat-anti-mouse IgG antibody was used for the control line. The assembled strips were then trimmed to 4 mm wide for testing. Schematics are represented in Figure.



**Schematics of the LFIA assembly (measurements in mm)**

**Figure 3.11.: Schematic view of a lectin-based lateral flow test strip using VTN-MAb conjugated AuNPs.**

### 3.13 Morphological analysis of the NCM (Nitrocellulose membrane)

During the standardization process, NCM pore diameters ranging from 8 to 15  $\mu\text{m}$  were utilized. The strip's porosity quality is important because the pore size of NCM influences the fluid flow through the strip. When NCM's pore size grows, it draws fluid in and wicks it more quickly than when its pore size is lower. However, the larger pore size of NCM also decreases its ability to bind proteins. Thus, a 10  $\mu\text{m}$  pore size was utilized for the construction of LFIA as indicated in figure 3.11 to modify fluid flow and protein binding on the NCM.

### 3.14 Morphology analysis of Sample pad, Conjugate pad and Absorbent pad

Appropriate sample, absorbent, and conjugate pad selection are essential to the success of lateral flow assays (LFAs). Fluid flow time, which controls the entire assay speed and results

interpretation, is a crucial factor in determining this decision. As the sample's first point of contact, the sample pad needs to strike a balance between allowing fluids to absorb quickly and avoiding particulate matter interference. Assuring effective sample transfer without sacrificing test specificity is possible with a pad that has the ideal porosity and thickness. Here the component of the selected sample pad was Glass fiber (GFB-R7) because of its ability to prevent non-specific binding of sample components, high absorption capacity, and ensure steady and uniform flow of the sample to the conjugate pad and helps to reduce background noise. The glass fiber is mainly composed of silica (silicon dioxide) mixed with various other ingredients. The main components of glass fiber are Silica ( $\text{SiO}_2$ ), Lime ( $\text{CaO}$ ), Magnesia ( $\text{MgO}$ ), Alumina ( $\text{Al}_2\text{O}_3$ ), Soda ( $\text{Na}_2\text{O}$ ), Potash ( $\text{K}_2\text{O}$ ), Boric oxide ( $\text{B}_2\text{O}_3$ ), etc.  $\text{CaO}$ , and  $\text{MgO}$  act as a stabilizing agent whereas  $\text{Al}_2\text{O}_3$  and  $\text{B}_2\text{O}_3$  showed linking capacity. On the other hand, the absorbent pad at the end of the strip functions as a fluid sink. Its ability to continuously draw fluid is essential for preserving a constant flow rate. Absorbent pads are made from cellulose fiber or a combination of cotton and glass fiber. These materials are chosen for their hydrophilic nature allowing liquid absorption and consistent flow. Here we have chosen AP080 for its high absorption capability and its higher thickness than the other type. The remaining component of lateral flow assay is the conjugate pad. The conjugate pad is a key component of lateral flow immunoassay. The labeled reagents are stored in the conjugate pad. In fluid dynamics, its job is to release the conjugate as optimally as possible without interfering with its activity. It's crucial to strike a balance between quick release and avoiding conjugation loss. The material of the conjugate pad is a polyester matrix. Polyester is a common material used for conjugate pads along with fiberglass and rayon. This synthetic composition ensures quick and uniform release of the dried conjugate. The polyester matrix is primarily composed of unsaturated polyester resins which are created from the reaction of polyhydric alcohols (e.g. Ethylene glycol) and unsaturated dibasic acids (e.g. maleic anhydride). Styrene is often used as a reactive diluent to reduce viscosity and is also used for cross-linking. Among the two categories of the conjugate pad, we have selected PT-R7 because of its better uniform movement of protein-conjugated nanoparticles.

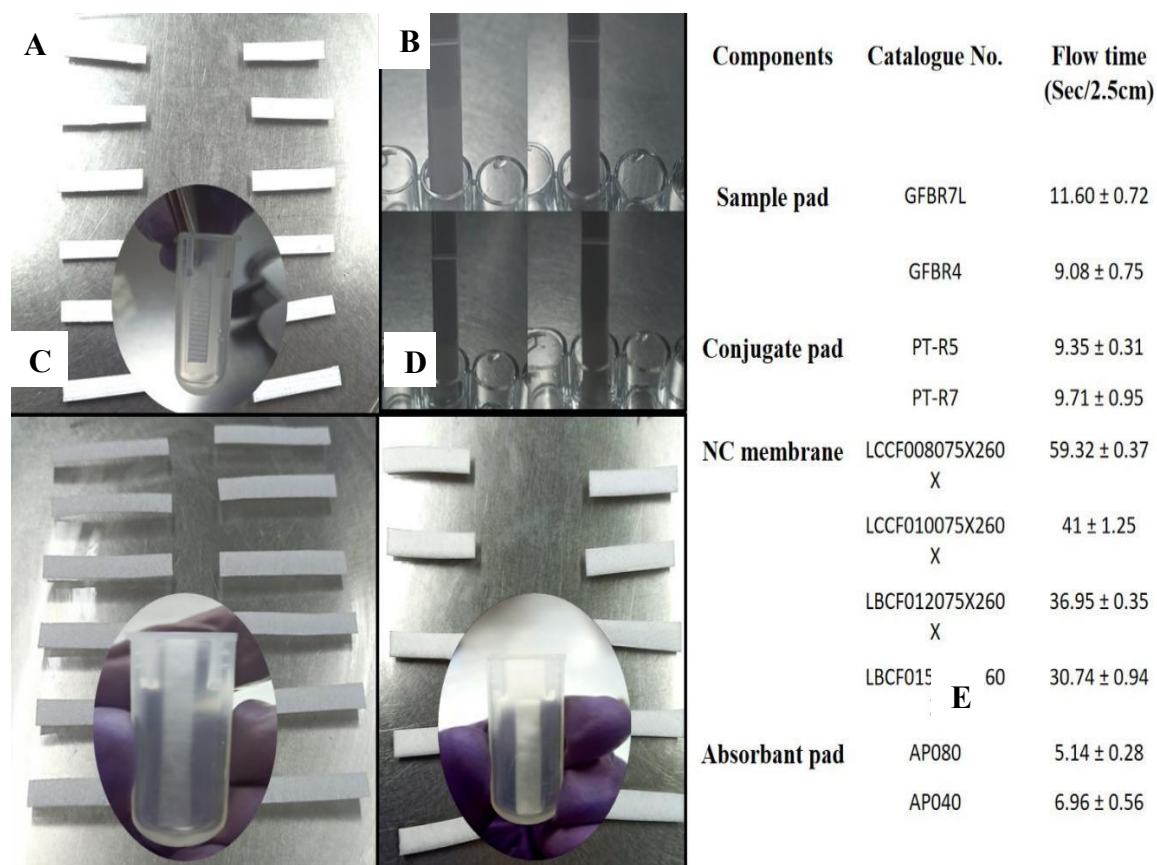


**Figure 3.11. A. Sample pad standardization, B. Conjugate pad standardization, C. NC membrane standardization, D. Absorbent pad standardization, E. table shows flow time of different categories of components.**

### 3.15 Characterization of Gold nanoparticles by using UV-Vis Spectrophotometry

Abcam’s Gold conjugation kit offers a streamlined approach to attaching antibodies or proteins to gold nanoparticles. This kit utilizes a covalent conjugation method that is both rapid and efficient, requiring less than 4 hours to complete [222]. However we have confirmed conjugation of anti-VTN mAb with gold nanoparticles by using Uv-Vis Spectrophotometry. The successful binding of the anti-VTN mAb to the gold nanoparticles from the Abcam (154873) gold conjugation kit was revealed by a shift in the UV absorption peaks following antibody conjugation [223, 224].

### 3.16 Control line optimization for AuNPs-Lectin-based LFIA

A crucial factor impacting the lateral flow assay's sensitivity and specificity is the antibody concentration immobilized on both the control and test lines. In order to confirm that the detected signal at the test line was actually caused by particular antigen-antibody interactions rather than non-specific causes, the employment of a secondary antibody at the control line

acted as a critical control to validate assay functionality. The assay's performance is firmly supported by this optimized condition, which also makes it possible to reliably detect the target analyte within the intended analytical range. After careful optimization, the best results in our assay were obtained with a control antibody concentration of 2  $\mu\text{g}/\mu\text{l}$  (in a 1  $\mu\text{l}$  volume). This concentration strikes a balance between specificity and sensitivity; too much of either could result in non-specific binding and false-positive results, while too little could possibly boost signal intensity.

### **3.17 Test line MAA (*Maackia amurensis agglutinin*) and DSA (*Datura stramonium agglutinin*) optimization for AuNPs- Lectin-based LFIA**

For the development of a gold nanoparticle lectin-based LFIA system test line standardization is an important parameter. In order to verify that specific antigen-antibody interactions or lectin-carbohydrate linkage, as opposed to non-specific ones, were the true origin of the signal that was recorded at the test line. An immunoassay for lateral flow was created to identify dengue infection. The assay's performance was largely dependent on the capture antibody concentrations being optimized. The concentration of 5  $\mu\text{g}/\mu\text{l}$  was found to be the most efficient for two lectins that were used as test lines i.e. DSA and MAA, producing a distinct line as seen in Figures 3.12. C and 3.12.D for DSA and figure 3.12.A and 3.12.B for MAA. The different dengue patient categories were then treated with these optimized concentrations. A control line was added utilizing the Goat Anti-Mouse IgG antibody as a marker to guarantee test reliability. In order to create a strong LFIA platform for wider use, this study concentrated on figuring out the optimal capture antibody concentrations for the test and control lines. Test line optimization was conducted with strict adherence to the experimental protocol.

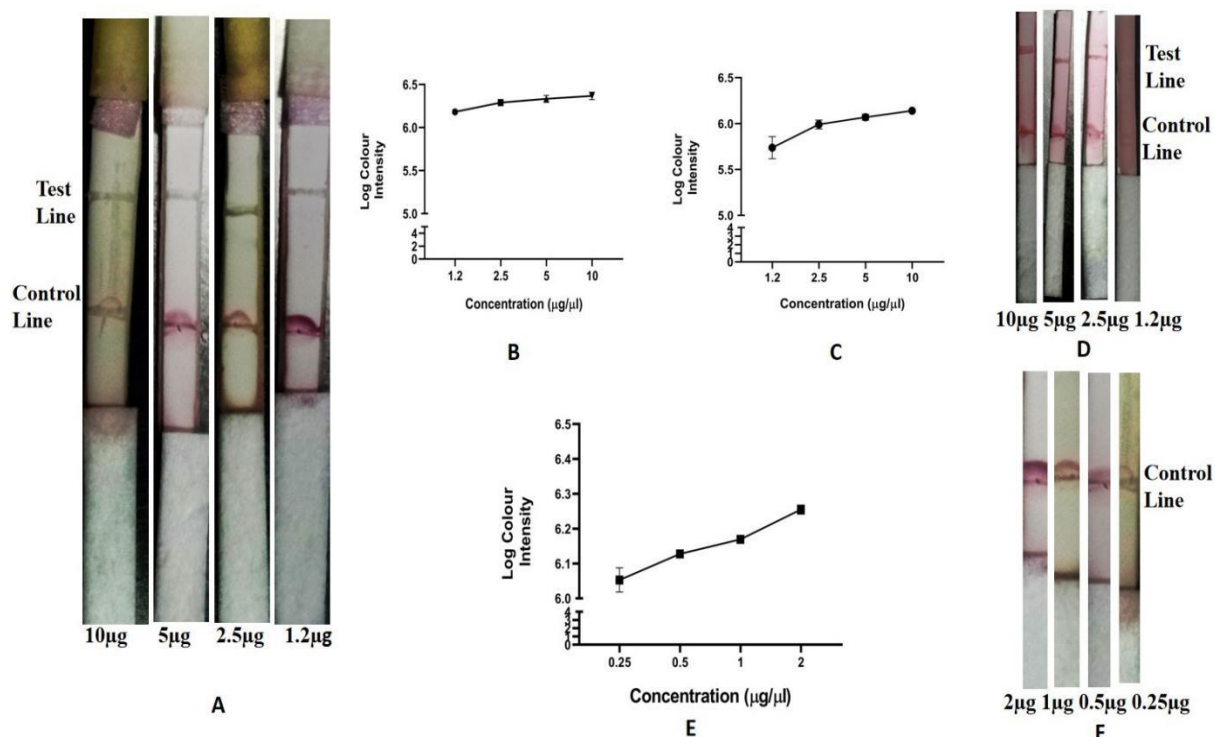


**Figure 3.12. Test and control line optimisation using point-of-care assay analysis. ANOVA is used first, then the Kruskal-Wallis test (K). A) Variations in MAA (*Maackia amurensis* agglutinin) concentration. B) Graph represents color intensity of different concentration of one lectin, i.e., of MAA (*Maackia amurensis* agglutinin). C) Graph represents color intensity of different concentration of another lectin, i.e., of DSA (*Datura stramonium* agglutinin). D) Different concentration of DSA (*Datura stramonium* agglutinin). E) Graph represents color intensity of different concentration of control line, i.e. Goat anti-mouse IgG antibody. F) Different concentration of control line (Goat anti-mouse IgG antibody)**

### 3.18 Synthesis of Silver Nanoparticles (AgNPs)

Silver nanoparticles were successfully synthesized using sodium borohydride as a reducing agent. The formation of these nanoparticles was evident by the distinctive bright yellow color of the resulting solution, a characteristic indicative of the presence of silver nanoparticles. This simple yet effective method provides a foundation for further exploration of silver nanoparticles and their potential applications.

### 3.19 Characterization of Silver nanoparticles through TEM and UV-Vis Spectrophotometry

UV/Vis spectrophotometry, TEM (Figures 3.13.), and DLS measurement were used to characterize the prepared AgNPs. The resulting AgNP solution has a distinctive absorption maximum at 401 nm, as shown by the UV/Vis spectra. Since the diameter of AgNPs and a



maximum of 401 nm suggests the presence of nanoparticles with dimensions of about 10 nm, which is consistent with the data from the literature [259].

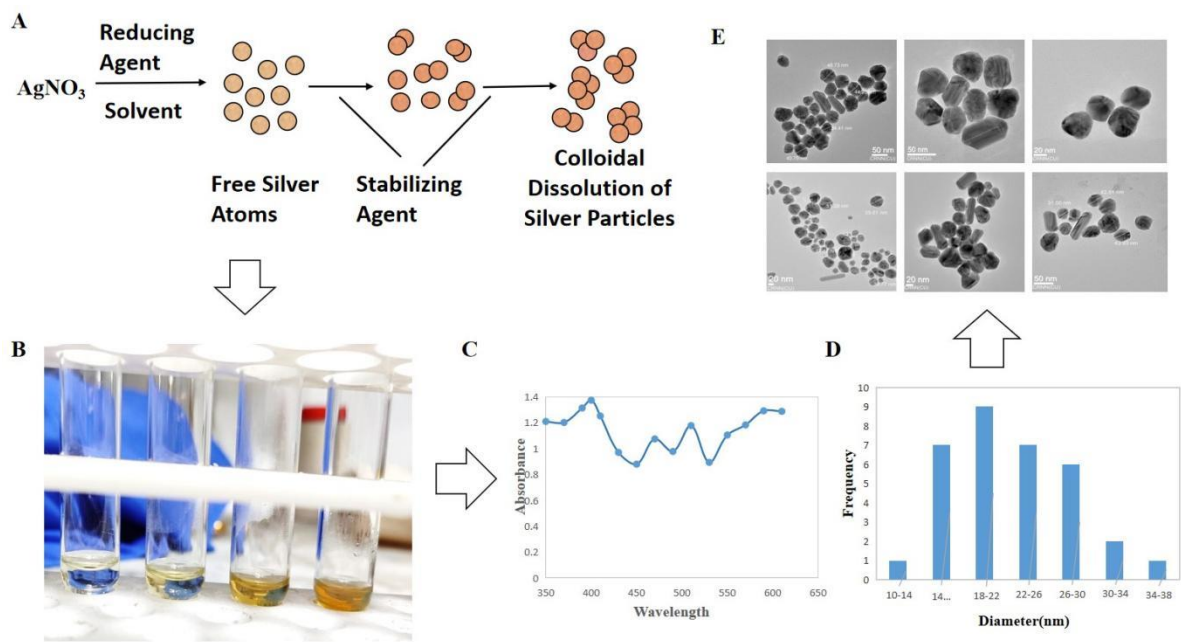


**Figure 3.13.: A) Chemical reaction behind the synthesis of Silver Nanoparticle Synthesis, B) Figure shows colour of solution of Silver nanoparticles gradually changed, C) Characteristic UV-Vis spectrum, with maximum absorbance at 401 nm, D) Bar graph represents size distribution of AgNPs. E) Transmission electron microscope (TEM) image of the synthesised AgNPs.**

Using information from TEM images, the diameter of AgNPs was directly determined, confirming the data. AgNPs were 15.43 nm in diameter on average (median 15.66 nm, SD 3.688 nm) according to TEM measurements. The distribution of AgNP particle sizes as seen by TEM is depicted in Figure 3.13. The physical characterization of silver nanoparticles was assessed by TEM analysis.

### 3.20 Characterization of Ab-conjugated AgNPs

The Z-average of the AgNPs-ab, as determined by the intensity distribution, is 39.24 nm, according to DLS measurement (Figure 3.14). Following the addition of the antibody to the solution containing the silver nanoparticles for one hour, data were collected. The modified AgNPs have a larger zeta potential (-22.35 mV) than the conjugated AgNPs, hence they ought to be more prone to aggregation. The antibody-coated AgNPs remained stable in the solution even when the Zeta potential increased. This supports earlier findings that nanoparticles become more stable when covered in proteins. Protein-coated nanoparticles do not combine because of hydrophobic and ionic interactions between proteins and nanoparticles.

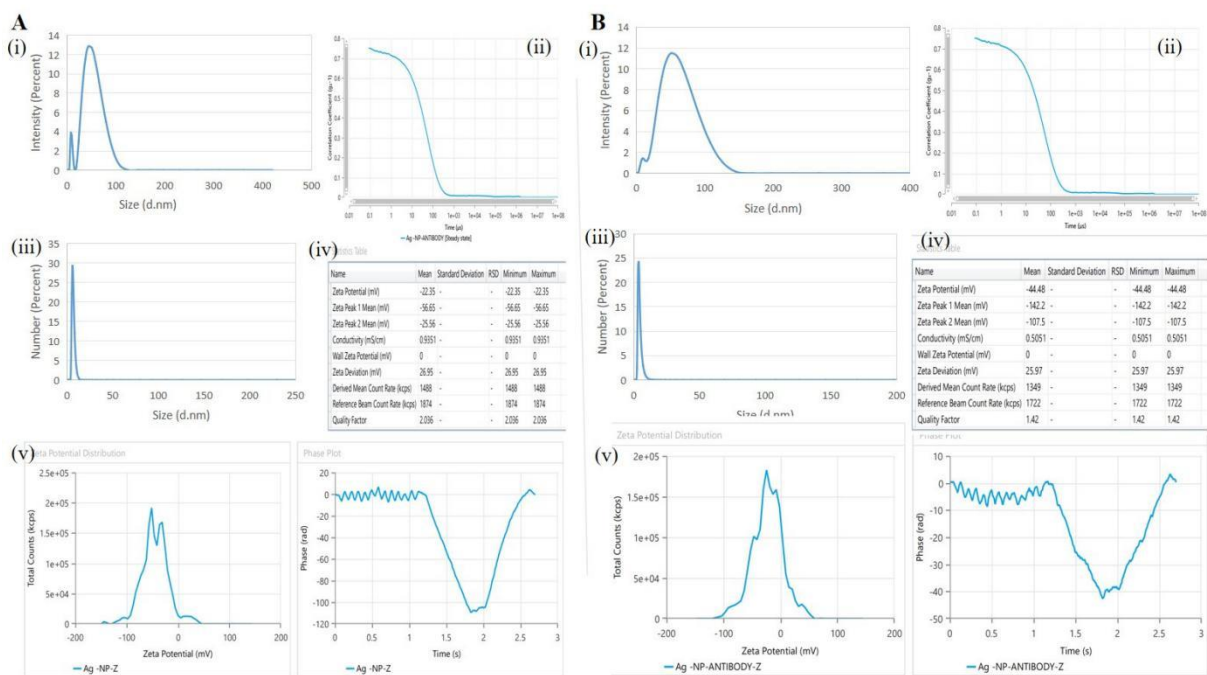


**Figure 3.14.: Dynamic light scattering (DLS) size distribution curves for AgNPs (A.[i] - A.[v] ) and AgNPs + Ab (B [i] - B [ii]):- (A1) intensity vs size of AgNPs, (B1) Correlation coefficient vs time of AgNPs , (C1) Number vs size of AgNPs, (A2) intensity vs size of AgNPs + Ab, (B2) Correlation coefficient vs time of AgNPs +Ab, (C2) Number vs size of AgNPs + Ab, (D1) Zeta potential graph of AgNPs, (D2) Zeta potential of AgNPs +Ab**

To assess the mean diameter of AgNPs, estimated by intensity distribution, dynamic light scattering was used. The polydispersity index (PDI) was evaluated through dynamic light scattering, which was 0.5311. The polydispersity index (PDI) is a measure of the heterogeneity of a sample based on size. The mean of the diameter of AgNPs was almost 30.9 nm. The mean and median AgNP diameter values obtained by DLS were greater than those obtained by TEM. This could be explained by the dispersant's interaction with the AgNPs' hydrodynamic diameter. While the DLS method measures the mean hydrodynamic diameter, which greatly favors the larger structures in the solution, TEM displays the diameter of the particles devoid of this aqueous and ionic payload. The mean particle size was thus higher according to DLS. The study by Souza et al. [260] described similar findings. Due to the non-narrow particle size distribution, the presence of larger particles may increase light scattering, leading to larger measured particles. Synthesized silver nanoparticles are of different sizes and different shapes in nature. The dynamic light scattering figure showed a heterogenic curve and the PDI value was 0.5311 which means the solution is heterogeneous in nature. To maintain the homogeneity, we used a standard silver dispersion kit. The concentration of the AgNPs solution is 0.02 mg/ml

and the diameter of the silver nanoparticle is 20 nm. Further, we characterized AgNPs through TEM and DLS as shown in Figure 3.15. and 3.16.

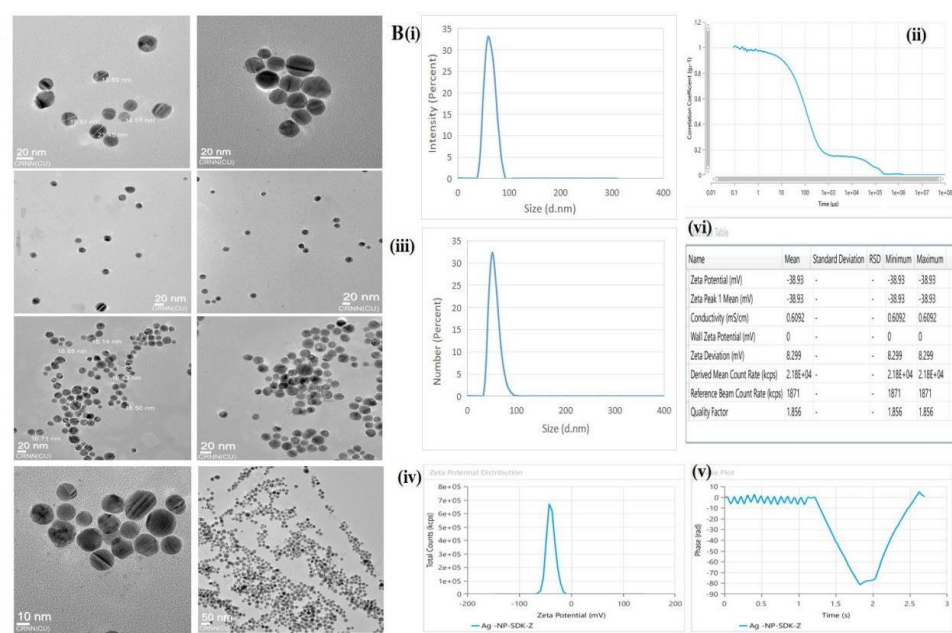


**Figure 3.15** A) TEM micrograph of the Silver dispersion kit, B.i) Intensity vs size of AgNPs, ii) Correlation coefficient vs time of AgNPs, iii) Number vs Size distribution of AgNPs, iv & v) zeta potential graph of AgNPs of silver dispersion kit, vi) Statistical table of AgNPs of Silver dispersion kit.

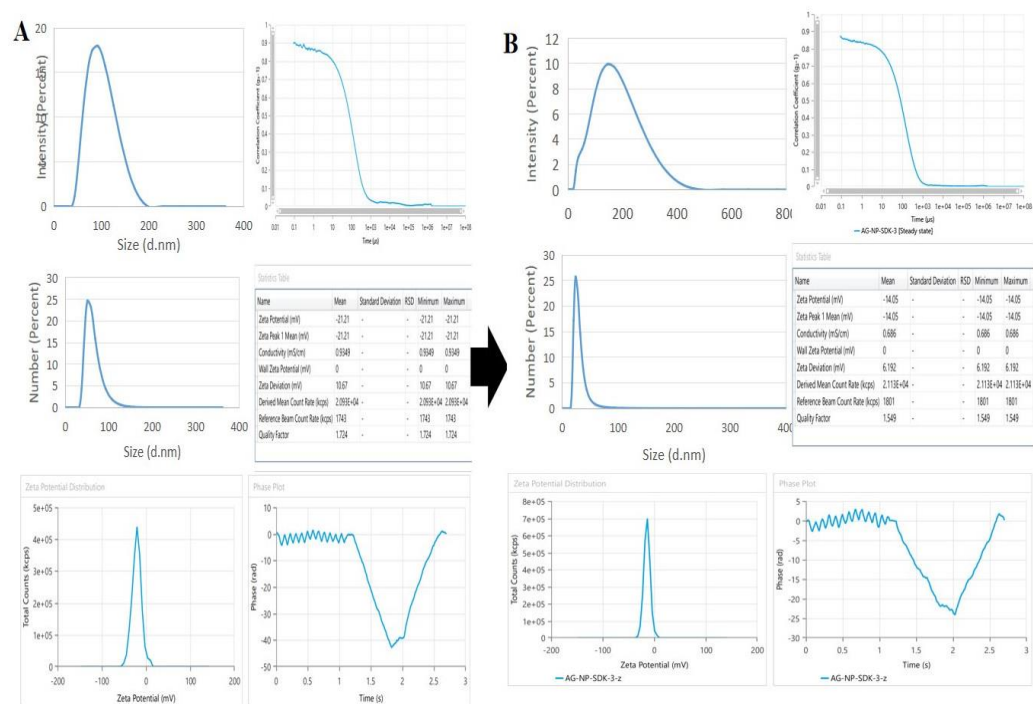


**Figure 3.16.:** Dynamic light scattering (DLS) size distribution curves for AgNPs of Silver dispersion kit which conjugated with antibody. A.i) Intensity vs Size of Ab conjugated AgNPs after 30 minutes, ii) Correlation coefficient vs time of Ab conjugated AgNPs, iii) Number vs Size, iv)





further bind with analytes present in patient sample, D i) Graph shows DLS of AgNPs- Intensity vs Size and ii) Correlation coefficient vs time of AgNPs.

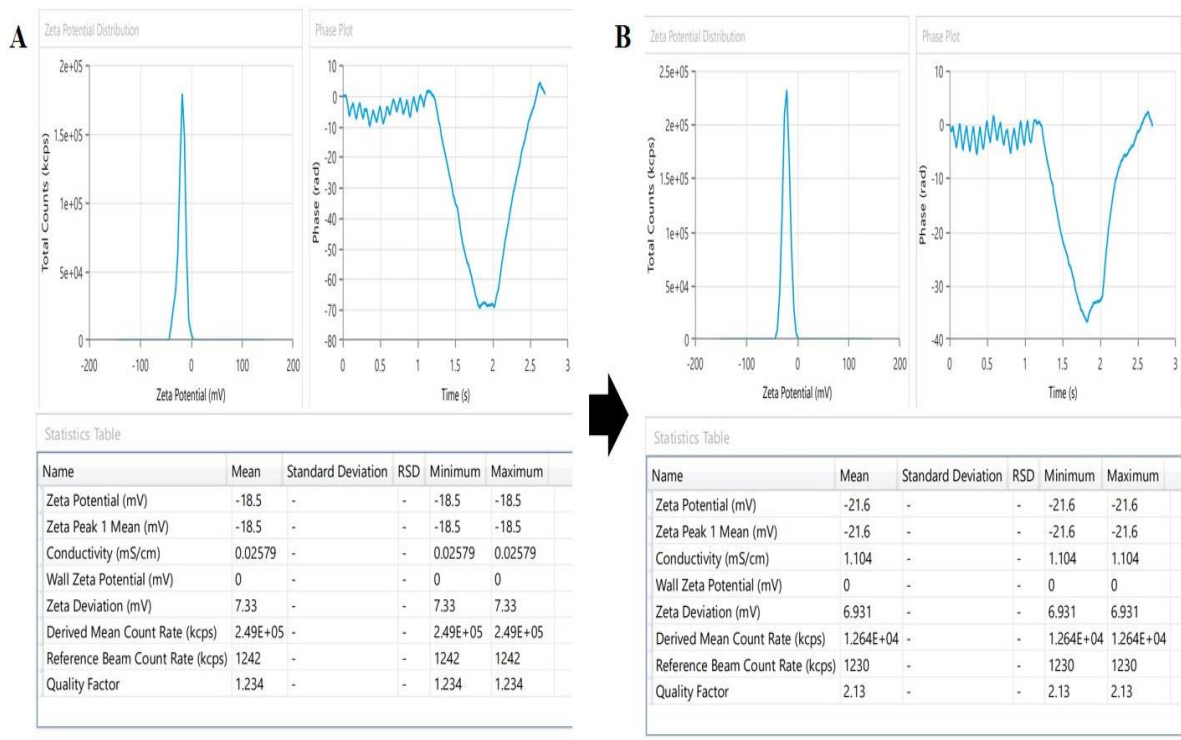
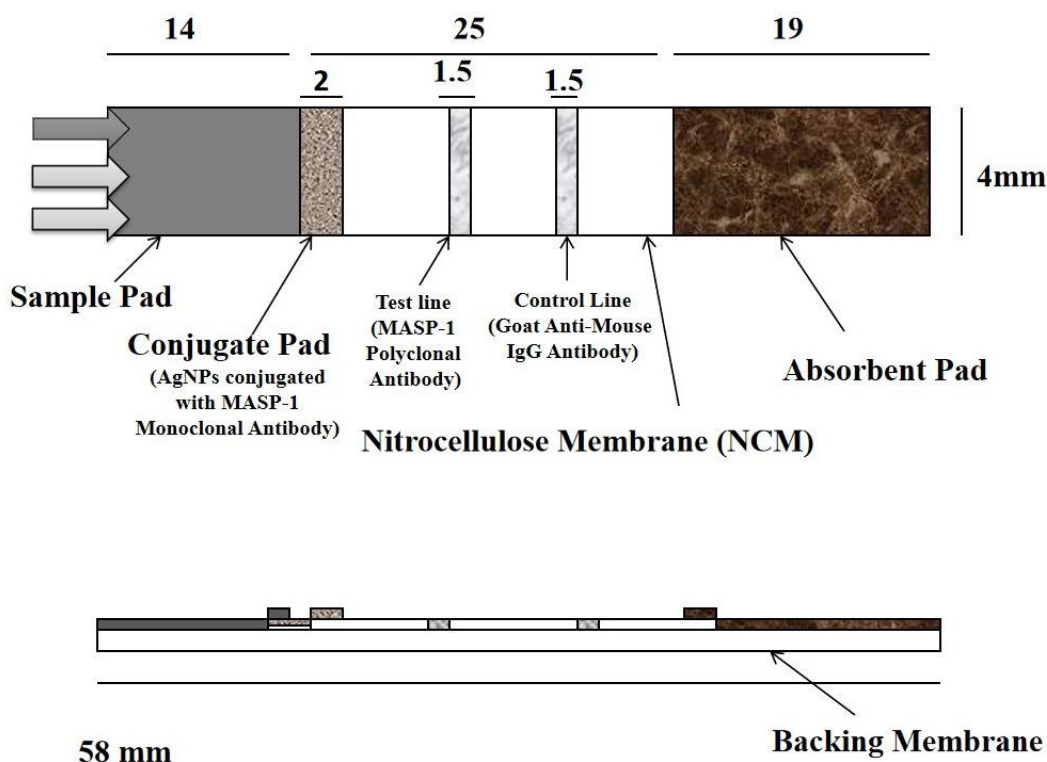


**Figure 3.18.** A) Graph represents Zeta potential of only AgNPs and value of zeta potential represents in statistical tabulate form, B) Graph represents zeta potential of Ab conjugated AgNPs and statistical table shows value of zeta potential.

### 3.22 Preparation of immunostrip for MASP-1-based LFIA using AgNPs

To conduct this experiments, we used a backing laminate with pre-assembled Nitrocellulose Membrane (NCM). A conjugate pad, containing MASP-1 monoclonal Antibody conjugated AgNPs, was placed on the NCM with 2 mm overlap. A sample pad was then placed on the conjugate pad with a 1 mm overlap. Finally, an absorbent pad was placed on the opposite end of the NCM with a 2 mm overlap. The overlap between each component is crucial for fluid wicking and efficient flow. For the test line, we used MASP-1 Polyclonal antibody, while a goat-anti mouse IgG antibody was used for the control line. The assembled strips were then trimmed to 4 mm wide for testing. Schematics represented in Figure.



**Schematics of the LFIA assembly (measurements in mm)**

**Figure 3.12.:** Schematic view of a lectin-based lateral flow test strip using MASP-1-MAb conjugated AgNPs.

### 3.23 Control and Test line optimization for LFIA by using AgNPs

The optimum concentration of capture antibody at the control line was found to be 2  $\mu\text{g}/\mu\text{l}$  (1  $\mu\text{l}$ ) in lateral flow immunoassay, which is shown in Figure 3.19. For the development of LFIA, Goat Anti Mouse IgG Antibody was used as a marker for the control line. Thus, LFIA was developed to determine the optimum concentration of capture antibody at the control line for further application. The optimum concentration of detection antibody (MASP-1 polyclonal antibody) at the test line was found to be 1  $\mu\text{g}/\mu\text{l}$  in lateral flow immunoassay, which is shown in Figure 3.19. For the development of LFIA, Goat-anti Mouse IgG antibody was used as a control line. Thus, LFIA was developed to determine the optimum concentration of detection antibody at the test line for further application.

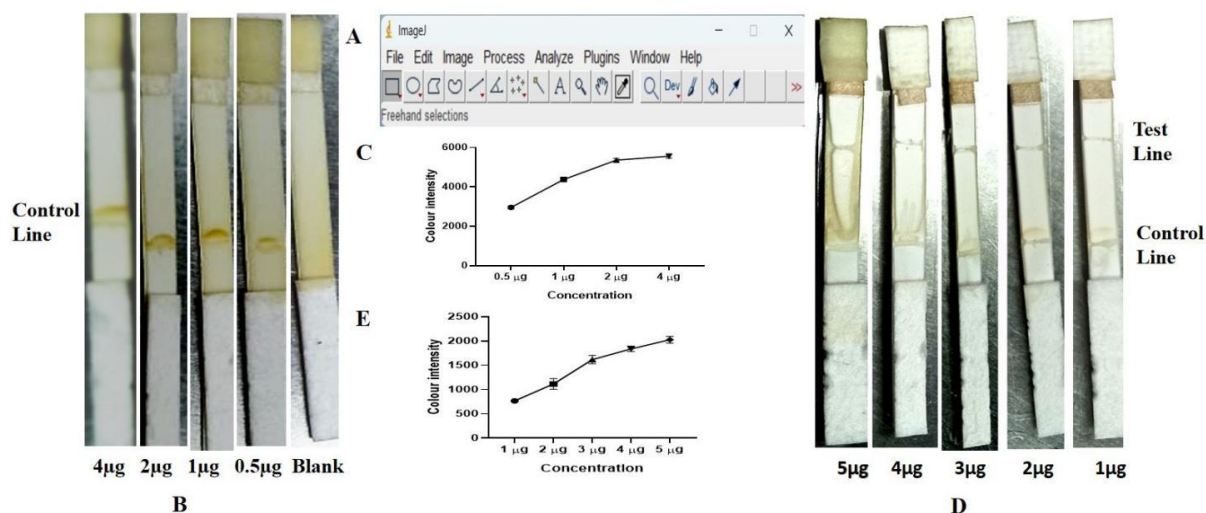


**Figure 3.19. Point of care immunoassay analysis of test and control line optimization. ANOVA followed by Kruskal-wallis test (K). (A) Obtained colour intensity by using ImageJ software, (B) Different concentration of Goat anti-mouse IgG antibody in lateral flow assay, (C) Graph represents colour intensity of different concentration of control line i.e. Goat anti-mouse IgG antibody. (D) Different concentration of Masp-1 polyclonal (test line) antibody in lateral flow assay, (E) Graph represents colour intensity of different concentration of test line.**

### 3.24 Validation of the newly developed Lectin-based assay using clinical samples

Three groups of patients were used to test the recently developed assay. For the newly developed assay we also performed the inter and intra-assay coefficient of variation (CV) to check variability. The intra-assay CV measures the variability within a single assay run while inter-assay CV measures the variability between different runs. Acceptable target values are generally : intra-assay CV< 10% and inter-assay < 15% [220].

For VTN, we used 50 patients with Dengue without a warning sign (DWoWS), 35 patients with Dengue with warning sign (DwWS), and 12 patients with severe Dengue (SD) illness. Dengue with both DWoWS and DwWS is considered non-severe. Through inter- and intra-assay testing, the recently created assay was validated. The assay yielded a %CV, which was calculated and displayed in the table. In short, intra-assay (MAA) non-severe Dengue infected patients had a coefficient of variation (%CV) of 1.07%, while severe Dengue patients had a %CV of 1.35%. For patients classified as non-severe, the intra-assay (DSA) variation (% CV) was 0.69%, while for those classified as severe, it was 0.63%. It was discovered that the VTN-MAA interaction had higher area under curve, sensitivity and specificity i.e. 0.93, 91.67% sensitivity and 83% specificity, while the VTN-DSA interaction displayed almost 0.9069, 91% sensitivity and 85% specificity. In case of VTN-DSA, it showed 40% positive predictive value

(PPV) and 98% Negative predictive value (NPV) whereas VTN-MAA showed 50% PPV and 98% NPV.

### **3.25 Validation of the newly developed MASP-1-based assay using clinical samples**

For MASP-1, we used 176 patients with DWoWS, 106 patients with DwWS and 20 patients with SD. MASP-1 test showed greater area under curve i.e. 0.9387. It showed 90% sensitivity but 85 % specificity although MASP-1 test was done on 302 study population. Lectin-based LFIA was applied on 97 dengue patients on the other hand MASP-1 based LFIA applied on 302 dengue patients and it showed 35% PPV and 99% NPV. Despite a lower positive predictive value, the silver nanoparticle-based LFIA demonstrated notable diagnostic performance in a larger patient population of 302 individuals. Our goal is to establish a silver nanoparticle-based LFIA for the rapid diagnosis of severe dengue, with the potential for future development of an electrochemical assay employing silver nanoparticles, which have been shown to possess good electrochemical activity compared to gold nanoparticles. A study suggested that AgNPs also provide a six-times more sensitive assay. The AgNP bioassay is particularly advantageous because it requires no additional solution to be added once it is employed in a biological sample, making it much simpler and more suitable for usage in a POC environment [221]. The intra-assay (MASP-1) non-severe Dengue infected patients had a coefficient of variation (%CV) of 7.08%, while SD patients had a %CV was 6.21% and interassay (MASP-1) Non-severe dengue patients had a coefficient of variation (%CV) of 7.02%, while SD patients had a %CV was 6.19%.

### **3.26 Comparison between assays with nomogram**

As demonstrated by this study, both AuNPs-based and AgNPs-based LFIA exhibit acceptable inter-assay and intra-assay coefficient of variations. These assays were further compared with conventional nomogram to compare assay performance.



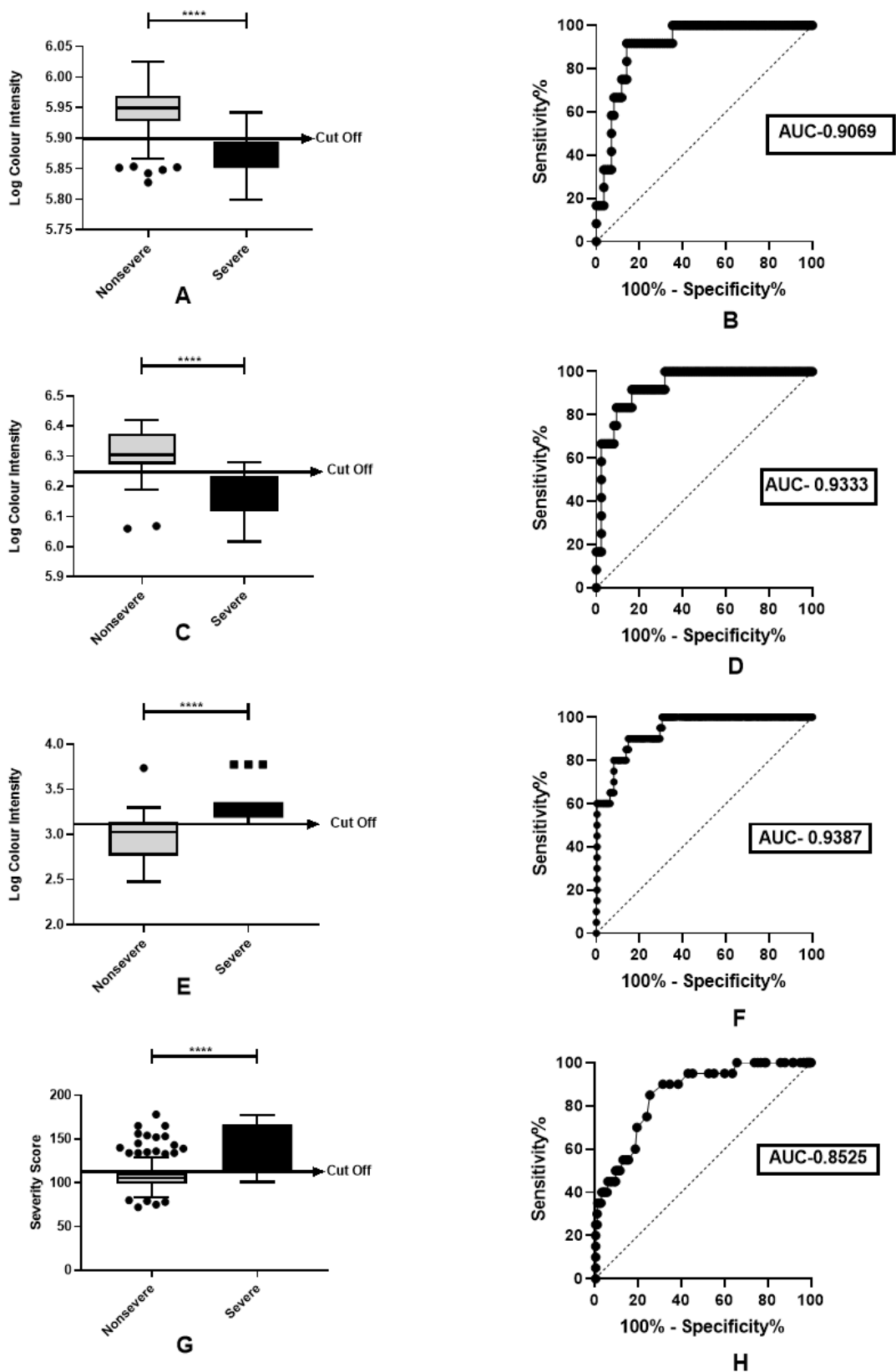


Figure 3.20. Validation of the newly developed assay using clinical samples. A) A graph showed the logarithmic color intensity of the LFIA strip when using DSA lectin, B) A receiver operating characteristic (ROC) curve analysis was performed to evaluate the diagnostic accuracy of the newly developed point-of-care assay using DSA lectin, C) A graph showed the logarithmic color

intensity of the LFIA strip when using MAA lectin, D) A receiver operating characteristic (ROC) curve analysis was performed to evaluate the diagnostic accuracy of the newly developed point-of-care assay using MAA lectin, E) A graph showed the logarithmic color intensity of the LFIA strip when using MASP-1 protein, F) A receiver operating characteristic (ROC) curve analysis was performed to evaluate the diagnostic accuracy of the newly developed point-of-care assay using MASP-1 protein, G) A graph showed the severity scores of dengue patients as calculated by a nomogram, H) A receiver operating characteristic (ROC) curve analysis was performed to evaluate the diagnostic accuracy of the severity score of dengue patients as calculated by a nomogram.

Table 3.6.: Inter- and intra-assay variation.

	Categories	Lectins/Proteins	Nonsevere Dengue	CV(%)	Severe Dengue	CV(%)
			Mean±SEM		Mean±SEM	
1	Inter-assay	DSA	5.91±0.004	0.72%	5.83±0.01	0.66%
		MAA	6.32±0.007	1.07%	6.18±0.02	1.37%
		MASP-1	2.96±0.01	7.02%	3.33±0.04	6.19%
2	Intra-assay	DSA	6.22±0.004	0.69%	6.15±0.01	0.63%
		MAA	6.31±0.007	1.07%	6.28±0.02	1.35%
		MASP-1	2.963±0.01	7.08%	3.34±0.04	6.21%

The results showed Mean ± SEM value of inter- and intra-assay followed by descriptive statistics. Abbreviations: DSA: *Datura stramonium* agglutinin, MAA: *Maackia amurensis* agglutinin, MASP-1: Mannose associated serine protease-1, CV: coefficient of variation.

## CHAPTER - 4

### Discussion

The majority of cases of dengue, an acute illness, are either asymptomatic or exhibit a variety of clinical signs and symptoms [225]. According to the World Health Organisation, dengue fever is hyperendemic in India, where yearly cyclical outbreaks are on the rise. In our study, the average age of dengue fever patients was almost in between 30-40 years old. The high frequency in this age group may be due to the fact that middle-aged persons typically work, either in the office or on the job in the field, which makes them more vulnerable to daytime mosquito bites. In this study, more male preponderance of dengue was noted than female. This was consistent with what Deshkar et al. Discovered [226]. In the Indian population, Garg et al. reported similar findings [227]. A higher incidence of dengue in men may result from more time spent outside or at work. High fever, headache, nausea, vomiting, skin rash, stomach pain, and arthralgia are common symptoms of adult dengue infection. Still, a few of these signs and symptoms are also seen in other infectious illnesses. The most prevalent symptoms reported by the patients in this study were headache, nausea, and abdominal discomfort. These findings were in line with studies conducted by Khan et al.[228] and Pan ST et al.[229]

Early detection of severe dengue is one of the most challenging areas in dengue research. There is a need for severe dengue patients to be identified and treated as soon as possible to reduce the death rate. In the early phase of the infection, dengue symptoms often mimic other common illnesses like flu, making it difficult to distinguish. Additionally, there is no single test to predict who will progress to severe dengue. Early intercession is crucial for better outcomes. In this study, the aim of this work is to investigate the possibility of using proteomics to find new indicators for severe dengue. In this study, we analyzed and compared the proteomics profile of severe and nonsevere dengue-infected patients followed by the identification of a statistically significant protein that might be useful for early prediction of severity of dengue infection. Further attempts have been made to utilize these severity biomarkers in the development of lateral flow immunoassay systems to predict severe dengue-infected patients. LC-MS/MS analysis identified 144 up-regulated proteins and 89 down-regulated proteins in severe dengue infection as compared to nonsevere dengue-infected patients. Among the different altered proteins identified through proteomics, three proteins showed promising results. Subsequently, these proteins were further validated by measuring their expression titers

through ELISA. These proteins are MASP-1 (Mannan-associated serine protease -1), VTN (Vitronectin) and Thrombospondin-1 (TSP-1). Currently, the molecular mechanism of dengue pathophysiology which occurs during severe conditions, is attributed to increased viral replication, apoptosis, proinflammatory cytokines, and complement activation. Although many molecular mechanisms have been proposed the exact role of effector proteins like TSP-1, VTN, and MASP-1 in pathology is not yet known.

In the case of TSP-1, decreased TSP-1 titer showed in severe dengue-infected patients than nonsevere dengue infection. To improve its diagnostic accuracy, we explored the combination of TSP-1 with selected biochemical parameters known to be significantly dysregulated in dengue infections, using CombiROC analysis, which helps researchers select the optimal marker combinations with an easy-to-use interface and a straightforward approach. The CombiROC tool is intended to choose multi-marker signatures from the assessed panel of markers. Reduced TSP-1 levels and platelet counts both inhibit clot formation and have the potential to start internal bleeding. The dengue virus can induce abrupt liver failure or asymptomatic transaminase increase as liver damage. Our research demonstrated a negative correlation between TSP-1 and transaminase levels, supporting the notion that both proteins are linked to the severity of dengue infections and that TSP-1 can be used as a potential biomarker to identify dengue severity.

VTN is another promising biomarker till now which had not been reported in the Indian cohort [230, 231] exhibiting greater protein folding alterations than thrombospondin-1 (TSP-1). We aimed to leverage VTN to enhance the accuracy of dengue severity prediction. Our research focused on developing a lateral flow immunoassay that can rapidly and reliably assess the severity of dengue infections. VTN is a multifunctional glycoprotein involved in platelet aggregation and coagulation. Its various isoforms circulate in the bloodstream and may influence dengue pathogenesis [232, 233]. Our analysis revealed higher VTN levels in non-severe dengue-infected patients as compared to severe cases. VTN expression was upregulated after infection but decreased overall in severe conditions. VTN exhibits structural flexibility and exists in both monomeric and multimeric forms with distinct functions. Severe dengue was associated with a decrease in the 10 kDa VTN isoform. VTN recruitment to injured tissues may contribute to decreased levels in severe cases. It plays a role in both the clotting cascade and vascular extracellular matrix regeneration [234, 235, 236]. According to our findings, VTN showed a “Mean  $\pm$  SEM” value of  $920.2 \pm 69.39$   $\mu\text{g/ml}$  in severe conditions which is almost 1.86 fold lower than the “Mean  $\pm$  SEM” value of  $1679 \pm 50.89$   $\mu\text{g/ml}$  in nonsevere conditions.

VTN revealed 75% sensitivity and almost 92% specificity as shown in Figure 3.7. VTN could successfully identify 15 out of 20 severe dengue cases and 260 cases out of 282 nonsevere dengue cases and could not identify 5 severe cases out of 20 cases. Additional comparisons were made between this VTN and a reported standardized severity nomogram. Nomogram could not identify correctly 3 severe cases out of 20 and 71 nonsevere cases out of 282, the sensitivity and specificity is 85% and 74%. According to this study, the VTN is more effective at detecting dengue severity than the previously published and standardized nomogram.

Human VTN has a high glycosylation level, and changes to its glycan moieties have been linked to human cancer [250, 251]. Using a high-throughput analysis, Mayampurath et al. discovered eight glycopeptides related to vitronectin 13 in human blood; however, they were only able to attach to two of the three N-glycosylation sites of vitronectin [252]. From the typical vitronectin, 15 glycans were identified and reported using a nonspecific digesting method with pronase [253]. The goal of the current study was to characterize patients with Dengue fever based on their glycosylation profiles of human VTN using two distinct lectin-based approaches: DSA (*Datura stramonium* agglutinin) and MAA (*Maackia amurensis* agglutinin). This was the first larger analysis of Dengue-infected patient samples. We were able to collect and visualize secondary antibodies on the control line and VTN on the lectin test line by using gold coupled with anti-VTN antibodies. Concentrations of control line 0.25–2  $\mu\text{g } \mu\text{L}^{-1}$  and concentration of test line 1.25–10  $\mu\text{g } \mu\text{L}^{-1}$  have been tested and detected as shown in Figure 3.12. We have chosen this concentration because titration analysis recommended that lower concentration ensure the clear signal development without saturation and it is suggested that in lateral flow assay antibody should be used in a LFIA which is 10 to 100 times lower than the concentration of analytes present in the plasma of infected patients sample [254, 255]. In the investigation, we showed that lectin binding, including DSA-VTN and MAA-VTN interaction, allowed the lectin-based lateral flow immunoassay method to characterize both severe and non-severe Dengue-infected patients. Our results indicate that DSA-VTN and MAA-VTN interactions are substantially higher in non-severe Dengue patients compared to severe participants (Figure 3.20.). The lectin LFIA technique shows that in nonsevere Dengue patients, the color intensity of lectin binding of VTN increases, suggesting a greater level of VTN concentration in nonsevere Dengue patients, which is also confirmed by VTN ELISA.

The color intensity data intra-assay for MAA in nonsevere cases had a "Mean  $\pm$  SEM" value of  $6.31 \pm 0.007$ ; this was higher than the color intensity data inter-assay for severe Dengue patients, who had a "Mean  $\pm$  SEM" value of  $6.18 \pm 0.02$  for MAA. Whereas, for DSA, the color

intensity data intra-assay for nonsevere patients was  $6.22 \pm 0.004$  higher than the severe Dengue patients with a "Mean  $\pm$  SEM" value of  $6.15 \pm 0.01$ . However, the interassay for MAA showed a coefficient variation in nonsevere Dengue infected patients of 1.07% and in severe with 1.37% whereas DSA showed a coefficient variation in nonsevere inter-assay with 0.72 % and for severe 0.66%. The general guidelines of the value of the coefficient variation of inter-assay and intra-assay should be less than 15% and 10%, acceptable targeted values [256, 257].

The lectin-based point-of-care immunological assay could correctly detect 11 out of 12 severe cases and 74 out of 85 nonsevere cases when employing MAA in the test line; however, DSA could identify 11 severe cases and 71 nonsevere cases. Further comparisons were made between this assay and a previously published, standardized severity nomogram. Nomogram's sensitivity and specificity were 85% and 74%, respectively, although it was unable to accurately identify three out of 20 severe cases and 71 out of 282 nonsevere cases. To ascertain the VTN level, this recently created test was also compared with a conventional ELISA. The specificity and sensitivity of the VTN ELISA were 92% and 75% respectively since it could detect 260 nonsevere cases out of 282 and 15 severe cases out of 20. This study demonstrates that for the detection of Dengue severity and ELISA, a lectin-based point of care is far more effective than an already established nomogram. Initially, a predictive POC test for severe Dengue can be used in the diagnosis process, and individuals can be tested for Dengue infection using a lectin-based Lateral Flow Immunoassay technique.

VTN also has another role. It acts as a complement regulator. Apart from plasma and other bodily fluids, VTN is present in connective tissue and is likely to play a significant role in connections between cells. Similar to clusterin, VTN attaches itself to the developing C5b-7, C5b-8, and C5b-9 complexes to stop them from being incorporated into cell membranes. VTN's N-terminal somatomedin B domain (SMB) controls cell adhesion and migration by binding PAI-1 and the urokinase receptor with great affinity. Since PAI-1's intact reactive center loop spontaneously inserts itself into the primary  $\beta$ -sheet of the molecule, rendering it inactive, it is an unusual member of the serpin family of serine protease inhibitors with an intrinsically short half-life [237].

The clinical spectrum of dengue ranges from mild to severe complications. Understanding the molecular mechanisms underlying the diverse clinical presentations of dengue is crucial for developing effective diagnostic and therapeutic strategies. Dengue virus activates the complement system through different mechanisms. Anti-DENV antibodies can stimulate

complement activation on infected endothelial cells, influencing immune response [238]. Additionally, the lectin pathway of the complement system plays a role in dengue infection, activated by antigen-antibody immune complexes [239]. MBL (Mannan binding lectin) is a key component of the lectin pathway and directly interacts with flaviviruses, such as DENV in vitro [240, 241]. On the surface of the virus, oligosaccharides, or glycoproteins, are recognized by MBL. Numerous studies on different viruses have shown that glycosylation affects the pathogenicity of the virus. Three structural proteins make up each flavivirus particle: the envelope (E), membrane (M), and capsid (C) [242]. The primary envelope glycoprotein on the surface of the virion, the E protein, is responsible for the virus's attachment and fusing onto target cells for successful replication [243]. The N-glycans of the E glycoprotein in virions derived from human hosts versus those from mosquito vectors most likely differ significantly in structure, which may have an impact on the target cell binding and infection efficiency in distinct ways [244]. The majority of virions produced in mammalian cells have complex types of glycans, with the exception of DENV, which has an additional high mannose in the second N-glycosylation site. In contrast, viruses derived from mosquito cells exhibit high-mannose and/or paucimannose glycans with terminal mannose residues [243].

MASP-1 (Mannose-binding lectin serine protease-1) is essential for complement activation, playing a vital role in the innate immune response but still now it is not reported in dengue infection. Recent research has increasingly implicated MASP-1 in the pathogenesis of dengue infection, particularly in severe cases. In this study, LC-MS/MS analysis has demonstrated an upregulation of MASP-1 levels in the plasma of patients with severe dengue infection compared to individuals with nonsevere dengue or healthy controls. This upregulation of MASP-1 suggests its potential involvement in the development of severe dengue complications. It has already been reported that the liver is the targeted organ of the dengue virus and MASP-1 is secreted mainly from the liver cells [239] so, Dengue virus might directly stimulate the production of MASP-1 from infected cells. This enhanced production could contribute to excessive complement activation, leading to inflammation and tissue damage. The overstated immune response observed in severe dengue patients, characterized by cytokine storm and activation of various immune cells, might contribute to increased MASP-1 production. MASP-1 triggers the production of IL-6 and IL-8 [245]. Our lab has previously investigated the production of IL-6 and IL-8 in severe conditions [246]. Additionally, MASP-1's dysregulation could be connected with abnormal immune responses affecting immune cell infiltration and molecular pathways like IL-6/JAK/STAT3 signaling [247]. Over all MASP-

l's role in immune modulation highlights its significance in different pathological and physiological conditions [248]. Dengue infection can damage endothelial cells and the lining of blood vessels. This damage could lead to the release of MASP-1 from these cells [249], further contributing to complement activation and vascular leakage, a hallmark of severe dengue infection. The upregulated MASP-1, in turn, can have several potential consequences in severe dengue like excessive complement activation. MASP-1 may play a central role in activating the complement cascade, leading to the generation of inflammatory mediators and opsonization (tagging) of pathogens for phagocytosis. However, uncontrolled activation of the complement system in severe dengue can lead to excessive inflammation and tissue damage. According to our findings, MASP-1 was significantly overexpressed in severe dengue infection. Severe dengue patients with a "Mean  $\pm$  SEM" value of  $20.12 \pm 0.7427$   $\mu\text{g/ml}$  for MASP-1 which was almost twofold higher than nonsevere dengue patients with a "Mean  $\pm$  SEM" value of  $9.713 \pm 0.4126$ . Western blot analysis also showed the overexpression of MASP-1 in severe dengue conditions. MASP-1 revealed 95% sensitivity and 76% specificity as shown in Figure 3.7. MASP-1 could successfully identify 18 severe cases out of 20 and 210 nonsevere cases out of 282 and could not identify only 2 severe cases out of 20. Additional comparisons were made between this MASP-1 immunoassay and a reported standardized severity nomogram. Nomogram could not identify correctly 3 severe cases out of 20 and 71 nonsevere cases out of 282, the sensitivity and specificity being 85% and 74% whereas MASP-1 could not identify only two severe cases. According to this study, the MASP-1 immunoassay is far more effective at detecting dengue severity than the previously published VTN ELISA and standardized nomogram. The association between MASP-1 upregulation and severe dengue has significant clinical and therapeutic implications. MASP-1 levels could potentially serve as a biomarker for identifying patients at risk of developing severe dengue complications.

Building upon our previous research, we are investigating the development of a more economically viable lateral flow immunoassay. This endeavor involves the conjugation of silver nanoparticles with MASP-1. Literature suggests that MASP-1, another protein identified through LC-MS/MS analysis and confirmed through ELISA and Western blotting, has the capacity to elevate endothelial permeability. This increase in permeability contributes to plasma leakage, a hallmark of severe dengue illness. MASP-1 is primarily explicit in the liver, a primary target organ of the dengue virus. Therefore, this study aims to employ a more affordable lateral flow immunoassay by utilizing MASP-1 in conjunction with synthesized AgNPs within a laboratory setting. The widespread application of AgNPs in diverse fields has



been steadily growing due to their unique properties. These properties have rendered them valuable in various applications, including household products, healthcare, food preservation, environmental conservation, etc.

Initially, AgNPs were synthesized utilizing silver nitrate ( $\text{AgNO}_3$ ) and sodium borohydride ( $\text{NaBH}_4$ ) as a reducing agent [258]. Subsequent to synthesis, the nanoparticles were characterized by using transmission electron microscopy (TEM). TEM analysis revealed that the nanoparticles exhibited a variety of shapes and sizes. In the following step, the nanoparticles were conjugated with an antibody, and this conjugation was characterized by dynamic light scattering (DLS). DLS data indicated a gradual increase in nanoparticle size, suggesting successful binding of the antibody to the silver nanoparticles. Further DLS analysis revealed a polydispersity index (PDI) value of 0.53, indicating a heterogeneous distribution of nanoparticle sizes. To enhance homogeneity, a standard silver dispersion kit was employed. This kit contained AgNPs with a uniform diameter of 20 nm, resulting in a more homogeneous distribution with a PDI value of 0.27. Subsequently, density gradient centrifugation was utilized to isolate nanoparticles based on their size within the synthesized AgNP solution. These separated nanoparticles were then employed as probes for the development of the lateral flow immunoassay. Characterization of the isolated silver nanoparticles by using TEM and DLS revealed a homogeneous distribution with nanoparticle sizes ranging from 10 to 30 nm. The DLS-determined PDI value of 0.27 was consistent with the PDI value of the standard silver dispersion kit. Additional DLS analysis confirmed the successful conjugation of the antibody to the AgNPs. To further validate the DLS findings, an agarose gel electrophoresis assay (AGE) was conducted. AGE results demonstrated that unconjugated AgNPs migrated at a faster rate compared to both antibody-conjugated AgNPs and analyte-bound antibody-conjugated AgNPs. This suggests that the unconjugated AgNPs were smaller in size, enabling them to travel the gel matrix more rapidly. The slower migration of antibody-conjugated AgNPs compared to unconjugated AgNPs suggests that the conjugation process increases the overall size of the nanoparticles. Analyte-bound antibody-conjugated AgNPs exhibited the slowest migration, indicating the successful binding of both the antibody and analyte to the AgNPs. Subsequently, the various components of the lateral flow immunostrip were assembled for the detection of MASP-1 in dengue-infected patients. Antibody-conjugated silver nanoparticles were incorporated into the conjugate pad of the LFIA strip. The patient sample was applied to the sample pad, allowing it to flow towards the conjugate pad. The antibody-conjugated silver nanoparticles bound to the target analytes present in the sample, formed complexes that

migrated towards the test line. The test line, precoated with antibodies, reacted with the complexes, resulting in the appearance of a brown-colored line. In this study, we successfully optimized the antibody concentrations used for the control and test lines. The primary objective of this research was to differentiate between severe and non-severe dengue patients based on the presence of MASP-1 in confirmed dengue cases. By utilizing silver-united anti-MASP-1 antibodies, we were able to detect and visualize secondary antibodies on the control line and MASP-1 antibodies on the test line. Various test line concentrations ranging from were evaluated and found to be perceptible, as illustrated in Figure 3.19. The selection of this concentration range was informed by titration analysis, which suggested that lower concentrations promote clear signal development without saturation. Additionally, it is recommended that the antibody concentration in lateral flow assays be 10 to 100 times lower than the analyte concentration present in the plasma of infected patients [254, 255]. In this investigation, we demonstrated that the MASP-1-based lateral flow immunoassay system is capable of differentiating between severe and non-severe dengue-infected patients. Our findings indicate that the interaction between AgNPs-conjugated MASP-1 and target analytes is significantly higher in severe dengue patients compared to non-severe cases (Figure 3.20). The LFIA technique revealed that severe dengue patients exhibit a more intense color reaction resulting from the binding of AgNPs-conjugated MASP-1 to analytes. This suggests a higher concentration of MASP-1 in severe dengue patients, a finding that was further confirmed by MASP-1 ELISA and Western blotting.

Intra-assay analysis of color intensity data for MASP-1 in non-severe cases revealed a Mean  $\pm$  SEM value of  $2.963 \pm 0.01$ . This value was slightly higher than the inter-assay color intensity data for non-severe dengue patients, which exhibited a Mean  $\pm$  SEM value of  $2.96 \pm 0.01$ . Conversely, the inter-assay color intensity result for severe patients was  $3.33 \pm 0.04$  lower than the intra-assay result for severe dengue patients, with a Mean  $\pm$  SEM value of  $3.34 \pm 0.04$ . Inter-assay coefficient variation for MASP-1 in non-severe and severe dengue-infected patients was 7.02% and 6.19%, respectively. Intra-assay coefficient variation for non-severe and severe cases was 7.08% and 6.21% respectively. General guidelines suggest that acceptable target values for inter-assay and intra-assay coefficient variation should be less than 15% and 10%, respectively [256, 257]. The MASP-1-based point-of-care (PoC) immunoassay correctly identified 18 out of 20 severe cases and 249 out of 282 non-severe dengue cases. Comparative analysis was conducted between this assay and a previously published, standardized dengue severity nomogram. The nomogram demonstrated a sensitivity of 85% and a specificity of 74%

but inappropriately classified three of 20 severe cases and 71 of 282 non-severe cases. To validate the MASP-1 levels, the newly developed test was compared with a conventional ELISA. The MASP-1 ELISA exhibited a specificity of 95% and a sensitivity of 74%, correctly diagnosing 210 non-severe cases out of 282 and 19 severe cases out of 20. In this study, we observed that while the MASP-1 ELISA miss-classified one severe case and Seventy-one non-severe cases, the MASP-1 LFIA miss-classified two severe cases and thirty-three non-severe cases. This study highlights that MASP-1-based and lectin-based point-of-care assays are significantly more effective than established nomograms for diagnosing dengue severity and using ELISA. Initially, a predictive point-of-care test for severe dengue can be employed in the diagnostic process. Subsequently, individuals can be further evaluated for dengue infection using lectin-based and MASP-1-based lateral flow immunoassay techniques.

Comparative analysis in between AuNPs-based and AgNPs-based LFIA demonstrated the superior performance of AgNPs as probes. The development of AgNPs-based LFIA is significantly more straightforward and economical than its AuNPs-based LFIA counterpart. Recent research has highlighted a rising preference for AgNPs due to their unique properties, including enhanced electrochemical activity.

Despite progress in applying these biomarkers to check the severity of dengue infection, further research is needed to fully understand the complex role of MASP-1 and VTN in dengue pathogenesis. Some key challenges include deciphering the exact mechanisms leading to MASP-1 upregulation and VTN, TSP-1 downregulation and its precise contribution to various pathological processes in severe dengue is crucial. Translating promising preclinical findings into safe and effective therapeutic interventions for human patients necessitates rigorous clinical trials. For lateral Flow Immunoassay, further validation is required before any of these biomarkers can be formulated as prognostic tests. A dengue diagnostic test and a prognostic POC test should ideally be used together for severe dengue cases. Patients who have a positive dengue test can then undergo a severity test. Patients who are at a high risk of developing a serious illness may be admitted to the hospital and closely watched by a doctor. Patients at low risk of serious illness and without clinical warning signals, however, can be sent home with greater confidence to recover.

## **CHAPTER - 5**

### **Summary & Future directions**

A major worldwide health problem is still dengue, a virus spread by mosquitoes that is most common in tropical and subtropical areas. Proper diagnosis of dengue severity in a timely manner is essential for efficient care and averting sequelae. Even though they are useful, traditional diagnostic techniques frequently lack the sensitivity and specificity needed to identify severe illnesses in their early stages. A new strategy that combines the measurement of platelet counts and thrombopoietin (TSP-1) levels has shown promise, according to recent studies. A remarkably substantial correlation between TSP-1 and platelet levels and the severity of dengue infections has been found using CombiROC analysis, a statistical approach used to assess the performance of diagnostic procedures. When compared to current diagnostic techniques, the combination of TSP-1 and platelet levels has many advantages. Its sensitivity and specificity are extraordinarily high, over 100%. In other words, there is less chance of false positives or negatives because the test can correctly identify people who have severe dengue as well as those who do not. The test only needs a blood sample and a laboratory analysis, making it very easy to do. It can therefore be applied in a variety of healthcare environments, including those with few resources. Although the initial results are encouraging, more investigation is required to confirm the therapeutic usefulness of the TSP-1 and platelet combination for dengue severity prediction. Extensive research with a variety of patient populations is required to verify the constancy of the observed correlation and assess the test's efficacy across various geographic contexts. Furthermore, research into the molecular pathways that connect TSP-1 and platelet counts to dengue severity may yield important new understandings of the disease's etiology. The combination of TSP-1 and platelet counts has the potential to completely change dengue treatment if it is shown through thorough clinical trials. Healthcare professionals can minimize mortality and morbidity by implementing focused treatments to enable early identification of individuals at risk of severe disease. This novel strategy underscores the value of biomarker-based diagnostics for better patient outcomes and is a major advancement in the fight against dengue.

The viral disease dengue, which is spread by mosquitoes, is a serious threat to international health, especially in tropical and subtropical areas. Timely and precise diagnosis is essential for efficient care and averting serious consequences. Even if they are trustworthy, traditional

diagnostic techniques are typically unavailable in environments with limited resources since they need laboratory space and skilled staff. A unique strategy using lectin-based Lateral Flow Immunoassay (LFIA) is being investigated as a solution to this problem.

Proteins called lectins attach themselves to particular carbohydrate structures. This technology has many benefits, such as being inexpensive, simple to use, and able to produce results quickly. The lectin-based LFIA can be used as a screening method to determine who has a Dengue infection, to start. In order to determine the likelihood of contracting a more severe form of the disease, a predictive POC test for severe Dengue can be given if the results are positive. Healthcare resources can be allocated more effectively. In this study, the lectin-based LFIA successfully detected glycoprotein i.e. VTN in the plasma sample of dengue-infected patients and predicted the severity of dengue infection. By providing rapid, accurate, and accessible diagnostics, this technology has the potential to improve patient outcomes and contribute to the global efforts to combat Dengue.

The current work emphasizes how important MASP-1 protein, which acts as a lectin, is to the pathophysiology of dengue infection, especially in severe cases. According to our research, patients with severe dengue illness had significantly higher levels of MASP-1 than patients with less severe infection. This finding raises the possibility that MASP-1 could be used as a biomarker to guide therapeutic measures and develop a MASP-1-based LFIA that can forecast the severity of a disease. LFIA tests may offer quick and precise answers at the point of care (POC) by utilizing their capacity to identify distinct glycan patterns linked to Dengue infection.

Although conventional biochemical criteria have been utilized as markers of dengue severity at the later stage of infection our investigation exposes their shortcomings in delivering prompt and precise evaluations within 4 to 5 days. The potential of MASP-1 as a more sensitive and specific marker for the course of the disease is highlighted by the early and substantial elevation of these levels in individuals with severe dengue. Additionally, our study has effectively shown that creating a lateral flow immunoassay with MASP-1 antibody-conjugated silver nanoparticles is feasible. This diagnostic tool has the potential to provide a quick, point-of-care method for identifying dengue early and determining its severity. Through the utilization of lateral flow technology and the special qualities of MASP-1, this immunoassay has the potential to greatly enhance patient outcomes and management.

In conclusion, the upregulation of MASP-1 in dengue infection, coupled with its potential as a biomarker for disease severity and the successful development of a lateral flow immunoassay,

presents promising avenues for advancing dengue research and clinical care. Continued investigations into the underlying mechanisms of MASP-1 dysregulation and its contribution to severe dengue complications are warranted. By elucidating these pathways, we can pave the way for the development of novel therapeutic strategies that target MASP-1 or its downstream signaling pathways, potentially improving clinical outcomes for patients with this enervating disease.

There is a great chance to include potential biomarkers employing gold and silver nanoparticles into POC immunoassay after they have been discovered. The development of sensitive and quick point-of-care (POC) immunoassays has been demonstrated by the use of gold and silver nanoparticles in electrochemical bioassays. These nanoparticles are perfect for biosensing applications because of their special qualities, which include good conductivity, biocompatibility, and simplicity of functionalization. Numerous research avenues are essential to improve these technologies' functionality and applicability even more. One important development in diagnostic technology is the capacity to identify many analytes at once in a single experiment i.e. multiplex assays.

**Multiplexing:** Multiplex assays provide a complete approach for illnesses with complicated pathophysiology, like dengue, where several variables might influence disease severity. Because of their speed and ease of use, lateral flow immunoassays (LFAs) make excellent candidates for multiplexing integration. In LFAs, multiplexing entails adding several test lines, each intended to detect a distinct biomarker, on a single strip. Analytes of different kinds can be distinguished from one another by coupling different kinds of nanoparticles or by utilizing nanoparticles with unique optical characteristics. For example, one test line may utilize gold nanoparticles, while other test lines may use silver or colored nanoparticles.

**Nanoparticle engineering:** The efficacy of gold and silver nanoparticles in immunoassays can be improved by adjusting their size, shape, and surface functionalization. Anisotropic nanoparticles, for instance, have special optical features that make them useful for improving sensitivity.

**Core-shell structures:** Developing core-shell nanoparticles with increased biocompatibility and conductivity can boost the sensor's overall performance. For instance, a silica core can enhance stability and bioconjugation, whereas a gold core with a silver shell can offer greater conductivity and biocompatibility.

**Electrode Material and Fabrication:** Selectivity and sensitivity can be increased by investigating electrode materials other than conventional gold and carbon, such as conducting polymers, graphene, and nanostructured materials. For example, graphene is a great choice for electrochemical sensing due to its enormous surface area and good conductivity. Creating integrated, low-cost, and miniaturized electrochemical sensors requires the development of sophisticated microfabrication processes. Complex electrode architectures can be precisely fabricated with the use of methods like soft lithography and 3D printing. Signal amplification can be improved and surface area can be increased by designing three-dimensional electrode designs. Using a variety of materials and production techniques, porous or hierarchical structures can be created to accomplish this.

**Integration with Microfluidics and Lab-on-a-Chip Devices:** Combining microfluidic platforms and electrochemical bioassays can produce completely automated, portable POC instruments. Microfluidics makes it possible to precisely manage sample handling and fluid flow, which improves performance and repeatability.

**Clinical Validation and Implementation:** To assess the new POC immunoassays' diagnostic accuracy, sensitivity, and specificity, comprehensive clinical studies must be conducted rigorously. In practical contexts, this will guarantee the device's dependability and efficacy. It is essential to provide interfaces that are both simple to use and intuitive for healthcare providers and patients to utilize at the point of treatment. The tool should be simple to use and understand in order to reduce mistakes and guarantee accurate findings.

To guarantee that the gadgets are widely accessible, it is imperative to develop manufacturing techniques that are both scalable and economical. Because of this, both rich and underdeveloped nations will be able to afford the POC immunoassays.

**Integration of artificial intelligence for data analysis and interpretation:** Artificial intelligence (AI) has the potential to completely transform healthcare when it is included in diagnostic platforms. 1. Artificial intelligence (AI) can greatly improve data analysis and interpretation in the field of point-of-care immunoassays. Artificial intelligence (AI) systems can detect patterns, correlations, and trends in complex datasets produced by these tests that may be invisible to human researchers. 2. This feature is especially helpful for diseases like dengue, which has complex pathophysiologies and many biomarkers that influence the severity of the disease. AI can be used to create predictive models that link biomarker profiles to the course of a disease, improving prognosis and diagnosis. Moreover, interpreting lateral flow

assays can be automated by AI-powered picture analysis, which lowers inter-observer variability and boosts productivity. Clinical decision-making will surely become more precise, instructive, and timely as AI develops and is included in point-of-care diagnostics.

By concentrating on these areas, scientists can enhance public health outcomes and hasten the creation of efficient point-of-care (POC) instruments for assessing dengue severity.



## References

1. Tsai, P. J., & Teng, H. J. (2016). Role of *Aedes aegypti* (Linnaeus) and *Aedes albopictus* (Skuse) in local dengue epidemics in Taiwan. *BMC infectious diseases*, 16, 1-20.
2. Ross, T. M. (2010). Dengue virus. *Clinics in laboratory medicine*, 30(1), 149-160.
3. Ross, T. M. (2010). Dengue virus. *Clinics in laboratory medicine*, 30(1), 149-160.
4. Falgout B., Pethel M., Zhang Y.M., Lai C.J. Both nonstructural proteins NS2B and NS3 are required for the proteolytic processing of dengue virus nonstructural proteins. *J. Virol.* 1991;65(5):2467–2475. [PMC free article] [PubMed] [Google Scholar] [Ref list]
5. Winkler G., Randolph V.B., Cleaves G.R., Ryan T.E., Stollar V. Evidence that the mature form of the flavivirus nonstructural protein NS1 is a dimer. *Virology*. 1988;162(1):187–196.
6. Muller D.A., Corrie S.R., Coffey J., Young P.R., Kendall M.A. Surface modified microprojection arrays for the selective extraction of the dengue virus NS1 protein as a marker for disease. *Anal. Chem.* 2012;84(7):3262–3268. doi: 10.1021/ac2034387
7. Xie X., Gayen S., Kang C., Yuan Z., Shi P.Y. Membrane topology and function of dengue virus NS2A protein. *J. Virol.* 2013;87(8):4609–4622. doi: 10.1128/JVI.02424-12.
8. Ashour J., Laurent-Rolle M., Shi P.Y., Garcia-Sastre A. NS5 of dengue virus mediates STAT2 binding and degradation. *J. Virol.* 2009;83(11):5408–5418. doi: 10.1128/JVI.02188-08.
9. [https://en.wikipedia.org/wiki/Dengue\\_fever](https://en.wikipedia.org/wiki/Dengue_fever)
10. <https://www.britannica.com/science/dengue>
11. SMITH CEG. The history of dengue in tropical Asia and its probable relationship to the mosquito *Aedes aegypti*. *J Trop Med Hyg* [Internet]. 1956 Oct [cited 2017 Oct 2];59(10):243–51. Available from: <http://www.ncbi.nlm.nih.gov/pubmed/13368255>
12. Halstead SB. Dengue. *Lancet* [Internet]. 2007 Nov 10 [cited 2017 Oct 2];370(9599):1644–52. Available from: <http://www.ncbi.nlm.nih.gov/pubmed/17993365>.
13. Kraemer MU, Sinka ME, Duda KA, Mylne AQ, Shearer FM, Barker CM, et al. The global distribution of the arbovirus vectors *Aedes aegypti* and *Ae. albopictus*. *Elife* [Internet].

2015 Jun 30 [cited 2017 Oct 2];4:e08347. Available from: <http://www.ncbi.nlm.nih.gov/pubmed/26126267>

14. Rodhain F, Rosen L. Mosquito vectors and dengue virus-vector relationships. In: Gubler DJ, Kuno G. Eds. Dengue and Dengue Haemorrhagic Fever. London: CAB International. 1997. p. 45–60.
15. Soundravally R, Hoti SL. Polymorphisms of the TAP 1 and 2 gene may influence clinical outcome of primary dengue viral infection. Scand J Immunol. 2008 June; 67(6): 618–25.
16. Chaturvedi U, Nagar R, Shrivastava R. Dengue and dengue haemorrhagic fever: Implications of host genetics. FEMS Immunol Med Mic. 2006; 47:155–166.
17. Wagenaar JFP, Mairuhu ATA, van Gorp ECM. Genetic influences on dengue virus infections. Dengue Bulletin. 2004; 28: 126–134.
18. Schnoor JL. The IPCC fourth assessment. Environ Sci Technol. 2007; 41: 1503.
19. Kyle JL, Harris E. Global spread and persistence of dengue. Annu Rev Microbiol. 2008; 62: 71–92.
20. Focks D, Barrera R. Dengue transmission dynamics: assessment and implications for control. In: Report of the scientific working group meeting on dengue, 1–5 October 2006. pp. 92–108. Geneva: WHO, 2007. Document No. TDR/SWG/08.
21. Morin, C. W., Comrie, A. C., & Ernst, K. (2013). Climate and dengue transmission: evidence and implications. *Environmental health perspectives*, 121(11-12), 1264-1272.
22. hoy, O. M. Sessions, D. J. Gubler, and E. E. Ooi, “Production of infectious dengue virus in *Aedes aegypti* is dependent on the ubiquitin proteasome pathway,” PLoS Neglected Tropical Diseases, vol. 9, no. 11, article e0004227, 2015.
23. N. B. Tjaden, S. M. Thomas, D. Fischer, and C. Beierkuhnlein, “Extrinsic incubation period of dengue: knowledge, backlog, and applications of temperature dependence,” PLoS Neglected Tropical Diseases, vol. 7, no. 6, 2013.
24. N. Nanaware, A. Banerjee, S. M. Bagchi, P. Bagchi, and A. Mukherjee, “Dengue virus infection: a tale of viral exploitations and host responses,” Viruses, vol. 13, no. 10, p. 1967, 2021.

25. E. G. Westaway, A. A. Khromykh, and J. M. Mackenzie, "Nascent Flavivirus RNA Colocalized \_in Situ\_ with Double-Stranded RNA in Stable Replication Complexes," *Virology*, vol. 258, no. 1, pp. 108–217, 1999.
26. V. Raquin and L. Lambrechts, "Dengue virus replicates and accumulates in *Aedes aegypti* salivary glands," *Virology*, vol. 507, pp. 75–81, 2017
27. Wu, S. J., G. Grouard-Vogel, et al. (2000). "Human skin Langerhans cells are targets of dengue virus infection." *Nat Med* **6**(7): 816-820.
28. Malasit, P. (1987). "Complement and dengue haemorrhagic fever/shock syndrome." *Southeast Asian J Trop Med Public Health* **18**(3): 316-320.
29. Halstead, S. B. (1992). "The XXth century dengue pandemic: need for surveillance and research." *World Health Stat Q* **45**(2-3): 292-298.
30. Mackenzie, J. S., D. J. Gubler, et al. (2004). "Emerging flaviviruses: the spread and resurgence of Japanese encephalitis, West Nile and dengue viruses." *Nat Med* **10**(12 Suppl): S98-109.
31. Dengue-National-Guidelines-2014 full.pdf. 2014.
32. Bhatt S, Gething PW, Brady OJ, Messina JP, Farlow AW MC, Et.al. The global distribution and burden of dengue. *Nature*. (496):504–7.
33. Brady OJ, Gething PW, Bhatt S, Messina JP, Brownstein JS, Hoen AG, et al. Refining the Global Spatial Limits of Dengue Virus Transmission by Evidence-Based Consensus. Reithinger R, editor. *PLoS Negl Trop Dis* [Internet]. 2012 Aug 7 [cited 2017 Oct 1];6(8):e1760. Available from: <http://dx.plos.org/10.1371/journal.pntd.0001760>
34. Wu W., Bai Z., Zhou H., Tu Z., Fang M., Tang B., et al. 2011. Molecular epidemiology of dengue viruses in southern China from 1978 to 2006. *Viol. J.* **8**(1): 322.
35. Rush B. 1951. An account of the bilious remitting fever: As it appeared in philadelphia, in the summer and autumn of the year 1780. *Am. J. Med.* **11**(5): 546–550.
36. WHO. Prevention and control of dengue and dengue haemorrhagic fever. 2003.
37. PAHO. 2019. Epidemiological update: dengue. PAHO/WHO, Washington. Available from [https://www.paho.org/hq/index.php?option=com\\_content&view=article&id=15360-9-](https://www.paho.org/hq/index.php?option=com_content&view=article&id=15360-9-)

august-2019-dengue-epidemiological-update&Itemid=42346&lang=en [accessed August 21 2020].

38. Were F. 2012. The dengue situation in Africa. *Paediatr. Int. Child Health*, **32**(sup1): 18–21.
39. Ooi E.E. and Gubler D.J. 2009. Dengue in Southeast Asia: epidemiological characteristics and strategic challenges in disease prevention. *Cad. Saúde Pública*, **25**: S115–S124.
40. Gubler D.J. 1998. Dengue and dengue hemorrhagic fever. *Clin. Microbiol. Rev.* **11**(3): 480–496
41. Ooi E.E. and Gubler D.J. 2009. Dengue in Southeast Asia: epidemiological characteristics and strategic challenges in disease prevention. *Cad. Saúde Pública*, **25**: S115–S124.
42. Taslim M., Arsunan A.A., Ishak H., Nasir S., and Usman A.N. 2018. Diversity of dengue virus serotype in endemic region of South Sulawesi Province. *J. Trop. Med.* **2018**: 9682784.
43. Kimura R. 1944. Inoculation of dengue virus into mice. *Nihon IgakuHoshasen Gakkai Zasshi*. **3379**: 629–633.
44. Hotta S. 1952. Experimental studies on dengue: I. Isolation, identification and modification of the virus. *J. Infect. Dis.* **90**(1): 1–9
45. Mustafa M.S., Rasotgi V., Jain S., and Gupta V. 2015. Discovery of fifth serotype of dengue virus (DENV-5): A new public health dilemma in dengue control. *Med. J. Armed Forces India*, **71**(1): 67–70.
46. National Vector Borne Disease Control Programme (NVBDPC). 2021. Government of India. Available from <https://nvbdcp.gov.in/index4.php?lang=1&level=0&linkid=431&lid=3715> [accessed August 20 2020].
47. R. George and L. Lum, *Clinical Spectrum of Dengue Infection. Dengue and Dengue Haemorrhagic Fever*, CAB International, New York, 1997.

48. Htun, N. S. N., Odermatt, P., Eze, I. C., Boillat-Blanco, N., D'Acremont, V., & Probst-Hensch, N. (2015). Is diabetes a risk factor for a severe clinical presentation of dengue?—review and meta-analysis. *PLoS neglected tropical diseases*, 9(4), e0003741.
49. World Health Organization. Dengue: guidelines for diagnosis, treatment, prevention and control. World Health Organization, Geneva (2009)
50. C.P. Simmons, J.J. Farrar, V.V. Nguyen, B. Wills Dengue *N Engl J Med*, 366 (2012), pp. 1423-1432.
51. A. Srikiatkachorn, A. Krautrachue, W. Ratanaprakarn, L. Wongtapradit, N. Nithipanya, S. Kalayanarooj, *et al.* Natural history of plasma leakage in dengue hemorrhagic fever: a serial ultrasonic study *Pediatr Infect Dis J*, 26 (2007), pp. 283-290
52. S. Kalayanarooj, D.W. Vaughn, S. Nimmannitya, S. Green, S. Suntayakorn, N. Kunentrasai, *et al.* Early clinical and laboratory indicators of acute dengue illness *J Infect Dis*, 176 (1997), pp. 313-321.
53. S. Nimmannitya Clinical spectrum and management of dengue haemorrhagic fever *Southeast Asian J Trop Med Public Health*, 18 (1987), pp. 392-397
54. S. Nimmannitya, S.B. Halstead, S.N. Cohen, M.R. Margiotta Dengue and chikungunya virus infection in man in Thailand, 1962–64. Observations on hospitalized patients with haemorrhagic fever *Am J Trop Med Hyg*, 18 (1969), pp. 954-971
55. S. Kalayanarooj, D.W. Vaughn, S. Nimmannitya, S. Green, S. Suntayakorn, N. Kunentrasai, *et al.* Early clinical and laboratory indicators of acute dengue illness *J Infect Dis*, 176 (1997), pp. 313-321.
56. I.K. Lee, W.H. Lee, J.W. Liu, K.D. Yang Acute myocarditis in dengue hemorrhagic fever: a case report and review of cardiac complications in dengue-affected patients *Int J Infect Dis*, 14 (2010), pp. e919-e922.
57. I.K. Lee, J.W. Liu, K.D. Yang Clinical characteristics, risk factors, and outcomes in adults experiencing dengue hemorrhagic fever complicated with acute renal failure *Am J Trop Med Hyg*, 80 (2009), pp. 651-655
58. World Health Organization (24 November 2023). "Meeting of the Strategic Advisory Group of Experts on Immunization, September 2023: conclusions and recommendations". *Weekly Epidemiological Record*. **98** (47): 599–620. hdl:10665/374327

59. Freedman DO (November 2023). "A new dengue vaccine (TAK-003) now WHO recommended in endemic areas; what about travellers?". *J Travel Med.* **30** (7): 1–3. doi:10.1093/jtm/taad132. PMID 37847608
60. <https://www.who.int/news-room/questions-and-answers/item/dengue-vaccines>.
61. <https://www.ema.europa.eu/en/medicines/human/EPAR/qdenga>
62. <https://www.who.int/news/item/15-05-2024-who-prequalifies-new-dengue-vaccine>
63. <https://timesofindia.indiatimes.com/city/lucknow/two-pharma-cos-set-to-begin-3rd-phase-of-human-trials-for-dengue-vaccine/articleshow/105506852.cms>
64. Alves AMB, Costa SM, Pinto PBA. Dengue Virus and Vaccines: How Can DNA Immunization Contribute to This Challenge? *Front Med Technol.* 2021 Apr 12;3:640964. doi: 10.3389/fmedt.2021.640964. PMID: 35047911; PMCID: PMC8757892.
65. <https://pib.gov.in/PressReleasePage.aspx?PRID=2045090>
66. Janeway Jr, C. A., Travers, P., Walport, M., & Shlomchik, M. J. (2001). The complement system and innate immunity. In *Immunobiology: The Immune System in Health and Disease. 5th edition*. Garland Science.
67. Dunkelberger, J. R., & Song, W. C. (2010). Complement and its role in innate and adaptive immune responses. *Cell research*, 20(1), 34-50.
68. Conde, J. N., Silva, E. M., Barbosa, A. S., & Mohana-Borges, R. (2017). The complement system in flavivirus infections. *Frontiers in microbiology*, 8, 213.
69. Beltrame, M. H., Catarino, S. J., Goeldner, I., Boldt, A. B. W., & de Messias-Reason, I. J. (2015). The lectin pathway of complement and rheumatic heart disease. *Frontiers in pediatrics*, 2, 148.
70. [https://en.wikipedia.org/wiki/Lectin\\_pathway](https://en.wikipedia.org/wiki/Lectin_pathway).
71. Bayly-Jones, C., Bubeck, D., & Dunstone, M. A. (2017). The mystery behind membrane insertion: a review of the complement membrane attack complex. *Philosophical Transactions of the Royal Society B: Biological Sciences*, 372(1726), 20160221.
72. Carr, J. M., Cabezas-Falcon, S., Dubowsky, J. G., Hulme-Jones, J., & Gordon, D. L. (2020). Dengue virus and the complement alternative pathway. *FEBS letters*, 594(16), 2543-2555.

73. Ricklin D., Hajishengallis G., Yang K., Lambris J.D. Complement: a key system for immune surveillance and homeostasis. *Nat. Immunol.* 2010;11:785–797. doi: 10.1038/ni.1923
74. Kjaer T.R., Thiel S., Andersen G.R. Toward a structure-based comprehension of the lectin pathway of complement. *Mol. Immunol.* 2013;56:413–422. doi: 10.1016/j.molimm.2013.05.007
75. Ricklin D., Hajishengallis G., Yang K., Lambris J.D. Complement: a key system for immune surveillance and homeostasis. *Nat. Immunol.* 2010;11:785–797. doi: 10.1038/ni.1923.
76. Matsushita M., Fujita T. Activation of the classical complement pathway by mannose-binding protein in association with a novel C1s-like serine protease. *J. Exp. Med.* 1992;176:1497–1502. doi: 10.1084/jem.176.6.1497.
77. Henriksen M.L., Brandt J., Andrieu J.-P., Nielsen C., Jensen P.H., Holmskov U., Jorgensen T.J.D., Palarasah Y., Thielens N.M., Hansen S. Heteromeric complexes of native collectin kidney 1 and collectin liver 1 are found in the circulation with MASPs and activate the complement system. *J. Immunol.* 2013;191:6117–6127. doi: 10.4049/jimmunol.1302121
78. Kjaer T.R., Thiel S., Andersen G.R. Toward a structure-based comprehension of the lectin pathway of complement. *Mol. Immunol.* 2013;56:413–422. doi: 10.1016/j.molimm.2013.05.007.
79. Degn S.E., Jensen L., Hansen A.G., Duman D., Tekin M., Jensenius J.C., Thiel S. Mannan-binding lectin-associated serine protease (MASP)-1 is crucial for lectin pathway activation in human serum, whereas neither MASP-1 nor MASP-3 is required for alternative pathway function. *J. Immunol.* 2012;189:3957–3969. doi: 10.4049/jimmunol.1201736.
80. Dahl M.R., Thiel S., Matsushita M., Fujita T., Willis a.C., Christensen T., Vorup-Jensen T., Jensenius J.C. MASP-3 and its association with distinct complexes of the mannan-binding lectin complement activation pathway. *Immunity.* 2001;15:127–135.
81. Thiel S. Complement activating soluble pattern recognition molecules with collagen-like regions, mannan-binding lectin, ficolins and associated proteins. *Mol. Immunol.* 2007;44:3875–3888. doi: 10.1016/j.molimm

82. Knittel T., Fellmer P., Neubauer K., Kawakami M., Grundmann A., Ramadori G. The complement-activating protease P100 is expressed by hepatocytes and is induced by IL-6 in vitro and during the acute phase reaction in vivo. *Lab. Investig.* 1997;77:221–230.
83. Thiel S., Jensen L., Degn S.E., Nielsen H.J., Gál P., Dobó J., Jensenius J.C. Mannan-binding lectin (MBL)-associated serine protease-1 (MASP-1), a serine protease associated with humoral pattern-recognition molecules: normal and acute-phase levels in serum and stoichiometry of lectin pathway components. *Clin. Exp. Immunol.* 2012;169:38–48. doi: 10.1111/j.1365-2249.2012.04584.x.
84. Frauenknecht V., Thiel S., Storm L., Meier N., Arnold M., Schmid J.-P., Saner H., Schroeder V. Plasma levels of mannan-binding lectin (MBL)-associated serine proteases (MASPs) and MBL-associated protein in cardio- and cerebrovascular diseases. *Clin. Exp. Immunol.* 2013;173:112–120. doi: 10.1111/cei.12093.
85. Saeed a, Baloch K., Brown R.J.P., Wallis R., Chen L., Dexter L., McClure C.P., Shakesheff K., Thomson B.J. Mannan binding lectin-associated serine protease 1 is induced by hepatitis C virus infection and activates human hepatic stellate cells. *Clin. Exp. Immunol.* 2013;174:265–273. doi: 10.1111/cei.12174.
86. Degn S.E., Jensen L., Hansen A.G., Duman D., Tekin M., Jensenius J.C., Thiel S. Mannan-binding lectin-associated serine protease (MASP)-1 is crucial for lectin pathway activation in human serum, whereas neither MASP-1 nor MASP-3 is required for alternative pathway function. *J. Immunol.* 2012;189:3957–3969. doi: 10.4049/jimmunol.1201736.
87. Megyeri M., Harmat V., Major B., Végh Á., Balczer J., Héja D., Szilágyi K., Datz D., Pál G., Závodszy P., Gál P., Dobó J. Quantitative characterization of the activation steps of mannan-binding lectin (MBL)-associated serine proteases (MASPs) points to the central role of MASP-1 in the initiation of the complement lectin pathway. *J. Biol. Chem.* 2013;288:8922–8934. doi: 10.1074/jbc.M112.446500.
88. Krarup A., Gulla K.C., Gál P., Hajela K., Sim R.B. The action of MBL-associated serine protease 1 (MASP1) on factor XIII and fibrinogen. *Biochim. Biophys. Acta.* 2008;1784:1294–1300. doi: 10.1016/j.bbapap.2008.03.020.
89. Megyeri M., Makó V., Beinrohr L., Doleschall Z., Prohászka Z., Cervenak L., Závodszy P., Gál P. Complement protease MASP-1 activates human endothelial cells: PAR4



activation is a link between complement and endothelial function. *J. Immunol.* 2009;183:3409–3416. doi: 10.4049/jimmunol.0900879.

90. Jani P.K., Kajdácsi E., Megyeri M., Dobó J., Doleschall Z., Futosi K., Tímár C.I., Mócsai A., Makó V., Gál P., Cervenak L. MASP-1 induces a unique cytokine pattern in endothelial cells: a novel link between complement system and neutrophil granulocytes. *PLoS ONE*. 2014;9:e87104. doi: 10.1371/journal.pone.0087104.
91. Boyd, N. A., Bradwell, A. R., & Thompson, R. A. (1993). Quantitation of vitronectin in serum: evaluation of its usefulness in routine clinical practice. *Journal of clinical pathology*, 46(11), 1042-1045.
92. Inuzuka, S., Ueno, T., Torimura, T., Tamaki, S., Sakata, R., Sata, M., ... & Tanikawa, K. (1992). Vitronectin in liver disorders: biochemical and immunohistochemical studies. *Hepatology*, 15(4), 629-636.
93. Yi, M., Sakai, T., Fässler, R., & Ruoslahti, E. (2003). Antiangiogenic proteins require plasma fibronectin or vitronectin for in vivo activity. *Proceedings of the National Academy of Sciences*, 100(20), 11435-11438.
94. Keasey, M. P., Jia, C., Pimentel, L. F., Sante, R. R., Lovins, C., & Hagg, T. (2018). Blood vitronectin is a major activator of LIF and IL-6 in the brain through integrin–FAK and uPAR signaling. *Journal of cell science*, 131(3), jcs202580.
95. Peng, L., Bhatia N., Parker, A. C., Zhu, Y., & Fay, W. P. (2002). Endogenous vitronectin and plasminogen activator inhibitor-1 promote neointima formation in murine carotid arteries. *Arteriosclerosis, thrombosis, and vascular biology*, 22(6), 934-939.
96. Milis, L., Morris, C. A., Sheehan, M. C., Charlesworth, J. A., & Pussell, B. (1993). Vitronectin-mediated inhibition of complement: evidence for different binding sites for C5b-7 and C9. *Clinical & Experimental Immunology*, 92(1), 114-119.
97. Preissner KT. Structure and biological role of vitronectin. *Annu Rev Cell Biol* 1991; 7:275-310.
98. Tschopp J, Masson D. Inhibition of the lytic activity of perforin (cytolysin) and of late complement components by proteoglycans. *Molecular Immunol* 1987; 24:907-13.
99. Pussell BA, Morris CA, Milis L et al. Inhibition of complement by protamine sulphate. *Proc 16th. Int Complement Workshop, Cambridge, UK. Complement Inflamm* 1992; 8:214.

100. Tschopp J, Mollnes TE. Antigenic crossreactivity of the alpha subunit of complement component C8 with the cysteine rich domain shared by complement component C9 and low density lipoprotein receptor. *Proc Nat Acad Sci USA* 1986; 83:4223-9.
101. Preissner, K. T., & Reuning, U. (2011, June). Vitronectin in vascular context: facets of a multitasking matricellular protein. In *Seminars in thrombosis and hemostasis* (Vol. 37, No. 04, pp. 408-424). © Thieme Medical Publishers.
102. Savage, B., & Ruggeri, Z. M. (2007). Platelet thrombus formation in flowing blood. *Platelets*, 359-367.
103. Reheman, A., Gross, P., Yang, H., Chen, P., Allen, D., Leytin, V., ... & Ni, H. (2005). Vitronectin stabilizes thrombi and vessel occlusion but plays a dual role in platelet aggregation. *Journal of Thrombosis and Haemostasis*, 3(5), 875-883.
104. Poole-Smith, B. K., Gilbert, A., Gonzalez, A. L., Beltran, M., Tomashek, K. M., Ward, B. J., ... & Ndao, M. (2014). Discovery and characterization of potential prognostic biomarkers for dengue hemorrhagic fever. *The American Journal of Tropical Medicine and Hygiene*, 91(6), 1218.
105. Moremen, K. W., Tiemeyer, M., & Nairn, A. V. (2012). Vertebrate protein glycosylation: diversity, synthesis and function. *Nature reviews Molecular cell biology*, 13(7), 448-462.
106. Tanabe, K., Deguchi, A., Higashi, M., Usuki, H., Suzuki, Y., Uchimura, Y., ... & Ikenaka, K. (2008). Outer arm fucosylation of N-glycans increases in sera of hepatocellular carcinoma patients. *Biochemical and biophysical research communications*, 374(2), 219-225.
107. Kitagaki-Ogawa, H., Yatohgo, T., Izumi, M., Hayashi, M., Kashiwagi, H., Matsumoto, I., & Seno, N. (1990). Diversities in animal vitronectins. Differences in molecular weight, immunoreactivity and carbohydrate chains. *Biochimica et Biophysica Acta (BBA)-General Subjects*, 1033(1), 49-56.
108. Uchibori-Iwaki, H., Yoneda, A., Oda-Tamai, S., Kato, S., Akamatsu, N., Otsuka, M., ... & Ogawa, H. (2000). The changes in glycosylation after partial hepatectomy enhance collagen binding of vitronectin in plasma. *Glycobiology*, 10(9), 865-874.
109. Sano, K., Miyamoto, Y., Kawasaki, N., Hashii, N., Itoh, S., Murase, M., ... & Ogawa, H. (2010). Survival signals of hepatic stellate cells in liver regeneration are regulated by

- glycosylation changes in rat vitronectin, especially decreased sialylation. *Journal of Biological Chemistry*, 285(23), 17301-17309.
110. Sano, K., Asanuma-Date, K., Arisaka, F., Hattori, S., & Ogawa, H. (2007). Changes in glycosylation of vitronectin modulate multimerization and collagen binding during liver regeneration. *Glycobiology*, 17(7), 784-794.
  111. Miyamoto, Y., Tanabe, M., Sakuda, K., Sano, K., & Ogawa, H. (2016). Sialylation of vitronectin regulates stress fiber formation and cell spreading of dermal fibroblasts via a heparin-binding site. *Glycoconjugate journal*, 33(2), 227-236.
  112. Pan, H., Lu, X., Ye, D., Feng, Y., Wan, J., & Ye, J. (2024). The molecular mechanism of thrombospondin family members in cardiovascular diseases. *Frontiers in Cardiovascular Medicine*, 11, 1337586
  113. Kuijpers, M. J., de Witt, S., Nergiz-Unal, R., van Kruchten, R., Korporaal, S. J., Verhamme, P., ... & Heemskerk, J. W. (2014). Supporting roles of platelet thrombospondin-1 and CD36 in thrombus formation on collagen. *Arteriosclerosis, thrombosis, and vascular biology*, 34(6), 1187-1192.
  114. Murphy MP (1999) Nitric oxide and cell death. *Biochim Biophys Acta* 1411:401–414. [https://doi.org/10.1016/s0005-2728\(99\) 00029-8](https://doi.org/10.1016/s0005-2728(99) 00029-8)
  115. Liu Z, Morgan S, Ren J, Wang Q, Annis DS, Mosher DF, Zhang J, Sorenson CM, Sheibani N, Liu B (2015) Thrombospondin-1 (TSP1) contributes to the development of vascular inflammation by regulating monocytic cell motility in mouse models of abdominal aortic aneurysm. *Circ Res* 117:129–141
  116. Agah A, Kyriakides TR, Lawler J, Bornstein P (2002) The lack of thrombospondin-1 (TSP1) dictates the course of Wound healing in double-TSP1/TSP2-null mice. *Am J Pathol* 161:831–839. [https://doi.org/10.1016/s0002-9440\(10\)64243-5](https://doi.org/10.1016/s0002-9440(10)64243-5)
  117. Malavige GN, Ogg GS (2017) Pathogenesis of vascular leak in dengue virus infection. *Front Immunol* 151:261–269
  118. Gubler DJ (1998) Dengue and dengue hemorrhagic fever. *Clin Microbiol Rev* 11:480–549
  119. Modhiran N, Watterson D, Muller DA, Panetta AK, Sester DP, Liu L, Hume DA, Stacey KJ, Young PR (2015) Dengue virus NS1 protein activates cells via Toll-like receptor 4

- and disrupts endothelial cell monolayer integrity. *Sci Transl Med* 7(304):304ra142. <https://doi.org/10.1126/scitranslmed.aaa3863>
120. Puerta-Guardo H, Glasner DR, Harris E (2016) Dengue virus NS1 disrupts the endothelial glycocalyx, leading to hyperpermeability *PLoS Pathog* 12(7):e1005738. <https://doi.org/10.1371/journal.ppat.1005738>
  121. Furuta T, Murao LA, Lan NT, Huy NT, Huong VT, Thuy TT, Tham VD, Nga CT, Ha TT, Ohmoto Y, Kikuchi M, Morita K, Yasunami M, Hirayama K, Watanabe N (2012) Association of mast cell-derived VEGF and proteases in Dengue shock syndrome. *PLoS Negl Trop Dis* 6:e1505. <https://doi.org/10.1371/journal.pntd.0001505>
  122. Steinberg BE, Goldenberg NM, Lee WL (2012) Do viral infections mimic bacterial sepsis? The role of microvascular permeability: a review of mechanisms and methods. *Antiviral Res* 93:2–15
  123. van de Weg CA, Pannuti CS, van den Ham HJ, de Araújo ES, Boas LS, Felix AC, Carvalho KI, Levi JE, Romano CM, Centrone CC, Rodrigues CL, Luna E, van Gorp EC, Osterhaus AD, Kallas EG, Martina BE (2014) Serum angiopoietin-2 and soluble VEGF receptor 2 are surrogate markers for plasma leakage in patients with acute dengue virus infection. *J Clin Virol* 60:328–335. <https://doi.org/10.1016/j.jcv.2014.05.001>
  124. Rogers NM, Sharif-Sanjani M, Csányi G, Pagano PJ, Isenberg JS (2014) Thrombospondin-1 and CD47 regulation of cardiac, pulmonary and vascular responses in health and disease. *Matrix Biol* 37:92–101. <https://doi.org/10.1016/j.matbio.2014.01.002>
  125. Nguyen MT, Ho TN, Nguyen VVC, Nguyen TH, Ha MT, Ta VT, Nguyen LDH, Simmons CP (2017) An evidence-based algorithm for early prognosis of severe dengue in the outpatient setting. *Clin Infect Dis* 64:656–663
  126. TriMark Publications, L. L. 2012. Point of Care Diagnostic Testing World Markets.
  127. Warsinke, A. 2009. Point-of-care testing of proteins. *Anal Bioanal Chem* 393, 5, 1393–1405.
  128. Frost & Sullivan. 2009. US point-of-care testing markets.
  129. Yager, P., Edwards, T., Fu, E., Helton, K., Nelson, K., Tam, M. R., and Weigl, B. H. 2006. Microfluidic diagnostic technologies for global public health. *Nature* 442, 7101, 412–418.

130. Lode, P. von. 2005. Point-of-care immunotesting: approaching the analytical performance of central laboratory methods. *Clin. Biochem.* 38, 7, 591–606.
131. C.D. Chin, V. Linder, and S.K. Sia, Lab-on-a-chip devices for global health: Past studies and future opportunities. *Lab on a Chip* 7, 41–57 (2007)
132. P. Yager, G.J. Domingo, and J. Gerdes, Point-of-care diagnostics for global health. *Annu. Rev. Biomed. Eng.* 10, 107–144 (2008)
133. S.K. Sia and L.J. Kricka, Microfluidics and point-of-care testing. *Lab Chip* 8, 1982–1983 (2008)
134. Spicuzza L, Campagna D, Di Maria C, Sciacca E, Mancuso S, Vancheri C, Sambataro G. An update on lateral flow immunoassay for the rapid detection of SARS-CoV-2 antibodies. *AIMS Microbiol.* 2023 Apr 13;9(2):375-401. doi: 10.3934/microbiol.2023020. PMID: 37091823; PMCID: PMC10113162.
135. Kettler, H.; White, K.; Hawkes, S.J.; UNDP/World Bank/WHO Special Programme for Research and Training in Tropical Diseases. Mapping the Landscape of Diagnostics for Sexually Transmitted Infections: Key Findings and Recommendations. 2004. <https://apps.who.int/iris/handle/10665/68990>.
136. Global Lateral Flow Assay Market Size by Type, by Technique, by Application, by End-user, by Geography and Forecast. Available online: <https://www.verifiedmarketresearch.com/product/lateral-flow-assay-market/>
137. Soh, J.H.; Chan, H.-M.; Ying, J.Y. Strategies for developing sensitive and specific nanoparticle-based lateral flow assays as point-of-care diagnostic device. *Nano Today* **2020**, 30, 100831.
138. Li, J.; Macdonald, J. Multiplexed lateral flow biosensors: Technological advances for radically improving point-of-care diagnoses. *Biosens. Bioelectron.* **2016**, 83, 177–192. [CrossRef]
139. Eltzov, E.; Guttel, S.; Kei, A.L.Y.; Sinawang, P.D.; Ionescu, R.E.; Marks, R.S. Lateral Flow Immunoassays—From Paper Strip to Smartphone Technology. *Electroanalysis* **2015**, 27, 2116–2130.
140. Anfossi, L.; Di Nardo, F.; Cavalera, S.; Giovannoli, C.; Spano, G.; Speranskaya, E.S.; Goryacheva, I.Y.; Baggiani, C. A lateral flow immunoassay for straightforward

- determination of fumonisin mycotoxins based on the quenching of the fluorescence of CdSe/ZnS quantum dots by gold and silver nanoparticles. *Microchim. Acta* **2018**, 185, 94
141. Parolo, C.; Sena-Torralba, A.; Bergua, J.F.; Calucho, E.; Fuentes-Chust, C.; Hu, L.; Rivas, L.; Alvarez-Diduk, R.; Nguyen, E.P.; Cinti, S.; et al. Tutorial: Design and fabrication of nanoparticle-based lateral-flow immunoassays. *Nat. Protoc.* **2020**, 15, 3788–3816.
  142. Damborský, P., Koczula, K. M., Gallotta, A., & Katrlík, J. (2016). Lectin-based lateral flow assay: proof-of-concept. *Analyst*, 141(23), 6444-6448.
  143. Bahadır, E.B.; Sezgentürk, M.K. Lateral flow assays: Principles, designs and labels. *TrAC-Trend. Anal. Chem.* **2016**, 82, 286–306.
  144. Quesada-González, D.; Merkoçi, A. Nanoparticle-based lateral flow biosensors. *Biosens. Bioelectron.* **2015**, 73, 47–63.
  145. Parolo, C.; Sena-Torralba, A.; Bergua, J.F.; Calucho, E.; Fuentes-Chust, C.; Hu, L.; Rivas, L.; Alvarez-Diduk, R.; Nguyen, E.P.; Cinti, S.; et al. Tutorial: Design and fabrication of nanoparticle-based lateral-flow immunoassays. *Nat. Protoc.* **2020**, 15, 3788–3816.
  146. <https://en.wikipedia.org/wiki/Nitrocellulose>
  147. Koczula, K. M., & Gallotta, A. (2016). Lateral flow assays. *Essays in biochemistry*, 60(1), 111-120.
  148. Reverberi R, Reverberi L. Factors affecting the antigen-antibody reaction. *Blood Transfus.* 2007 Nov;5(4):227-40. doi: 10.2450/2007.0047-07. PMID: 19204779; PMCID: PMC2581910.
  149. Vanoss, C. J. (1995). Hydrophobic, Hydrophilic and Other Interactions in Epitope Paratope Binding. *Molecular Immunology*, 32(3), 199-211.
  150. Wild, D. (2013). *The immunoassay handbook : theory and applications of ligand binding, ELISA, and related techniques* (4th ed.). Oxford ; Waltham, MA: Elsevier.
  151. Bahadır, E. B. & Sezgenturk, M. K. (2016). Lateral flow assays: Principles, designs and labels. *Trac-Trends in Analytical Chemistry*, 82, 286-306.

152. Yu, L., Li, P., Ding, X. & Zhang, Q. (2017b). Graphene oxide and carboxylated graphene oxide: Viable two-dimensional nanolabels for lateral flow immunoassays. *Talanta*, 165, 167- 175
153. Chen, Y., Chen, Q., Han, M., Zhou, J., Gong, L., Niu, Y., Zhang, Y., He, L. & Zhang, L. (2016). Development and optimization of a multiplex lateral flow immunoassay for the simultaneous determination of three mycotoxins in corn, rice and peanut. *Food Chemistry*, 213, 478-484.
154. Posthuma-Trumpie, G. A., Korf, J. & van Amerongen, A. (2009). Lateral flow (immuno) assay: its strengths, weaknesses, opportunities and threats. A literature survey. *Analytical and Bioanalytical Chemistry*, 393(2), 569-582.
155. Dykman, L. & Khlebtsov, N. (2012). Gold nanoparticles in biomedical applications: recent advances and perspectives. *Chemical Society Reviews*, 41(6), 2256-2282.
156. Shyu, R.-H., Shyu, H.-F., Liu, H.-W. & Tang, S.-S. (2002). Colloidal gold-based immunochromatographic assay for detection of ricin. *Toxicon*, 40(3), 255-258.
157. Kolm, C., Mach, R. L., Krska, R. & Brunner, K. (2015). A rapid DNA lateral flow test for the detection of transgenic maize by isothermal amplification of the 35S promoter. *Analytical Methods*, 7(1), 129-134.
158. Bu, T., Huang, Q., Yan, L. Z., Huang, L. J., Zhang, M. Y., Yang, Q. F., Yang, B. W., Wang, J. L. & Zhang, D. H. (2018). Ultra technically-simple and sensitive detection for Salmonella Enteritidis by immunochromatographic assay based on gold growth. *Food Control*, 84, 536-543.
159. Quesada-Gonzalez, D. & Merkoci, A. (2015). Nanoparticle-based lateral flow biosensors. *Biosensors & Bioelectronics*, 73, 47-63.
160. Gurunathan, S.; Park, J.H.; Han, J.W.; Kim, J.H. Comparative assessment of the apoptotic potential of silver nanoparticles synthesized by *Bacillus tequilensis* and *Calocybe indica* in MDA-MB-231 human breast cancer cells: Targeting p53 for anticancer therapy. *Int. J. Nanomed.* 2015, 10, 4203–4222. [CrossRef] [PubMed]
161. Li, W.R.; Xie, X.B.; Shi, Q.S.; Zeng, H.Y.; Ou-Yang, Y.S.; Chen, Y.B. Antibacterial activity and mechanism of silver nanoparticles on *Escherichia coli*. *Appl. Microbiol. Biotechnol.* 2010, 8, 1115–1122. [CrossRef] [PubMed]

162. Mukherjee, P.; Ahmad, A.; Mandal, D.; Senapati, S.; Sainkar, S.R.; Khan, M.I.; Renu, P.; Ajaykumar, P.V.; Alam, M.; Kumar, R.; et al. Fungus-mediated synthesis of silver nanoparticles and their immobilization in the mycelial matrix: A novel biological approach to nanoparticle synthesis. *Nano Lett.* 2001, 1, 515–519. [CrossRef]
163. Chernousova, S.; Epple, M. Silver as antibacterial agent: Ion, nanoparticle, and metal. *Angew. Chem. Int. Ed.* 2013, 52, 1636–1653. [CrossRef] [PubMed]
164. Li, C.Y.; Zhang, Y.J.; Wang, M.; Zhang, Y.; Chen, G.; Li, L.; Wu, D.; Wang, Q. In vivo real-time visualization of tissue blood flow and angiogenesis using Ag<sub>2</sub>S quantum dots in the NIR-II window. *Biomaterials* 2014, 35, 393–400. [CrossRef] [PubMed]
165. SonDI, I.; Salopek-SonDI, B. Silver nanoparticles as antimicrobial agent: A case study on *E. coli* as a model for Gram-negative bacteria. *J. Colloid Interface Sci.* 2004, 275, 177–182. [CrossRef] [PubMed]
166. C. T. Matea , T. Mocan , F. Zaharie , C. Iancu and L. Mocan , *Chem. Cent. J.*, 2015, **9** , 55 —62
167. M. P. Monopoli , C. Aberg , A. Salvati and K. A. Dawson , *Nat. Nanotechnol.*, 2012, **7** , 779 —786
168. Wu, K. H., Huang, W. C., Chang, S. C., & Shyu, R. H. (2022). Colloidal silver-based lateral flow immunoassay for detection of profenofos pesticide residue in vegetables. *RSC advances*, 12(21), 13035-13044.
169. Noguera, P. S., Posthuma-Trumpie, G. A., van Tuil, M., van der Wal, F. J., Boer, A. d., Moers, A. P. H. A. & van Amerongen, A. (2011). Carbon Nanoparticles as Detection Labels in Antibody Microarrays. Detection of Genes Encoding Virulence Factors in Shiga Toxin Producing *Escherichia coli*. *Analytical Chemistry*, 83(22), 8531-8536.
170. Posthuma-Trumpie, G. A., Wichers, J. H., Koets, M., Berendsen, L. B. J. M. & van Amerongen, A. (2012). Amorphous carbon nanoparticles: a versatile label for rapid diagnostic (immuno)assays. *Analytical and Bioanalytical Chemistry*, 402(2), 593-600.
171. Aldus, C. F., Van Amerongen, A., Ariëns, R. M. C., Peck, M. W., Wichers, J. H. & Wyatt, G. M. (2003). Principles of some novel rapid dipstick methods for detection and characterization of verotoxigenic *Escherichia coli*. *Journal of Applied Microbiology*, 95(2), 380-389.



172. Blažková, M., Javůrková, B., Fukal, L. & Rauch, P. (2011). Immunochromatographic strip test for detection of genus *Cronobacter*. *Biosensors and Bioelectronics*, 26(6), 2828-2834.
173. Takalkar, S., Baryeh, K. & Liu, G. D. (2017). Fluorescent carbon nanoparticle-based lateral flow biosensor for ultrasensitive detection of DNA. *Biosensors & Bioelectronics*, 98, 147-154.
174. Huang, X., Aguilar, Z. P., Xu, H., Lai, W. & Xiong, Y. (2016). Membrane-based lateral flow immunochromatographic strip with nanoparticles as reporters for detection: A review. *Biosensors and Bioelectronics*, 75, 166-180.
175. Wang, D.-B., Tian, B., Zhang, Z.-P., Deng, J.-Y., Cui, Z.-Q., Yang, R.-F., Wang, X.-Y., Wei, H.-P. & Zhang, X.-E. (2013). Rapid detection of *Bacillus anthracis* spores using a superparamagnetic lateral-flow immunological detectionsystem. *Biosensors and Bioelectronics*, 42, 661-667.
176. Gas, F., Baus, B., Quere, J., Chapelle, A. & Dreanno, C. (2016). Rapid detection and quantification of the marine toxic algae, *Alexandrium minutum*, using a superparamagnetic immunochromatographic strip test. *Talanta*, 147, 581-589.
177. van de Rijke, F., Zijlmans, H., Li, S., Vail, T., Raap, A. K., Niedbala, R. S. & Tanke, H. J. (2001). Upconverting phosphor reporters for nucleic acid microarrays. *Nat Biotech*, 19(3), 273- 276.
178. Tu, D., Zheng, W., Liu, Y., Zhu, H. & Chen, X. (2014). Luminescent biodetection based on lanthanide-doped inorganic nanoprobe. *Coordination Chemistry Reviews*, 273–274, 13-29.
179. Zhao, P., Wu, Y., Zhu, Y., Yang, X., Jiang, X., Xiao, J., Zhang, Y. & Li, C. (2014a). Upconversion fluorescent strip sensor for rapid determination of *Vibrio anguillarum*. *Nanoscale*, 6(7), 3804-3809.
180. Greenwald, R., Esfandiari, J., Lesellier, S., Houghton, R., Pollock, J., Aagaard, C., Andersen, P., Hewinson, R. G., Chambers, M. & Lyashchenko, K. (2003). Improved serodetection of *Mycobacterium bovis* infection in badgers (*Meles meles*) using multiantigen test formats. *Diagnostic Microbiology and Infectious Disease*, 46(3), 197-203.

181. Yoshida, R., Muramatsu, S., Akita, H., Saito, Y., Kuwahara, M., Kato, D., Changula, K., Miyamoto, H., Kajihara, M., Manzoor, R., Furuyama, W., Marzi, A., Feldmann, H., Mweene, A., Masumu, J., Kapeteshi, J., Muyembe-Tamfum, J. J. & Takada, A. (2016). Development of an Immunochromatography Assay (QuickNavi-Ebola) to Detect Multiple Species of Ebolaviruses. *Journal of Infectious Diseases*, 214, S185-S191.
182. Huang, Y., Wen, Y. Q., Baryeh, K., Takalkar, S., Lund, M., Zhang, X. J. & Liu, G. D. (2017). Lateral flow assay for carbohydrate antigen 19-9 in whole blood by using magnetized carbon nanotubes. *Microchimica Acta*, 184(11), 4287-4294.
183. Liang, R. L., Deng, Q. T., Chen, Z. H., Xu, X. P., Zhou, J. W., Liang, J. Y., Dong, Z. N., Liu, T. C. & Wu, Y. S. (2017a). Europium (III) chelate microparticle-based lateral flow immunoassay strips for rapid and quantitative detection of antibody to hepatitis B core antigen. *Scientific Reports*, 7.
184. Schaefer, T. J., Panda, P. K., & Wolford, R. W. (2022). Dengue Fever. National Library of Medicine. *StatPearl Publishing* | <https://tinyurl.com/223vjd8e> | Accessed on August, 26, 2022.
185. Li, J., & Macdonald, J. (2016). Multiplexed lateral flow biosensors: Technological advances for radically improving point-of-care diagnoses. *Biosensors and Bioelectronics*, 83, 177-192.
186. Najjioullah F, Viron F, Césaire R. Evaluation of four commercial real- time RT-PCR kits for the detection of dengue viruses in clinical samples. *Virol J*. 2014;11(1):4-8. doi:10.1186/1743-422X-11-164
187. Chattopodhyay, D., & Sen, M. R. (1999). Circulating immune complex in murine autoimmune hepatitis.
188. Raja A, Ranganathan UD & Ramalingam B, Clinical value of specific detection of immune complex-bound antibodies in pulmonary tuberculosis. *Diagn Microbiol Infect Dis*, 56 (2006) 281.
189. Muyzer G, De Waal EC, Uitterlinden AG. Profiling of complex microbial populations by denaturing gradient gel electrophoresis analysis of polymerase chain reaction-amplified genes coding for 16S rRNA. *Appl Environ Microbiol*. 1993 Mar 1; 59(3):695–700. PMID: 7683183.

190. Moss, J., Woodrow, D. F., Guillon, J.-C., and Gresser, I. (1982). Tubular Aggregates and Interferon. *The Lancet*. 320, 1277–1278. doi: 10.1016/s0140-6736(82)90130-1.
191. Jaiswal, P., Datta, S., Sardar, B., Chaudhuri, S. J., Maji, D., Ghosh, M., et al. (2018). Glycoproteins in circulating immune complexes are biomarkers of patients with indian PKDL: a study from endemic districts of West Bengal, India. *PLoS ONE* 13:e0192302. doi: 10.1371/journal.pone.0192302.
192. Stoll, M. S., and Hounsell, E. F. (1987). Selective purification of reduced oligosaccharides using a phenylboronic acid bond elut column: potential application in HPLC, mass spectrometry, reductive amination procedures and antigenic/serum analysis. *Biomed. Chromatogr.* 2, 249–253. doi: 10.1002/bmc.1130020605.
193. Hageman, J. H., and Kuehn, G. D. (1992). Boronic acid matrices for the affinity purification of glycoproteins and enzymes. *Methods Mol. Biol.* 11, 45–72. doi: 10.1385/0-89603-213-2:45.
194. Bassil, E., Hu, H., and Brown, P. H. (2004). Use of phenylboronic acids to investigate boron function in plants. Possible role of boron in transvacuolar cytoplasmic strands and cell-to-wall adhesion. *Plant physiol.* 136, 3383–3395. doi: 10.1104/pp.104.040527.
195. Lowry, O. H., Rosebrough, N. J., Farr, A. L., and Randall, R. J. (1951). Protein measurement with the folin phenol reagent. *J. Biol. Chem.* 193, 265–275.
196. Nguyen, T. H., Trieu, H. T., Okamoto, K., Ninh, T. T. H., Ha, T. T. N., Morita, K., et al. (2013). Proteomic profile of circulating immune complexes in dengue infected patients. *J. Trop. Dis.* 1:109. doi: 10.4172/2329-891X.1000109.
197. Singh, S. K., Bimal, S., Dinesh, D. S., Gupta, A. K., Sinha, P. K., Bimal, R., et al. (2005). Towards identifying immunogenic targets in visceral leishmaniasis: role of 17 kDa and 63 kDa phosphoproteins. *Am. J. Immunol.* 1, 96–100. doi: 10.3844/ajisp.2005.96.100.
198. Engvall E. and Perlmann P. (1971) *Immunochem.* 8: p. 871-874.
199. Engvall E. and Perlmann P. (1972) *J. Immunol.* 109: p. 129-135.
200. Conde JN, da Silva EM, Allonso D, Coelho DR, Andrade IDS, de Medeiros LN, Menezes JL, Barbosa AS, Mohana-Borges R. Inhibition of the Membrane Attack Complex by Dengue Virus NS1 through Interaction with Vitronectin and Terminal Complement Proteins. *J Virol.* 2016 Oct 14;90(21):9570-9581. doi: 10.1128/JVI.00912-16. PMID: 27512066; PMCID: PMC5068511.

201. Kraivong R, Punyadee N, Liszewski MK, Atkinson JP, Avirutnan P. Dengue and the Lectin Pathway of the Complement System. *Viruses*. 2021 Jun 24;13(7):1219. doi: 10.3390/v13071219. PMID: 34202570; PMCID: PMC8310334.
202. [https://omicstutorials.com/overview-of-recent-advancements-in-proteomics-bioinformatics-tools/#google\\_vignette](https://omicstutorials.com/overview-of-recent-advancements-in-proteomics-bioinformatics-tools/#google_vignette).
203. Han, B., Cheng, D., Luo, H. *et al*. Peptidomic analysis reveals novel peptide PDLC promotes cell proliferation in hepatocellular carcinoma via Ras/Raf/MEK/ERK pathway. *Sci Rep* **14**, 18757 (2024). <https://doi.org/10.1038/s41598-024-69789-3>.
204. Wu, K. H., Huang, W. C., Shyu, R. H., & Chang, S. C. (2020). Silver nanoparticle-base lateral flow immunoassay for rapid detection of Staphylococcal enterotoxin B in milk and honey. *Journal of Inorganic Biochemistry*, *210*, 111163.
205. Sastry, M.; Patil, V.; Sainkar, S.R. Electrostatically controlled diffusion of carboxylic acid derivatized silver colloidal particles in thermally evaporated fatty amine films. *J. Phys. Chem. B* 1998, 102, 1404–1410.
206. Tomaszewska, E.; Soliwoda, K.; Kadziola, K.; Celichowski, G.; Cichomski, M.; Szmaja, W.; Grobelny, J. Detection limits of DLS and UV-vis spectroscopy in characterization of polydisperse nanoparticles colloids. *J. Nanomater.* 2013, 2013, 313081
207. Joshi, M.; Bhattacharyya, A. Characterization techniques for nanotechnology applications in textiles. *Indian J. Fiber Text. Res.* 2008, 33, 304–317
208. Williams, D.B.; Carter, C.B. *The Transmission Electron Microscope*; Springer Verlag: New York, NY, USA, 2009.
209. Wu, K. H., Huang, W. C., Shyu, R. H., & Chang, S. C. (2020). Silver nanoparticle-base lateral flow immunoassay for rapid detection of Staphylococcal enterotoxin B in milk and honey. *Journal of Inorganic Biochemistry*, *210*, 111163.
210. Lin, P.C.; Lin, S.; Wang, P.C.; Sridhar, R. Techniques for physicochemical characterization of nanomaterials. *Biotechnol. Adv.* 2014, 32, 711–726.
211. Tomaszewska, E.; Soliwoda, K.; Kadziola, K.; Celichowski, G.; Cichomski, M.; Szmaja, W.; Grobelny, J. Detection limits of DLS and UV-vis spectroscopy in characterization of polydisperse nanoparticles colloids. *J. Nanomater.* 2013, 2013, 313081

212. Dieckmann, Y.; Cölfen, H.; Hofmann, H.; Petri-Fink, A. Particle size distribution measurements of manganese-doped ZnS nanoparticles. *Anal. Chem.* 2009, 81, 3889–3895.
213. Lange, H. Comparative test of methods to determine particle size and particle size distribution in the submicron range. *Part. Part. Syst. Charact.* 1995, 12, 148–157.
214. Kowalczyk, B., Lagzi, I., & Grzybowski, B. A. (2011). Nanoseparations: Strategies for size and/or shape-selective purification of nanoparticles. *Current Opinion in Colloid & Interface Science*, 16(2), 135-148.
215. Jimenez, M. S., Luque-Alled, J. M., Gomez, T., & Castillo, J. R. (2016). Evaluation of agarose gel electrophoresis for characterization of silver nanoparticles in industrial products. *Electrophoresis*, 37(10), 1376-1383.
216. Nguyen, M. T.; Ho, T. N.; Nguyen, V. V. C.; Nguyen, T. H.; Ha, M. T.; Ta, V. T.; Nguyen, L. D. H.; Phan, L.; Han, K. Q.; Duong, T. H. K., et al. An Evidence-Based Algorithm for Early Prognosis of Severe Dengue in the Outpatient Setting. *Clin. Infect. Dis.* 2017, 64, 656–663. DOI: 10.1093/cid/ciw863.
217. Rodriguez EL, Poddar S, Iftekhar S, Suh K, Woolfork AG, Ovbude S, Pekarek A, Walters M, Lott S, Hage DS. Affinity chromatography: A review of trends and developments over the past 50 years. *J Chromatogr B Analyt Technol Biomed Life Sci.* 2020 Nov 10;1157:122332. doi: 10.1016/j.jchromb.2020.122332. Epub 2020 Aug 14. PMID: 32871378; PMCID: PMC7584770.
218. Poole-Smith BK, Gilbert A, Gonzalez AL, Beltran M, Tomashek KM, Ward BJ, Hunsperger EA, Ndao M. Discovery and characterization of potential prognostic biomarkers for dengue hemorrhagic fever. *Am J Trop Med Hyg.* 2014 Dec;91(6):1218-26. doi: 10.4269/ajtmh.14-0193. Epub 2014 Oct 27. PMID: 25349378; PMCID: PMC4257649.
219. Liu Z, Zhao Q, Han Q, Gao M, Zhang N (2008) Serum thrombospondin-1 is altered in patients with hemorrhagic fever with renal syndrome. *J Med Virol* 80:1799–1803. <https://doi.org/10.1002/jmv.21270>.
220. [https://influentialpoints.com/Training/coefficient\\_of\\_variation-principles-properties-assumptions.htm](https://influentialpoints.com/Training/coefficient_of_variation-principles-properties-assumptions.htm).

221. Beck, F., Horn, C., & Baeumner, A. J. (2022). Ag nanoparticles outperform Au nanoparticles for the use as label in electrochemical point-of-care sensors. *Analytical and Bioanalytical Chemistry*, 1-9.
222. <https://www.abcam.com/en-us/products/conjugation-kits/gold-conjugation-kit-40nm-20-od-ab154873>
223. Kamel, M., Maher, S., El-Baz, H., Salah, F., Sayyouh, O., & Demerdash, Z. (2022). Non-invasive detection of SARS-CoV-2 antigen in saliva versus nasopharyngeal swabs using nanobodies conjugated gold nanoparticles. *Tropical Medicine and Infectious Disease*, 7(6), 102.
224. Oliveira, J. P., Prado, A. R., Keijok, W. J., Antunes, P. W. P., Yapuchura, E. R., & Guimarães, M. C. C. (2019). Impact of conjugation strategies for targeting of antibodies in gold nanoparticles for ultrasensitive detection of 17 $\beta$ -estradiol. *Scientific reports*, 9(1), 13859.
225. Atakuri SR, Nayak P. Correlation of C-reactive protein and neutrophil counts as early indicators of severe dengue in children. *Int J Contemp Pediatric* 2017; 4: 450-454.
226. Deshkar ST, Raut, SR, Khadse RK. Dengue infection in central India: A 5 years study at a tertiary care hospital. *Int J Res Med Sci* 2017; 5: 2483-2489.
227. Garg A, Garge J, Rao YK, Upadhyay GC, Sakhuja S. Prevalence of dengue among clinically suspected febrile episodes at a teaching hospital in north India. *J Infect Dis Immun* 2011; 3(5): 85-89.
228. KhanE, Siddiqui J, Shakoor S, Mehraj V, Jamil B, Hasan R. Dengue outbreak in Karachi, Pakistan, 2006: Experience at a tertiary care center. *Trans R Soc Trop Med Hyg* 2007; 101(11): 1114-1119.
229. Pan ST, Su PA, Chen KT, Lin HJ, Lai WP. Comparison of the clinical manifestations exhibited by dengue and non-dengue patients among children in a medical center in southern Taiwan. *J Acute Med* 2014; 4(2): 53-56.
230. Poole-Smith BK, Gilbert A, Gonzalez AL, Beltran M, Tomashek KM, Ward BJ, Hunsperger EA, Ndao M. Discovery and characterization of potential prognostic biomarkers for dengue hemorrhagic fever. *Am J Trop Med Hyg*. 2014 Dec;91(6):1218-26. doi: 10.4269/ajtmh.14-0193. Epub 2014 Oct 27. PMID: 25349378; PMCID: PMC4257649.

231. Paul, M., Saha, B., & Mukhopadhyay, S. (2023). Development of a novel lectin-based gold nanoparticle point-of-care immunoassay for rapid diagnosis of patients with severe Dengue infection. *Journal of Immunoassay and Immunochemistry*, 44(5-6), 418-435.
232. Seiffert D, Schleef RR. Two functionally distinct pools of vitronectin (Vn) in the blood circulation: identification of a heparin-binding competent population of Vn within platelet alpha-granules. *Blood*. 1996;88:552–560. [PubMed] [Google Scholar] [Ref list]
233. Preissner KT, Reuning U. Vitronectin in vascular context: facets of a multitasked matricellular protein. *Semin Thromb Hemost*. 2011;37:408–424. [PubMed] [Google Scholar] [Ref list]
234. Minor, K. H.; Peterson, C. B. Plasminogen Activator Inhibitor Type 1 Promotes the Self-Association of Vitronectin into Complexes Exhibiting Altered Incorporation into the Extracellular Matrix. *J. Biol. Chem.* 2002, 277, 10337–10345. DOI: 10.1074/jbc.M109564200
235. Izumi M, Yamada KM, Hayashi M. Vitronectin exists in two structurally and functionally distinct forms in human plasma. *Biochim Biophys Acta*. 1989;990:101–108. [PubMed] [Google Scholar] [Ref list]
236. Stefansson S, Haudenschild CC, Lawrence DA. Beyond fibrinolysis: the role of plasminogen activator inhibitor-1 and vitronectin in vascular wound healing. *Trends Cardiovasc Med*. 1998;8:175–180. [PubMed] [Google Scholar] [Ref list]
237. <https://www.sinobiological.com/research/complement-system/vitronectin#:~:text=Complement%20Regulator%20of%20Complement%20System%3A%20Vitronectin%20%2F%20VTN%20Function,tumor%20cell%20adhesion%20and%20migration.>
238. Shresta S. Role of complement in dengue virus infection: protection or pathogenesis?. *MBio*. 3(1), 10-1128 (2012).
239. Kraivong R, Punyadee N, Liszewski MK, Atkinson JP, & Avirutnan P. Dengue and the lectin pathway of the complement system. *Viruses*. 13(7), 1219 (2021).
240. Fuchs A, Lin TY, Beasley DW, Stover CM, Schwaebler WJ, Pierson TC, Diamond MS. Direct complement restriction of flavivirus infection requires glycan recognition by mannose-binding lectin. *Cell Host Microbe*. 8, 186–195 (2010).

241. Avirutnan P, Hauhart RE, Marovich MA, Garred P, Atkinson JP, Diamond MS. Complement-mediated neutralization of dengue virus requires mannose-binding lectin. *mBio*. 2 (2011).
242. Perera R., Kuhn RJ. Structural proteomics of dengue virus. *Curr. Opin. Microbiol.* 11, 369–377 (2008).
243. Hacker K, White L, de Silva AM. N-linked glycans on dengue viruses grown in mammalian and insect cells. *J. Gen. Virol.* 90, 2097–2106 (2009).
244. Dejnirattisai W, Webb AI, Chan V, Jumnainsong A, Davidson A, Mongkolsapaya J, Screaton G. Lectin switching during dengue virus infection. *J. Infect. Dis.* 203, 1775-1783 (2011).
245. Jani PK, Kajdacs E, Megyeri M, Dobo J, Doleschall Z, Futosi K, & Cervenak L. MASP-1 induces a unique cytokine pattern in endothelial cells: a novel link between complement system and neutrophil granulocytes. *PloS one*. 9(1), e87104 (2014).
246. Patra, G., Mallik, S., Saha, B., & Mukhopadhyay, S. (2019). Assessment of chemokine and cytokine signatures in patients with dengue infection: A hospital-based study in Kolkata, India. *Acta tropica*, 190, 73-79
247. Xian, L., Cheng, S., Chen, W., Zhong, C., Hu, Z., & Deng, X. (2024). Systematic analysis of MASP-1 serves as a novel immune-related biomarker in sepsis and trauma followed by preliminary experimental validation. *Frontiers in Medicine*, 11, 1320811.
248. Németh, Z., Debreczeni, M. L., Kajdácsi, E., Dobó, J., Gál, P., & Cervenak, L. (2023). Cooperation of Complement MASP-1 with Other Proinflammatory Factors to Enhance the Activation of Endothelial Cells. *International Journal of Molecular Sciences*, 24(11), 9181.
249. Debreczeni, M. L., Németh, Z., Kajdácsi, E., Schwaner, E., Makó, V., Masszi, A., ... & Cervenak, L. (2019). MASP-1 increases endothelial permeability. *Frontiers in immunology*, 10, 991.
250. Benachour, H.; Leroy-Dudal, J.; Agniel, R.; Wilson, J.; Briand, M.; Carreiras, F.; Gallet, O. Vitronectin (Vn) Glycosylation Patterned by Lectin Affinity Assays—A Potent Glycoproteomic Tool to Discriminate Plasma Vn from Cancer Ascites Vn. *J. Mol. Recognit.* 2018, 31(5), e2690. DOI: 10.1002/jmr.2690.



251. Mayampurath, A.; Song, E.; Mathur, A.; Yu, C. Y.; Hammoud, Z.; Mechref, Y.; Tang, H. Label-Free Glycopeptide Quantification for Biomarker Discovery in Human Sera. *J. Proteome Res.* 2014, *13*(11), 4821–4832. DOI: 10.1021/pr500242m.
252. Mayampurath, A. M.; Yu, C. Y.; Song, E.; Balan, J.; Mechref, Y.; Tang, H. Computational Framework for Identification of Intact Glycopeptides in Complex Samples. *Anal. Chem.* 2014, *86*, 453–463. DOI: 10.1021/ac402338u.
253. Hua, S.; Hu, C. Y.; Kim, B. J.; Totten, S. M.; Oh, M. J.; Yun, N.; Nwosu, C. C.; Yoo, J. S.; Lebrilla, C. B.; An, H. J. Glyco-Analytical Multispecific Proteolysis (Glyco-AMP): A Simple Method for Detailed and Quantitative Glycoproteomic Characterization. *J. Proteome Res.* 2013, *12*, 4414–4423. DOI: 10.1021/pr400442y.
254. Omidfar, Kobra et al. “Lateral Flow Assay: A Summary of Recent Progress for Improving Assay Performance.” *Biosensors* vol. 13,9 837. 23 Aug. 2023, doi:10.3390/bios13090837
255. Çam D, Öktem HA. Optimizations needed for lateral flow assay for rapid detection of pathogenic E. coli. *Turk J Biol.* 2017 Dec 18;41(6):954-968. doi: 10.3906/biy-1705-50. PMID: 30814860; PMCID: PMC6353270.
256. <https://salimetrics.com/calculating-inter-and-intra-assay-coefficients-of-variability/>
257. <https://www.enzo.com/note/cv-in-elisa-how-to-reduce-them-and-why-theyre-important/>
258. Wu, K. H., Huang, W. C., Shyu, R. H., & Chang, S. C. (2020). Silver nanoparticle-base lateral flow immunoassay for rapid detection of Staphylococcal enterotoxin B in milk and honey. *Journal of Inorganic Biochemistry*, *210*, 111163.
259. Tomaszewska, E.; Soliwoda K.; Kadziola, K.; Celichowski, G.; Cichomski, M.; Szmaja, W.; Grobelny, J. Detection limits of DLS and UV-vis spectroscopy in characterization of polydisperse nanoparticles colloids. *J. Nanomater.* 2013, 2013, 313081.
260. Souza, T.G.F.; Ciminelli, V.S.T.; Mohallem, N.D.S. A Comparison of TEM and DLS Methods to Characterize Size Distribution of Ceramic Nanoparticles. *J. Phys. Conf. Ser.* 2016, 733.

# Permission for Figure

18/08/2024, 16:16

RightsLink Printable License

ELSEVIER LICENSE  
TERMS AND CONDITIONS

Aug 18, 2024

This Agreement between Moumita Paul ("You") and Elsevier ("Elsevier") consists of your license details and the terms and conditions provided by Elsevier and Copyright Clearance Center.

License Number	5851861364876
License date	Aug 18, 2024
Licensed Content Publisher	Elsevier
Licensed Content Publication	Biosensors and Bioelectronics
Licensed Content Title	Multiplexed lateral flow biosensors: Technological advances for radically improving point-of-care diagnoses
Licensed Content Author	Jia Li,Joanne Macdonald
Licensed Content Date	Sep 15, 2016
Licensed Content Volume	83
Licensed Content Issue	n/a
Licensed Content Pages	16
Start Page	177
End Page	192
Type of Use	reuse in a thesis/dissertation

Portion	figures/tables/illustrations
Number of figures/tables/illustrations	2
Format	print
Are you the author of this Elsevier article?	No
Will you be translating?	No
Title of new work	Development of a Point-Of-Care Immunoassay System for Rapid Diagnosis of Severe Dengue
Institution name	Calcutta School of Tropical Medicine
Expected presentation date	Dec 2024
Portions	Figure 1 A & B
The Requesting Person / Organization to Appear on the License	Moumita Paul
Requestor Location	Moumita Paul Department of Laboratory Medicine, Calcutta School of Tropical Medicine  Kolkata, West Bengal 700073 India Attn: Moumita Paul
Publisher Tax ID	GB 494 6272 12
Total	0.00 USD
Terms and Conditions	

INTRODUCTION

1. The publisher for this copyrighted material is Elsevier. By clicking "accept" in connection with completing this licensing transaction, you agree that the following terms and conditions apply to this transaction (along with the Billing and Payment terms and conditions established by Copyright Clearance Center, Inc. ("CCC"), at the time that you

opened your RightsLink account and that are available at any time at <https://myaccount.copyright.com>).

## GENERAL TERMS

2. Elsevier hereby grants you permission to reproduce the aforementioned material subject to the terms and conditions indicated.

3. Acknowledgement: If any part of the material to be used (for example, figures) has appeared in our publication with credit or acknowledgement to another source, permission must also be sought from that source. If such permission is not obtained then that material may not be included in your publication/copies. Suitable acknowledgement to the source must be made, either as a footnote or in a reference list at the end of your publication, as follows:

"Reprinted from Publication title, Vol /edition number, Author(s), Title of article / title of chapter, Pages No., Copyright (Year), with permission from Elsevier [OR APPLICABLE SOCIETY COPYRIGHT OWNER]." Also Lancet special credit - "Reprinted from The Lancet, Vol. number, Author(s), Title of article, Pages No., Copyright (Year), with permission from Elsevier."

4. Reproduction of this material is confined to the purpose and/or media for which permission is hereby given. The material may not be reproduced or used in any other way, including use in combination with an artificial intelligence tool (including to train an algorithm, test, process, analyse, generate output and/or develop any form of artificial intelligence tool), or to create any derivative work and/or service (including resulting from the use of artificial intelligence tools).

5. Altering/Modifying Material: Not Permitted. However figures and illustrations may be altered/adapted minimally to serve your work. Any other abbreviations, additions, deletions and/or any other alterations shall be made only with prior written authorization of Elsevier Ltd. (Please contact Elsevier's permissions helpdesk [here](#)). No modifications can be made to any Lancet figures/tables and they must be reproduced in full.

6. If the permission fee for the requested use of our material is waived in this instance, please be advised that your future requests for Elsevier materials may attract a fee.

7. Reservation of Rights: Publisher reserves all rights not specifically granted in the combination of (i) the license details provided by you and accepted in the course of this licensing transaction, (ii) these terms and conditions and (iii) CCC's Billing and Payment terms and conditions.

8. License Contingent Upon Payment: While you may exercise the rights licensed immediately upon issuance of the license at the end of the licensing process for the transaction, provided that you have disclosed complete and accurate details of your proposed use, no license is finally effective unless and until full payment is received from you (either by publisher or by CCC) as provided in CCC's Billing and Payment terms and conditions. If full payment is not received on a timely basis, then any license preliminarily granted shall be deemed automatically revoked and shall be void as if never granted. Further, in the event that you breach any of these terms and conditions or any of CCC's Billing and Payment terms and conditions, the license is automatically revoked and shall be void as if never granted. Use of materials as described in a revoked license, as well as any use of the materials beyond the scope of an unrevoked license, may constitute copyright infringement and publisher reserves the right to take any and all action to protect its copyright in the materials.

9. Warranties: Publisher makes no representations or warranties with respect to the licensed material.

10. **Indemnity:** You hereby indemnify and agree to hold harmless publisher and CCC, and their respective officers, directors, employees and agents, from and against any and all claims arising out of your use of the licensed material other than as specifically authorized pursuant to this license.

11. **No Transfer of License:** This license is personal to you and may not be sublicensed, assigned, or transferred by you to any other person without publisher's written permission.

12. **No Amendment Except in Writing:** This license may not be amended except in a writing signed by both parties (or, in the case of publisher, by CCC on publisher's behalf).

13. **Objection to Contrary Terms:** Publisher hereby objects to any terms contained in any purchase order, acknowledgment, check endorsement or other writing prepared by you, which terms are inconsistent with these terms and conditions or CCC's Billing and Payment terms and conditions. These terms and conditions, together with CCC's Billing and Payment terms and conditions (which are incorporated herein), comprise the entire agreement between you and publisher (and CCC) concerning this licensing transaction. In the event of any conflict between your obligations established by these terms and conditions and those established by CCC's Billing and Payment terms and conditions, these terms and conditions shall control.

14. **Revocation:** Elsevier or Copyright Clearance Center may deny the permissions described in this License at their sole discretion, for any reason or no reason, with a full refund payable to you. Notice of such denial will be made using the contact information provided by you. Failure to receive such notice will not alter or invalidate the denial. In no event will Elsevier or Copyright Clearance Center be responsible or liable for any costs, expenses or damage incurred by you as a result of a denial of your permission request, other than a refund of the amount(s) paid by you to Elsevier and/or Copyright Clearance Center for denied permissions.

### LIMITED LICENSE

The following terms and conditions apply only to specific license types:

15. **Translation:** This permission is granted for non-exclusive world **English** rights only unless your license was granted for translation rights. If you licensed translation rights you may only translate this content into the languages you requested. A professional translator must perform all translations and reproduce the content word for word preserving the integrity of the article.

16. **Posting licensed content on any Website:** The following terms and conditions apply as follows: Licensing material from an Elsevier journal: All content posted to the web site must maintain the copyright information line on the bottom of each image; A hyper-text must be included to the Homepage of the journal from which you are licensing at <http://www.sciencedirect.com/science/journal/xxxxx> or the Elsevier homepage for books at <http://www.elsevier.com>; Central Storage: This license does not include permission for a scanned version of the material to be stored in a central repository such as that provided by Heron/XanEdu.

Licensing material from an Elsevier book: A hyper-text link must be included to the Elsevier homepage at <http://www.elsevier.com>. All content posted to the web site must maintain the copyright information line on the bottom of each image.

**Posting licensed content on Electronic reserve:** In addition to the above the following clauses are applicable: The web site must be password-protected and made available only to bona fide students registered on a relevant course. This permission is granted for 1 year only. You may obtain a new license for future website posting.



**17. For journal authors:** the following clauses are applicable in addition to the above:

### **Preprints:**

A preprint is an author's own write-up of research results and analysis, it has not been peer-reviewed, nor has it had any other value added to it by a publisher (such as formatting, copyright, technical enhancement etc.).

Authors can share their preprints anywhere at any time. Preprints should not be added to or enhanced in any way in order to appear more like, or to substitute for, the final versions of articles however authors can update their preprints on arXiv or RePEc with their Accepted Author Manuscript (see below).

If accepted for publication, we encourage authors to link from the preprint to their formal publication via its DOI. Millions of researchers have access to the formal publications on ScienceDirect, and so links will help users to find, access, cite and use the best available version. Please note that Cell Press, The Lancet and some society-owned have different preprint policies. Information on these policies is available on the journal homepage.

**Accepted Author Manuscripts:** An accepted author manuscript is the manuscript of an article that has been accepted for publication and which typically includes author-incorporated changes suggested during submission, peer review and editor-author communications.

Authors can share their accepted author manuscript:

- immediately
  - via their non-commercial person homepage or blog
  - by updating a preprint in arXiv or RePEc with the accepted manuscript
  - via their research institute or institutional repository for internal institutional uses or as part of an invitation-only research collaboration work-group
  - directly by providing copies to their students or to research collaborators for their personal use
  - for private scholarly sharing as part of an invitation-only work group on commercial sites with which Elsevier has an agreement
- After the embargo period
  - via non-commercial hosting platforms such as their institutional repository
  - via commercial sites with which Elsevier has an agreement

In all cases accepted manuscripts should:

- link to the formal publication via its DOI
- bear a CC-BY-NC-ND license - this is easy to do
- if aggregated with other manuscripts, for example in a repository or other site, be shared in alignment with our hosting policy not be added to or enhanced in any way to appear more like, or to substitute for, the published journal article.

**Published journal article (JPA):** A published journal article (PJA) is the definitive final record of published research that appears or will appear in the journal and embodies all value-adding publishing activities including peer review co-ordination, copy-editing, formatting, (if relevant) pagination and online enrichment.

Policies for sharing publishing journal articles differ for subscription and gold open access articles:

**Subscription Articles:** If you are an author, please share a link to your article rather than the full-text. Millions of researchers have access to the formal publications on ScienceDirect, and so links will help your users to find, access, cite, and use the best available version.

Theses and dissertations which contain embedded PJAs as part of the formal submission can be posted publicly by the awarding institution with DOI links back to the formal publications on ScienceDirect.

If you are affiliated with a library that subscribes to ScienceDirect you have additional private sharing rights for others' research accessed under that agreement. This includes use for classroom teaching and internal training at the institution (including use in course packs and courseware programs), and inclusion of the article for grant funding purposes.

**Gold Open Access Articles:** May be shared according to the author-selected end-user license and should contain a [CrossMark logo](#), the end user license, and a DOI link to the formal publication on ScienceDirect.

Please refer to Elsevier's [posting.policy](#) for further information.

18. **For book authors** the following clauses are applicable in addition to the above: Authors are permitted to place a brief summary of their work online only. You are not allowed to download and post the published electronic version of your chapter, nor may you scan the printed edition to create an electronic version. **Posting to a repository:** Authors are permitted to post a summary of their chapter only in their institution's repository.

19. **Thesis/Dissertation:** If your license is for use in a thesis/dissertation your thesis may be submitted to your institution in either print or electronic form. Should your thesis be published commercially, please reapply for permission. These requirements include permission for the Library and Archives of Canada to supply single copies, on demand, of the complete thesis and include permission for Proquest/UMI to supply single copies, on demand, of the complete thesis. Should your thesis be published commercially, please reapply for permission. Theses and dissertations which contain embedded PJAs as part of the formal submission can be posted publicly by the awarding institution with DOI links back to the formal publications on ScienceDirect.

### **Elsevier Open Access Terms and Conditions**

You can publish open access with Elsevier in hundreds of open access journals or in nearly 2000 established subscription journals that support open access publishing. Permitted third party re-use of these open access articles is defined by the author's choice of Creative Commons user license. See our [open access license policy](#) for more information.

#### **Terms & Conditions applicable to all Open Access articles published with Elsevier:**

Any reuse of the article must not represent the author as endorsing the adaptation of the article nor should the article be modified in such a way as to damage the author's honour or reputation. If any changes have been made, such changes must be clearly indicated.

The author(s) must be appropriately credited and we ask that you include the end user license and a DOI link to the formal publication on ScienceDirect.

If any part of the material to be used (for example, figures) has appeared in our publication with credit or acknowledgement to another source it is the responsibility of the user to ensure their reuse complies with the terms and conditions determined by the rights holder.

#### **Additional Terms & Conditions applicable to each Creative Commons user license:**

**CC BY:** The CC-BY license allows users to copy, to create extracts, abstracts and new works from the Article, to alter and revise the Article and to make commercial use of the Article (including reuse and/or resale of the Article by commercial entities), provided the user gives appropriate credit (with a link to the formal publication through the relevant DOI), provides a link to the license, indicates if changes were made and the licensor is not represented as endorsing the use made of the work. The full details of the license are available at <http://creativecommons.org/licenses/by/4.0>.

**CC BY NC SA:** The CC BY-NC-SA license allows users to copy, to create extracts, abstracts and new works from the Article, to alter and revise the Article, provided this is not done for commercial purposes, and that the user gives appropriate credit (with a link to the formal publication through the relevant DOI), provides a link to the license, indicates if changes were made and the licensor is not represented as endorsing the use made of the work. Further, any new works must be made available on the same conditions. The full details of the license are available at <http://creativecommons.org/licenses/by-nc-sa/4.0>.

**CC BY NC ND:** The CC BY-NC-ND license allows users to copy and distribute the Article, provided this is not done for commercial purposes and further does not permit distribution of the Article if it is changed or edited in any way, and provided the user gives appropriate credit (with a link to the formal publication through the relevant DOI), provides a link to the license, and that the licensor is not represented as endorsing the use made of the work. The full details of the license are available at <http://creativecommons.org/licenses/by-nc-nd/4.0>. Any commercial reuse of Open Access articles published with a CC BY NC SA or CC BY NC ND license requires permission from Elsevier and will be subject to a fee.

Commercial reuse includes:

- Associating advertising with the full text of the Article
- Charging fees for document delivery or access
- Article aggregation
- Systematic distribution via e-mail lists or share buttons

Posting or linking by commercial companies for use by customers of those companies.

## 20. Other Conditions:

v1.10

Questions? [customercare@copyright.com](mailto:customercare@copyright.com).

---



# Thesis

## ORIGINALITY REPORT

13%

SIMILARITY INDEX

### PRIMARY SOURCES

[www.research.manchester.ac.uk](http://www.research.manchester.ac.uk)

Internet

386 words — 1%

[www.ncbi.nlm.nih.gov](http://www.ncbi.nlm.nih.gov)

Internet

346 words — 1%

[www.frontiersin.org](http://www.frontiersin.org)

Internet

337 words — 1%

[coek.info](http://coek.info)

Internet

243 words — 1%

[globalresearchonline.net](http://globalresearchonline.net)

Internet

172 words — 1%

[digitalcommons.uri.edu](http://digitalcommons.uri.edu)

Internet

169 words — 1%

[docksci.com](http://docksci.com)

Internet

156 words — < 1%

[www.mdpi.com](http://www.mdpi.com)

Internet

141 words — < 1%

Arab, Jennifer Suz. "Modeling dengue viral infection, insect transmission and multiplex PCR in humanized mice", Proquest, 2014.

ProQuest

113 words — < 1%

Goutam Patra, Sudeshna Mallik, Bibhuti Saha, Sumi Mukhopadhyay. "Assessment Of Chemokine And Cytokine Signatures In Patients With Dengue Infection: A Hospital-Based Study In Kolkata, India", Acta Tropica, 2018  
Crossref 102 words — < 1%

[www.irjmets.com](http://www.irjmets.com)  
Internet 83 words — < 1%

[www.nature.com](http://www.nature.com)  
Internet 78 words — < 1%

Sourav Datta, Manab Ghosh, Moumita Paul, Prantiki Halder, Sudeshna Mallik, Sumi Mukhopadhyay, Bibhuti Saha, Pratip Kumar Kundu. "Comprehensive Investigation of Fever cases enrolled during 2019 Dengue outbreaks from three hyperendemic regions of North 24 parganas district of West Bengal, India", Journal of Medical Virology, 2021  
Crossref 77 words — < 1%

[cni.co.id](http://cni.co.id)  
Internet 75 words — < 1%

[nopr.niscpr.res.in](http://nopr.niscpr.res.in)  
Internet 66 words — < 1%

Kowalczyk, B.. "Nanoseparations: Strategies for size and/or shape-selective purification of nanoparticles", Current Opinion in Colloid & Interface Science, 201104  
Crossref 65 words — < 1%

Amudhan Murugesan, Mythreyee Manoharan. "Dengue Virus", Elsevier BV, 2020  
Crossref 64 words — < 1%

Kuo-Hui Wu, Wen-Chien Huang, Shu-Chen Chang, Ching-Hua Kao, Rong-Hwa Shyu. "Colloidal silver-based lateral flow immunoassay for rapid detection of melamine in milk and animal feed", Materials Chemistry and Physics, 2019

Crossref

59 words — < 1%

Goutam Patra, Bibhuti Saha, Sumi Mukhopadhyay. "Study of serum VEGF levels in patients with severe dengue infection admitted in a tertiary care hospital in Kolkata", Journal of Medical Virology, 2019

Crossref

57 words — < 1%

academic.oup.com

Internet

55 words — < 1%

Sakuni Rankothgedera, Inoshi Atukorala, Chandrika Fernando, Duminda Munidasa, Lalith Wijayarathne, Preethi Udagama. "A potential diagnostic serum immunological marker panel to differentiate between primary and secondary knee osteoarthritis", PLOS ONE, 2021

Crossref

54 words — < 1%

Maria S. Jimenez, Jose M. Luque-Alled, Teresa Gomez, Juan R. Castillo. "Evaluation of agarose gel electrophoresis for characterization of silver nanoparticles in industrial products", ELECTROPHORESIS, 2016

Crossref

53 words — < 1%

Hong-Jie Kuo, Ing-Kit Lee, Jien-Wei Liu. "Analyses of clinical and laboratory characteristics of dengue adults at their hospital presentations based on the World Health Organization clinical-phase framework:

50 words — < 1%

Emphasizing risk of severe dengue in the elderly", Journal of Microbiology, Immunology and Infection, 2017

Crossref

[journals.plos.org](https://journals.plos.org)

Internet

39 words — < 1%

Ana Luísa Tomás, Miguel P. de Almeida, Fernando Cardoso, Mafalda Pinto, Eulália Pereira, Ricardo Franco, Olga Matos. "Development of a Gold Nanoparticle-Based Lateral-Flow Immunoassay for Pneumocystis Pneumonia Serological Diagnosis at Point-of-Care", Frontiers in Microbiology, 2019

Crossref

38 words — < 1%

L. MILIS. "Vitronectin-mediated inhibition of complement: evidence for different binding sites for C5b-7 and C9", Clinical & Experimental Immunology, 06/28/2008

Crossref

38 words — < 1%

[www.rsc.org](http://www.rsc.org)

Internet

35 words — < 1%

[wwwnc.cdc.gov](http://wwwnc.cdc.gov)

Internet

34 words — < 1%

[www.ecdc.europa.eu](http://www.ecdc.europa.eu)

Internet

31 words — < 1%

[listens.online](http://listens.online)

Internet

29 words — < 1%

[www.researchgate.net](http://www.researchgate.net)

Internet

29 words — < 1%

Shijith Thoms, Richard A Gonsalves, Jomy Jose, Samer H. Zyoud, Anupama R Prasad, Julia Garvasis. "Plant-Based Synthesis, characterization Approaches, Applications and Toxicity of Silver Nanoparticles: A Comprehensive Review", Journal of Biotechnology, 2024  
Crossref 24 words — < 1%

Ali, Farzana. "Identifying Biomarkers for Treatment Response in Depression Using Neuroimaging and Actigraphy", State University of New York at Stony Brook, 2023  
ProQuest 22 words — < 1%

Haoxuan Xiong, Peipei Hu, Meimei Zhang, Yanping Li, Zhenqiang Ning. "Recent advances of nanozyme-enhanced lateral flow assay sensing in clinic diagnosis", Microchemical Journal, 2024  
Crossref 21 words — < 1%

[hal-riip.archives-ouvertes.fr](http://hal-riip.archives-ouvertes.fr)  
Internet 21 words — < 1%

Dongyou Liu. "Molecular Detection of Human Viral Pathogens", CRC Press, 2019  
Publications 20 words — < 1%

Kaifa Wei, Yuhan Li. "Global evolutionary history and spatio-temporal dynamics of dengue virus type 2", Scientific Reports, 2017  
Crossref 19 words — < 1%

[link.springer.com](http://link.springer.com)  
Internet 19 words — < 1%

Goutam Patra, Bibhuti Saha, Sumi Mukhopadhyay. "The relationship between

changes in IL-2 / IL-18 and liver enzyme with dengue severity",  
Cytokine, 2021

Crossref

M Schmitt. "Aortic valve endocarditis causing fatal myocardial infarction caused by ostial coronary artery obliteration", Heart, 3/1/2004

Crossref

Xuewu Li, Gaiping Zhang, Qingtang Liu, Chunhua Feng et al. "Development of immunoassays for the detection of sulfamethazine in swine urine", Food Additives & Contaminants: Part A, 2009

Crossref

dspace.bracu.ac.bd

Internet

Soumya Jose, Roshni Jerome, Ajai Krishnan, Ozhiparambhil AnilKumar Jagan, Dongmei Li, Veena Menon. "Differential Expression Patterns of Indoleamine 2,3-Dioxygenase 1 and Other Tryptophan and Arginine Catabolic Pathway Genes in Dengue Correlate with Clinical Severity-Pilot Study Results", Viral Immunology, 2023

Crossref

Viral Genome Replication, 2009.

Crossref

Heeyoun Hwang, Ju Yeon Lee, Hyun Kyoung Lee, Gun Wook Park, Hoi Keun Jeong, Myeong Hee Moon, Jin Young Kim, Jong Shin Yoo. "In-depth analysis of site-specific N-glycosylation in vitronectin from human plasma by tandem mass spectrometry with immunoprecipitation", Analytical and Bioanalytical Chemistry, 2014

Crossref

Londono Zuluaga, Nathalia. "Impacts of engineered nanoparticles (TiO<sub>2</sub>, ZnO, Ag) on aquatic microbial communities.", Southern Illinois University at Carbondale

ProQuest

14 words — < 1%

Marcia H. Beltrame, Angelica B.W. Boldt, Sandra J. Catarino, Hellen C. Mendes et al. "MBL-associated serine proteases (MASPs) and infectious diseases", Molecular Immunology, 2015

Crossref

14 words — < 1%

[aiimsrajkot.edu.in](http://aiimsrajkot.edu.in)

Internet

14 words — < 1%

[docplayer.net](http://docplayer.net)

Internet

14 words — < 1%

[www.abcam.cn](http://www.abcam.cn)

Internet

14 words — < 1%

Mashayekhi, . "Enhancing the Detection of Biomolecules Using Aqueous Two-Micellar Systems", Proquest, 2014.

ProQuest

13 words — < 1%

Srinivas Murthy, Jay Keystone, Niranjana Kissoon. "Infections of the Developing World", Critical Care Clinics, 2013

Crossref

13 words — < 1%

Szymanski, Mateusz S., and Robert A. Porter. "Preparation and quality control of silver nanoparticle-antibody conjugate for use in electrochemical immunoassays", Journal of Immunological Methods, 2013.

Crossref

13 words — < 1%

acikbilim.yok.gov.tr

Internet

13 words — < 1%

extension.mmsu.edu.ph

Internet

12 words — < 1%

khazna.ku.ac.ae

Internet

12 words — < 1%

new.paho.org

Internet

12 words — < 1%

scholarworks.gsu.edu

Internet

12 words — < 1%

www.imcjms.com

Internet

12 words — < 1%

www.tandfonline.com

Internet

12 words — < 1%

www.voicesoffriends.org

Internet

12 words — < 1%

Boyang Sun, Haiyu Wu, Pei Jia, Yuanyuan Cao,  
Chenyu Xuan, Qinlin Feng, Huiqi Yan, Li Wang.

"Dual-modal lateral flow immunoassay based on cauliflower-  
like ReS2@Pt core-shell nanospheres mediated ultra-sensitive  
detection of deoxynivalenol in food samples", Chemical  
Engineering Journal, 2024

Crossref

11 words — < 1%

C. Anandharamakrishnan, S. Parthasarathi. "Food  
Nanotechnology - Principles and Applications",  
CRC Press, 2019

Publications

11 words — < 1%



Dandan Ma, Yuting Wang, Qijia Zhang, Chao Wang, Yixuan Du, Dongbing Liang, Jiachen Shen, Xing Pan, Enze Sheng, Dong Zhu. "Hierarchical magneto-colorimetric labels for immediate lateral flow immunoassay of chlorothalonil residues", Talanta, 2024

Crossref

11 words — < 1%

Kuo-Hui Wu, Wen-Chien Huang, Shu-Chen Chang, Rong-Hwa Shyu. "Colloidal silver-based lateral flow immunoassay for detection of profenofos pesticide residue in vegetables", RSC Advances, 2022

Crossref

11 words — < 1%

Naik, Laxmana, Rajan Sharma, Bimlesh Mann, Kiran Lata, Y.S. Rajput, and B. Surendra Nath. "Rapid screening test for detection of oxytetracycline residues in milk using lateral flow assay", Food Chemistry, 2017.

Crossref

11 words — < 1%

Robert S. Matson. "Applying Genomic and Proteomic Microarray Technology in Drug Discovery", CRC Press, 2019

Publications

11 words — < 1%

[api.research-repository.uwa.edu.au](http://api.research-repository.uwa.edu.au)

Internet

11 words — < 1%

11 words — < 1%

[bmccomplementmedtherapies.biomedcentral.com](http://bmccomplementmedtherapies.biomedcentral.com)

Internet

[pure.strath.ac.uk](http://pure.strath.ac.uk)

Internet

11 words — < 1%

[www.nursingcenter.com](http://www.nursingcenter.com)

Internet

11 words — < 1%

"Advances in Medical Physics and Healthcare Engineering", Springer Science and Business Media LLC, 2021

Crossref

10 words — < 1%

"Cardiac Function and Heart Failure", Journal of the American College of Cardiology, 20060221

Crossref

10 words — < 1%

"Neglected Tropical Diseases and Conditions of the Nervous System", Springer Nature, 2014

Crossref

10 words — < 1%

"Poster Presentations", FEBS Journal, 07/2009

Crossref

10 words — < 1%

Abdulkadir, Abubakar Shettima. "Diesel Particulate Extract Induced Immunotoxicity: Hybrid Study in Pulmonary Cells", Southern University and Agricultural and Mechanical College, 2024

ProQuest

10 words — < 1%

Ahmed Fares, Abdou Mahdy, Gamal Ahmed. "Unraveling the mysteries of silver nanoparticles: synthesis, characterization, antimicrobial effects and uptake translocation in plant—a review", Planta, 2024

Crossref

10 words — < 1%

Claudio Parolo, Amadeo Sena-Torralba, José Francisco Bergua, Enric Calucho et al. "Tutorial: design and fabrication of nanoparticle-based lateral-flow immunoassays", Nature Protocols, 2020

Crossref

10 words — < 1%

De Decker, Sophie, Muriel Vray, Viridiana Sistek, Bhety Labeau, Antoine Enfissi, Dominique Rousset, and Séverine Matheus. "Evaluation of the Diagnostic

10 words — < 1%

Accuracy of a New Dengue IgA Capture Assay (Platelia Dengue IgA Capture, Bio-Rad) for Dengue Infection Detection", PLoS Neglected Tropical Diseases, 2015.

Crossref

Francesco Piraino, Šeila Selimović, Krzysztof Iniewski. "Diagnostic Devices with Microfluidics", CRC Press, 2017

Publications

10 words — < 1%

Huang, Xiaolin, Zoraida P. Aguilar, Hengyi Xu, Weihua Lai, and Yonghua Xiong. "Membrane-based lateral flow immunochromatographic strip with nanoparticles as reporters for detection: A review", Biosensors and Bioelectronics, 2016.

Crossref

10 words — < 1%

[aac.asm.org](http://aac.asm.org)

Internet

10 words — < 1%

[archive.org](http://archive.org)

Internet

10 words — < 1%

do Couto Rodrigues, Sílvia Maria. "Dissecting the Mechanisms Governing Skin Wound Healing Induced by an Umbilical Cord Blood-Derived Product", Universidade de Coimbra (Portugal), 2024

ProQuest

10 words — < 1%

[etheses.whiterose.ac.uk](http://etheses.whiterose.ac.uk)

Internet

10 words — < 1%

[www.science.gov](http://www.science.gov)

Internet

10 words — < 1%

"Human Emerging and Re-emerging Infections", Wiley, 2015

Crossref

9 words — < 1%

Abhay P. S. Rathore, Manouri Senanayake, Arjuna Salinda Athapathu, Sunethra Gunasena et al. "Serum chymase levels correlate with severe dengue warning signs and clinical fluid accumulation in hospitalized pediatric patients", Scientific Reports, 2020

Crossref

9 words — < 1%

Anne-Marie Lambeir, José Fernando Díaz Pereira, Pablo Chacón, Geert Vermeulen et al. "A prediction of DPP IV/CD26 domain structure from a physico-chemical investigation of dipeptidyl peptidase IV (CD26) from human seminal plasma", Biochimica et Biophysica Acta (BBA) - Protein Structure and Molecular Enzymology, 1997

Crossref

9 words — < 1%

Ballegaard, V., A.K. Haugaard, P. Garred, S.D. Nielsen, and L. Munthe-Fog. "The lectin pathway of complement: Advantage or disadvantage in HIV pathogenesis?", Clinical Immunology, 2014.

Crossref

9 words — < 1%

C. R. O'Riordan. "Characterization of the oligosaccharide structures associated with the cystic fibrosis transmembrane conductance regulator", Glycobiology, 11/01/2000

Crossref

9 words — < 1%

Dalot, Ana Sofia Barradas. "Plasmonic Nanostars for Sensitive Sers-Based Immunodetection", Universidade NOVA de Lisboa (Portugal), 2024

ProQuest

9 words — < 1%

Dias, Ana Sofia Abrantes. "Development and Validation of an Analytical Method for Quantification of Dopamine Metabolism in Plasma Samples by LC-MS/MS", Universidade de Coimbra (Portugal), 2024

ProQuest

9 words — < 1%

G. Zhang, X. Wang, A. Zhi, Y. Bao, Y. Yang, M. Qu, J. Luo, Q. Li, J. Guo, Z. Wang, J. Yang, G. Xing, S. Chai, T. Shi, Q. Liu. "Development of a lateral flow immunoassay strip for screening of sulfamonomethoxine residues", Food Additives & Contaminants: Part A, 2008

Crossref

9 words — < 1%

Kerry Atkinson, David Mabey. "Revolutionizing Tropical Medicine", Wiley, 2019

Crossref

9 words — < 1%

Khokon Kanti Bhowmik, Md. Abdul Barek, Md. Abdul Aziz, Mohammad Safiqul Islam. "A systematic review and meta-analysis of abnormalities in hematological and biochemical markers among Bangladeshi COVID-19 cases", Health Science Reports, 2022

Crossref

9 words — < 1%

Lionel Mandell, Mark Woodhead, Santiago Ewig, Antoni Torres. "Respiratory Infections", CRC Press, 2019

Publications

9 words — < 1%

Mahendra Rai, Graciela Avila-Quezada. "Nanotechnology in Plant Health", CRC Press, 2024

Publications

9 words — < 1%

Michael J. Myers, Michael P. Murtaugh. "Cytokines in Animal Health and Disease", CRC Press, 2020

Publications

9 words — < 1%

Soliman, H.. "Loop mediated isothermal amplification combined with nucleic acid lateral flow strip for diagnosis of cyprinid herpes virus-3", Molecular and Cellular Probes, 201002

Crossref

9 words — < 1%

T. Pullaiah, Maddi Ramaiah. "Handbook of Research on Herbal Liver Protection - Hepatoprotective Plants", CRC Press, 2021  
Publications

9 words — < 1%

ecth2018.org  
Internet

9 words — < 1%

encyclopedia.pub  
Internet

9 words — < 1%

escholarship.org  
Internet

9 words — < 1%

fjps.springeropen.com  
Internet

9 words — < 1%

idoc.pub  
Internet

9 words — < 1%

mdpi-res.com  
Internet

9 words — < 1%

openaccess.iyte.edu.tr  
Internet

9 words — < 1%

oro.open.ac.uk  
Internet

9 words — < 1%

wjoud.com  
Internet


9 words — < 1%

www.medrxiv.org  
Internet

9 words — < 1%



# Development of a novel lectin-based gold nanoparticle point-of-care immunoassay for rapid diagnosis of patients with severe Dengue infection

Moumita Paul<sup>a</sup>, Bibhuti Saha<sup>b</sup>, and Sumi Mukhopadhyay <sup>a</sup>

<sup>a</sup>Department of Laboratory Medicine, School of Tropical Medicine, Kolkata, India; <sup>b</sup>Department of Infectious Diseases & Advanced Microbiology, School of Tropical Medicine, Kolkata, India

## ABSTRACT

Rapid diagnosis of patients with severe Dengue infection can be useful for the efficient clinical management of cases caused by the Dengue virus. Lateral Flow Immunoassay (LFIA) have been broadly used for rapid Dengue diagnosis, because of their quick readouts with the human eye, simplicity of use, and affordability. Despite the availability of several commercial Dengue point-of-care assays, none has shown to be successful in discriminating between severe and nonsevere forms of Dengue infection. In the current study, for the first time, a novel lectin-based point-of-care assay for the early detection of patients with severe Dengue infection with gold-adorned sheets as detection labels is being reported. In this assay, Dengue severity was diagnosed by detecting the glycosylation profile of vitronectin, a known Dengue severity marker. Two lectins were employed namely DSA (*Datura stramonium*) and MAA (*Maackia amurensis*) that can recognize specific glycans like galactose Gal-(1–4) GlcNAc and sialic acid in an (α2–3) linkage, which displayed high sensitivity and high specificity, i.e. 90% and 85% for DSA and 90.91% and 95% for MAA. The new assay has a detection limit of 5 µg µl<sup>-1</sup> and enables the quick (30 min) and sensitive detection of severe Dengue cases. The reported point-of-care immunoassay exhibits considerable promise for early identification of patients with Dengue severity.

## KEYWORDS

Dengue fever; DSA (*Datura stramonium*); MAA (*Maackia amurensis*)

## Introduction

One of the most prevalent arboviral diseases is Dengue, affecting human beings. Several tropical and subtropical regions in the world are affected by this disease.<sup>[1,2]</sup> As per the World Health Organization (WHO), this disease is largely indigenous to South-East Asia and the Western Pacific. In recent years, multiple epidemics have occurred in Kolkata, a Dengue hyperendemic area in West Bengal, India. In India and throughout the world, Dengue infection is still one of the biggest health issues. Dengue is caused by four serotypes.<sup>[3]</sup> *Aedes* mosquitoes are the primary vectors of Dengue virus transmission (i.e. *Aedes aegypti* and *Aedes albopictus*).

**CONTACT** Sumi Mukhopadhyay  [drsumimukhopadhyay@gmail.com](mailto:drsumimukhopadhyay@gmail.com)  Department of Laboratory Medicine, Calcutta School of Tropical Medicine, West Bengal, India

© 2023 Taylor & Francis

The interplay between the viral component and the host's genetic and immunological makeup greatly influences the pathological outcome of Dengue infection.<sup>[4]</sup> Clinical symptoms caused by the Dengue virus infection range from self-limiting Dengue-without-warning- sign (DWOWS), Dengue-with-warning-sign (DWWS) to life-threatening severe-Dengue (SD) infection.<sup>[5]</sup> Currently, there are no vaccines available for Dengue prevention. There are no antiviral drugs also for Dengue infection.<sup>[6]</sup> To reduce the rate of fatalities, appropriate laboratory-based early diagnosis of febrile cases which might become severe is highly necessary.

One of the most challenging areas in Dengue disease management has been the early diagnosis of Dengue severity.<sup>[7]</sup> Antigen capture-enzyme linked immunosorbent assay and laboratory-based reverse transcription polymerase chain reaction (RT-PCR) are already applied to diagnose Dengue, but none of these assays can predict Dengue severity. No such test for the detection of Dengue severity is being reported or commercially available.<sup>[8]</sup> This study aimed to develop a simple, highly sensitive, and low-cost point-of-care immunoassay using gold conjugated vitronectin monoclonal antibody and lectin (DSA{*Datura stramonium*} and MAA{*Maackia amurensis*}) which detect glycosylated VTN rapidly.

Vitronectin (VTN) is a multifunctional glycosylated protein, present in the extracellular matrix of tissues, blood, amniotic fluid, and urine.<sup>[9]</sup> VTN is a part of the extracellular matrix that affects cell adhesion and cell necrosis.<sup>[10]</sup> Similar to fibronectin, VTN is an adhesion protein found in plasma that contains the amino acids arginine, glycine, and aspartic acid (RGD).<sup>[11]</sup> Human glycoprotein broadly has two types of glycosylation, N-linked and O-linked modification, respectively, in which glycan is attached to the asparagines or serine and threonine residues. Though VTN is reported in Dengue infection, its application in the development of point of care immunoassay to detect the severity of Dengue infection is still unknown.<sup>[12]</sup> This test will aid in the early detection of severe Dengue cases and provide a predictive evaluation for the progression of the disease severity.

Approximately 30% of human VTN is glycosylated. Changes in glycosylation of plasma VTN may be associated with cellular functions, related to different physiological states.<sup>[13]</sup> According to mass spectrometry and chromatography data, VTN has an N-glycan with outer fucosylation.<sup>[14]</sup> A post-translational alteration known as glycosylation involves the attachment of glycans, which are sugar molecules, to specific locations on the protein's backbone. During cellular functions and cirrhosis, VTN's glycosylation modulates cellular functions.<sup>[15,16]</sup> De N-glycosylation and desialylation of VTN in humans, swine, and rodents have also been shown to improve collagen-binding activity.<sup>[17]</sup> When compared to normal VTN, dermal fibroblast and hepatic stellate cell proliferation are significantly reduced by desialylated VTN (deNeu-VN) but not by desialylated VTN that has been deN-glycosylated



(deN-gly-VN).<sup>[18]</sup> According to these findings, VTN and its glycosylation should be essential in the remodeling of organs and tissues where collagen is the primary constituent.

The altered glycosylation profile of vitronectin in disease can thus be conveniently read through a simple lectin binding assay. These lectin-recognized carbohydrates can thus be created in a high throughput platform for LFIA.<sup>[19]</sup> Lectins are glycan-binding proteins that recognize the glycan epitope of free carbohydrates or glycoprotein.<sup>[20]</sup> For direct and accurate detection of functional glycans on intact glycoproteins taking into account accessibility, the lectin binding-based method provides an interesting strategy. Lectins are a widespread class of natural proteins that bind with specific glycans. Due to their specificity and diversity, lectins can be useful tools in molecular research.

DSA (*Datura stramonium*) and MAA (*Maackia amurensis*) are one of the most widely studied lectins due to their wide range of biological functions, such as immune stimulating activity. MAA can recognize specific glycans like sialic acid in  $\alpha 2-3$  linkage, whereas DSA is specific for galactose Gal-(1-4) GlcNAc.<sup>[21]</sup> The present study was designed to evaluate the potential of lectin affinity-based approaches for characterizing the glycosylation pattern of human VTN from Dengue-infected patient's plasma samples in LFIA format.

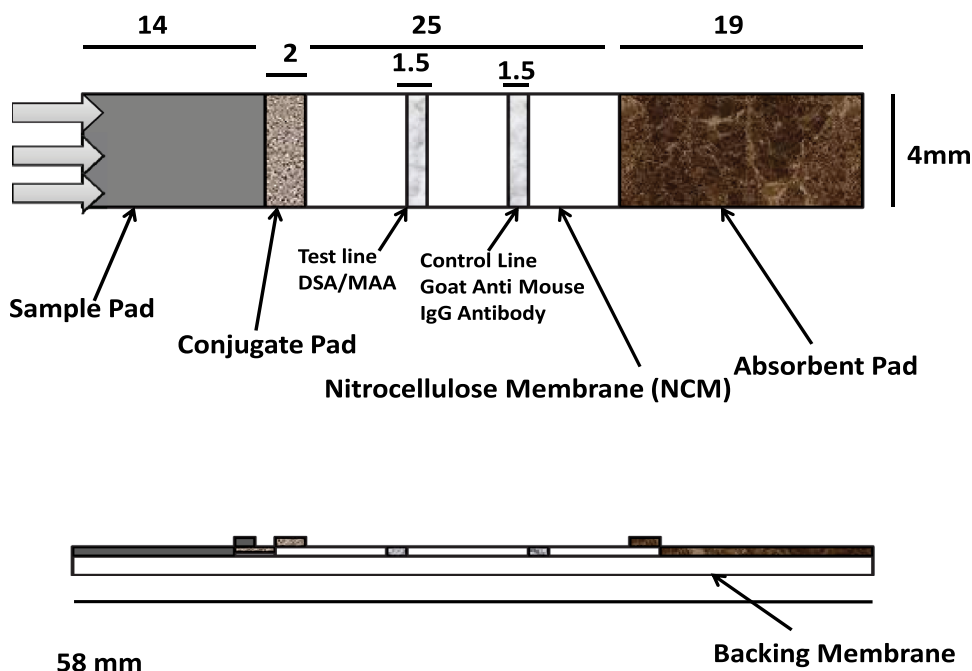
## Method

### Study population

A total of 30 confirmed Dengue patients enrolled at the Calcutta School of Tropical Medicine during the period of June to November 2021, evaluated in this study. After a clinical evaluation, an NS1 IgM antibody capture enzyme-linked immunosorbent test (MAC-ELISA) and an IgM/IgG ELISA were used to confirm the diagnosis of Dengue infection. Among the 30 subjects, patients (PT) 1-10 were included in the category of Dengue without warning sign (DWOWS), PT 11-20 were included in the category of Dengue with warning sign (DWWS), and PT 21-30 were included in the category of severe Dengue (SD).

### Preparation of immunostrip

For the studies, a backing laminate with a 10  $\mu$ m porosity Nitrocellulose Membrane (NCM) preassembled on its surface was used. By removing the adhesive tape from the sample pad side, a 4 mm wide conjugate pad was put together on the NCM. The conjugate pad was stuck on the strip so that it overlaps on the NCM by 2 mm. This overlap is crucial for the fluid's ability to move freely across the strip because the wicking motion helps move the fluid from one layer to the next. On the conjugate pad, a sample pad was similarly positioned with a 1 mm overlap. The absorbent pad was assembled on the strip with an overlap of 2 mm on



#### Schematics of the LFIA assembly (measurements in mm)

**Figure 1.** Illustrates the dimension of components on assembled LFIA strip along with the side view. Abbreviations: LFIA: lateral flow immunoassay.

the NCM from another end. As the absorbent pad acts as a tool and pulls the fluid from the strip to the end, this overlap is an important consideration. The presence of moisture on the strip surface may diffuse the fluid throughout the pad and affect the flow pattern. After putting the necessary components on the plastic backing laminate, the sheet was trimmed into 4 mm strips. Schematics are represented in [Figure 1](#). For the experiments, a backing laminate with a preassembled NCM with a 10 mm porosity was used. By removing the adhesive tape from the sample pad side, a conjugate pad measuring 4 mm broad was put together on the NCM.

#### Conjugation of gold nanoparticles with anti-VTN mAb

We use gold nanoparticles as optical probes to provide a meaningful signal in the presence of the targeted biomarker. We used Gold Conjugated Kit (40 nm, 200D, ab154873) for the preparation of Gold conjugated Antibody which is used as a detection probe for lectin-based lateral flow immunoassay. Stock antibody (Anti-Vitronectin Monoclonal Antibody raised in mouse {Invitrogen CSI003–0202}) was diluted with the gold antibody diluent provided in the kit to 0.1 mg/ml. For each reaction in a clean 1.5 ml, microfuge tube 42  $\mu$ l of gold reaction buffer was

added followed by 12  $\mu\text{L}$  of diluted antibody. Forty-five microliters of the mixture was added to a vial of gold. Finally, 5  $\mu\text{L}$  of EL Gold Quencher was added to yield 50  $\mu\text{L}$  of 20 OD gold conjugated anti-VTN antibody, i.e. AuNP-anti-VTN.

### ***Nitrocellulose membrane selection***

As a membrane for strip development, nitrocellulose is frequently utilized (i.e. NCM). Advanced Microdevices Pvt. Ltd. of Ambala, Haryana, India, provided the Easypack membrane kit device. The kit comprises different pore sizes of NCM, i.e. 8, 10, 12, and 15  $\mu\text{m}$ , which were used in the standardization process. The porosity of the strip is crucial because the NCM pore size affects how fluid flows through the strip. To study the flow time of different porosity of the NCM lump together on the strips, flow time is an important morphology for selecting NCM with appropriate pore size.

### ***Sample-pad, conjugate-pad, and absorbent-pad selection***

For developing a lateral flow assay, we used different components like a Sample pad (glass fiber; GFB-R7L), Conjugate pad (Cellulose fiber; PT-R7, R-1816J E02), NC Membrane (CNPF-SN12, MEMBRANE TECHNOLOGY), and Absorbent Pad (Cellulose; AP080), procured from Advanced Microdevices Pvt. Ltd. Ambala, Haryana, India.

### ***Assembly of the immunostrip for the detection of Dengue severity***

Plastic backing laminate ( $4 \times 25$  mm) requires three elements on the surface, sticker for sample pad meeting at one end. The sample pad receives the sample, retains it while forwarding it to the conjugate pad, and then releases it to the NCM. Using a paper cutter, a sheet of the conjugate pad ( $4 \times 2$  mm) was cut, the adhesive label on the sample pad side was removed, and the conjugate pad sheet was assembled on the backing laminate with a 2 mm overlap on NCM. Throughout the LFIA shelf life, the conjugate pad maintains the protein bioconjugates' stability. For the LFIA study, the conjugate pad should reliably and effectively release the bioconjugate. After that, the sample pad sheet ( $4 \times 14$  mm) adhered to the backing laminate so that it overlapped the conjugate pad but was no longer attached to NCM. On the other side of the strip, the absorbent pad sheet ( $4 \times 19$  mm) adhered in a similar pattern. To confirm the consistent construction, the strip was flattened on a level surface using a plastic cover sheet. It was then seen that the sample pad had no folds or aberrations. A paper cutter was used to cut the sheet into 4 mm-wide strips, which were then placed in a desiccator until they were needed.

### ***Control line and test line optimization***

The standard running protocol for the LFIA development consists of an assembly of the elements like an absorbent pad at the plastic backing laminate preassembled with NCM. In the beginning, a laminated NC membrane for standardization was carried out. At first, the NC membrane was kept in a hot air oven at 55°C for 20 min to eliminate moisture if any. For Control line optimization, 1 µl of capture antibody, i.e. Goat Anti-Mouse IgG Antibody (#31160 invitrogen), and for test line optimization, different concentrations of two lectins, i.e. MAA (vector lab-L-1310) or DSA (vector lab-L-1180), were lined on the NCM and dried at room temperature overnight in front of the dehumidifier. After that, microcentrifuge tubes were taken. Various concentrations of the capture antibody, i.e. 0.25, 0.5, 1, and 2 µg/µl, were prepared within a microcentrifuge tube and lined on the NCM, and various concentrations of lectins, i.e. 10, 5, 2.5, and 1.25 µg/µl, on the test line were prepared in a microcentrifuge tube and lined on the NC membrane; 2 µl of gold conjugated detection antibody (Anti-VTN Mab) was applied on the conjugated pad and kept overnight at room temperature. LFIA strip is also used for the detection of severe and nonsevere Dengue-infected patients with optimized lectin concentration.

### ***Quantification of color intensity***

The intensity of dots and lines was quantified using ImageJ 1.49 v software. After converting the photos to RGB format, the proper color was chosen. A line created by hand encircled the intensity, and the measure icon was used to measure the area, minimum, and maximum values. A plot profile throughout the illuminated region was created using a rectangle that was drawn. To establish a baseline for the data, column averages to the left and right of the point were utilized. The signals were suitably scaled if various exposure times were employed.

### ***LFIA strips testing with clinical samples***

Confirmed Dengue patients were enrolled in the indoor Calcutta School of Tropical Medicine from June to November 2021. Thirty patients were included in this study. Clinical and laboratory-based diagnostic confirmation tests were performed using NS1 and IgM/IgG capture ELISA and PCR tests. Plasma samples were collected from Dengue-infected patients in the course of their indoor admission to the Calcutta School of Tropical Medicine, West Bengal. During their stay in the hospital, hematocrit and platelet counts were measured using automated cell counters (SYSMEX Model No. XP100), and liver function was tested using an Autoanalyser (ERBA Model No. EM360), which were utilized for development of nomograms. A nomogram was used to predict the

severity of severe Dengue patients. The nomogram is used by totaling the points assigned on the scales for each independent parameter, i.e. NS1, platelet, HCT, SGOT, and SGPT.<sup>[22]</sup>

By loading human plasma from Dengue infected patients, the viability of the generated immunostrips as instruments for determining the severity of Dengue infection was examined in triplicate trials. A sample pad containing 50 µl of positive or negative human plasma was added to the case of strips where the conjugates were made up of AuNP-anti-VTNMab. Capillary pressures caused samples to travel from the conjugate pad to the membrane, where they met the lectin test lines and control lines and finally into the absorbent pad during the first 5 min of the test, and the findings were visually assessed within 30 min. Using the Image J program, the color intensity in the test and control lines of each strip was further quantified. The assay performance was calculated by determining sensitivity, specificity, and the inter- and intra-assay coefficient of variation (CV). To calculate the reproducibility of this assay, samples in triplicate from each set were assayed by two independent experiments. Further assay performance is validated through standard ELISA determining VTN titers of severe and nonsevere Dengue patients.

### ***Determination of circulating glyco-proteins (VTN) titres***

To measure the levels of plasma circulating glycoproteins (VTN) in different categories of Dengue infected patients, stored plasma of Dengue patients was thawed, and levels of VTN were evaluated using standard ELISA kits (Ray Biotech, ISO 13,485 Certified, 3607 Parkway Suite 100, Norcross, GA 30,092, Catalog #: ELH-VTN). The tests were carried out as per the manufacturer's instruction. Samples used for this assay include severe and nonsevere Dengue patients.

### ***Statistics***

First, the D'Agostino and Pearson omnibus normality tests were used to perform a normality test on each data set. Analyses using a single non-parametric ANOVA (i.e. Kruskal-Wallis test) and t-test (Mann-Whitney-Test) were performed, and *P* values below 0.05 were considered statistically significant. Area-under-curve (AUC) values that were statistically significant were also calculated. Applied statistical analysis utilizing the Graph-Pad Prism statistical program (Graph-Pad Software Inc., San Diego, CA).

### **Ethics statement**

This study received ethical permission from the Clinical Research Ethical Committee of Calcutta School of Tropical Medicine (CREC-STM/461 dated 18/06/2018), following the Helsinki protocol.

### **Result**

#### ***Morphological analysis of the NCM***

Different pore sizes of NCM, i.e. 8, 10, 12, and 15  $\mu\text{m}$ , were used in the standardization process. Since the pore size of NCM affects the flow of fluid through the strip, the strip's porosity quality is crucial. An increase in pore size of NCM increases the wicking rate and pulls fluid at a faster rate as compared to the NCM with a smaller pore size, but the protein-binding capacity of NCM is reduced with the increase in pore size. Thus, to adjust fluid flow and protein binding on the NCM, having 10  $\mu\text{m}$  pore size was used for the development of LFIA as shown in Table 1.

#### ***Control line optimization using LFIA***

The optimum concentration of capture antibody at the control line was found to be 2  $\mu\text{g}/\mu\text{l}$  (1  $\mu\text{l}$ ) which is shown in Figure 2e-f.

#### ***Test line DSA (Datura stamonium agglutinin) optimization using LFIA***

The optimum concentration of DSA was found to be 5  $\mu\text{g}/\mu\text{l}$  for LFIA. A cleared line was found in this concentration which is shown in Figure 2c,d. This concentration of DSA was applied to different categories of Dengue-infected patients which are shown in Figure 3c.

#### ***Test line MAA (Maackia amurensis agglutinin) optimization using LFIA***

The optimum concentration of MAA was found to be 5  $\mu\text{g}/\mu\text{l}$  for LFIA. A cleared line was found in this concentration which is shown in Figure 2a,b. This

**Table 1.** Flow time analysis of different pore sizes of NC membrane.

Strips	Pore size of NC membrane	Flow time (sec/2.5 cm)
A	8 $\mu\text{m}$	59.32 $\pm$ 0.3765
B	10 $\mu\text{m}$	41 $\pm$ 1.25
C	12 $\mu\text{m}$	36.95 $\pm$ 0.3567
D	15 $\mu\text{m}$	30.74 $\pm$ 0.9483

The results showed Mean  $\pm$  SEM value of flow time. Abbreviations: NC membrane-nitrocellulose membrane.

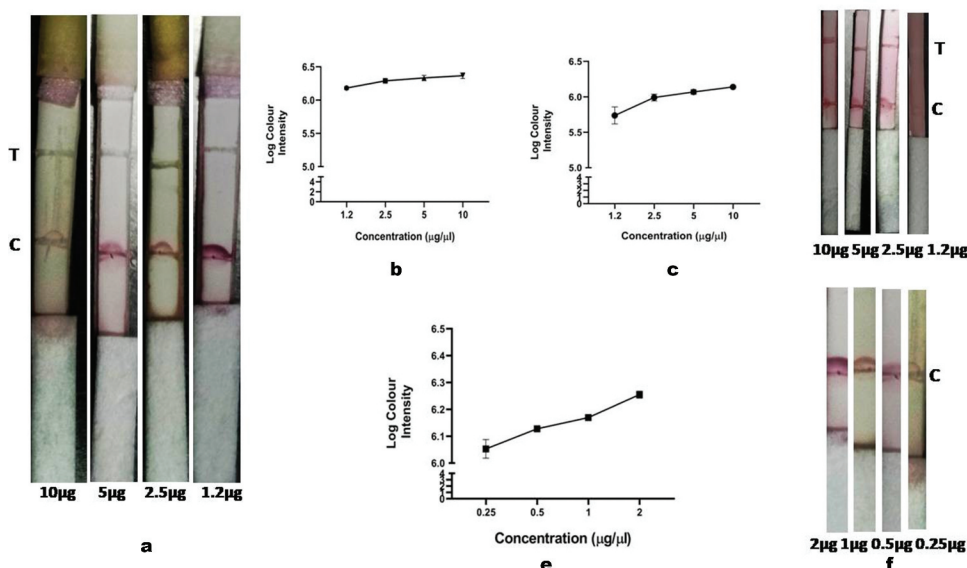


**Figure 2.** Point of care assay analysis of test line and control line optimization. ANOVA followed by Kruskal–Wallis test (K). a) Different concentration of MAA (*Maackia amurensis* agglutinin). b) Graph represents color intensity of different concentration of one lectin, i.e., of MAA (*Maackia amurensis* agglutinin). c) Graph represents color intensity of different concentration of another lectin, i.e., of DSA (*Datura stramonium* agglutinin). d) Different concentration of DSA (*Datura stramonium* agglutinin). e) Graph represents color intensity of different concentration of control line, i.e. Goat anti-mouse IgG antibody. f) Different concentration of control line (Goat anti-mouse IgG antibody).

concentration of MAA was applied to different categories of Dengue-infected patients which are shown in Figure 3d. For the development of LFIA Goat Anti-Mouse IgG Antibody was used as a marker for the control line. Thus, LFIA was developed to determine the optimum concentration of capture antibody at the control line and test line for further application. The experimental protocol was followed for the development of LFIA for test line optimization.

### Validation of the newly developed assay using clinical samples

The newly developed assay was tested with different categories of Dengue-infected patients, i.e. 10 patients with Dengue without a warning sign (DWoWS), 10 patients with Dengue with a warning sign (DwWS), and 10 patients with severe Dengue (SD) infection. Nonsevere Dengue infection includes both DWoWS and DwWS. The study population included severe and nonsevere Dengue patients.<sup>[23]</sup>

The newly developed assay was validated by performing inter and intra assay. The %CV observed in this assay was determined as shown in Table 2.

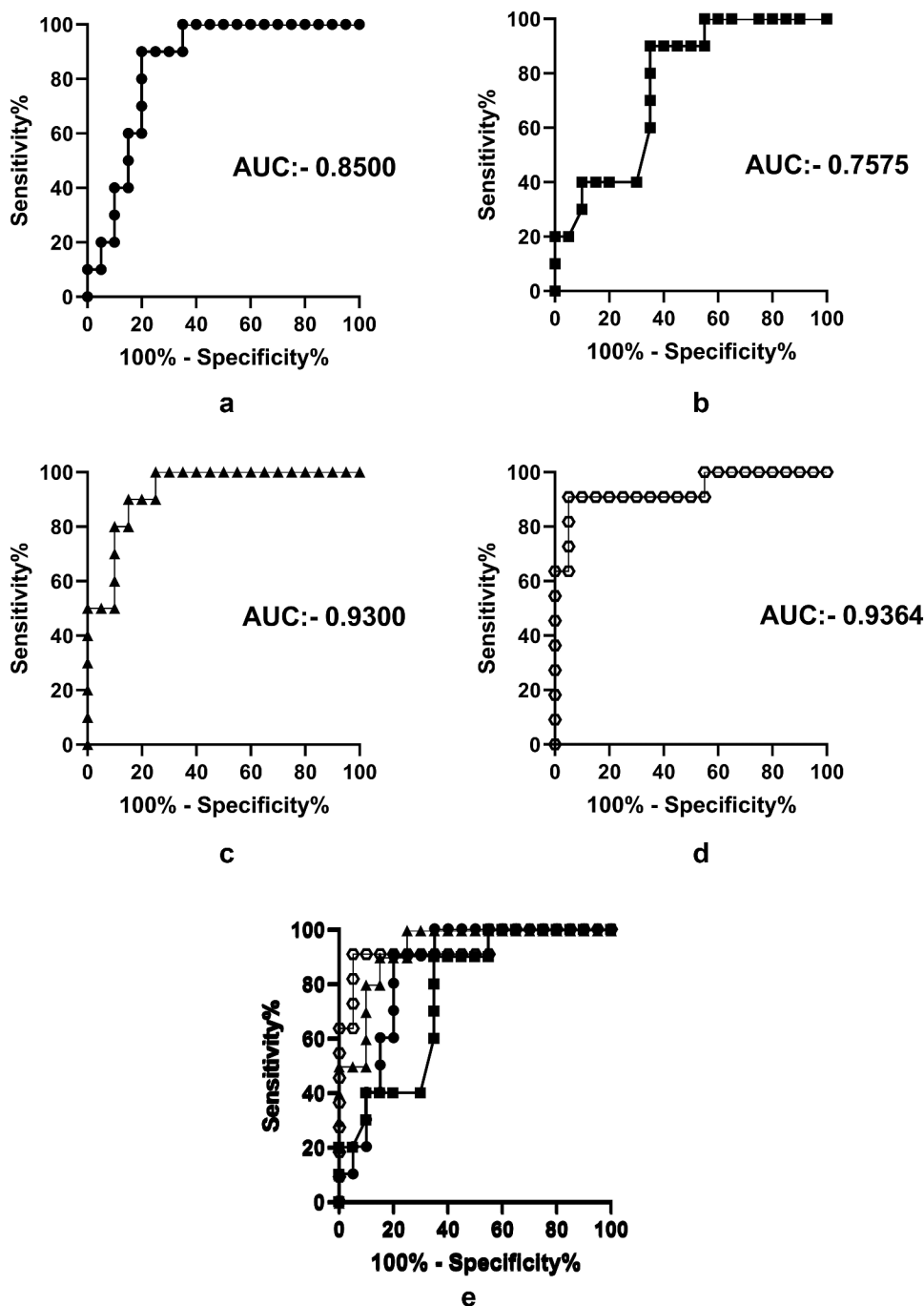


**Figure 3.** Receiver operating characteristics curve (ROC) analysis of severe and non-severe Dengue infected patients. a) ROC analysis of VTN level as obtained through standard ELISA had 90% sensitivity and 80% specificity. b) ROC analysis of severity score of Dengue patients as obtained from nomogram calculation had 90% sensitivity and 65% specificity. c) ROC analysis of newly developed point-of-care assay using DSA had 90% sensitivity and 85% specificity and d) ROC curve analysis of newly developed point-of-care assay using MAA had 90.91% sensitivity and 95% specificity. Abbreviations: VTN: vitronectin, DSA: Datura stramonium agglutinin, MAA: Maackia amurensis agglutinin, CV: coefficient of variation.



Briefly, the coefficient of variation (%CV) for intra-assay (MAA) non-severe Dengue infected patients was 0.81% and, for severe Dengue patients, was 1.3%.

**Table 2.** Inter- and intra-assay variation.

Categories	MEAN±SD Inter-assay (DSA)	CV (%)	MEAN±SD Inter-assay (MAA)	CV (%)	MEAN±SD Intra-assay (DSA)	CV (%)	MEAN±SD Intra-assay (MAA)	CV (%)
Nonsevere	5.912 ± 0.053	0.89%	6.329 ± 0.051	0.81%	5.938 ± 0.053	0.89%	6.331 ± 0.051	0.81%
Severe	5.822 ± 0.031	0.5345%	6.156 ± 0.082	1.339	5.845 ± 0.031	0.5355%	6.102 ± 0.082	1.34%

The results showed Mean ± SEM value of inter- and intra-assay followed by descriptive statistics. Abbreviations: DSA: *Datura stramonium* agglutinin, MAA: *Maackia amurensis* agglutinin, CV: coefficient of variation.

About the intra-assay (DSA) variation, the % CV was 0.899% for nonsevere and 0.5355% for severe patients.

The sensitivity and specificity were found to be higher for VTN-MAA interaction, i.e. 90.91% sensitivity and 95% specificity, whereas VTN-DSA interaction showed 90% sensitivity and 85% specificity. Though there is no such assay available that can predict Dengue severity, we cannot compare this assay with any standard assay. However, we compare the assay performance through the standard severity-determining nomogram which can generate severity scores (Figure 3).

### **Comparison between assay with nomogram and VTN ELISA**

From this nomogram, we also get the percentage of the predicted risk factor of severity. Among the Dengue patients enrolled in the study, the nomogram was applied and it yielded a sensitivity of 90% and specificity of 65%. The area under the curve (AUC) was 0.7575, whereas ELISA of VTN yielded a sensitivity of 90% and specificity of 80% and AUC being 0.8500 (Figure 4).

### **Characteristics of blood parameters of clinical samples used for LFIA testing**

According to the patients clinical presentation, they were categorized into Dengue without warning sign (DWoWS), Dengue with a warning sign (DwWS), and severe Dengue (SD). Nonsevere Dengue infection includes both DWoWS and DwWS. The study population included DWoWS, DwWS, and SD. Biochemical results showed that low concentrations (Mean ± SEM) of serum glutamic oxaloacetic transaminase (SGOT; 46.70 ± 10.09 IU/L) and serum glutamic-pyruvic transaminase (SGPT; 32 ± 4.115 IU/L) were obtained in the DWoWS sera. In patients with DwWS,

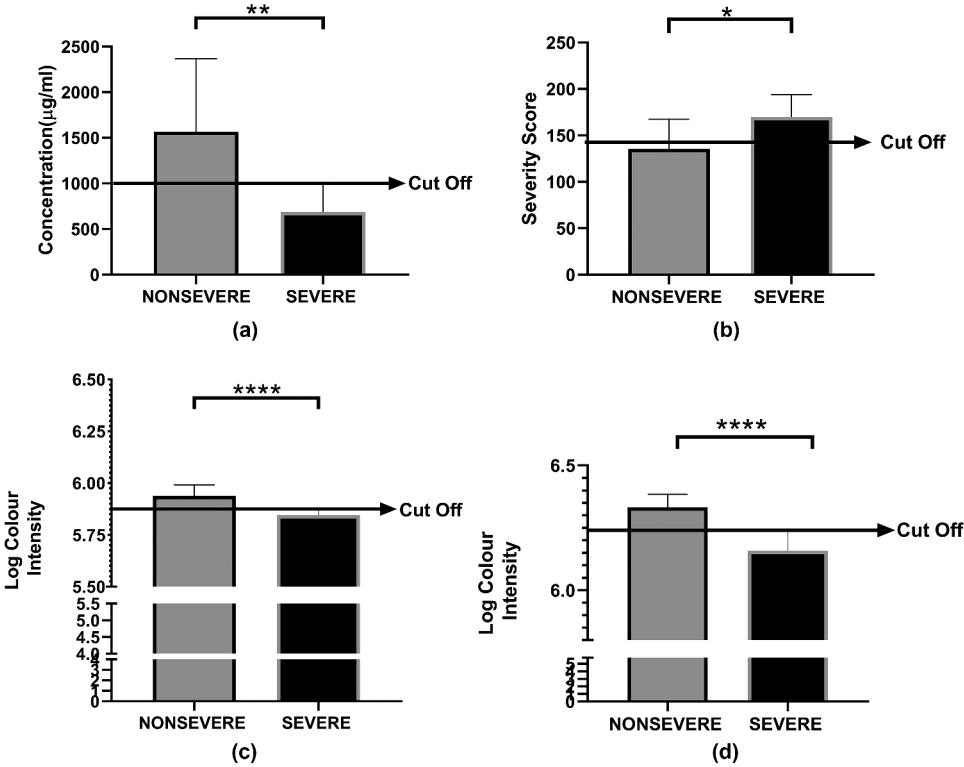


**Figure 4.** a) Levels of vitronectin (VTN) of nonsevere and severe Dengue infected patients. Study subjects are significantly different from each category. b) Graph represents severity score of severe and nonsevere Dengue patients. c) Graph represents the log value of color intensity of LFIA strip using DSA lectin. d) Graphical representation of colour intensity of LFIA strip using MAA lectin. All analysis performed were unpaired t test followed by Mann–Whitney method.

SGOT ( $160.4 \pm 27.37$  IU/L) and SGPT ( $77.50 \pm 13.65$  IU/L) were lower than the patients with SD ( $205.8 \pm 58.13$  IU/L) and ( $158.5 \pm 40.63$  IU/L), respectively, as shown in Table 3.

**Table 3.** Laboratory parameters of the study population

	DWOWS (n = 10)	DWWS (n = 10)	SD (n = 10)	
Laboratory measure	MEAN±SEM	MEAN±SEM	MEAN±SEM	ANOVA analysis (P value)
Platelet ( $\times 10^3/\mu\text{l}$ )	128800 ± 22898	66800 ± 8700	44400 ± 10696	0.0068
SGOT (U/L)	46.70 ± 10.09	160.4 ± 27.37	205.8 ± 58.13	0.0004
SGPT (U/L)	32 ± 4.115	77.5 ± 13.65	158.5 ± 40.63	0.0029
Hematocrit (%)	36.87 ± 0.9435	38.90 ± 1.840	36.65 ± 2.442	0.6419
Nomogram Score	109.4 ± 3.519	161.6 ± 7.196	169.8 ± 7.684	<.0001

The statistical analyses were performed using ANOVA followed by Kruskal–Wallis test (K) significance is indicated by  $P < 0.05$ . Biochemical results showed the value of mean ± SEM.

Abbreviations: DWOWS: Dengue without warning sign, DWWS: Dengue with warning sign, SD: severe Dengue, SGOT: serum glutamic-oxaloacetic transaminase, SGPT: serum glutamic-pyruvic transaminase.

## Discussion

To enhance disease management and reduce healthcare system costs globally, there is a demand for point-of-care diagnostic technologies that enable quick and affordable screening/diagnosis of infectious diseases. In the case of Dengue infection, there is no such assay that can predict the severity of Dengue-infected patients. This study demonstrated for the first time a reliable and affordable, lateral flow technology, well suited to point-of-care Dengue severity diagnostics. Considering this, the new aspect of the current study develops a point-of-care platform for diagnosis based on a strip-based test using VTN in combination with gold nanoparticles. The LFIA created is dependent on AuNPs' capacity to interface with anti-VTN antibodies to form conjugates that are employed as recognition tools capable of associating with VTN present in the plasma of patients with Dengue infection, then VTN-AuNP-Anti-VTN binds with lectins present in NCM as a test line. VTN is a glycosylated protein and a severity biomarker in Dengue-infected patients. However, the application of this protein in the development of point-of-care immunoassay is an innovative concept for early detection of the severity of Dengue infection. Glycosylation patterns are altered in several human diseases.<sup>[24]</sup> The lectin-based LFIA was developed and optimized for the detection of glycosylated VTN, particularly those coupled with sialic acid and N-acetylglucosamine residues. These two methods were based on the binding affinity of two different lectins with glycoproteins of current Dengue biomarkers, i.e. vitronectin (VTN). Changes in the connections between carbohydrate moieties can have a significant impact on the glycosylation state of VTN. To detect VTN glyco-patterns, two lectins were used which showed the most binding affinity with Plasma VTN,<sup>[21]</sup> i.e. (i) *Datura stamonium* agglutinin (DSA) recognizes (GlcNAc)<sub>2-4</sub> and (ii) *Maackia amurensis* lectin (MAA) recognizes terminal  $\alpha$ -2,3 sialylation of VTN were employed. To the best of our knowledge, this study is the first to apply the binding affinity of lectins with glycoproteins in the LFIA system for severity detection of Dengue infection. A higher sensitivity of detection was observed with ImageJ software, allowing discriminating fine differences of lectin binding.

VTN, a versatile glycoprotein found in blood and ECM, is essential to several physiological functions. Severe Dengue is characterized by endothelial dysfunction that causes the vascular leak. The crucial period, which occurs 3–6 days following the beginning of the disease, is when vascular leak usually becomes clinically noticeable.<sup>[25,26]</sup> Human VTN is highly glycosylated, and alterations in its glycan moieties were reported in human cancer.<sup>[21,27]</sup> Vitronectin circulates in the blood, usually as an inactive monomer, until it is recruited to regulate coagulation and platelet aggregation.<sup>[28,29]</sup> Vitronectin is mostly produced by the liver. In plasma, the level of vitronectin is associated with chronic liver disease.<sup>[30-33]</sup> Mayampurath et al. found eight vitronectin

glycopeptides in human blood using a high-throughput study; however, they were only able to bind to two of the three N-glycosylation sites of vitronectin.<sup>[33]</sup> A nonspecific digesting approach using pronase was used to identify and report 15 glycans from the standard vitronectin.<sup>[34]</sup> Our present study described the first larger analysis of Dengue-infected patient samples to characterize severe and non-severe Dengue-infected patients using glycosylation profiles of human VTN through two different lectin-based approaches, i.e. DSA (*Datura stramonium* agglutinin) and MAA (*Maackia amurensis* agglutinin). The use of gold conjugated with anti-VTN antibodies allowed us to capture and visualize secondary antibodies on the control line and VTN on the lectin test line. Concentrations of control line  $0.25\text{--}2\text{ }\mu\text{g mL}^{-1}$  and concentration of test line  $1.25\text{--}10\text{ }\mu\text{g mL}^{-1}$  have been tested and detected as shown in [Figure 2a–f](#).

The VTN oligomer has two distinct capabilities that could have implications for DENV infection and pathogenesis. First, the oligomer binds to heparin, a known receptor for DENV<sup>[35]</sup> Second, it regulates coagulation by forming a bridge between integrin and fibrin to induce platelet aggregation to inhibit plasma leakage.<sup>[30,31]</sup> The overall VTN glycosylation was measured by the lectin-based LFIA system. VTN levels in severe and nonsevere Dengue infected patients and discriminant patterns of lectin interactions were compared.

In the present paper, we demonstrated that the lectin-based lateral flow immunoassay system revealed the characterization of severe and non-severe Dengue infected patients through lectin binding, including DSA-Vtn and MAA-Vtn interaction. According to our findings, [Figure 4](#) shows that DSA-Vtn and MAA-Vtn interactions are significantly higher in non-severe Dengue patients than in severe subjects. The color intensity of lectin binding of VTN increases in nonsevere Dengue patients, as demonstrated by the lectin LFIA system, indicating a higher level of VTN concentration in nonsevere Dengue patients, which is also corroborated with VTN ELISA. The intraassay of the color intensity data with a “Mean  $\pm$  SD” value of  $6.331 \pm 0.051$  for MAA in Nonsevere was higher than severe Dengue patients with a “Mean  $\pm$  SD” value of  $6.102 \pm 0.0825$  for MAA, whereas for DSA, the intraassay of the color intensity data is  $5.938 \pm 0.053$  in Nonsevere Dengue patient is higher than severe Dengue patients with “Mean  $\pm$  SD” value of  $5.845 \pm 0.031$  but the interassay of MAA showed lower coefficient variation in nonsevere Dengue infected patients than DSA which is 0.8137% for nonsevere MAA and 0.89% for nonsevere DSA. While using MAA in the test line of the lectin-based point-of-care immune assay, the assay could successfully identify 9 out of 10 severe cases and 19 out of 20 nonsevere cases, but DSA could identify 15 nonsevere cases and 9 severe cases. This assay was further compared with an already reported standardized severity nomogram. Nomogram could not identify correctly seven such nonsevere patients and one severe patient, the sensitivity

and specificity being 90% and 65%. This newly developed assay was also compared with standard ELISA to determine VTN level. VTN ELISA could identify 15 nonsevere and 9 severe cases therefore the specificity and sensitivity were 80% and 90%. This study shows that a lectin-based point of care is much better than an already standardized nomogram for the detection of Dengue severity and ELISA. A lectin-based Lateral Flow Immunoassay method can be utilized to test individuals for Dengue infection initially, and if possible, a predictive POC test for severe Dengue can be employed in the diagnosis process. Patients who will be identified as having a non-severe Dengue infection, that is, with and without warning signs and low risk for Dengue infection, can be more confidently sent home to recover, whereas patients who will be identified as having a severe Dengue infection can be hospitalized and monitored by a physician.

There are some limitations in this study which include a small number of study subjects recruited. Before the widespread implementation of this assay, it must be evaluated in a larger cohort of patients.

## Disclosure statement

No potential conflict of interest was reported by the authors.

## Funding

The work was supported by the Life Sciences Research Board [LSRB-339].

## ORCID

Sumi Mukhopadhyay  <http://orcid.org/0000-0003-1400-3715>

## Financial support

This study received financial support from LSRB, DRDO, Govt. of India [O/o DG(TM)/81/48222/LSRB-339/BTB/2019].

## References

- [1] Katzelnick, L. C.; Coloma, J.; Harris, E. Dengue: Knowledge Gaps, Unmet Needs, and Research Priorities. *Lancet Infect. Dis.* **2017**, *17*, e88–e100. DOI: [10.1016/S1473-3099\(16\)30473-X](https://doi.org/10.1016/S1473-3099(16)30473-X).
- [2] Bhatt, S.; Gething, P.; Brady, O.; Messina, J.; Farlow, A.; Moyes, C.; Drake, J. M.; Brownstein, J. S.; Hoen, A. G.; Sankoh, O. The Global Distribution and Burden of Dengue. *Nature*. **2013**, *496*(7446), 504–507. DOI: [10.1038/nature12060](https://doi.org/10.1038/nature12060).
- [3] Broor, S.; Devi, L. S. Arboviral Infections in India. *Ind. Jour. Healt. Scie.* **2015**, *2*(3), 192–202. DOI: [10.5958/2394-2800.2015.00035.8](https://doi.org/10.5958/2394-2800.2015.00035.8).

- [4] Lai, S. C.; Huang, Y. Y.; Wey, J. J.; Tsai, M. H.; Chen, Y. L.; Shu, P. Y.; Chang, S. F.; Hung, Y. J.; Hou, J. N.; Lin, C. C. Development of Novel Dengue NS1 Multiplex Lateral Flow Immunoassay to Differentiate Serotypes in Serum of Acute Phase Patients and Infected Mosquitoes. *Front. Immunol.* **2022**, *13*, 852452. DOI: [10.3389/fimmu.2022.852452](https://doi.org/10.3389/fimmu.2022.852452).
- [5] Thein, T. L.; Gan, V. C.; Lye, D. C.; Yung, C. F.; Leo, Y. S.; Halstead, S. B. Utilities and Limitations of the World Health Organization 2009 Warning Signs for Adult Dengue Severity. *PLoS Negl. Trop. Dis.* **2013**, *7*(1), e2023. DOI: [10.1371/journal.pntd.0002023](https://doi.org/10.1371/journal.pntd.0002023).
- [6] Thisyakorn, U.; Thisyakorn, C. Latest Developments and Future Directions in Dengue Vaccines. *Ther. Adv. Vaccines.* **2014**, *2*(1), 3–9. DOI: [10.1177/2051013613507862](https://doi.org/10.1177/2051013613507862).
- [7] Bhat, V. G.; Chavan, P.; Ojha, S.; Nair, P. K. Challenges in the Laboratory Diagnosis and Management of Dengue Infections. *Open Microbiol. J.* **2015**, *9*, 33–37. DOI: [10.2174/1874285801509010033](https://doi.org/10.2174/1874285801509010033).
- [8] Araújo, F. M. C.; Brilhante, R. S. N.; Cavalcanti, L. P. G.; Rocha, M. F. G.; Cordeiro, R. A.; Perdigão, A. C. B.; Miralles, I. S.; Araújo, L. C.; Lima, E. G.; Sidrim, J. J. C. Detection of the Dengue Non-Structural 1 Antigen in Cerebral Spinal Fluid Samples Using a Commercially Available Enzyme-Linked Immunosorbent Assay. *J. Virol. Methods.* **2011**, *177*(1), 128–131. DOI: [10.1016/j.jviromet.2011.07.003](https://doi.org/10.1016/j.jviromet.2011.07.003).
- [9] Boyd, N. A.; Bradwell, A. R.; Thompson, R. A. Quantitation of Vitronectin in Serum: Evaluation of Its Usefulness in Routine Clinical Practice. *J. Clin. Pathol.* **1993**, *46*, 1042–1045. DOI: [10.1136/jcp.46.11.1042](https://doi.org/10.1136/jcp.46.11.1042).
- [10] Inuzuka, S.; Ueno, T.; Torimura, T.; Tamaki, S.; Sakata, R.; Sata, M.; Yoshida, H.; Tanikawa, K. Vitronectin in Liver Disorders: Biochemical and Immunohistochemical Studies. *Hepatology.* **1992**, *15*, 629–636. DOI: [10.1002/hep.1840150413](https://doi.org/10.1002/hep.1840150413).
- [11] Savage, B.; Ruggeri, Z. M. Platelet Thrombus Formation in Flowing Blood. *Platelets.* **2007**, *2*, 359–367.
- [12] Poole-Smith, B. K.; Beltran, A.; Gonzalez, A. L.; Gilbert, M.; Tomashek, K. M.; Ward, B. J.; Hunsperger, E. A.; Ndao, M. Discovery and Characterization of Potential Prognostic Biomarkers for Dengue Hemorrhagic Fever. *Am. J. Trop. Med. Hyg.* **2014**, *91* (6), 1218–1226. DOI: [10.4269/ajtmh.14-0193](https://doi.org/10.4269/ajtmh.14-0193).
- [13] Moremen, K. W.; Tiemeyer, M.; Nairn, A. V. Vertebrate Protein Glycosylation: Diversity, Synthesis and Function. *Nat. Rev. Mol. Cell Biol.* **2012**, *13*, 448–462. DOI: [10.1038/nrm3383](https://doi.org/10.1038/nrm3383).
- [14] Tanabe, K.; Deguchi, A.; Higashi, M.; Usuki, H.; Suzuki, Y.; Uchimura, Y.; Ikenaka, K.; Ikenaka, K. Outer Arm Fucosylation of N-Glycans Increases in Sera of Hepatocellular Carcinoma Patients. *Biochem. Biophys. Res. Commun.* **2008**, *374*(2), 219–225. DOI: [10.1016/j.bbrc.2008.06.124](https://doi.org/10.1016/j.bbrc.2008.06.124).
- [15] Uchibori-Iwaki, H.; Yoneda, A.; Oda-Tamai, S.; Kato, S.; Akamatsu, N.; Otsuka, M.; Murase, K.; Kojima, K.; Suzuki, R.; Maeya, Y., et al. The Changes in Glycosylation After Partial Hepatectomy Enhance Collagen Binding of Vitronectin in Plasma. *Glycobiology.* **2000**, *10*, 865–874. DOI: [10.1093/glycob/10.9.865](https://doi.org/10.1093/glycob/10.9.865).
- [16] Sano, K.; Miyamoto, Y.; Kawasaki, N.; Hashii, N.; Itoh, S.; Murase, M.; Date, K.; Yokoyama, M.; Sato, C.; Kitajima, K., et al. Survival Signals of Hepatic Stellate Cells in Liver Regeneration are Regulated by Glycosylation Changes in Rat Vitronectin, Especially Decreased Sialylation. *J. Biol. Chem.* **2010**, *285*, 17301–17309. DOI: [10.1074/jbc.M109.077016](https://doi.org/10.1074/jbc.M109.077016).
- [17] Sano, K.; Asanuma-Date, K.; Arisaka, F.; Hattori, S.; Ogawa, H. Changes in Glycosylation of Vitronectin Modulate Multimerization and Collagen Binding During Liver Regeneration. *Glycobiology.* **2007**, *17*, 784–794. DOI: [10.1093/glycob/cwm031](https://doi.org/10.1093/glycob/cwm031).

- [18] Miyamoto, Y.; Tanabe, M.; Ogawa, K.; Sakuda, K.; Sano, H.; Ogawa, H. Sialylation of Vitronectin Regulates Stress Fiber Formation and Cell Spreading of Dermal Fibroblasts via a Heparin-Binding Site. *Glycoconjugate. J.* **2016**, 33(2), 227–236. DOI: [10.1007/s10719-016-9660-8](https://doi.org/10.1007/s10719-016-9660-8).
- [19] Solis, D.; Bovin, N. V.; Davis, A. P.; Jiménez-Barbero, J.; Romero, A.; Roy, R. S.; Gabius, H. J.; Gabius, H.-J. A Guide into Glycosciences: How Chemistry, Biochemistry and Biology Cooperate to Crack the Sugar Code. *Biochim. Biophys. Acta.* **2015**, 1850(1), 186–235. DOI: [10.1016/j.bbagen.2014.03.016](https://doi.org/10.1016/j.bbagen.2014.03.016).
- [20] Varki, A.; Etzler, M. E.; Cummings, R. D.; Esko, J. D. Discovery and Classification of Glycan-Binding Proteins. In *Essentials. Of Glycobiology*, 2nd.; Varki, A., Cummings, R. D., Esko, J. D., Freeze, H. H., Freeze, P., Bertozzi, C. R., Hart, G. W., Etzler, M. E., Eds. Cold Spring Harbor (NY): Cold Spring Harbor Laboratory Press, **2009**.
- [21] Benachour, H.; Leroy-Dudal, J.; Agniel, R.; Wilson, J.; Briand, M.; Carreiras, F.; Gallet, O. Vitronectin (Vn) Glycosylation Patterned by Lectin Affinity Assays—A Potent Glycoproteomic Tool to Discriminate Plasma Vn from Cancer Ascites Vn. *J. Mol. Recognit.* **2018**, 31(5), e2690. DOI: [10.1002/jmr.2690](https://doi.org/10.1002/jmr.2690).
- [22] Nguyen, M. T.; Ho, T. N.; Nguyen, V. V. C.; Nguyen, T. H.; Ha, M. T.; Ta, V. T.; Nguyen, L. D. H.; Phan, L.; Han, K. Q.; Duong, T. H. K., et al. An Evidence-Based Algorithm for Early Prognosis of Severe Dengue in the Outpatient Setting. *Clin. Infect. Dis.* **2017**, 64, 656–663. DOI: [10.1093/cid/ciw863](https://doi.org/10.1093/cid/ciw863).
- [23] Ajlan, B. A.; Alafif, M. M.; Alawi, M. M.; Akbar, N. A.; Aldigs, E. K.; Madani, T. A. Assessment of the New World Health Organization's Dengue Classification for Predicting Severity of Illness and Level of Healthcare Required. *PLoS Negl. Trop. Dis.* **2019**, 13, e0007144. DOI: [10.1371/journal.pntd.0007144](https://doi.org/10.1371/journal.pntd.0007144).
- [24] Tian, Y.; Kelly-Spratt, K. S.; Kemp, C. J.; Zhang, H. J. Mapping Tissue-Specific Expression of Extracellular Proteins Using Systematic Glycoproteomic Analysis of Different Mouse Tissues. *J. Proteome Res.* **2010**, 9(11), 5837–5847. DOI: [10.1021/pr1006075](https://doi.org/10.1021/pr1006075).
- [25] Malavige, G. N.; Ogg, G. S. Pathogenesis of Vascular Leak in Dengue Virus Infection. *Immunology.* **2017**, 151, 261–269. DOI: [10.1111/imm.12748](https://doi.org/10.1111/imm.12748).
- [26] Inuzuka, S.; Ueno, T.; Torimura, T.; Tamaki, S.; Sakata, R.; Sata, M.; Yoshida, H.; Tanikawa, K. Vitronectin in Liver Disorders: Biochemical and Immunohistochemical. *Hepatology.* **1992**, 15(4), 629–636. DOI: [10.1002/hep.1840150413](https://doi.org/10.1002/hep.1840150413).
- [27] Mayampurath, A.; Song, E.; Mathur, A.; Yu, C. Y.; Hammoud, Z.; Mechref, Y.; Tang, H. Label-Free Glycopeptide Quantification for Biomarker Discovery in Human Sera. *J. Proteome Res.* **2014**, 13(11), 4821–4832. DOI: [10.1021/pr500242m](https://doi.org/10.1021/pr500242m).
- [28] Seiffert, D.; Schleef, R. R. Two Functionally Distinct Pools of Vitronectin (Vn) in the Blood Circulation: Identification of a Heparin-Binding Competent Population of Vn within Platelet Alpha-Granules. *Blood.* **1996**, 88(2), 552–560.
- [29] Preissner, K. T.; Reuning, U. Vitronectin in Vascular Context: Facets of a Multitalented Matricellular Protein. *Semin. Thromb. Hemost.* **2011**, 37, 408–424. DOI: [10.1055/s-0031-1276590](https://doi.org/10.1055/s-0031-1276590).
- [30] Akama, T.; Yamada, K. M.; Seno, N.; Matsumoto, I.; Kono, I.; Kashiwagi, H.; Funaki, T.; Hayashi, M. Immunological Characterization of Human Vitronectin and Its Binding to Glycosaminoglycans. *J. Biochem.* **1986**, 100(5), 1343–1351. DOI: [10.1093/oxfordjournals.jbchem.a121840](https://doi.org/10.1093/oxfordjournals.jbchem.a121840).
- [31] Patra, G.; Mallik, S.; Saha, B.; Mukhopadhyay, S. Assessment of Chemokine and Cytokine Signatures in Patients with Dengue Infection: A Hospital-Based Study in Kolkata, India. *Actatropica.* **2019**, 190, 73–79. DOI: [10.1016/j.actatropica.2018.10.017](https://doi.org/10.1016/j.actatropica.2018.10.017).

- [32] vanAken, B. E.; Seiffert, D.; Thinnies, T.; Loskutoff, D. J. Localization of Vitronectin in the Normal and Atherosclerotic Human Vessel Wall. *Histochem. Cell Biol.* **1997**, *107*, 313–320. DOI: [10.1007/s004180050116](https://doi.org/10.1007/s004180050116).
- [33] Mayampurath, A. M.; Yu, C. Y.; Song, E.; Balan, J.; Mechref, Y.; Tang, H. Computational Framework for Identification of Intact Glycopeptides in Complex Samples. *Anal. Chem.* **2014**, *86*, 453–463. DOI: [10.1021/ac402338u](https://doi.org/10.1021/ac402338u).
- [34] Hua, S.; Hu, C. Y.; Kim, B. J.; Totten, S. M.; Oh, M. J.; Yun, N.; Nwosu, C. C.; Yoo, J. S.; Lebrilla, C. B.; An, H. J. Glyco-Analytical Multispecific Proteolysis (Glyco-AMP): A Simple Method for Detailed and Quantitative Glycoproteomic Characterization. *J. Proteome Res.* **2013**, *12*, 4414–4423. DOI: [10.1021/pr400442y](https://doi.org/10.1021/pr400442y).
- [35] Minor, K. H.; Peterson, C. B. Plasminogen Activator Inhibitor Type 1 Promotes the Self-Association of Vitronectin into Complexes Exhibiting Altered Incorporation into the Extracellular Matrix. *J. Biol. Chem.* **2002**, *277*, 10337–10345. DOI: [10.1074/jbc.M109564200](https://doi.org/10.1074/jbc.M109564200).





RESEARCH ARTICLE

# Decreased Thrombospondin-1 Titers Are Hallmarks of Patients with Severe Dengue Infection

Moumita Paul<sup>1</sup> · Deep Basu<sup>1</sup> · Sudeshna Mallik<sup>2</sup> ·  
Chaity Roy<sup>1</sup> · Bibhuti Saha<sup>2</sup> · Sumi Mukhopadhyay<sup>1</sup>

Received: 10 December 2022 / Revised: 8 May 2023 / Accepted: 19 March 2024  
© The Author(s), under exclusive licence to The National Academy of Sciences, India 2024

**Abstract** Severe dengue is a life-threatening complication. Biological markers that can predict or serve as correlates for rapid identification of disease severity are urgently needed. *Thrombospondin-1 (TSP-1)* is a matricellular functional protein that plays an important role in the extracellular matrix. In the present investigation, the level of TSP-1 was investigated for its possible utility as a dengue severity marker. Accordingly, confirmed dengue cases were enrolled from July to November of 2020. Plasma from all the study subjects was subjected to the standard enzyme-linked immunosorbent assay test for TSP-1 analysis. This study showed that the TSP-1 titers significantly decreased in severe dengue (SD) patients in contrast to those with a milder form of dengue infection. This is the first study demonstrating that a combination of parameters like TSP-1 titers and platelets exhibit sensitivity and specificity of 100% with an AUC of 1.000 in predicting severity. The investigation revealed that low TSP-1 titers along with decreased platelet are novel indicators of dengue severity.

**Keywords** Dengue · Severity · TSP-1 · Platelet

**Significance Statement:** We investigated the status of TSP-1 and its possible utility as a dengue severity marker. This is the first study demonstrating that a combination of parameters like TSP-1 titers and platelets exhibit sensitivity and specificity of 100% with an AUC of 1.000 in predicting severity.

✉ Sumi Mukhopadhyay  
drsumimukhopadhyay@gmail.com

<sup>1</sup> Department of Laboratory Medicine, Calcutta School of Tropical Medicine, 108, C.R. Avenue, Kolkata, West Bengal 700073, India

<sup>2</sup> Department of Tropical Medicine, Calcutta School of Tropical Medicine, 108, C.R. Avenue, Kolkata, West Bengal 700073, India

## Introduction

Dengue displays a broad range of clinical manifestations like dengue-without-warning-signs (DWOWS), showing symptoms such as fever, nausea, rash, aches, pain, and leukopenia. Dengue-with-warning-signs (DWWS) usually shows abdominal pain, persistent vomiting, clinical fluid accumulation, bleeding, restlessness, liver enlargement of > 2 cm, an increased hematocrit level with decreased platelet count. Patients with Severe Dengue (SD) become fatal over time. Simple markers to reliably identify severe dengue patients are lacking and are much needed to avoid unnecessary hospitalization, reduce disease burden, and control the potential severity of the infection [1]. In search of such markers, we have previously demonstrated a high VEGF (vascular endothelial growth factor) level in severe dengue cases [2]. VEGF stimulates endothelial permeability by inducing nitric oxide (NO) and can contribute to inflammation, while thrombospondin (TSP-1) inhibits NO synthesis; thus, VEGF and TSP-1 have an antagonistic relationship and contribute to disease pathogenesis [3]. The current study was undertaken to investigate the utility of TSP-1 in combination with other laboratory parameters for further improving the sensitivity and specificity limits to diagnose severe dengue cases. Recent data have also suggested that TSP-1 is also responsible for capillary architecture [4]. It was reported that downregulation of TSP-1 in diabetic wounds resulted in capillaries having increased permeability and delayed wound healing [5–7]. The cause of this increase in vascular permeability is believed to be manifold with cytokines such as TNF- $\alpha$  and dengue NS1 antigen, factors such as VEGF, and activation of NF- $\kappa$ B, all likely to be contributing factors [8–13]. TSP-1 is a potent activator of the NF- $\kappa$ B pathway and is strongly associated with TNF- $\alpha$  expression [14].

Hence, the role of TSP-1 in vascular leakage and its association with dengue severity must be evaluated. Many studies have shown that elderly patients are more susceptible to this infection, resulting in an increased mortality rate. To improve this situation, more studies are essential to figuring out the underlying cause and management of the severity of this infection.

To overcome this situation, it is imperative to establish a reliable dengue severity biomarker that shows 100% sensitivity and specificity to avoid unnecessary hospitalization and control the potential severity of the infection. This study was thus undertaken to identify the role of thrombospondin-1 as a potential biomarker for the identification of dengue severity. Cutoff values of TSP-1 for different categories of Dengue were determined and compared to that of healthy controls. A clinician examined all the patients thoroughly, and NS1, IgM/IgG capture ELISA, and RT-PCR were used to confirm disease diagnosis. Platelet counts and hematocrit were assessed with the aid of an automatic cell counter (SYSTEM version No.- XP100). Liver function checked using an autoanalyzer (ERBA version No.- EM360). Additionally, an effort was made to correlate several routine parameters, including platelet count, SGOT, and SGPT, to the TSP-1 levels in the blood plasma. Further, CombiROC, a freely available web-based software tool, was also adopted to determine sensitivity and specificity limits of a combination of laboratory parameters.

## Methods

A cross-sectional, analytical study was performed. A total of 57 dengue patients were enrolled in the study. While most of the patients were admitted at Calcutta School of Tropical Medicine from July to November 2020, some patients were also enrolled from outbreaks in North and South 24 Parganas, Howrah, and Hooghly. They were well informed about the study being conducted and gave written consent for participation. Peripheral blood was therefore drawn from individuals who gave their consent. Following clinical assessment, the NS1 IgM antibody capture enzyme linked immunosorbent assay (MAC-ELISA), IgM/IgG ELISA, and RT-PCR were used to confirm the diagnosis of dengue fever. The enrolled subjects were classified into dengue-without-warning-sign (DWOWS), dengue-with-warning-sign (DWWS), and severe-dengue (SD) according to the WHO 2016 guidelines, based on their clinical symptoms. Out of the 57 dengue-infected patients, 27 had secondary dengue illness, whereas 30 had initial dengue infection. Additionally, ten healthy donors (HD) who had no recent medical history were enlisted as a control group. Blood samples of all the enrolled subjects, both patients and healthy, were collected separately. Five milliliters of blood was collected from

each individual by venipuncture and into a sterile tube. The collected blood was immediately processed, and centrifugation was used to separate the plasma for ten minutes at 900 g. The isolated plasma was stored at  $-80^{\circ}\text{C}$  temperature till further use. All the experiments were performed using this stored plasma. Routine biochemical tests of blood samples were carried out utilizing the auto-analyzer ERBA XL 600 to define the pathological state of the study individuals. These measurements include serum glutamic oxaloacetic transaminase (SGOT) and serum glutamic oxaloacetic transaminase (SGOT) (SGPT). Hematocrit (HCT) and platelet count (PLT) were also assessed using a 3-part cell counter like the KX-21. The values from each sample were examined and analyzed.

*Thrombospondin-1* levels were evaluated using commercially available ELISA kits in different categories of dengue infected patients (Ray Biotech). The tests were carried out in accordance with the manufacturer's instruction manual. Calculating the medians and interquartile ranges allowed for the analysis of the results from each set of studies (IQR). In order to compare multiple groups, one-way ANOVA with Kruskal–Wallis tests was performed because the numerical variables had a nonparametric distribution. Descriptive statistics were used to calculate mean SEM values. Differences were considered statistically significant if their p values were less than 0.05. To assess the statistical differences in laboratory parameters between each group, the Mann–Whitney test was used. If necessary, Spearman's correlation was used. The generated data were examined using statistical analysis tools (GraphPad). The most effective parameter combinations with the corresponding sensitivity, specificity, and accuracy were chosen with the aid of CombiROC (area under the curve).

## Result and Discussion

There were 25 DwoWS, 22 DWWS, and 10 SD in the study population. Out of the 57 patients with confirmed dengue infection, 30 patients were identified as having primary dengue infection and 27 as having secondary infection. Patients with DwoWS, DWWS, or SD had fever (96, 100, 100%), myalgia (4, 18.18, 40%), headache (4, 9.09, 40%), abdominal pain (4, 4.54, 40%), ascites (0, 4.54, 20%) and bleeding (0, 0, 20%), respectively. Biochemical results showed 4.29-fold low platelets in SD than DWOWS and 1.73-fold low in DWWS than DWOWS. The platelet level is significantly ( $<0.0001$ ) low in SD patients than DWOWS and DWWS. Low platelet count, or thrombocytopenia, is a characteristic of dengue infection [15–17]. The serum glutamic-oxaloacetic-transaminase (SGOT) were 2.67-fold higher in DWWS than DWOWS and 5.55-fold higher in SD than DWOWS. The serum glutamic- pyruvic transaminase

(SGPT) level was 2.06-fold lower in DWOVS than DWWS and 5.64-fold lower find DWOVS than SD patients. The hematocrit level of SD patients was 1.20-fold higher than DWOVS and DWWS patients (Table 1).

Decreased *Thrombospondin-1* titers ( $P < 0.0001$ ) were obtained in severe dengue infection. *In vitro* suppression of TSP-1 transcription in endothelial cells was observed during viral infections, leading to reduction in TSP-1 protein accumulation in the extracellular matrix of endothelial cells [18]. A similar molecular response may also be responsible for decrease in TSP-1 levels during dengue infection. Among patients with severe dengue infection, *Thrombospondin-1* (TSP-1) level is 2.14-fold lower in DWOVS, 2.14-fold lower in DWWS and 3.92-fold lower in SD than healthy donor (HD). TSP-1 level is upregulated in HD with “mean  $\pm$  SEM” value of  $8,616,109 \pm 1121$  ng/ml as compared DWOVS ( $7519 \pm 557.9$  ng/ml), DWWS ( $7496 \pm 421.8$  ng/ml) and SD ( $4102 \pm 251.9$  ng/ml) (Fig. 1). In addition, thrombospondin-1 cutoff of 4818 ng/

mL with a promising AUC—0.9234 showed its potential to be a novel indicator of dengue severity (Fig. 1). It was reported that increased consumption or insufficient production of TSP-1 may lead to impairment of the integrity of capillary and small vessels.

*Thrombospondin-1* had a positive correlation with platelet and negative correlation with SGOT, SGPT and HCT. This information may indicate that there is a possible association of *thrombospondin-1* with platelet in dengue severity. A blood coagulation system gets initiated in response to the vascular injuries, resulting in aggregation of platelets at the site of vascular leakage. Aggregated platelets release TSP-1, which gets incorporated into fibrin clots and acts as a substrate for fibrin and factor XIIIa [19]. This localized accumulation and increased consumption of platelets may also be responsible for the decreased TSP-1 levels. To predict severity of severe dengue patients a nomogram was utilized [20]. The nomogram is used by totaling the points assigned on the scales for each independent parameter, i.e., platelet,

**Table 1** Biochemical parameters of the study subjects

Laboratory measure	DWOVS ( $n=25$ )		DWWS ( $n=22$ )		SD ( $n=10$ )		ANOVA <sup>@</sup>	Mann–Whitney $U$ test nonsevere vs severe $p^*$
	Mean $\pm$ SEM	Median	Mean $\pm$ SEM	Median	Mean $\pm$ SEM	Median		
Platelet ( $\times 10^3/\mu\text{l}$ )	$141,400 \pm 10,711$	140,000	$81,545 \pm 7758$	70,000	$32,900 \pm 4173$	30,000	<0.0001	<0.0001
SGOT (IU/L)	$46.44 \pm 4.943$	41	$124.3 \pm 13.29$	122	$258 \pm 63.75$	174.5	<0.0001	<0.0001
SGPT (IU/L)	$32.64 \pm 4.046$	29	$67.55 \pm 12.09$	44	$184.4 \pm 43.21$	130	<0.0001	<0.0001
Hematocrit (%)	$35.94 \pm 1.125$	38	$35.99 \pm 1.328$	37.30	$43.45 \pm 2.909$	47	0.0621	0.0310

\*Mann–Whitney  $U$  test between nonsevere vs severe Dengue cases. The statistical significance is indicated by  $P < 0.05$

@ ANOVA followed by Kruskal–Wallis test (K)

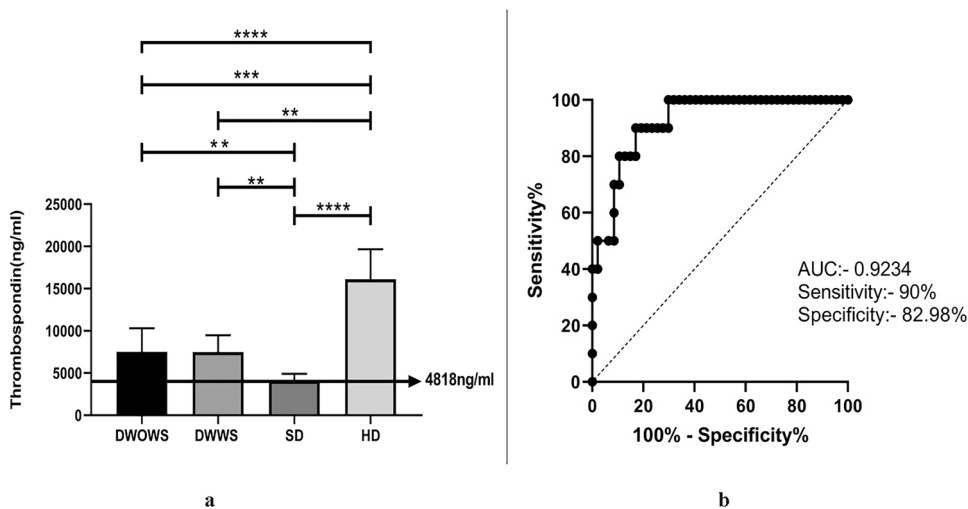


**Fig. 1 a** Levels of *Thrombospondin 1* (TSP1) of dengue without warning sign (DwoWS), dengue with warning signs (DWWS) and severe dengue (SD). Study subjects are significantly different from each category. One-way ANOVA with Kruskal–wallis test was done for comparing different study categories and Dunn’s multiple com-

parisons test was done for repeated measures. Symbols (\*) represent statistical significant differences ( $P < 0.05$ ) between different groups. **b** Receiver operating characteristics curve analysis obtained the cutoff value (4818 ng/ml), AUC=0.9234, Sensitivity—90% and Specificity—82.98%

HCT, SGOT and SGPT. From this nomogram, we also got percentage of predicted risk factor of severity. Percentage of risk factor of severe dengue patient has negative correlation with TSP-1. Decreased level of TSP-1 may indicate that risk factor of severity of dengue patients (Table 2).

CombiROC offers a straightforward process and an intuitive user interface to assist researchers in choosing the best marker combinations. The CombiROC tool, which is designed to select multi-marker signatures from the panel of markers evaluated, is accessible at <http://CombiROC.eu>

**Table 2** Correlation of *Thrombospondin-1* with laboratory parameters

Serial number	Laboratory parameters	Spearman r	p value
1	Platelet ( $\times 10^3/\mu\text{l}$ )	0.4570	0.0189
2	HCT (%)	− 0.5455	0.0039
3	SGOT (IU/I)	− 0.3707	0.0401
4	SGPT (IU/I)	− 0.3933	0.0235
5	Percentage of predicted risk factor of severity	− 0.3168	0.0435

and was used to investigate the best marker combination. Based on the maximum area under the curve (AUC), sensitivity (SE), and specificity (SP), the ideal marker or marker combination is selected. Figure 2 presents the obtained best marker on multiple receiver operating characteristics (ROC) curve. TSP-1 also plays an important role in platelet aggregation and vascular dysfunction. Although TSP-1 is secreted from various sources, including macrophages and smooth muscle cells, platelets are its major source of secretion [21]. Almost 25% of the platelet secreted proteins is made up of TSP-1 [22]. Thrombocytopenia, was negatively correlated with disease severity and plasma TSP-1 levels. Therefore, the decrease in TSP-1 levels could be attributed to the low platelet count leading to decreased synthesis of the protein.

TSP-1 is also involved in responses to inflammation which may get affected in reverse by the decreased serum TSP-1 levels leading to further aggravation of the dysfunction [23, 24]. The more severely infected patients showed lower levels of platelets and TSP-1 in their blood (Fig. 1b). One of the outcomes of dengue infection is fluid loss through vascular leakages causing depletion of intravascular volume and hemoconcentration [25]. Patients show increased levels

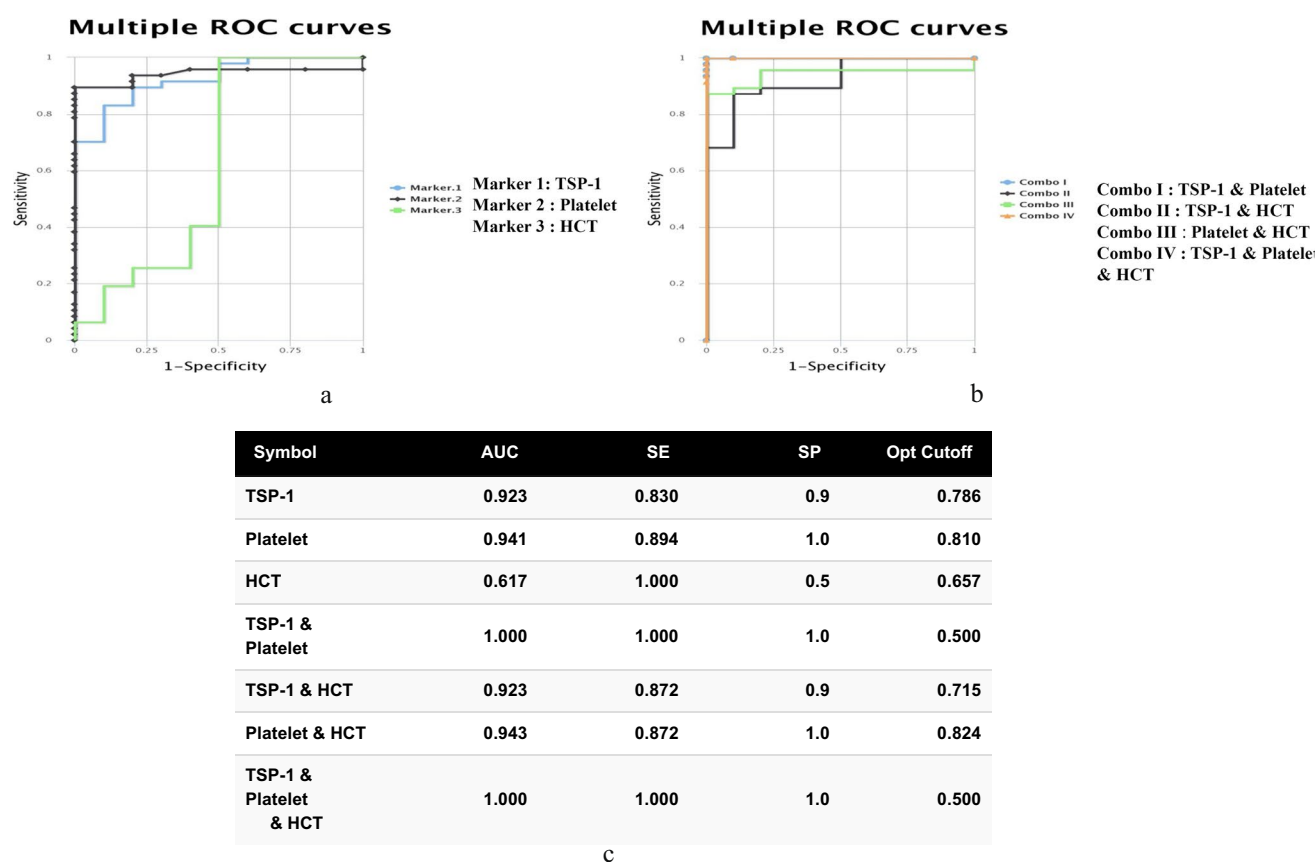


**Fig. 2** a–b Multiple receiver operating characteristic (ROC) curve as a function of sensitivity vs 1-specificity to compare the performance of markers and combos for TSP-1 PLATELET and HCT. c The per-

formance of combination of biomarkers via receiver operating characteristic (ROC) curve analysis

of hematocrit from the third day of the infection. A negative correlation was obtained between TSP-1 levels and hematocrit, while hematocrit showed a positive correlation with dengue severity. It can be hypothesized that as TSP-1 is downregulated, activity of endothelial nitric oxide synthase (eNOS) and soluble guanylate cyclase (sGC) is enhanced, leading to vasodilation and increased permeability. Plasma escapes into the body from the vessels, leaving behind the larger RBCs, thus giving a higher hematocrit value of ("Mean  $\pm$  SEM")  $43.4 \pm 2.9$ .

Decreased platelets along with decreased TSP-1 levels limits clot formation and can initiate internal bleeding. Liver injury caused by dengue virus can range from asymptomatic transaminase elevation to acute liver failure. Our study revealed a negative correlation between TSP-1 and the transaminase levels, further validating an association of these proteins with dengue infection severity and the use of TSP-1 as a novel biomarker in dengue severity identification.

## Conclusion

CombiROC analysis has shown a very high association of TSP-1 and platelet combination with Dengue severity. If suitably implemented, can help detection of severe Dengue with extremely high sensitivity and specificity, which is almost higher (100%) than VEGF, as shown in our previous study. While most diagnostic methods are time-consuming, this can be developed into a rapid diagnostic kit for point of care diagnosis.

**Acknowledgements** This study received funding support from LSRB, DRDO, Govt. of India [O/o DG(TM) /81/48222/LSRB-339/ BTB/2019].

## Declarations

**Conflict of interest** The authors have declared that no competing interests exist.

**Ethical approval** The Clinical Research Ethical Committee of the Calcutta School of Tropical Medicine granted this study clearance in accordance with ethical guidelines (CREC-STM/461 dated 18/06/2018), ensuing the Helsinki protocol.

**Consent for publication** All authors have agreed for publication of this manuscript in its current form.

## References

- Zhang H, Zhou YP, Peng HJ, Zhang XH, Zhou FY, Liu ZH, Chen XG (2014) Predictive symptoms and signs of severe dengue disease for patients with dengue fever: a meta-analysis. *Biomed Res Int* 2014:1–10. <https://doi.org/10.1155/2014/359308>
- Patra G, Saha B, Mukhopadhyay S (2019) Study of serum VEGF levels in patients with severe dengue infection admitted in a tertiary care hospital in Kolkata. *J Med Virol* 91:1873–1876. <https://doi.org/10.1002/jmv.25529>
- Murphy MP (1999) Nitric oxide and cell death. *Biochim Biophys Acta* 1411:401–414. [https://doi.org/10.1016/s0005-2728\(99\)00029-8](https://doi.org/10.1016/s0005-2728(99)00029-8)
- Liu Z, Morgan S, Ren J, Wang Q, Annis DS, Mosher DF, Zhang J, Sorenson CM, Sheibani N, Liu B (2015) Thrombospondin-1 (TSP1) contributes to the development of vascular inflammation by regulating monocytic cell motility in mouse models of abdominal aortic aneurysm. *Circ Res* 117:129–141
- Agah A, Kyriakides TR, Lawler J, Bornstein P (2002) The lack of thrombospondin-1 (TSP1) dictates the course of Wound healing in double-TSP1/TSP2-null mice. *Am J Pathol* 161:831–839. [https://doi.org/10.1016/s0002-9440\(10\)64243-5](https://doi.org/10.1016/s0002-9440(10)64243-5)
- Malavige GN, Ogg GS (2017) Pathogenesis of vascular leak in dengue virus infection. *Front Immunol* 151:261–269
- Gubler DJ (1998) Dengue and dengue hemorrhagic fever. *Clin Microbiol Rev* 11:480–549
- Modhiran N, Watterson D, Muller DA, Panetta AK, Sester DP, Liu L, Hume DA, Stacey KJ, Young PR (2015) Dengue virus NS1 protein activates cells via Toll-like receptor 4 and disrupts endothelial cell monolayer integrity. *Sci Transl Med* 7(304):304ra142. <https://doi.org/10.1126/scitranslmed.aaa3863>
- Puerta-Guardo H, Glasner DR, Harris E (2016) Dengue virus NS1 disrupts the endothelial glycocalyx, leading to hyperpermeability. *PLoS Pathog* 12(7):e1005738. <https://doi.org/10.1371/journal.ppat.1005738>
- Furuta T, Murao LA, Lan NT, Huy NT, Huong VT, Thuy TT, Tham VD, Nga CT, Ha TT, Ohmoto Y, Kikuchi M, Morita K, Yasunami M, Hirayama K, Watanabe N (2012) Association of mast cell-derived VEGF and proteases in Dengue shock syndrome. *PLoS Negl Trop Dis* 6:e1505. <https://doi.org/10.1371/journal.pntd.0001505>
- Steinberg BE, Goldenberg NM, Lee WL (2012) Do viral infections mimic bacterial sepsis? The role of microvascular permeability: a review of mechanisms and methods. *Antiviral Res* 93:2–15
- van de Weg CA, Pannuti CS, van den Ham HJ, de Araújo ES, Boas LS, Felix AC, Carvalho KI, Levi JE, Romano CM, Centrone CC, Rodrigues CL, Luna E, van Gorp EC, Osterhaus AD, Kallas EG, Martina BE (2014) Serum angiopoietin-2 and soluble VEGF receptor 2 are surrogate markers for plasma leakage in patients with acute dengue virus infection. *J Clin Virol* 60:328–335. <https://doi.org/10.1016/j.jcv.2014.05.001>
- Rogers NM, Sharifi-Sanjani M, Csányi G, Pagano PJ, Isenberg JS (2014) Thrombospondin-1 and CD47 regulation of cardiac, pulmonary and vascular responses in health and disease. *Matrix Biol* 37:92–101. <https://doi.org/10.1016/j.matbio.2014.01.002>
- Nguyen MT, Ho TN, Nguyen VVC, Nguyen TH, Ha MT, Ta VT, Nguyen LDH, Simmons CP (2017) An evidence-based algorithm for early prognosis of severe dengue in the outpatient setting. *Clin Infect Dis* 64:656–663
- Quirino-Teixeira AC, Andrade FB, Pinheiro M, Rozini SV, Hottz ED (2022) Platelets in dengue infection: more than a numbers game. *Platelets* 33:176–183. <https://doi.org/10.1080/09537104.2021.1921722>
- Azeredo ELD, Monteiro RQ, de-Oliveira Pinto LM, (2015) Thrombocytopenia in dengue: interrelationship between Virus and the Imbalance between coagulation and fibrinolysis and inflammatory mediators. *Mediators Inflamm* 2015:1–16. <https://doi.org/10.1155/2015/313842>
- Khaiboullina SF, Morzunov SP, St. Jeor SC, Rizvanov AA, Lombardi VC (2016) Hantavirus Infection suppresses thrombospondin-1 expression in cultured endothelial cells in a strain-specific



- manner. *Front Microbiol* 7:1077. <https://doi.org/10.3389/fmicb.2016.01077>
18. Liu Z, Zhao Q, Han Q, Gao M, Zhang N (2008) Serum thrombospondin-1 is altered in patients with hemorrhagic fever with renal syndrome. *J Med Virol* 80:1799–1803. <https://doi.org/10.1002/jmv.21270>
  19. Tarabozetti G, Roberts D, Liotta LA, Giavazzi R (1990) Platelet thrombospondin modulates endothelial cell adhesion, motility, and growth: a potential angiogenesis regulatory factor. *J Cell Biol* 111:765–772
  20. Lopez-Dee Z, Pidcock K, Gutierrez LS (2011) Thrombospondin-1: multiple paths to inflammation. *Mediators Inflamm* 2011:296069. <https://doi.org/10.1155/2011/296069>
  21. Greenaway J, Gentry PA, Feige JJ, LaMarre J, Petrik JJ (2005) Thrombospondin and vascular endothelial growth factor are cyclically expressed in an inverse pattern during bovine ovarian follicle development. *Biol Reprod* 72(5):881071–881078. <https://doi.org/10.1095/biolreprod.104.031120>
  22. Adane T, Getawa S (2021) Coagulation abnormalities in Dengue fever infection: a systematic review and meta-analysis. *PLoS Negl Trop Dis* 15:e0009666. <https://doi.org/10.1371/journal.pntd.0009666>
  23. Narizhneva NV, Razorenova OV, Podrez EA, Chen J, Chandrasekharan UM, DiCorleto PE, Plow EF, Topol EJ, Byzova TV (2005) Thrombospondin-1 up-regulates expression of cell adhesion molecules and promotes monocyte binding to endothelium. *FASEB J* 19:1158–1160
  24. Rajapakse S (2011) Dengue shock. *J Emerg Trauma Shock* 4:120–127. <https://doi.org/10.4103/0974-2700.76835>
  25. Azin FR, Gonçalves RP, Pitombeira MH, Lima DM, Branco IC (2012) Dengue: profile of hematological and biochemical dynamics. *Rev Bras Hematol Hemoter* 34:36–41. <https://doi.org/10.5581/1516-8484.20120012>

**Publisher's Note** Springer Nature remains neutral with regard to jurisdictional claims in published maps and institutional affiliations.

Springer Nature or its licensor (e.g. a society or other partner) holds exclusive rights to this article under a publishing agreement with the author(s) or other rightsholder(s); author self-archiving of the accepted manuscript version of this article is solely governed by the terms of such publishing agreement and applicable law.

# In Silico Molecular Docking and in Vitro Analysis of Eugenol as Free Radical Scavenger in Patients with Dengue Infection



Moumita Paul, Sourav Misra, Goutam Patra, Sourav Datta, Bibhuti Saha, and Sumi Mukhopadhyay

**Abstract** Infection by the Dengue virus (DENV) threatens global public health due to its high prevalence and the lack of effective treatments. Oxidative and cytotoxic damage plays an important role in Dengue pathogenesis and may serve as an important target for treatment. DENV infection activates Keap1/Nrf2 signaling pathway that leads to transcription of downstream antioxidant and detoxification genes such as HMOX-1, SOD2, NQO1, etc. In this study, both the molecular docking technique and In-Vitro experiments were performed to show potentiality of Eugenol as an activator of Keap1/Nrf2 signaling pathway. The molecular docking work concludes that Eugenol can actually induce Keap1/Nrf2 signaling pathway with a significant change in negative Firedock Global-Energy value, AScore value and as well as experimentally, Eugenol demonstrated promising antioxidant potential and free radical (RNS) scavenging activity.

**Keywords** Keap1/Nrf2 · RNS · DENV · Eugenol · DPPH · PatchDock · FireDock · BioVia discovery studio · Global-energy value · ArgusLab · AScore value

## 1 Introduction

Dengue-infection is a mosquito-borne viral infection spreading rapidly throughout the world, particularly in tropical or subtropical countries (Mapalagamage et al. 2018). Dengue-virus belongs to the family-Flaviviridae and genus-Flavivirus and might cause dengue-infection. According to WHO guidelines in 2009, Dengue infection has been classified based on their symptoms: Dengue-without warning-sign

---

M. Paul · S. Misra · G. Patra · S. Datta · S. Mukhopadhyay (✉)  
Department of Laboratory Medicine, School of Tropical Medicine, Government of West Bengal,  
108, C. R. Avenue, Kolkata, West Bengal 700073, India

B. Saha  
Department of Tropical Medicine, Department of Health and Family Welfare, School of Tropical  
Medicine, Government of West Bengal, 108, C. R. Avenue, Kolkata, West Bengal 700073, India

© The Author(s), under exclusive license to Springer Nature Singapore Pte Ltd. 2021  
M. Mukherjee et al. (eds.), *Advances in Medical Physics and Healthcare Engineering*,  
Lecture Notes in Bioengineering, [https://doi.org/10.1007/978-981-33-6915-3\\_55](https://doi.org/10.1007/978-981-33-6915-3_55)

583

(DWOVS) (Nausea, Vomiting, Aches, and pain leucopenia), Dengue-with warning-signs (DWWS) (Abdominal pain or tenderness, persistent vomiting, clinical-fluid-accumulation, Mucosal-bleeding, Restlessness) and Severe-dengue (SD) (Severe plasma-leakage, Severe bleeding). A current model calculates 390 million belongings each year, with ninety-six million cases manifesting with a minimum of some clinical displays. As per WHO, the South-East Asia and Western Pacific regions square measure extremely endemic for this sickness (Ahmad et al. 2018). In India, Kolkata is a hyperendemic region and has witnessed many Dengue epidemics in current years. So far, dengue infection remains the number one pathological state, in Asian nations and around the world (World Health Organization 2011).

Viral infections usually cause the enhanced expression of proinflammatory cytokines. Reactive-Oxygen and Nitrogen-species (i.e. ROS, RNS) are generated in the monocytes, macrophages, and many other resistant cells in viral infections. However excessive secretion of ROS, RNS makes the inequity between these peroxidant and antioxidants leading oxidative-stress which may cause many deleterious effects on the host. Damages induced by oxidative-stresses and changes into redox status are being identified in some patients with Dengue infection which suggests the crucial role of oxidative-stress in Dengue pathogenesis (Chaturvedi and Nagar 2009). NO is one such extremely reactive molecule and considered as major peroxidant in the body which can spread through cells. The enzyme NO synthase produces NO. Peroxynitrite is also harmful when it is there in high concentration, oxidizing genetic material, lipids, and oxidizing and nitrating proteins thus peroxynitrite enhances oxidative stresses (Chaturvedi and Nagar 2009). Defense against such excessive free radical accumulation and reticence of the RNS is important cytoprotective mechanisms that are regulated and controlled by the activation of Keap1/Nrf2 signaling pathway (Olagnier et al. 2014). Keap1-Nrf2 signaling cascade is the key controller pathway against prolonged oxidative stresses. Nrf2 (nuclear factor E2-related factor 2) belongs to family of leucine zipper transcription protein factors. It binds with Maf-Proteins to the regulatory promoter region of downstream Nrf2 targeted genes and enhances expression of >200 oxidative stress-related genes to protect the cell from oxidative stress-induced damages (Barrera-Rodríguez 2018; Kansanen et al. 2013; Leung et al. 2019). The transactivation of Nrf2 targeted genes within the cell is strictly regulated and maintained at its basal level by Keap1, a cytoplasmic adaptor protein molecule of the Cullin3 based E3- ligase complex (David et al. 2017). The 605-residue human Nrf2 protein is composed of seven Nrf2-ECH homology (Neh1–7) domains all that have distinct functions. The N-terminal Neh2 domain mediates interaction with C-terminal portion of Keap1 that tightly regulates the permanency of Nrf2 (Tonelli et al. 2018). Keap1 (Kelch-like ECH-associated protein 1) contains five domains of which the C terminal portion of Keap1 or the Kelch domain interacts with Neh2 domain. The other domains of Keap1 namely BTB domain and IVR help in homo dimerization of Keap1 and interacting with Cullin3 (Taguchi et al. 2011). Neh2 domain is bound to Kelch domain in homeostasis. Keap1 protein moderates Cul3 E3 complex for ubiquitination, which leads to continuous ubiquitination and destruction of Nrf2 during non-stressed conditions (Tong et al. 2006). This kind of



quenching interaction keeps up lower basal expression of Nrf2 mediated cytoprotective gene transcription. However, when cell experiences oxidative stress, Keap1 gets inactivated and the poly-ubiquitination of Nrf2 is halted and newly synthesized Nrf2 proteins bypass Keap1 mediated degradation resulting in accumulation of the Nrf2 in cytoplasm. Consequently, Nrf2 gets accessed into nucleus, transcribes downstream Nrf2 targeted genes like SOD2, HMOX1, etc. (Theodore et al. 2008).

Thus the administration of antioxidant molecules to Dengue infected patients may limit virus-mediated cell damage and restrict the patient to go into severe conditions. Any phytochemical that has potent antioxidant activity and proved to be less toxic to human body can be employed in Dengue pathogenesis. Eugenol, a very common natural phytochemical suffice all our requirements to study its beneficial role in Dengue-induced oxidative stress and in future it may open up novel treatment methods for Dengue-associated diseases. Eugenol (4-allyl-2-methoxy phenol (EUG)) a hydrocarbon is present as yellow viscous oil (de Araújo Lopes et al. 2018). This is an associate with aromatic and phenolic compound from the category of phenylpropanoids (Barboza et al. 2018). It is a key component of cloves and found in bay leaves and all spices (Barboza et al. 2018; Ghofran et al. 2019). This is utilized in food industry (Nagababu et al. 2010)) as a preservative compound, appreciated due to its inhibitor property (Zhang et al. 2009). Eugenol shows numerous biological activities like bactericide, (Xu et al. 2016) antifungal (Chami et al. 2005; Gayoso et al. 2005) antiallergic (Kim et al. 1998; Corrêa et al. 2008) properties. Eugenol conjointly has medication, chemoprotective effects furthermore it has antioxidant-activity (Yogalakshmi et al. 2010) credited due to the existence of the phenolic cluster in its structure. For that reason, Eugenol has attracted several researchers. Numerous studies also opine that Eugenol has bioactive terpenes that inhibit ROS production in human neutrophil. Eugenol is a helpful pain reliever, and has antioxidant-activity. Taken together the current study aims to investigate the effectiveness of Eugenol (if any) in Dengue infection.

## 2 Materials and Methods

### 2.1 *In-Silico Analysis*

**Protein preparation:** The X-ray Crystallographic structure of Keap1-Neh2 complex (PDB ID 3ZGC) was obtained from the Protein Data Bank (PDB) at a resolution of 2.2 Å. Water molecules, ligands, and other hetero atoms were removed from protein complex and obtained the C-terminal Kelch domain (A and B chain) of Keap1 and the Neh domain (C chain) of Nrf2 separately by using Biovia Discovery Studio client software.

**Ligand Preparation:** The 3D structure of Eugenol was obtained and downloaded from the PUBCHEM database. The proteins and ligand were saved as PDB format for further analysis.

**Automatic Docking:** The computational molecular docking was accomplished by PatchDock server. Protein-small ligand platform of PatchDock was employed for docking by using clustering Root-Mean-Square-Deviation (RMSD) value of 4.0 (Chaturvedi et al. 2016). Neh domain of Nrf2 was docked against Kelch domain of Keap1 and Eugenol was docked against Kelch domain followed by docking of Neh domain against Kelch-Eugenol complex domain in separate pair of docking analysis. In both analyses, the complexes were sorted based on their PatchDock scores produced by the server. Further, PatchDock score refinement was accomplished by using FireDock server. The most stable conformations of desired protein–protein and the protein–ligand complexes were selected based on highest negative Global Energy (GE) value given by the FireDock server. Further validation was done by implementing flexible algorithm with ArgusLab 4.0.1 Docking Engine. The grid box was generated for assortment and formation of the dynamic binding pocket where the ligand could actually bind using grid resolution of 0.40 Å. Docking calculation was performed using AScore scoring function and the complexes that were best docked were chosen depending on the least AScore calculated by ArgusLab (Chikhi and Bensegueni 2008). The conformations of the complexes were envisaged by Discovery Studio software for further analysis.

## 2.2 *In-Vitro Experiments*

**Chemicals:** The subsequent compounds used for inhibitor activities, obtained from Sigma-Aldrich: Eugenol (4-allyl-2-methoxyphenol), Ascorbic acid. DPPH was purchased from Himedia. Ethanol was purchased from Merck. Griess chemical agent was purchased from Sigma. NO colorimetric assay kit from Cayman, subsequent experimental procedures were applied to gauge the radical scavenging activity of Eugenol.

**Study Population:** Enrolled 37 Dengue patients at Calcutta School of Tropical Medicine from July 2019 to October 2019 after obtaining their consent. They were confirmed by both Dengue-NS1/IgM ELISA, and RT-PCR. They are classified into Dengue-without warning-sign (DWOWS), Dengue-with warning-signs (DWWS) according to WHO 2009 criteria through their symptoms. We had also enrolled 15 Healthy Donors (HD) with no history of illness in the past 3 months.

**Serum separation and processing:** Venous blood was collected from all patients and healthy. Five ml of blood were collected by venipuncture into a germ-free clot-activated tube and blood was separated by centrifugation process at 2000 RPM for ten minutes, stored in -20 °C temperature and clear serum were used for experiments.

**DPPH assay:** To assess the antioxidant potential of Eugenol, DPPH assay based on the methods of Brand-Williams et al. with small modification (Szerlauth et al. 2019) was used. Diphenyl-1-picrylhydrazyl (DPPH) has a radical-scavenger effect and has the ability to donate hydrogen, especially those with a phenolic cluster in their structure. This method is based on electron transport. It produces a purple ethanolic solution. Free radical molecules are decreased by the antioxidant molecules, producing yellowish ethanolic solution. Different concentrations (1.5–5.5  $\mu\text{g/ml}$ ) of Eugenol and Ascorbic acid (standard) were used, mixed with equivolume of DPPH solution. Optical density was measured at 492 nm after 30 min incubation at room temperature. The radical scavenging activity was calculated in percentage from the following formula: % scavenging [DPPH] =  $[(A_0 - A_1)/A_0] \times 100$ . Where  $A_0$  was the absorbance of the control and  $A_1$  was the absorbance of the samples. IC<sub>50</sub> value was interpolated from the standard graph.

**Serum Nitrite and Nitrate measurement:** Reactive-nitrogen-species were determined by estimating the stable merchandise of nitrite and nitrate. Total nitrite + nitrate was considered by utilizing a nitrate and nitrite colorimetric-assay-kit (Cayman, USA) in the serum sample, following the manufacturer's directions. This assay determine nitrite + nitrate depending on the enzymatic translation of nitrate to nitrite by nitrate reductase enzyme. The reaction following a quantitative chemical analysis detection of nitrite by Griess reaction supported by the diazotization-reaction within which acidified  $\text{NO}_2^-$  produces a nitrosating agent that reacts with sulphanilic acid to yield the anion particle. This particle is then combined to N-(1-naphthyl) ethylenediamine making deep purple chromophoric chemical group spin off that absorbs light-wavelength at 540 nm.

**Statistical Analysis:** All analysis was performed using Graph-Pad Prism statistics software (Graph-Pad-Software-Inc., San-Diego, CA, USA). As the numeric variables had nonparametric distribution, One-way ANOVA with Kruskal–Wallis tests was used to differentiate more groups, respectively. Mann–Whitney test was used to compare two groups. For Mean  $\pm$  SEM values, we used descriptive statistics. Differences with p values smaller than 0.05 were considered to be statistically significant.

### 3 Results

**In-Silico Results:** To find the potentiality of Eugenol as an antioxidant molecule and whether it could enhance the Keap1/Nrf2 pathway, two different sets of analysis on molecular docking were done. The first set of docking analysis showed Neh domain of Nrf2 docked against Kelch domain of Keap1 protein via PatchDock server. The docking result shows FireDock GE value of  $-48.90$  with 10 conventional Hydrogen-bonding (SER363, ASN382, SER508, GLN530, TYR572, SER602, ASN387, GLY574, GLY386 of Keap1), 3 salt bridges (ARG380, ARG415, ARG483

of Keap1), 3 electrostatic interactions (ARG415 of Keap1, GLU78, GLU79 of Nrf2) and 2 hydrophobic interactions (GLU82, THR80, GLY81 of Nrf2)—a sum total of 18 Non-bonding interactions (Table 1). In the other set of docking analysis, Eugenol was docked against Kelch domain of Keap1 and the most stable Keap1-Eugenol complex structure was chosen on the basis of highest negative Firedock GE value. Then, Neh domain of Nrf2 was docked against Keap1-Eugenol complex via PatchDock server. The docking result shows decreased FireDock GE value of -38.04 with 2 conventional Hydrogen bonding (ASN382, TYR572 of Keap1), 1 Salt bridge (ARG380 of Keap1) and 4 electrostatic interactions (ARG380, ARG483 of Keap1, and GLU78 of Nrf2)—a total of 7 Non-bonding interactions (Table 2) demonstrating Eugenol prevents Keap1 to bind Nrf2 and thus bypassing proteasomal destruction of Nrf2. ArgusLab flexible docking analysis also shows similar kind of results. Nrf2 when docked against Keap1 best Ligand Pose energy of −5.80586 kcal/mol was obtained and when Nrf2 docked against Keap1-Eugenol complex best Ligand Pose energy of −5.53895 kcal/mol was obtained.

**Study Population:** Dengue-patients were classified into DWOWS, DWWS as per 2009 WHO guidelines. They were categorized according to their symptoms and the result of the biochemical test.

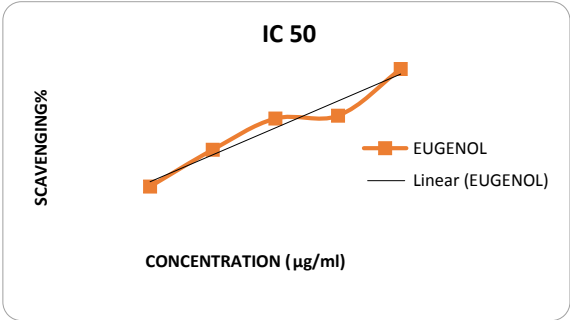
**Table 1** Amino acids involved in non-bonding interactions in Nrf2-Keap1 docked complex (obtained from Discovery Studo software)

Neh2 Domain of Nrf2 interacting with Kelch Domain of Keap1	
Bond Donor to bond acceptor	Type of bond
1. keap1:ARG380:NH1—nrf2:GLU82:OE1	Salt bridge
2. keap1:ARG415:NH2—nrf2:GLU79:OE2	Salt bridge
3. keap1:ARG483:NH1—nrf2:GLU79:OE1	Salt bridge
4. keap1:ARG415:NH1—nrf2:ASP77:OD2	Electrostatic
5. keap1:ARG415:NH1—nrf2:GLU79:OE1	Electrostatic
6. keap1:SER363:OG—nrf2:GLU82:OE2	Conventional hydrogen bond
7. keap1:ASN382:ND2—nrf2:GLU82:OE1	Conventional hydrogen bond
8. keap1:SER508:OG—nrf2:GLU79:OE2	Conventional hydrogen bond
9. keap1:GLN530:NE2—nrf2:GLU78:O	Conventional hydrogen bond
10. keap1:GLN530:NE2—nrf2:GLU78:OE1	Conventional hydrogen bond
11. keap1:TYR572:OH—nrf2:GLU78:OE2	Conventional hydrogen bond
12. keap1:SER602:OG—nrf2:THR80:O	Conventional hydrogen bond
13. keap1:ASN387:N—nrf2:GLY76:O	Conventional hydrogen bond
14. keap1:GLY574:CA—nrf2:GLU78:OE1	Conventional hydrogen bond
15. keap1:GLY386:CA—nrf2:GLY76:O	Conventional hydrogen bond
16. nrf2:GLU78:C,O;GLU79:N—keap1:TYR525	Electrostatic
17. nrf2:GLU82:OE2—keap1:TYR334	Hydrophobic
18. nrf2:THR80:C,O;GLY81:N—keap1:TYR572	Hydrophobic

**Table 2** Amino acids involved in non-bonding interactions when Nrf2 docked against Keap1-Eugenol complex (obtained from Discovery Studio software)

Neh2 Domain interacting with Kelch Domain in presence of Eugenol	
Bond Donor to Bond acceptor	Type of bond
1. keap1:ARG380:NH2—nrf2:GLU82:OE2	Salt bridge
2. keap1:ARG380:NH1—nrf2:GLU82:OE1	Electrostatic
3. keap1:ARG483:NH1—nrf2:GLU78:OE2	Electrostatic
4. keap1:ARG483:NH2—nrf2:GLU78:OE1	Electrostatic
5. keap1:ASN382:ND2—nrf2:GLU82:OE1	Conventional hydrogen bond
6. keap1:TYR572:OH—nrf2:GLU79:OE1	Conventional hydrogen bond
7. nrf2:GLU78:OE1—keap1:TYR525	Electrostatic

**Fig. 1** Determination of IC 50 of Eugenol



**DPPH Assay:** The antioxidant property of Eugenol was determined by using DPPH scavenging assay followed by gross IC<sub>50</sub> value determination. The IC<sub>50</sub> of Eugenol was 3.02 µg/ml. A standard curve was prepared using ascorbic acid in different concentrations. The DPPH—scavenging capacity, was calculated from the graph through linear regression (R<sup>2</sup> = 0.941). Thus Eugenol’s ability to sequester free radicals within the DPPH solution was obtained (Fig. 1).

3.1 Determination of Nitrite and Nitrate Level

High concentration of nitrite and nitrate was observed in the patients with DWWS (57.25 ± 5.9 µM) compared with patients with DWOWS (42.71 ± 5.5 µM) and HD (23.56 ± 2.6 µM) (Fig. 2). Though there was no significant difference between patients with DWWS and DWOWS (*p* = 0.3077). The level of nitrite + nitrate level is significantly higher in DWWS than HD (*p* = 0.0340).

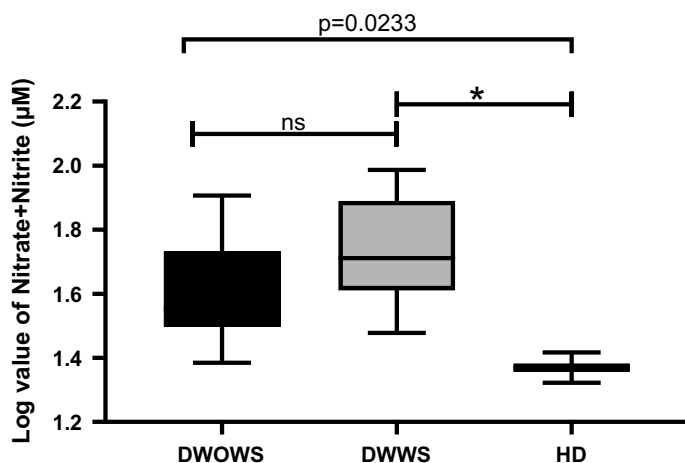


**Fig. 2** Nitrite and Nitrate values in serum samples ( $\mu\text{M}$  of  $\text{NO}_2^-$  and  $\text{NO}_3^-$ ) of patients with Dengue without warning sign (DWOWS,  $n = 19$ ), Dengue with Warning sign (DWWS,  $n = 18$ ), and Healthy Donors (HD,  $n = 15$ ) measured by Griess reaction. Results were expressed by the median value using the box plot. Symbols (\*) represent statistically significant differences ( $p = 0.0340$ ) between DWWS and HD. Nitrite and Nitrate level is comparatively higher in DWWS ( $p = 0.0233$ ) than DWOWS and HD. One-way ANOVA with Kruskal–Wallis test was done for comparing different study categories and Dunn’s multiple comparisons test was done for repeated measures

### 3.2 Determination of Nitrite and Nitrate level After Eugenol Treatment

From Figs. 1 and 2, the antioxidant property of Eugenol was obtained and additionally high nitrite + nitrate level was found in patients with Dengue with warning signs. Further following Srejayar and Rao.et.al protocol the RNS quenching ability of Eugenol was investigated. Serum samples containing high nitrite + nitrate level were treated with/without Eugenol for 150 min, room temperature, subsequent to which Griess reagent was added and Optical Density was measured at 546 nm after 30 min incubation (Fig. 3).

Interestingly, very low amounts of nitrite and nitrate were obtained in the eugenol treated serum of dengue infected patients ( $28.37 \pm 4.9 \mu\text{M}$ ) as compared to samples without eugenol treatment ( $59.14 \pm 5.9 \mu\text{M}$ ). Thus, 2.1 fold reduced nitrite and nitrate were obtained in the serum of dengue patients when it was treated with eugenol.

## 4 Discussion

Dengue infection is one of the fastest spreading viral infections, threatening the whole world. Its cure and treatment have become a major concern. In this respect, the current

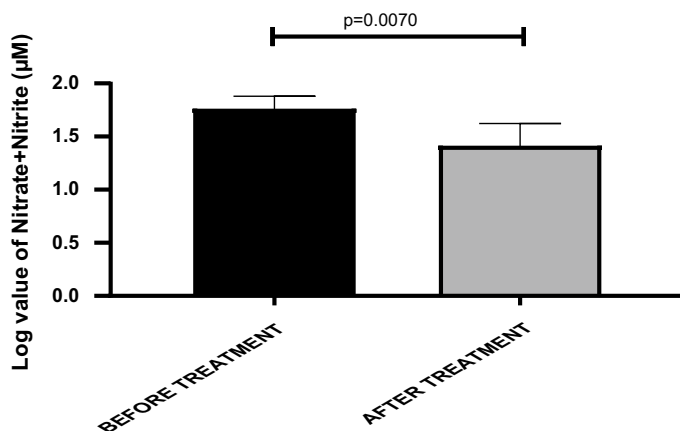


**Fig. 3** Nitrite and nitrate value of patients with dengue infection before Eugenol treatment and after Eugenol treatment. Results were expressed, using Mann–Whitney test. Nitrite and Nitrate level is significantly reduced ( $p = 0.0070$ ) after Eugenol treatment

study tried to find out a natural cure for dengue pathogenesis and found Eugenol to be a potent candidate for our studies. Eugenol was demonstrated to modulate the antioxidative Keap1-Nrf2 pathway through In Silico studies and could results in reduction in the free radical accumulation during Dengue infection through in vitro serum analysis. In this investigation, In Silico studies showed a reduction in free energies as well as diminution in the number of non- bonding interactions. Though the changes obtained in the free energy by the docking engines may seem very little and insignificant but all these changes are moderated by only a single molecule of Eugenol. Decreasing the number of non-bonding interactions inbetween Keap1 and Nrf2 is evident that Eugenol binds with Keap1 in the same interacting domain where Nrf2 binds. The lowering in the negative FireDock GE value as well as AScore pose energy value indicates that Keap1 cannot bind Nrf2 so firmly that it can act as an adaptor protein molecule for the Cul3 E3 ligase as long as Eugenol is bound to it. This propounds that newly synthesized Nrf2 can then bypass Keap1 mediated proteasomal degradation pathway which might lead to summoning up of Nrf2 in the cytosol followed by translocation into nucleus where it can induce transcription of oxidative stress-related genes (Fig. 4).

Eugenol, a compound, containing phenolic resin clusters, exhibits antioxidant-property by ending radical species through the loss of atom. In step with the results of our study, Eugenol had the foremost powerful antioxidant-activity. Nitric oxide is an essential chemical moderator, generated by neurons, macrophages, endothelial cells etc., and is implicated in many physiological processes. NO produced in macrophages and epithelial cells acts as an important molecule in the regulation of the diameter of blood vessels, inhibiting WBC adhesion and platelet aggregation. A balanced quantity of NO in the body is essential to maintain vital metabolic activities, a decreased or increased level, however may be deleterious to health. Figure 2,

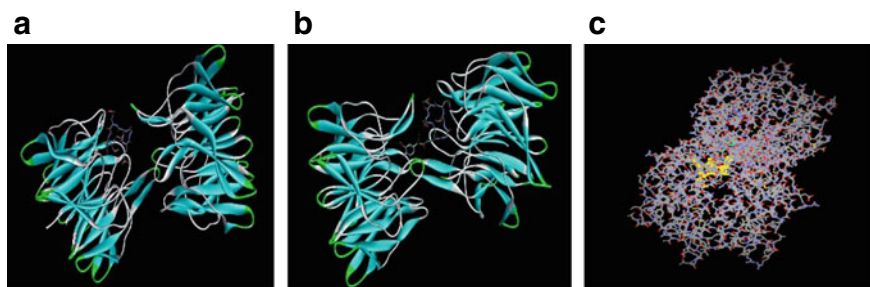


**Fig. 4** **a** Neh domain interacting with Kelch domain. **b** Neh domain interacting with Eugenol-Kelch complex (Discovery Studio visualization). **c** Neh domain interacting with Eugenol-Kelch complex (ArgusLab visualization)

demonstrated, higher concentration of Reactive Nitrogen species (nitrite + nitrate) in Dengue with warning sign. In the acute phase of Dengue infection, the amount of Reactive-Nitrogen-Species remains high in infection, causing major pathophysiological effects. Therefore, the RNS quenching ability of Eugenol was next investigated, Fig. 3 demonstrated the amount of nitrite + nitrate, which is drastically reduced after Eugenol treatment. This may be caused by occurrence of antioxidant properties in the Eugenol, which competes with oxygen, doing a reaction with nitric oxide and thereby blocking the formation of nitrite and nitrate. This, therefore, demonstrates the usefulness of Eugenol in Dengue infection.

## 5 Conclusion

Thus, In-Silico analysis concludes that Keap1 cannot bind Nrf2 to that extend so that it can degrade Nrf2 by Proteasomal pathway as long as Eugenol is bound to Keap1. So, Keap1-Nrf2 pathway can be modulated in presence of Eugenol which ultimately leads to cytoprotection during oxidative stress. We conclude from the above discussion that Eugenol has an antioxidant activity by scavenging the free Reactive-Nitrogen-Species. Eugenol thus could be a possible drug candidate for treating Dengue infections. However, our conclusions must be verified in a larger study population.



## References

- Ahmad MH, Ibrahim MI, Mohamed Z, Ismail N, Abdullah MA, Shueb RH, Shafei MN (2018) The sensitivity, specificity and accuracy of warning signs in predicting severe dengue, the severe dengue prevalence and its associated factors. *Int J Environ Res Public Health* 15(9)
- Barboza JN, da Silva Maia Bezerra Filho C, Silva RO, Medeiros JVR, de Sousa DP (2018) An overview on the anti-inflammatory potential and antioxidant profile of Eugenol. *Oxid Med Cell Longev* 2018:3957262. <https://doi.org/10.1155/2018/3957262>. PMID: 30425782; PMCID: PMC6217746
- Barrera-Rodríguez R (2018) Importance of the Keap1-Nrf2 pathway in NSCLC: is it a possible biomarker? *Biomed Rep* 9(5):375–382
- Chami F, Chami N, Bennis S, Bouchikhi T, Remmal A (2005) Oregano and clove essential oils induce surface alteration of *Saccharomyces cerevisiae*. *Phytother Res* 19(5):405–408
- Chaturvedi UC, Nagar R (2009) Nitric oxide in dengue and dengue haemorrhagic fever: necessity or nuisance? *FEMS Immunol Med Microbiol* 56(1):9–24
- Chaturvedi I, Sinha S, Chaudhary PP (2016) A molecular docking study to understand the interaction between anti-cancerous compounds and 12bp DNA sequences: poly (dA-dT) 12 and poly (dG-dC) 12. *J Sci* 1(4)
- Chikhi A, Bensegueni A (2008) Docking efficiency comparison of Surflex, a commercial package and Arguslab, a licensable freeware. *J Comput Sci Syst Biol* 1(01):081–086
- Corrêa MFP, Melo GO, Costa SS (2008) Substâncias de origem vegetal potencialmente úteis na terapia da Asma. *Rev Bras Farm* 18:785–797
- David JA, Rifkin WJ, Rabbani PS, Ceradini DJ (2017) The Nrf2/Keap1/ARE pathway and oxidative stress as a therapeutic target in type II diabetes mellitus. *J Diab Res* 2017:4826724. <https://doi.org/10.1155/2017/4826724>. Epub 2017 Aug 20. PMID: 28913364; PMCID: PMC5585663
- de Araújo Lopes A, da Fonseca FN, Rocha TM, de Freitas LB, Araújo EVO, Wong DVT, Júnior RCPL, Leal LKAM (2018) Eugenol as a promising molecule for the treatment of dermatitis: antioxidant and anti-inflammatory activities and its nanoformulation. *Oxid Med Cell Longev* 2018:8194849. <https://doi.org/10.1155/2018/8194849>. PMID: 30647816; PMCID: PMC6311755
- Gayoso CW, Lima EO, Olivera VT et al (2005) Sensitivity of fungi isolated from onychomycosis to *Eugenia caryophyllata* essential oil and eugenol. *Fitoterapia* 76:247–249
- Ghofran O, Safari T, Shahraki MR (2019) Effects of eugenol on pain response to the formalin test and plasma antioxidant activity in high fructose drinking water in male rats. *Int J Prev Med* 10
- Kansanen E, Kuosmanen SM, Leinonen H, Levenon AL (2013) The Keap1-Nrf2 pathway: mechanisms of activation and dysregulation in cancer. *Redox Biol* 1(1):45–49
- Kim HM, Lee EH, Hong SH et al (1998) Effect of *Syzygium aromaticum* extract on immediate hypersensitivity in rats. *J Ethnopharmacol* 60(2):125–131
- Leung CH, Zhang JT, Yang GJ, Liu H, Han QB, Ma DL (2019) Emerging screening approaches in the development of Nrf2–Keap1 protein-protein interaction inhibitors. *Int J Mol Sci* 20(18):4445
- Mapalagamage M, Handunnetti S, Premawansa G, Thillainathan S, Fernando T, Kanapathippillai K, Wickremasinghe R, De Silva AD, Premawansa S (2018) Is total serum nitrite and nitrate (NO<sub>x</sub>) level in dengue patients a potential prognostic marker of dengue hemorrhagic fever? In: *Disease markers*
- Nagababu, E., Rifkind, J. M., Boindala, S., & Nakka, L. (2010). Assessment of antioxidant activity of eugenol in vitro and in vivo. In: *Free radicals and antioxidant protocols*. Humana Press, pp 165–180
- Olagnier D, Peri S, Steel C, van Montfort N, Chiang C et al (2014) Cellular oxidative stress response controls the antiviral and apoptotic programs in dengue virus-infected dendritic cells. *PLoS Pathog* 10(12):e1004566. <https://doi.org/10.1371/journal.ppat.1004566>
- Szerlauth A, Muráth S, Viski S, Szilagyi I (2019) Radical scavenging activity of plant extracts from improved processing. *Heliyon* 5(11):e02763

- Taguchi K, Motohashi H, Yamamoto M (2011) Molecular mechanisms of the Keap1-Nrf2 pathway in stress response and cancer evolution. *Genes Cells* 16:123–140
- Theodore M, Kawai Y, Yang J, Kleshchenko Y, Reddy SP, Villalta F, Arinze IJ (2008) Multiple nuclear localization signals function in the nuclear import of the transcription factor Nrf2. *J Biol Chem* 283:8984–8994
- Tonelli C, Chio IIC, Tuveson DA (2018) Transcriptional regulation by Nrf2. *Antioxid Redox Signal* 29(17):1727–1745
- Tong KI, Katoh Y, Kusunoki H, Itoh K, Tanaka T, Yamamoto M (2006) Keap1 recruits Neh2 through binding to ETGE and DLG motifs: characterization of the two-site molecular recognition model. *Mol Cell Biol* 26:2887–2900
- World Health Organization (2011) Comprehensive guidelines for prevention and control of dengue and dengue haemorrhagic fever. Revised and expanded edition. WHO Regional Office for South-East Asia, New Delhi, India
- Xu JG, Liu T, Hu QP, Cao XM (2016) Chemical composition, antibacterial properties and mechanism of action of essential oil from clove buds against *staphylococcus aureus*. *Molecules* 21(9):1194–1206
- Yogalakshmi B, Viswanathan P, Anuradha CV (2010) Investigation of antioxidant, anti-inflammatory and DNA protective properties of eugenol in thioacetamide-induced liver injury in rats. *Toxicology* 268(3):204–212
- Zhang H, Chen X, He JJ (2009) Pharmacological action of clove oil and its application in oral care products. *Oral Care Ind* 19:23–24

## RESEARCH ARTICLE

# Comprehensive investigation of fever cases enrolled during 2019 dengue outbreaks from three hyperendemic regions of North 24 Parganas district of West Bengal, India

Sourav Datta<sup>1</sup> | Manab Ghosh<sup>2</sup> | Moumita Paul<sup>1</sup> | Prantiki Halder<sup>2</sup> |  
Sudeshna Mallik<sup>2</sup> | Sumi Mukhopadhyay<sup>1</sup>  | Bibhuti Saha<sup>2</sup> | Pratip Kumar Kundu<sup>3</sup>

<sup>1</sup>Department of Laboratory Medicine, Kolkata, West Bengal, India

<sup>2</sup>Department of Tropical Medicine, Kolkata, West Bengal, India

<sup>3</sup>School of Tropical Medicine, Kolkata, West Bengal, India

## Correspondence

Sumi Mukhopadhyay, Department of Laboratory Medicine, 108, C.R. Ave, Kolkata 700073, West Bengal, India.

Email: [drsumimukhopadhyay@gmail.com](mailto:drsumimukhopadhyay@gmail.com)

## Funding information

WBHSTBT; Defence Research and Development Organisation

## Abstract

For the past several decades, dengue fever has been emerging in epidemic proportions in several regions of the world. During August–September 2019, an increasing number of fever cases were being reported from some areas of North 24 Parganas district of West Bengal, India. Accordingly, outbreak investigation of fever cases from these affected areas of Bongoan, Barasat, and Habra was carried out. To characterize clinical and biochemical features of fever cases as well as to investigate the utility of CRP as a Dengue severity marker in resource-limited settings. We systematically enrolled 108 patients from the affected region of North 24 Parganas. Standard diagnostic assays along with routine serological and biochemical parameters were performed. Of the 108 patients, 77 (71%) were confirmed with Dengue infection followed by 22 (20%) DENV seronegative and 9 (8%) coinfecting DENV cases. Among the 77 confirmed Dengue patients, 53 (69%) had primary infection while 24 (31%) had secondary infection. Among the DENV clinical symptoms, fever ( $r = 0.50$ ;  $p = 0.004$ ), headache ( $r = 0.40$ ;  $p = 0.03$ ) and abdominal pain ( $r = -0.40$ ;  $p = 0.02$ ) were found to bear significant correlation with DENV viral load. The predominant circulating serotype was found to be DENV2. CRP Dengue severity cut-off level of 10.15 mg/L (AUC: 0.85; 86% sensitivity, 77% specificity) was obtained. CRP had correlation with viral load ( $r = 0.4$ ,  $p = 0.05$ ) within febrile phase of infection. The performance of biomarkers can be influenced by local epidemiology, geography, and several patient factors, therefore, CRP Dengue severity cut-off value may be region-specific. This study for the first time attempts to estimate CRP Dengue severity cut-off value based on routine immunoturbidometric evaluation from Dengue Hyperendemic zones of North 24 Parganas, West Bengal, Eastern India.

## KEYWORDS

CRP, dengue, ELISA, RT-PCR, West Bengal

## 1 | INTRODUCTION

Arthropod-borne infectious diseases are considered to be one of the major contributors to global mortality and disability.<sup>1</sup> In India, every year during the monsoon and post-monsoon period, a large number

of individuals get affected with Dengue and Chikungunya, which almost occur in epidemic proportion causing significant morbidity and mortality.<sup>2</sup> An upsurge of all these infections during these periods can impose significant challenges to the healthcare system. To reduce the rate of fatalities appropriate laboratory-based diagnoses of febrile

illness are highly necessary. Dengue virus is a flavivirus transmitted by *Aedes* mosquito occurring in the tropical and subtropical area of the world with a huge disease burden.<sup>3</sup> All four types of different serotypes can cause a diverse range of unpredictable clinical symptoms of dengue infection.<sup>4</sup> However, the sensitivity of clinical symptoms is significantly low to discriminate among different categories of dengue infection within the early phase.<sup>5</sup> As a consequence, dengue-infected individuals are often essential for triage, suitable treatment, which can create pressure on the resource-limited health care system. A useful and reliable simple biomarker is thus needed to discriminate between the mild and severe forms of dengue infection within the febrile phase. C-reactive protein (CRP) is an acute-phase protein that can get synthesized by the hepatic cells of the liver at the early phase of infection.<sup>6</sup> The level of CRP can increase up to 25% in presence of inflammation. CRP stimulates the complement pathway of the innate immune response during microbes' infection, resulting in the increased inflammatory response and host defense to infection.<sup>7</sup> This early inflammatory marker can also discriminate between dengue and malaria infection.<sup>8</sup> Accordingly in this study, we studied the level of this inflammatory marker in an Indian cohort from North 24 Parganas, West Bengal. Here, we also investigated the level of CRP in between DENV seropositive and seronegative samples. We also studied the correlation between viral load and CRP in the acute phase of infection. Scrub typhus also an arthropod-borne infection is caused by the bacterium *Orientia tsutsugamushi* and transmitted to humans through the bite of the trombiculid mite.<sup>9</sup> Another common disease during the monsoon period is Typhoid, which is a waterborne infection caused by *Salmonella* sp.<sup>10, 11</sup> For the past few decades, the state of West Bengal in India has been plagued with a huge arthropod-borne disease burden. Among the 11 districts of West Bengal, North 24 Parganas has time and again been affected with Dengue infection in epidemic proportions. This study reports the detailed investigation of the Dengue outbreak in three affected regions of North 24 Parganas, West Bengal as well as the utility of CRP as a Dengue severity biomarker in a resource-limited setting.

## 2 | MATERIAL AND METHODS

### 2.1 | Ethical approval

This study received ethical permission from the Clinical Research Ethical Committee of Calcutta School of Tropical Medicine (CREC-STM/408 dated 21.12.2017) and ethical standards were maintained as per the act of the 1964 Helsinki Declaration and its later amendments.

### 2.2 | Study population

Patients with suspected dengue fever were enrolled from the sub-divisional Govt hospitals of three municipality areas, that is, Bongaon, Barasat, and Habra of North 24 Parganas in the state of West Bengal during August–September 2019. Geographically, North 24 Parganas

extends in the tropical zone from latitude 22°11'6" north to 23°15'2" north and from longitude 88°20' east to 89°5' east; it is situated in the eastern region of the country at an elevation of 13 m above sea level. The monsoon season spans from June to September with an average precipitation of 1579 mm. The district lies within the Ganges-Brahmaputra delta. Taken together, rapidly growing urbanization, favorable temperature, rainfall, and humidity make ideal grounds for Dengue viral transmission in this hugely populated district. During the post-monsoon period too small clogged drains, water-storing practices of the local residents serve as ideal breeding grounds for mosquito and dengue transmission.

### 2.3 | Diagnostic tests

Dengue was confirmed on the basis of NS1 and immunoglobulin M (IgM) enzyme-linked immunosorbent assay (ELISA) and polymerase chain reaction (PCR) test positivity, Chikungunya by MAC IgM ELISA (InBios), Typhoid through Widal test (Tulip tidal test), and Scrub Typhus through IgM ELISA test (InBios). Five milliliters of peripheral blood was collected from 108 clinically suspected patients during their indoor admission in the sub-divisional govt. hospitals of North 24 Parganas, West Bengal. Sera and plasma were prepared from the whole blood of patients and were stored at -20°C for downstream processing. All the enrolled Dengue patients exhibited any four of the following symptoms: fever, nausea, abdominal pain, myalgia, vomiting, fluid accumulation, and retro-orbital pain. Based on their symptoms, the patients were classified according to WHO criteria of dengue disease severity.<sup>12</sup> Chikungunya patients were characterized by small joint pain, nausea, rash, headache.<sup>13</sup> As per World Health Organization, symptoms of Scrub and Typhoid are very similar to Dengue and Chikungunya, that is, fever, headache, and rash. All the clinically suspected patients ( $n = 108$ ) were enrolled for detection of NS1 antigen by Dengue NS1 Ag MICROELISA (J.Mitra&Co.Pvt.Ltd.) of Anti Dengue IgM & IgG antibody in patient's sera was determined using Anti Dengue IgM & IgG ELISA kit (Panbio) following manufacturer's instruction.

### 2.4 | Dengue viral load determination and serotyping

To quantify the viral load, DENV infected febrile phase patients were selected for real-time PCR-based viral RNA quantification. Briefly, viral RNA was isolated from 140 µl of serum sample of dengue patients using a viral RNA extraction kit (Qiagen). Dengue viral load among patients was quantified using Taqman based Real-Time PCR (Genome Diagnostic Pvt. Ltd.).<sup>14</sup> The Specific Master Mix in the kit contains reagents and enzymes for the specific amplification of the Dengue genome and for the direct detection of the specific amplicon in fluorescence channel FAM. External positive Standards are supplied in the kit which allows the determination of the gene load. Real-time PCR was programmed in an ABI Prism 7500 instrument. Confirmed dengue patients in their febrile phase of infection were selected for detecting all four serotypes of dengue infection. The

samples were processed as per the manufacturer's protocol (Genome Diagnostic Pvt. Ltd.).<sup>14</sup> Multiplex reverse-transcription polymerase chain reaction (RT-PCR) reactions were performed following the steps of real-time PCR-based dengue viral RNA quantification. Four different fluorescence channels were used for the detection of specific DENV serotypes. Positive control was used to interpret the data with the unknown samples.

## 2.5 | Biochemical parameters

Complete blood count (CBC test) of the enrolled patients was performed using an automated cell counter (SYSMEX Model No-XP100). The serum of the enrolled samples was also analyzed for liver enzymes along with CRP. All the tests were performed following standard protocols on an automated biochemistry analyzer (ERBA Model No-EM360).<sup>15</sup> CRP was measured by turbidimetric immunoassay to quantitate the level of CRP in samples. The method is based on the end-point reaction of antigen-antibody.

## 2.6 | Statistical analysis

The counting method was used to differentiate among categorical variables by using absolute number (*n*) and percentage (%) while, biochemical data were analyzed by calculating mean  $\pm$  SEM and Median value followed by Mann-Whitney *U* test. One-way analysis of variance was performed to study the comparison among continuous variables. CRP threshold was determined using receiver operating characteristic curve (ROC) analysis followed by the Youden index. Spearman's correlation was also performed between DENV clinical symptoms and viral load. A *p* < 0.05 was considered significant for the entire test performed. Statistical analysis was performed using the Graph-Pad Prism statistics software (Graph-Pad Software Inc.).<sup>16</sup>

## 3 | RESULTS

### 3.1 | Demography and clinical parameters

In the present study, we systematically enrolled 108 patients from three hyperendemic regions of North 24 Paraganas, West Bengal during the monsoon period from August 2019 to September 2019. Among the patients, predominantly male patients 57% (*n* = 61) were infected with DENV followed by female patients 43% (*n* = 47). The prevailing infected age group were between 20 and 40 (*n* = 51 [47.2%]). Out of 108 patients, laboratory-confirmed dengue patients were 71% (*n* = 77) and dengue coinfected patients were 8% (*n* = 9) followed by dengue seronegative patients were 20% (*n* = 22) (Figure 1). Among the 22 infected DENV seronegative patients, four were infected with Chikungunya (*n* = 2) and Scrub Typhus (*n* = 2), two were coinfecting with Scrub + Chikungunya (*n* = 1) and Scrub + Typhoid (*n* = 1), rest of the Dengue seronegative patients (*n* = 16) showed clinical symptoms of hepatomegaly, enlarged liver, and other febrile illness. Further among the Dengue coinfecting patients, five were infected with Dengue + Chikungunya and four were with Dengue + Scrub. According to the WHO<sup>17</sup> criteria, we further categorized the Dengue patients into Dengue without Warning sign (DwoWS) (*n* = 44), Dengue with a Warning sign (DwWS) (*n* = 26), and Severe Dengue (SD) (*n* = 7). Out of 77 dengue infected patients, NS1 based serological test confirmed patients were 100% (*n* = 77), primary infected patients were 69% (*n* = 53) and secondary infected patients were 31% (*n* = 24) (Figure 1). During the time of blood collection, fever (74%) was the most common symptom among the Dengue seropositive patients compared to Dengue seronegative patients. Additionally, other Dengue-specific symptoms such as Nausea (83.33%), Rash (70%), Myalgia (82%), Headache (72%) were predominantly found in seropositive samples (Table 1). The symptoms among different categories of DENV infection, DwoWS, DwWS, and SD had fever along with nausea (20%, 31%, and 57%), vomiting

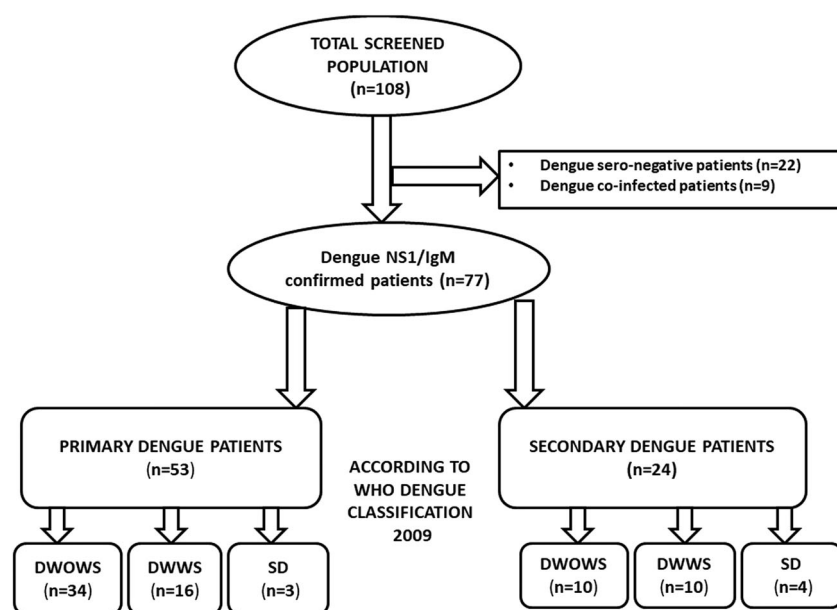


**FIGURE 1** Flowchart diagram showing the distribution of enlisted study population. Dengue without Warning Sign (DwoWS), Dengue With Warning Signs (DWWS), and Severe Dengue (SD)

(9%, 15%, and 29%), abdominal pain (14%, 20%, and 71%) and myalgia (32%, 46%, and 71%). Among the dengue seronegative patients, myalgia and headache were predominantly found in Chikungunya and Scrub Typhus infected population. Dengue and Chikungunya coinfecting patients showed the typical characteristics of rash and small joint pain. In the case of Scrub and Dengue coinfecting patients, myalgia and rash were predominantly found.

### 3.2 | Detection of DENV viral load and serotypes by qRT-PCR

Furthermore, we analyzed the DENV infected patient population for the presence of viral load and different dengue serotypes. Previous studies have demonstrated that high viral load can be detected within the febrile phase (1–4 days) of dengue infection. In our study population, 32 DENV patients were in this category, therefore these patients were analyzed for their viral load and serotype detection. Total 32 patients were included on the basis of low platelet count (mean < 85 000/ $\mu$ l), high Hematocrit (HCT) (mean > 41.2), and dengue clinical symptoms. Among the DENV clinical symptoms, fever ( $r = 0.491$ ;  $p = 0.004$ ), headache ( $r = 0.375$ ;  $p = 0.03$ ) and abdominal pain ( $r = -0.403$ ;  $p = 0.02$ ) were found to bear statistically significant correlation with DENV viral load (Table 2). Among the infected patients, predominant serotypes were DENV2 ( $n = 14$ ) followed by DENV3 ( $n = 5$ ). Co-circulation of multiple dengue serotypes was observed in seven patients, that is, DENV2 + DENV3 ( $n = 5$ ) and DENV1 + DENV2 ( $n = 2$ ). No positive results were found for DENV4 infection.

### 3.3 | Biochemical parameter of infected patients at the time of hospital visit

Blood parameters like platelet count demonstrated a 1.2-fold decrease in DENV seropositive samples compared to seronegative samples with a statistical significance of 0.023 (Table 3). According to

the WHO (2009) criteria, the low platelet count is a significant characteristic of dengue-infected patients. Furthermore, a 0.93-fold increase of hematocrit was observed in DENV seropositive samples compared to DENV seronegative samples (Table 3). A different biochemical parameter was tested among the dengue-infected population. The level of liver enzymes such as serum glutamic oxaloacetic transaminase (SGOT) and serum glutamic pyruvic transaminase (SGPT) were higher in DENV seropositive samples compared to DENV seronegative samples with a statistical significance of 0.01 (Mann–Whitney  $U$  test) (Table 3). Furthermore, levels of albumin and globulin in the blood of infected patients were significantly low in DENV seropositive samples compared DENV seronegative with a  $p = 0.007$  and 0.04, respectively (Mann–Whitney  $U$  test). One of the inflammatory marker CRP levels was quite low in the DENV population with a median value of 4.50 mg/L (Table 3). DENV seronegative patients had a fivefold increased (median value) level of CRP compared to DENV seropositive with a statistical significance of 0.0008 (Mann–Whitney  $U$  test). DENV seronegative population ( $n = 22$ )

**TABLE 2** Variation of clinical symptoms (febrile phase) with dengue viral loads

Clinical symptoms (febrile phase)	Spearman correlation	$p$ value
Fever	<b>0.491</b>	<b>0.0041</b>
Nausea	0.272	0.1307
Headache	<b>0.375</b>	<b>0.0341</b>
Myalgia	-0.276	0.1260
Rash	-0.121	0.5088
Vomiting	0.013	0.9437
Abdominal Pain	<b>-0.403</b>	<b>0.0221</b>
Clinical Fluid Accumulation	-0.220	0.2249
Hemorrhage	0.223	0.2184

Note: The statistical significance is indicated by  $p < 0.05$  and their corresponding spearman correlation value has been bold faced. Statistical analysis was performed using Graph-pad Prism statistic software.

**TABLE 1** Demography of the subjected study population among DENV seropositive, coinfecting DENV and DENV seronegative samples

Clinical symptoms	Dengue without warning sign ( $n = 35$ )	Dengue with warning sign ( $n = 27$ )	Severe dengue ( $n = 10$ )
Fever (number, percentage)	35; 100%	24; 88%	9; 90%
Nausea (number, percentage)	17; 48%	14; 51%	6; 60%
Rash (number, percentage)	9; 25%	10; 37%	0
Myalgia (number, percentage)	17; 48%	14; 51%	6; 60%
Headache (number, percentage)	25; 71%	20; 74%	7; 70%
Abdominal Pain (number, percentage)	8; 22%	14; 51%	5; 50%
Clinical fluid accumulation (number, percentage)	0	3; 11%	4; 40%
Hemorrhage (number, percentage)	0	0	3; 30%



**TABLE 3** Comparison of laboratory parameter levels in blood from DENV seropositive ( $n = 77$ ), coinfecting DENV ( $n = 9$ ), and DENV seronegative ( $n = 22$ )

Laboratory measure	DENV seropositive samples ( $n = 77$ )		Coinfecting DENV samples ( $n = 9$ )		DENV seronegative samples ( $n = 22$ )		ANOVA <sup>a</sup> analysis ( $p$ value)	DENV seropositive samples vs. coinfecting DENV samples (Mann-Whitney U test)		DENV seronegative samples vs. coinfecting DENV samples (Mann-Whitney U test)		DENV seropositive samples vs. DENV seronegative samples (Mann-Whitney U test)	
	Mean $\pm$ SEM	Median	Mean $\pm$ SEM	Median	Mean $\pm$ SEM	Median		Median	U test	Median	U test	Median	U test
Platelets	82 872 $\pm$ 6229	85 500	83 222 $\pm$ 15 717	82 000	116 417 $\pm$ 11 175	945 000	0.023	ns	ns	ns	ns	0.0206	ns
Haematocrit	37.86 $\pm$ 0.639	37.55	33.03 $\pm$ 2.202	34.40	35.42 $\pm$ 1.240	35.00	0.02	0.04	ns	ns	ns	ns	ns
SGOT	100.6 $\pm$ 11.58	70.50	60.30 $\pm$ 13.96	51.00	75.11 $\pm$ 16.94	62.00	0.01	ns	ns	ns	ns	0.015	0.015
SGPT	63.92 $\pm$ 7.044	44.00	36.44 $\pm$ 10.20	30.00	35.00 $\pm$ 6.22	26.00	0.012	ns	ns	ns	ns	0.018	0.018
CRP	10.20 $\pm$ 1.566	4.70	9.770 $\pm$ 5.808	2.00	22.50 $\pm$ 3.831	20.95	0.0011	ns	0.018	ns	0.0014	0.007	0.007
Albumin	3.571 $\pm$ 0.048	3.600	3.489 $\pm$ 0.108	3.600	3.733 $\pm$ 0.1038	3.800	0.0063	ns	ns	ns	ns	0.007	0.007
Globulin	3.071 $\pm$ 0.053	3.00	3.144 $\pm$ 0.213	3.100	3.381 $\pm$ 0.115	3.500	0.051	ns	ns	ns	ns	0.04	0.04

Note: The statistical significance is indicated by  $p < 0.05$ . @ANOVA followed by Kruskal-Wallis test (K).

Abbreviation: ANOVA, analysis of variance.

<sup>a</sup>Mann-Whitney U test. Statistical analysis was performed using Graph-pad Prism statistic software.

consisted of patients with Scrub ( $n = 2$ ), Chikungunya ( $n = 2$ ), Scrub + Chikungunya ( $n = 1$ ), Scrub + Typhoid ( $n = 1$ ), and other febrile illness ( $n = 16$ ).

### 3.4 | Laboratory characteristic of DENV population

One of the most common hematological findings observed in the DENV population was low platelet count (mean  $\pm$  SEM) in SD (24 500/ $\mu$ L  $\pm$  8878) compared to DWWS (55 000/ $\mu$ L  $\pm$  6659) and DWoWS (142 000/ $\mu$ L  $\pm$  7060) (Table 4). Furthermore, 1.06-fold increased hematocrit was observed in SD patients compared to DWWS. In addition, we also studied the level of SGOT and SGPT in different categories of DENV infection. Increased level (Mean  $\pm$  SEM) of SGOT (204.4 IU/L  $\pm$  57.15) and SGPT (169.70 IU/L  $\pm$  26.37) were obtained in SD patients compared to DWWS (126.7 IU/L  $\pm$  16.86 and 110.4 IU/L  $\pm$  12.86, respectively) (Table 4).

### 3.5 | CRP as diagnostic predictor of dengue severity

In patients with DENV infection, the mean  $\pm$  SEM value of CRP level in SD patients (27.89 mg/L  $\pm$  6.90) were higher compared to DWoWS (9.71 mg/L  $\pm$  2.14) and DWWS (6.36 mg/L  $\pm$  1.31) with a statistical significance of 0.003 (Figure 2). The ROC curve analysis was performed for DWoWS/DWWS versus SD patients. Regardless of the phase of illness, for DWoWS/DWWS versus SD, the AUC value is 0.85 with a CRP cutoff of 10.15 mg/L (Sensitivity: 86%, Specificity: 77%, Likelihood ratio: 3.750) (Figure 2). The level of CRP was also analyzed on the basis of days of illness. A higher level of CRP was observed in 1–3 days (14.28 mg/L  $\pm$  2.82) of infection compared to 4–6 and 7–10 (7.49 mg/L  $\pm$  3.98, 8.94 mg/L  $\pm$  2.37, respectively) days of infection with a statistical significance of 0.036 (Figure 2). Furthermore, a correlation study was performed between CRP and laboratory parameters. The increased level of CRP was positively correlated with SGOT ( $r = 0.25$  with  $p = 0.02$ ), SGPT ( $r = 0.24$  with  $p = 0.03$ ) and HCT ( $r = 0.318$  with  $p = 0.004$ ), while negatively correlated with platelet ( $r = -0.344$  with  $p = 0.002$ ) Again, CRP was positively correlated with viral load ( $r = 0.4$ ,  $p = 0.05$ ) within febrile phase of infection (Figure 3).

## 4 | DISCUSSION

Since 1990, epidemics of Dengue in India have become more frequent, especially in urban zones. The epidemiology of Dengue in India was first reported in Chennai (1780), followed by the first outbreak in Kolkata (1963).<sup>18–20</sup> Presently the geographical range of DENV infection has shifted from urban to rural areas,<sup>21 22</sup> However, there have been several studies in urban areas, while this is the first study of DENV infection in the hyperendemic region of North 24 Parganas.

**TABLE 4** Comparison of laboratory parameter levels in blood from patients who were positive for DENV infection

Laboratory measure	Dengue without Warning Sign (n = 44)		Dengue with Warning Sign (n = 26)		Severe Dengue (n = 7)		ANOVA <sup>a</sup> analysis
	Mean ± SEM	Median	Mean ± SEM	Median	Mean ± SEM	Median	
Platelets (/μl)	142 886 ± 7061	134 500	55 346 ± 6659	43 500	24500 ± 8878	16 500	<0.0001
Haematocrit (%)	36.32 ± 0.728	35.60	38.57 ± 0.984	38.05	41.20 ± 1.742	40.50	0.026
SGOT (IU/l)	57.33 ± 5.203	48	126.7 ± 16.86	120	204.4 ± 57.15	144	<0.0001
SGPT (IU/l)	47.12 ± 4.202	38.50	110.4 ± 12.86	98	169.70 ± 26.37	144	<0.0001
CRP (mg/L)	6.36 ± 1.314	2.70	9.712 ± 2.149	4.800	27.89 ± 6.902	37.60	0.003

Note: The statistical significance is indicated by  $p < 0.05$ . <sup>a</sup>ANOVA followed by Kruskal–Wallis test (K). Statistical analysis was performed using Graph-pad Prism statistic software

Abbreviation: ANOVA, analysis of variance.

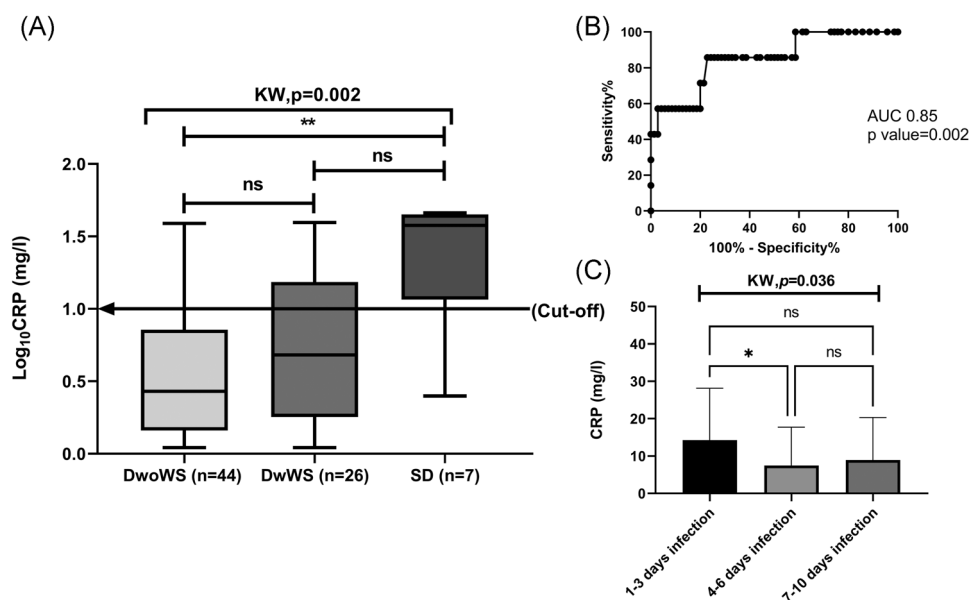


**FIGURE 2** (A) C-reactive protein (CRP) level in the blood from Dengue without Warning Sign (DwoWS), Dengue with Warning Signs (DWWS), and Severe Dengue (SD). Study subjects are significantly different from each other. (B) Receiver operating characteristics curve analysis obtained the cut-off value (10.15 mg/L) and AUC = 0.85. Arrow line showing the severity cutoff value (10.15 mg/L) obtained from the Youden index. AUC, area under the curve. (C) Day wise changes of the level of CRP. Study subjects are significantly from each other

In the present study, the serological and clinical report indicates that the outbreak was predominantly due to dengue viral transmission. More male patients were infected compared to females. In our study population, we found 47% of infected patients were within the age group of 20–40. A similar result was reported by Bandyopadhyay et al. (2012) from the Calcutta School of Tropical Medicine.<sup>23</sup> Study populations were enrolled from three hyperendemic regions (Bongaon, Barasat, and Habra) of North 24 Parganas. The majority of the infected patients showed typical clinical manifestations of Dengue such as fever (74%), nausea (83%), rash (70%), headache (72%).

Additionally, DWWS characteristics such as abdominal pain and clinical fluid accumulation were seen in a maximum number of DENV positive populations compared to DENV negative. Typical clinical manifestations of SD, such as gum bleeding was observed within three DENV seropositive patients. This current finding showed

similarities with the studies done by Eamchan et al. in Thailand (2008).<sup>24</sup>

RT-PCR-based nucleic acid detection is one of the novel molecular methods to diagnose dengue infection successfully. Here we used RT-PCR-based Dengue viral load detection and serotyping of the acute phase infected DENV population. Total 32 DENV patients were enlisted based on low platelet count and high HCT to detect different serotypes of dengue infection, among this population, male  $n = 21$  (65%) were predominant followed by female 11 (35%). The prevalent age group of the infected patients was 20–50 years. High viral load ( $2 \times 10^7$  copies/ml) was detected within the febrile phase of disease compared to the defervescence period ( $3 \times 10^5$  copies/ml). Higher viral load in acute phase patients might have induced cellular immune response, which cleared the plasma viremia at the defervescence period. Our data also demonstrated that viral load was



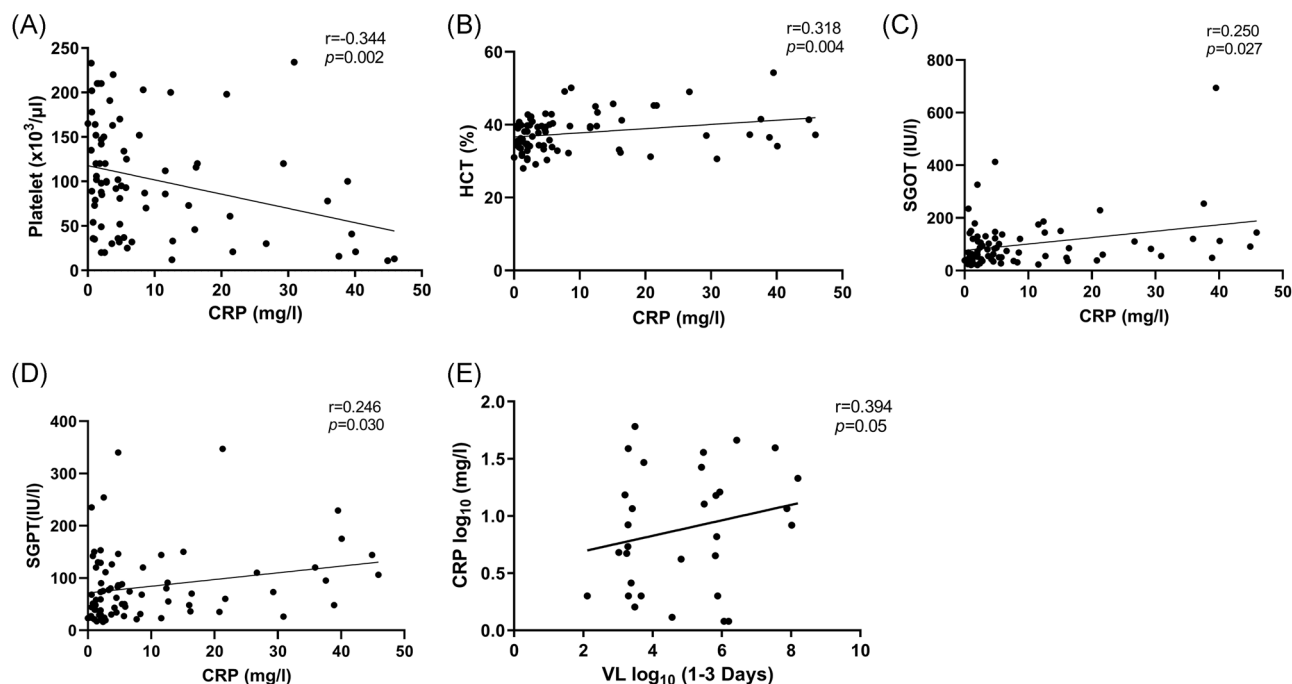


**FIGURE 3** Correlation of CRP with biochemical parameters and viral load. (A) CRP versus platelet, (B) CRP versus HCT, (C) CRP versus SGOT, (D) CRP versus SGPT, (E) CRP versus Viral load. Statistical analysis was performed using Graph-pad Prism statistic software. CRP, C-reactive protein; SGOT, serum glutamic oxaloacetic transaminase; SGPT, serum glutamic pyruvic transaminase

positively correlated with fever ( $r = 0.491$ ,  $p = 0.004$ ), headache ( $r = 0.375$ ,  $p = 0.034$ ) and negatively correlated with abdominal pain ( $r = -0.403$ ,  $p = 0.022$ ) within the febrile phase of infection indicating that clinical symptoms bear direct correlation with viral load. DENV2 was predominantly found in the study population, followed by DENV3. According to Dey et al. study, in 2016 predominant serotype of Dengue in Kolkata was DENV2.<sup>25</sup> In 2012, the reemergence of the DENV3 serotype in Kolkata caused a major DENV outbreak with a considerable number of severe cases.<sup>26</sup> This serotype shift can cause Antibody-dependent enhancement (ADE) where pre-existing antibodies against primary infection fail to neutralize the virus caused by different dengue serotypes.

CRP is a highly conserved pentraxin family of proteins.<sup>27</sup> It is an acute-phase protein that is rapidly synthesized in the presence of inflammation. The level of CRP in plasma can increase up to 25% in the presence of inflammatory disorder.<sup>28</sup> CRP level can increase up to 1000-fold within a few hours after the introduction of bacterial infection.<sup>7</sup> In our study, the level of CRP in the DENV seronegative population was five times (median value) higher than the DENV seropositive population. However, in this study, we analyzed our findings exclusively in the Dengue virus-infected population. Evidence suggested that a high viral load evokes the macrophages to produce several proinflammatory cytokines. IL6 is the major proinflammatory cytokine that can stimulate the liver cells to produce CRP.<sup>29</sup>

A higher level of CRP in DENV infection indicates a higher rate of inflammation which may cause severe hepatitis, kidney injury, organ dysfunction, and other poor outcomes. Previously, Chen et al. had reported an elevated level of CRP during the febrile phase of

infection in SD patients compared to non-severe (defined using 2009 WHO classification).<sup>30</sup> Our analysis established an elevated level of CRP in SD patients compared to DwoWS/DwWS with a statistical significance of 0.0028. CRP's turbidimetric immunoassay showed reasonable sensitivity (86%) and specificity (77%) for SD detection with a cutoff value of 10.15 mg/L. Furthermore, a higher level of CRP was obtained in the 1–3 days (febrile phase) of infection compared to 4–6 and 7–10 days. Our study also demonstrated that higher viral load was positively correlated with the level of CRP. So within the febrile phase of infection higher CRP level was significantly associated with the prediction of SD infection. Furthermore, laboratory parameters were also showed a significant correlation with CRP. Our current study revealed that SD patients had decreased platelet count, increased liver enzymes and were clinically associated with fluid accumulation and liver enlargement.

Although this is the first effort to study dengue outbreaks from the hyperendemic regions of North 24 Parganas, this study has several limitations. Large numbers of febrile phase patients are required further to investigate the pathogenicity of DENV infection in rural areas. Cohort studies are needed in these hyperendemic regions for better patient health care management.

In conclusion, this study demonstrates the clinical and biochemical parameters of the hospitalized patients in the three municipalities' areas of North 24 Parganas. The continuous spread of DENV serotypes can invade new areas and populations, thereby increasing health problems. The clinical symptoms of Dengue are pretty similar to other febrile phase infections such as Chikungunya, Scrub, and Typhoid. Such nonspecific clinical symptoms thus make

proper diagnosis considerably challenging. Necessary and reliable laboratory facilities in rural areas to detect different types of febrile infection can overcome this issue. This study also demonstrated that CRP might be used as a marker within the febrile phase to detect individuals with the risk of dengue severity. This finding suggested that patients with DENV infection with a high CRP value should get intensive hospital care with routine monitoring. Thus, appropriate vector control, systematic tracking of infected individuals, community awareness, rapid diagnosis are key features for better patient health care management and restricting the increasing number of dengue cases.

## ACKNOWLEDGMENTS

We are thankful to WBHESTBT (File no: BT (Estt)/RD-65/2017), the Government of West Bengal, India, and LSRB. DRDO Govt. of India [O/o DG(TM)/81/48222/LSRB-339/BTB/2019], which made it possible to carry out this study. This study received financial support from WBHESTBT (File no: BT (Estt)/RD-65/2017), Government of West Bengal, India, and LSRB. DRDO Govt. of India [O/o DG(TM)/81/48222/LSRB-339/BTB/2019].

## CONFLICT OF INTERESTS

The authors declare that there are no conflict of interests.

## AUTHOR CONTRIBUTIONS

Sourav Datta and Sudeshna Mallik designed the study and wrote the manuscript. Sourav Datta performed all experiments. Sourav Datta and Moumita Paul collected samples and performed the statistical analysis. Pratip Kumar Kundu provided administrative support to conduct the study. Bibhuti Saha, Manab Ghosh, Prantiki Halder, and Sumi Mukhopadhyay helped in clinical interpretation and collection of samples. Manab Ghosh helped in the diagnosis and supportive treatment of the enrolled subjects. Funding recipients Bibhuti Saha and Sumi Mukhopadhyay.

## DATA AVAILABILITY STATEMENT

The data that support the findings of this study are available from the corresponding author upon reasonable request.

## ORCID

Sumi Mukhopadhyay  <http://orcid.org/0000-0003-1400-3715>

## REFERENCES

- Wilder-Smith A, Gubler DJ, Weaver SC, Monath TP, Heymann DL, Scott TW. Epidemic arboviral diseases: priorities for research and public health. *Lancet Infect Dis*. 2017;17:e101-e106. doi:10.1016/S1473-3099(16)30518-7
- Broor S, Devi LS. Arboviral infections in India. *Indian J Heal Sci Care*. 2015;2:192. doi:10.5958/2394-2800.2015.00035.8
- Heilman JM, De Wolff J, Beards GM, Basden BJ. Dengue fever: a wikipedia clinical review. *Open Med*. 2014;8:105-15.
- Guzman MG, Gubler DJ, Izquierdo A, Martinez E, Halstead SB. Dengue infection. *Nat Rev Dis Prim*. 2016;2:16055. doi:10.1038/nrdp.2016.55
- Guzman MG, Perez AB, Fuentes O, Kouri G. Dengue, dengue hemorrhagic fever. Hegggenhougen HK, *International Encyclopedia of Public Health*. Academic Press; 2008. 98-119. doi:10.1016/B978-012373960-5.00564-5
- Gewurz H. Biology of C-reactive protein and the acute phase response. *Hosp Pract*. 1982;17:67-81. doi:10.1080/21548331.1982.11702332
- Sproston NR, Ashworth JJ. Role of C-reactive protein at sites of inflammation and infection. *Front Immunol*. 2018;9:754. doi:10.3389/fimmu.2018.00754
- Epelboin L, Boullé C, Ouar-Epelboin S, et al. Discriminating malaria from dengue fever in endemic areas: clinical and biological criteria, prognostic score and utility of the C-reactive protein: a retrospective matched-pair study in French Guiana. *PLOS Negl Trop Dis*. 2013;7:e2420.
- Rao PN, Van Eijk AM, Choubey S, et al. Dengue, chikungunya, and scrub typhus are important etiologies of non-malarial febrile illness in Rourkela, Odisha, India. *BMC Infect Dis*. 2019;19:572. doi:10.1186/s12879-019-4161-6
- Stanaway JD, Reiner RC, Blacker BF, et al. The global burden of typhoid and paratyphoid fevers: a systematic analysis for the Global Burden of Disease Study 2017. *Lancet Infect Dis*. 2019;19:369-381. doi:10.1016/S1473-3099(18)30685-6
- Sharma Y, Arya V, Jain S, Kumar M, Deka L, Mathur A. Dengue and typhoid co-infection-study from a government hospital in North Delhi. *J Clin Diagnostic Res*. 2014;8:DC09-DC11. doi:10.7860/JCDR/2014/9936.5270
- Srikiathachorn A, Rothman AL, Gibbons RV, et al. Dengue-how best to classify it. *Clin Infect Dis*. 2011;53:563-567. doi:10.1093/cid/cir451
- Rueda JC, Santos AM, Angarita JL, et al. Demographic and clinical characteristics of chikungunya patients from six Colombian cities, 2014-2015. *Emerg Microbes Infect*. 2019;8:1490-1500. doi:10.1080/22221751.2019.1678366
- Najioullah F, Viron F, Césaire R. Evaluation of four commercial real-time RT-PCR kits for the detection of dengue viruses in clinical samples. *Viral J*. 2014;11(1):4-8. doi:10.1186/1743-422X-11-164
- Nair A, Jayakumari C, Jabbar PK, et al. Prevalence and associations of hypothyroidism in Indian patients with type 2 diabetes mellitus. *J Thyroid Res*. 2018;2018:5386129. doi:10.1155/2018/5386129
- Patra G, Mallik S, Saha B, Mukhopadhyay S. Assessment of chemokine and cytokine signatures in patients with dengue infection: a hospital-based study in Kolkata, India. *Acta Trop*. 2019;190:73-79.
- WHO. *Dengue: Guidelines for Diagnosis, Treatment Prevention and Control*. World Health Organisation; 2009.
- Sarkar JK, Chatterjee SN, Chakravarty SK. Haemorrhagic fever in Calcutta: some epidemiological observations. *Indian J Med Res*. 1964;52:651-659.
- Chatterjee SN, Chakravarti SK, Mitra AC, Sarkar JK. Virological investigation of cases with neurological complications during the outbreak of haemorrhagic fever in Calcutta. *J Indian Med Assoc*. 1965;45:314-316.
- Dengue-vector-prevalence-and-virus-infection-in-a-rural-area-in-south-India\_Enhanced-Reader.pdf.
- Taraphdar D, Sarkar A, Bhattacharya MK, Chatterjee S. Sero diagnosis of dengue activity in an unknown febrile outbreak at the Sili-guri Town, District Darjeeling, West Bengal. *Asian Pac J Trop Med*. 2010;3:364-366. doi:10.1016/S1995-7645(10)60088-0
- Sarkar A, Taraphdar D, Chatterjee S. Investigations of recurrent outbreaks of unknown fever, establish rural dengue activity in West Midnapore, a coastal district in West Bengal, India. *Arch Clin Microbiol*. 2010;18:534-538. doi:10.3823/215

23. Bandyopadhyay B, Bhattacharyya I, Adhikary S, et al. A comprehensive study on the 2012 dengue fever outbreak in Kolkata, India. *ISRN Virol.* 2013;2013:1-5. doi:10.5402/2013/207580
24. Eamchan P, Nisalak A, Foy HM, Chareonsook OA. Epidemiology and control of dengue virus infections in Thai villages in 1987. *Am J Trop Med Hyg.* 1989;41:95-101. doi:10.4269/ajtmh.1989.41.95
25. Dey M, Sengupta M, Chatterjee RM, Barik G. Co-circulation of all dengue serotypes among patients attending a tertiary care hospital in Kolkata. *Virol Immunol J.* 2018. 2(9):doi:10.23880/vij-16000184
26. Saha K, Ghosh M, Firdaus R, et al. Changing pattern of dengue virus serotypes circulating during 2008–2012 and reappearance of dengue serotype 3 may cause outbreak in Kolkata, India. *J Med Virol.* 2016;88:1697-1702. doi:10.1002/jmv.24529
27. Du Clos TW. Pentraxins: structure, function, and role in inflammation. *ISRN Inflamm.* 2013;2013:1-22. doi:10.1155/2013/379040
28. Gabay C, Kushner I. Acute-phase proteins and other systemic responses to inflammation. *N Engl J Med.* 1999;340:448-454. doi:10.1056/NEJM199902113400607
29. Sun XJ, Meng HX, Shi D, et al. Elevation of C-reactive protein and interleukin-6 in plasma of patients with aggressive periodontitis. *J Periodontal Res.* 2009;44:311-316. doi:10.1111/j.1600-0765.2008.01131.x
30. Chen CC, Lee IK, Liu JW, Huang SY, Wang L. Utility of C-reactive protein levels for early prediction of dengue severity in adults. *Biomed Res Int.* 2015;2015:936062. doi:10.1155/2015/936062

**How to cite this article:** Datta S, Ghosh M, Paul M, et al. Comprehensive investigation of fever cases enrolled during 2019 dengue outbreaks from three hyperendemic regions of North 24 Parganas district of West Bengal, India. *J Med Virol.* 2022;94:540-548. doi:10.1002/jmv.27430